

**Mineral Magnetic and Palaeomagnetic Properties
of Continental Shelf Sediments**

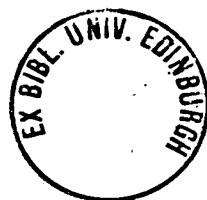
by

D.J.Watson

PhD

University of Edinburgh

1989



Declaration

I declare that this thesis was composed by myself and that the work it describes is my own, except where stated in the text.

David Watson

**This thesis is dedicated to my ever supportive parents,
John and Mary**

Acknowledgements

At Edinburgh University, Department of Geophysics, my thanks to Dr. Roy Thompson for his patient supervision and Prof. Ken Creer, the Head of Department for his support and access to the palaeomagnetic laboratories. Amongst the staff and students in the dept, all of whom have been extremely helpful, special thanks to Hazel Brown and Ian Snowball for proof reading, Mike Stewart and Tony Morris for assistance with computer packages, Helen McKeating for service above and beyond the call of duty and the technical staff, Alan, Alex and Colin, whose practical expertise was only surpassed by their exceptional humour. Also Prof. G. Boulton for access to material from the Barents Sea and Dr Barbara Maher for her assistance in processing it.

At the British Geological Survey, many thanks to Dr. N. Fannin for his advice and assistance in gaining access to B.G.S material, G. Tulloch for his practical advice and assistance, and D. Long, A. Stevenson, A. Fyfe and the many other BGS staff for all the help they have given over the past four years.

Thanks to Dr. J.P. Smith and Mr B. Bucknall for their assistance with XRF work at Wolverhampton Polytechnic; Arshad Beg for his assistance with heavy mineral extraction at Strathclyde University and G. Reid for access to material from the Moray Firth.

This work was undertaken whilst in receipt of a NERC studentship.

Abstract

A range of palaeomagnetic and mineral magnetic techniques have been applied to UK continental shelf materials and to sediment cores from Spitsbergen.

Palaeomagnetic analysis of British Geological Survey vibrocore and gravity core material was found to be technically possible. An easily measurable natural remanent magnetisation that was stable under alternating field demagnetisation was observed. However, the downcore natural remanent magnetisation records were found to be too short to contain a magnetic polarity change and lacked sufficient features for a successful match to secular variation master curves. Slightly shallow inclinations were observed in many of the UK continental shelf cores. The Spitsbergen sediment cores produced a confused palaeomagnetic record, containing pronounced shallow inclinations. These shallow inclinations are thought to reflect both geomagnetic and sedimentary causes.

Mineral magnetic analysis showed varying grain sizes of magnetite as the principal magnetic remanence carrier in UK continental shelf core and grab samples. In addition, considerable amounts of high coercivity minerals, principally haematite were found in many areas.

Whole core magnetic susceptibility was successfully used as a sediment core logging tool both onboard British Geological Survey sampling ships and in land based laboratories. Whole core susceptibility was found to reflect changes in core lithology and the presence of local features eg drop stones. Susceptibility in both stored cores and stored subsamples was observed to be stable over time. Mass specific susceptibility measurements on surface sediment samples was observed to be an effective means of mapping sediment distribution in the Firth of Clyde and the Moray Firth. Sediment particle size were observed to have a great influence on susceptibility, with peak susceptibilities seen in the mud fractions. Higher coercivity minerals were often observed in the sand fractions, whereas magnetite was found to dominate the magnetic mineral assemblage in the mud fraction. The variable coercivity found in sand samples was used as a sediment source indicator in the Moray Firth. Mineral magnetic studies on sediments from Spitsbergen

showed evidence of considerable variations in the sedimentary regime with pronounced contrasts in magnetite/haematite ratio.

Chemical analysis of UK continental shelf cores showed a strong positive relationship between whole core susceptibility and iron content. Additional correlations were found between iron, susceptibility and other potentially valuable chemical constituents.

List of Tables

Table no Page no.

2.1	30	A table showing some of the magnetic properties of a range of magnetic minerals.
3.1	50	A comparison of instrument readings of chemical susceptibility standards between shore and ship based laboratories.
4.1	82	χ and SIRM properties of subsamples from Flett cores repeated after two years.
4.2	82	The range of mineral magnetic data for cores from Flett area.
7.1	147	χ and SIRM/χ ratio values for various grain size fractions from the Moray Firth.
9.1a	184	Chemical data for samples from UK continental shelf cores.
9.1b	184	Chemical ratio and magnetic data for samples analysed by XRF.
9.2	185	Correlation coefficients between chemical constituents and volume susceptibility for some UK continental shelf sediments.

Figure List

Figure no	Page no.	
1.1	4	Principal frequency bands of the geomagnetic spectrum.
1.2	7	Typical lake sediment secular variation records.
1.3	8	Declination values for Firth of Clyde.
1.4	9	Palaeomagnetic results from DSDP site 552A.
1.5	10	Comparison of mineral magnetic data for IOS core S8-79-4 with its record of late Pleistocene palaeoclimate variations.
1.6	11	Magnetic susceptibility vs magnetite content for grab samples from the Canadian shelf.
1.7	12	Contour map of susceptibility variation in core-top samples from the Argentine Basin.
2.1	17	Log. SIRM ($\text{Am}^2\text{kg}^{-1}$) vs. log. χ (m^3kg^{-1}) for 1000 natural samples.
2.2	18	Log. SIRM vs log. K for natural samples.
2.3	21	Diagram of coil design for Digico susceptibility bridge.
2.4	22	Chemical calibration of Bartington susceptibility equipment.
2.5	23	Cross calibration of Bartington whole core and subsample susceptibility measurements.
2.6	24	Whole core susceptibility of core 56-10 53VE.
2.7	27	Cross-calibration of electromagnet and Trilec pulse-magnetiser.
2.8	28	Forward IRM curves for magnetite, haematite and a mixed assemblage of magnetite and haematite.
2.9	31	Empirically derived normalised IRM curves for various grain sizes of magnetite and haematite.

Figure no	Page no.	
2.10	32	SIRM/ χ vs $(B_0)_{CR}$ diagram.
2.11	33	Diagram showing the principal features of a hysteresis loop.
2.12	34	Diagram of magnetic extraction equipment.
2.13	36	Curie balance data for two magnetite standards.
2.14	38	The relationship of particle size and χ .
2.15	39	IRM curves for splits from particle size analysis.
2.16	40	IRM curves for splits from shaking table.
3.1	43	The position of the Peach sea area.
3.2	44	Pinger data for the Peach area sea bed.
3.3	45	Position of sample stations in the Peach area.
3.4	47	Downcore palaeomagnetic data for core 56-10 32VE.
3.5	49	AF demagnetisation results for pilot samples from core 56-10 32VE.
3.6	51	Whole core susceptibility profiles for cores from the Peach area.
3.7	59	Whole core susceptibility profiles for cores 56-09 169VE, 56-10 42CS and 56-10 28VE.
3.8	60	Composite map of median whole core susceptibility values and sea bed sediment types for part of the Peach sea area.
3.9	62	Normalised IRM acquisition curves for subsamples from core 56-10 32VE.
3.10	64	Curie point analysis on a magnetic extract from core 56-10 32VE
3.11	67	Geological log of core 56-10 32VE.
4.1	70	The position of the Miller, Flett and Judd sea areas.
4.2	71	Sample station positions in the Flett area.

Figure no Page no.

4.3 a-c	75	Whole core susceptibility profiles for cores from the Flett area.
4.4a	79	Whole core susceptibility profiles for core 61-03 42CS taken from 1986-1988.
4.4b	80	Whole core susceptibility profiles for core 61-03 30CS taken from 1986-1987.
4.5	83	Mineral magnetic data for subsamples from core 61-03 42CS.
4.6	84	IRM acquisition curves for subsamples from core 61-03 42CS.
4.7	85	Curie point analysis for a magnetic extract from core 61-03 42CS.
4.8	87	Downcore palaeomagnetic data for subsamples from 61-03 42CS.
4.9	88	Alternating field demagnetisation results for pilot samples from core 61-03 42CS.
4.10 a,b	89	Geological logs of cores 61-03 41CS and 61-03 43CS.
4.11a	90	Geotechnical data for core 61-03 41CS.
4.11b	90	Geotechnical data for core 61-03 42CS.
5.1	97	The Central North Sea study area.
5.1b	98	Sample station positions in the Central North Sea.
5.2	99	The location of previous palaeomagnetic work in the North Sea.
5.3	100	Palaeomagnetic results for central North Sea from Stoker et al (1983).
5.4	102	Whole core susceptibility results for 22 cores from the Central North Sea.
5.5a	105	Whole core susceptibility profile for core 58-02 231VE.
5.5b	105	Lithological description of core 58-02 231VE.
5.6	107	Mineral magnetic results for subsamples from core 58-02 231VE.

Figure no	Page no.	
5.7	109	IRM curves for pilot samples from 58-02 231VE.
5.8	110	IRM curves for splits from shaking table on a subsample from core 58-02 231VE.
5.9	111	IRM curves for particle size splits from core 58-02 231VE.
5.10	113	Curie point analysis on magnetic extracts from core 58-02 231VE.
5.11	114	Downcore palaeomagnetic results for core 58-02 122VE.
5.12	115	Alternating field demagnetisation data for pilot samples from core 58-02 122VE.
6.1	120	Map showing density of sample stations and geophysical data lines in the Firth of Clyde.
6.2	121	Solid geology of coastal areas adjoining the Firth of Clyde.
6.3	122	Distribution of sediments in the Firth of Clyde based on Folk classification.
6.4	123	Areas of manganese mineralization in the Firth of Clyde.
6.5	127	Magnetic susceptibility distribution in the mud fraction of Firth of Clyde grab samples.
6.6	128	χ distribution in the sand fraction of grab samples from the Firth of Clyde.
6.7	129	The relationship of SIRM to χ in Firth of Clyde grab samples.
6.8	131	IRM acquisition curves illustrating the range of magnetic mineralogies encountered in the mud fraction of grab samples from the Firth of Clyde.
6.9	132	Back-field IRM curves for the sand fraction of grab samples from the Firth of Clyde.
6.10	134	Particle size vs. χ for Firth of Clyde sediments.
6.11	135	Distribution of clastic material in the grain-size spectrum of sediments.

Figure no	Page no.	
6.12	137	Coring sites in the Firth of Clyde from the <i>M.V. John Murray</i> .
6.13	138	Whole core susceptibility data for John Murray cores 1B and 11A from the Firth of Clyde.
6.14	139	Composition of gravel samples from the Clyde.
7.1	142	BGS geophysical survey lines and geological sample station coverage in the Moray Firth.
7.2	144	A geological sketch map of the geology of coastal areas adjoining the Moray Firth.
7.3	145	Particle size distribution of surface sediments in the Moray Firth.
7.4	146	The bathymetry of the Moray Firth.
7.5	148	Particle size vs χ for two samples from the Moray Firth.
7.6	149	Acquisition IRM curves for the sand fraction of samples from the Moray Firth.
7.7	150	Coercivity vs SIRM/ χ ratio for pilot samples from the Moray Firth.
7.8	152	Diagram of principal transport paths and sediment sinks in the Moray Firth area.
8.1	155	Map showing core sites around Spitsbergen used in this study.
8.2	156	Location map of coring sites in the Kara Sea, Norwegian Sea and Barents Shelf.
8.3	157	Geological sketch map of Spitsbergen.
8.4	159	Inclination and declination data for short cores from the Barents Shelf.
8.5	160	Inclination data for long cores from the Barents Shelf.
8.6	161	Correlation of palaeomagnetic records between cores from the Norwegian Sea and Barents Shelf.
8.7	162	Examples of mineral magnetic analysis of Norwegian sea cores.

Figure no	Page no.	
8.8	165	Palaeomagnetic results for Spitsbergen , site 3.
8.9	166	Palaeomagnetic results for Spitsbergen, site 4.
8.10	167	Palaeomagnetic results for Spitsbergen, site 5.
8.11	168	Palaeomagnetic results for Spitsbergen, site 8.
8.12	171	Mineral magnetic results for Spitsbergen, site 3.
8.13	172	Mineral magnetic results for Spitsbergen, site 4.
8.14	173	Mineral magnetic results for Spitsbergen, site 5.
8.15	174	Mineral magnetic results for Spitsbergen, site 8.
8.16	175	Biplot of HIRM against χ for samples from Spitsbergen sites 3,4,5 and 8. Core 5a and 5b represent the top section and base section of the core from site 5.
8.17	177	Histogram of palaeomagnetic inclination data for Icelandic lava flows.
8.18	177	Histogram of palaeomagnetic inclination data for Aleutian Island lava flows.
8.19	177	Histogram of palaeomagnetic inclinations from site 8 of this study.
9.1a	186	Iron content vs susceptibility for 17 continental shelf core samples.
9.1b	186	Susceptibility vs carbonate content for 17 continental shelf samples.
9.2	187	The relationship between nickel content and (a) iron content, (b) volume susceptibility.
9.3	188	The relationship between phosphate content and (a) iron content, (b) volume susceptibility for 17 continental shelf core samples.
9.4	189	The relationship between zinc content and (a) iron content, (b) volume susceptibility for 17 continental shelf core samples.

Figure no Page no.

9.5	190	The relationship between magnesium oxide content and (a) iron content, (b) volume susceptibility for 17 continental shelf core samples.
9.6	191	The relationship between aluminium oxide content and (a) iron content, (b) volume susceptibility for 17 continental shelf core samples.
9.7	192	The relationship between manganese oxide content and (a) iron content, (b) volume susceptibility for 17 continental shelf core samples.
9.8	193	The relationship between copper oxide content and (a) iron content, (b) volume susceptibility for 17 continental shelf core samples.
9.9	194	The relationship between sulphate content and volume susceptibility for 17 continental shelf core samples.
9.10	195	A plot of Fe/Mn ratio against SIRM/χ ratio for 17 samples from the UK continental shelf.
10.1	201	A plot of SIRM/χ ratio against coercivity with grid of mineralogies.

TABLE OF CONTENTS

1 Introduction	1
1.1 Preamble	1
1.2 UK Continental shelf survey	1
1.3 Geomagnetic Field	2
1.4 Palaeomagnetism	3
1.5 Mineral Magnetism	5
2 Techniques and Instrumentation	13
2.1 BGS/IGS Sampling Techniques	13
2.2 Subsampling for magnetic analysis	13
2.3 Palaeomagnetic and Mineral magnetic techniques and terminology.	14
1 Magnetic Susceptibility Measurements	19
2 NRM measurement	20
3 Alternating Field Demagnetisation	25
4 IRM acquisition	25
5 IRM measurement	26
6 IRM interpretation	26
2.4 Magnetic Mineral Extraction Equipment	29
2.5 Curie temperature analysis	35
2.6 Geological Techniques	37
1 Particle size work	37
2 Heavy Liquid Separation	37
3 Shaking Table	41
4 XRF 41	
3 Peach area	42
3.1 Background	42
3.2 Ship board sampling and magnetic measurement procedures	42
3.3 Laboratory sampling and magnetic measurement procedures	46
3.4 Results	46
1 Palaeomagnetic Results	46
2 Mineral magnetic data	48
3 Geological core logs	61
3.5 Discussion	61
1 Palaeomagnetic Parameters	61
2 Mineral Magnetic Parameters	63
3 Deck Operations	66
3.6 Significant Points	68
4 Flett Area	69
4.1 Background	69
4.2 Sampling and Measurement Procedures	72
1 Shipboard Procedures	72
2 Shore based procedures and measurements	73
4.3 Results	74
1 Whole core susceptibility results	74
2 Repeat whole core susceptibility results	78
3 Repeat subsample measurements.	78
4 Mineral Magnetic Data from subsamples	78
5 IRM acquisition curves	81
6 Thermomagnetic Analysis	81
7 Palaeomagnetic results	86
8 Geological Data	86
4.4 Discussion	91
1 Whole core susceptibility	91
2 Repeat Measurements	92
3 Palaeomagnetic data	93
4 Mineral Magnetic Results	93
4.5 Significant Points	95
5 Central North Sea	96

5.1 Introduction	96
5.2 Core Selection and Magnetic Measurement Procedures	96
5.3 Results	101
1 Whole Core Susceptibility	101
2 Mineral Magnetic Data - Core 58-02 231VE	106
3 Shaking Table and Particle Size Results	108
4 Thermomagnetic Results	112
5 Palaeomagnetic Results	112
5.4 Discussion	116
1 Whole Core Susceptibility	116
2 Mineral magnetic Data	116
3 Extraction	116
4 Palaeomagnetic Results	117
5.5 Significant Points	118
6 Firth of Clyde	119
6.1 Background	119
1 Sample Distribution	124
2 Onshore Geology	124
3 Surface Deposits	124
4 Manganese Distribution	125
6.2 Measurements	125
6.3 Results	126
1 Susceptibility Results	126
2 SIRM/ χ Results	130
3 IRM Results	130
4 Particle Size Results	130
6.4 Discussion	130
6.5 Significant Points	140
7 The Moray Firth	141
7.1 Introduction	141
7.2 Geological Background	143
7.3 Sample Selection and Measurement Procedures	143
7.4 Results	147
1 Susceptibility Data	147
2 IRM analysis	147
3 SIRM/ χ and coercivity results	147
7.5 Discussion	151
7.6 Significant Points	153
8 Spitsbergen	154
8.1 Background	154
1 The Geology of Spitsbergen	154
2 Previous palaeomagnetic work in the Spitsbergen area	158
8.2 Sampling	158
8.3 Measurement	158
8.4 Results	163
1 Palaeomagnetic Results	163
2 Mineral Magnetic Results	164
8.5 Discussion	170
1 Palaeomagnetic Results	170
2 Mineral Magnetic Results	176
8.6 Significant Points	180
9 Chemical Analysis	181
9.1 Introduction	181
9.2 Subsampling and Measurement Techniques	182
1 Sample selection	182
2 XRF measurement	182
3 Carbonate Content Measurement	182
9.3 Results	183
9.4 Discussion	196

Appendix A. - British Geological Survey marine exploration equipment descriptions. -
See folder at rear of volume.

CHAPTER 1

INTRODUCTION

1.1 Preamble

This thesis is largely concerned with assessing the potential for the practical application of palaeomagnetic and mineral magnetic techniques in the continental shelf environment. The practicality aspect refers both to the identification of appropriate magnetic instrumentation and to the likely limitations on interpretations of the magnetic results.

1.2 UK Continental shelf survey

The British Geological Survey (BGS), formerly known as The Institute of Geological Sciences (IGS) has been engaged in a survey of the UK continental shelf since 1967. Their work has been directed either towards specific small scale projects, for example surveys for offshore gravel resources (Deegan et al 1973), or towards the wider objective of preparing geological maps of the whole UK continental shelf. The majority of their survey work was completed by 1989.

As a result of over 20 years of survey activity, a large archive of geological and geophysical data has been gathered. For example there are over 200 000km of seismic lines, samples from 30 000 geological sampling stations and cores from over 500 boreholes. Much of this geological and geophysical material is in a raw form. It is currently being used in the preparation of new geological maps of the sea bed. The published material based on the continental shelf survey, is to be found in various formats. These are specific project reports (Deegan et al 1973), internal reports (Long, (1979)), papers in journals (Stoker et al 1983) and various scale geological maps (eg Evans 1985). Access to much unpublished data and to partially complete interpretations was made possible by kind permission of the BGS.

Much of the original sample material on which the BGS work had been based has been retained in storage. A strictly enforced archiving system has

resulted in a near complete retention of material from all BGS sampling sites. The resulting sample stock consists of sea floor grab samples, vibrocores, gravity cores and borehole sections. The grab samples and vibro and gravity cores provided the basic raw material for this thesis.

During 1985 and 1986 BGS were still operating sampling vessels and I participated in cruises onboard the vessel *M.V. British Magnus*, in November 1985 and the vessel *M.V. Kommander Subsea* in October 1986. These two cruises gave opportunities to obtain fresh sample material and to employ magnetic susceptibility core logging techniques in a sea going laboratory. This maritime experience also proved invaluable in terms of assessing the effects of BGS handling techniques on core quality, with particular reference to its possible influence on magnetic properties.

1.3 Geomagnetic Field

The behaviour of the Earth's geomagnetic field has been the subject of detailed study and observation for several hundred years, with work dating back to the 15th century when William Gilberte (*De Magneta* 1600) noted the resemblance of the geomagnetic field to that of a uniformly magnetised sphere. Gauss (1839) first established the source of the magnetic field as being within the Earth by using spherical harmonic models. These models have been expanded to the present preferred representation of dipole and non-dipole parts adding to make the total geomagnetic field. The best fitting dipole for the present field is tilted at about 11.5° to the rotational axis. Non-dipole components consisting of a number of continental size foci of maxima and minima distributed over the globe represent the rest of the field.

Historical records of magnetic directions date back to 1570 (Barraclough 1982) with intensity data becoming available for many locations from 1850 onwards (Tarling, 1983). Extensive cataloging of past records has been carried out by several workers, the most comprehensive catalogue being that of Veinberg and Shibaev (1969). Such data sets have been used in attempts to model the geomagnetic field and associated behaviour of the earth's core (Gubbins 1982).

Cook (1973) summarises the behaviour of the geomagnetic field as seen in observatory records as follows:-

- a) A growth of some non-dipole features and decline of others.
- b) An average westward drift of features of the non-dipole field by 0.2° per year.
- c) A westward rotation of the dipole by 0.05° longitude per year.
- d) A decrease in the main dipole moment of about 0.05% per year.
- e) A decrease in the angle of tilt of the geocentric dipole of about 0.02° per year.

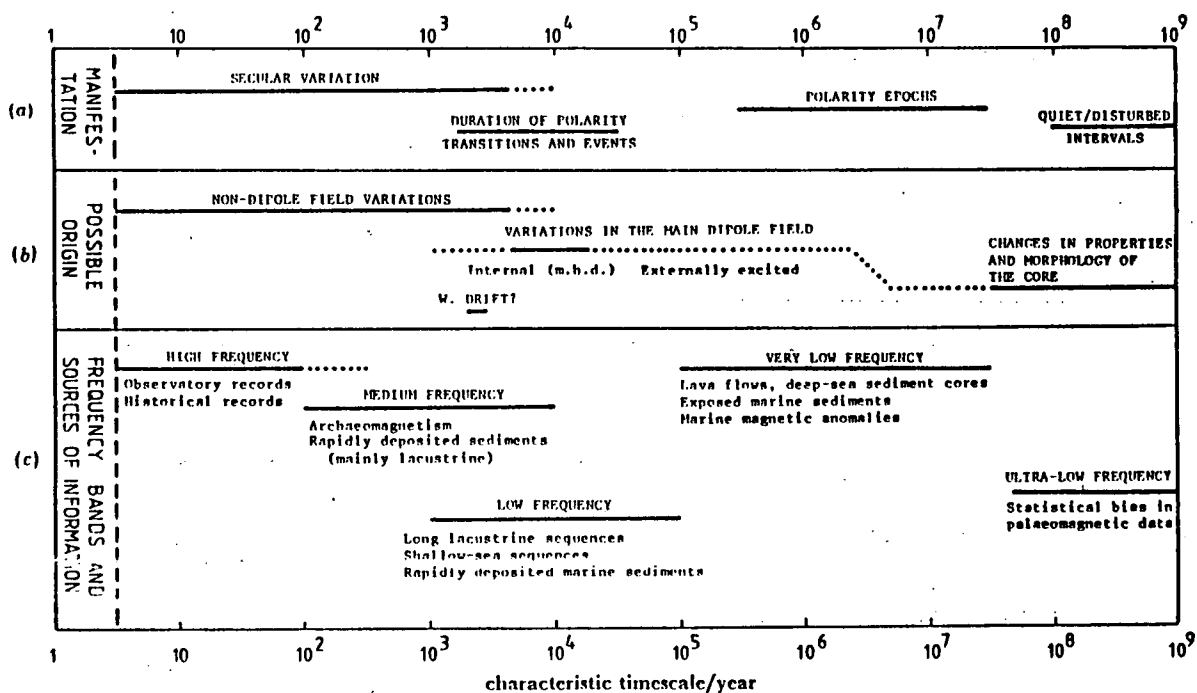
1.4 Palaeomagnetism

The geomagnetic field is unique amongst geophysical processes in that we do not need to rely solely on contemporary observations of its behaviour. It leaves a detailed record of its activities behind, locked into for example, rocks, sediments, and pottery. The study of these records, termed palaeomagnetism is a well established subject very effectively reviewed in works such as Tarling (1983) and Collinson (1983).

Palaeomagnetic studies have given an insight into the past behaviour of the geomagnetic field. Fig 1.1 from Barton, (1982) illustrates the major features and the associated evidence of geomagnetic variation. Time scales of geomagnetic activity range from high frequency (fraction of a second) pulses to long period (100 000 year) reversals. Variation occurs in both intensity, and direction of the field with frequent complete reversals being a dominant long term feature.

In relation to sedimentary studies, the most significant features are (a) *secular variation* which occurs on a time scale from one year to thousands of years and involves small shifts (up to 30°) in field direction; (b) *polarity excursions*, defined by Thompson (1977) as a sequence of virtual geomagnetic poles which extend beyond 45 degrees of latitude from the pole and return to the original latitude after a short period of time; (c) *polarity reversals*, complete 180 degree shifts in direction on a time scale of $10^5 - 10^6$ years.

Of most relevance to this thesis is the record of secular variation as found in high deposition rate ($>1\text{mm pa.}$) sediments (eg lakes, marine margins). The pioneering work of Mackereth (1971) demonstrated that lake sedimentary



- Fig 1.1 Principal frequency bands of the geomagnetic spectrum of internal origin, showing (a) how the variations are manifested, (b) hypothesized origins, (c) frequency band classification and sources of observed data (Barton 1982).

sequences from Lake Windermere held a high quality record of secular variation. Following this original work on Lake Windermere, secular variation data has been obtained from Europe, Near East, New Zealand, Australia, Japan and the Americas (Creer 1985) eg Fig. 1.2. There is sufficient data in many areas to construct type or master-curves based on collated data from any one region. High resolution data is also available in high-deposition rate sediments (>1mm pa) from marine environments (eg Bishop 1975 Fig 1.3, Austin, 1987).

Palaeomagnetic techniques are applied as a standard tool on Deep Sea Drilling Project (DSDP) vessels. When used on deep ocean cores they provide a record of long term variations of the geomagnetic field, usually in the form of a polarity reversal record, eg Shackleton et al, (1984), fig 1.4. Due to lower sedimentation rates in deep sea environments than lakes, the temporal resolution of deep sea cores is usually too limited for secular variation studies.

1.5 Mineral Magnetism

As a consequence of palaeomagnetic investigations on lake sediments, a parallel line of research evolved to study the magnetic mineralogy of sediments. Early work by Thompson et al (1977) demonstrated the use of magnetic susceptibility (χ) as a tool for correlation between lake sediment cores. The mineralogy based line of magnetic studies has expanded into the use of a large number of artificial remanence and magnetization derived parameters as reviewed by Thompson and Oldfield (1986) in their work 'Environmental Magnetism'.

The use of magnetic mineralogies has been extended away from lake sediments and been found to be effective in many other environments. It has been used for example, as a sediment tracer in fluvial situations (Walling et al 1979); as an indicator of soil formation environments (Maher 1986); in the identification of atmospheric particles (Hunt 1986); as a correlation tool and environmentally sensitive indicator in peats (Richardson 1986, Williams 1988), as a recorder of change of environment of deposition in deep sea sediments (Robinson 1986 fig 1.5, Bloemendal 1983); as a means of differentiating glacial diamicts (Walden et al 1987); and for understanding biological environments eg in the case of magnetotactic bacteria (Petersen et al 1986).

In addition to its environmental modelling role, susceptibility has been

demonstrated as an effective heavy mineral exploration tool. Puranen (1977), showed the use of susceptibility as a method for locating iron deposits in glacial tills. Currie and Bornhold (1983) used susceptibility as a heavy mineral reconnaissance technique on marine grab samples taken from the Canadian continental shelf. Fig 1.6 taken from their work emphasised the relationship between magnetite content and magnetic susceptibility . Susceptibility has also been successfully applied as a sedimentary mapping tool in ocean basins (Sachs and Ellwood 1988) Fig 1.7.

Much current attention is being directed at investigating the effect of hydrocarbon seepage on mineral magnetic properties. In particular the effect of hydrocarbons on authigenic magnetite formation in sea bed sediments (Elmore et al 1987, Barton 1988) is of commercial interest.

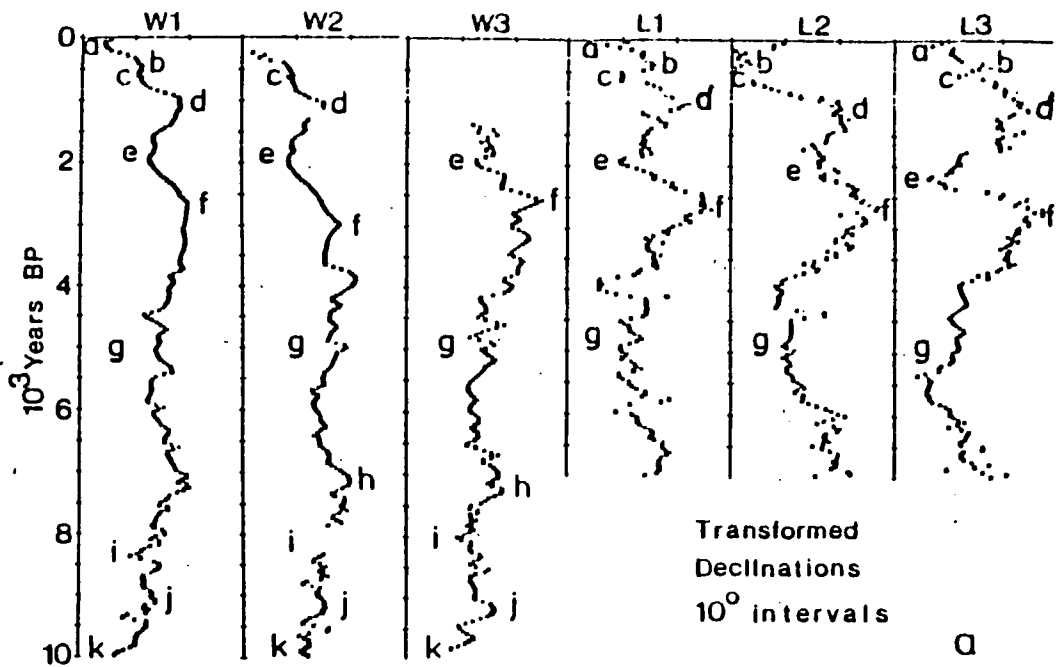


Fig. 1a. Transformed declinations plotted against preferred time for three Lake Windermere cores (W1-3) and three Loch Lomond cores (L1-3). Symbols refer to characteristic features which may be sharp (e.g. 'f') or drawn out (e.g. 'g').

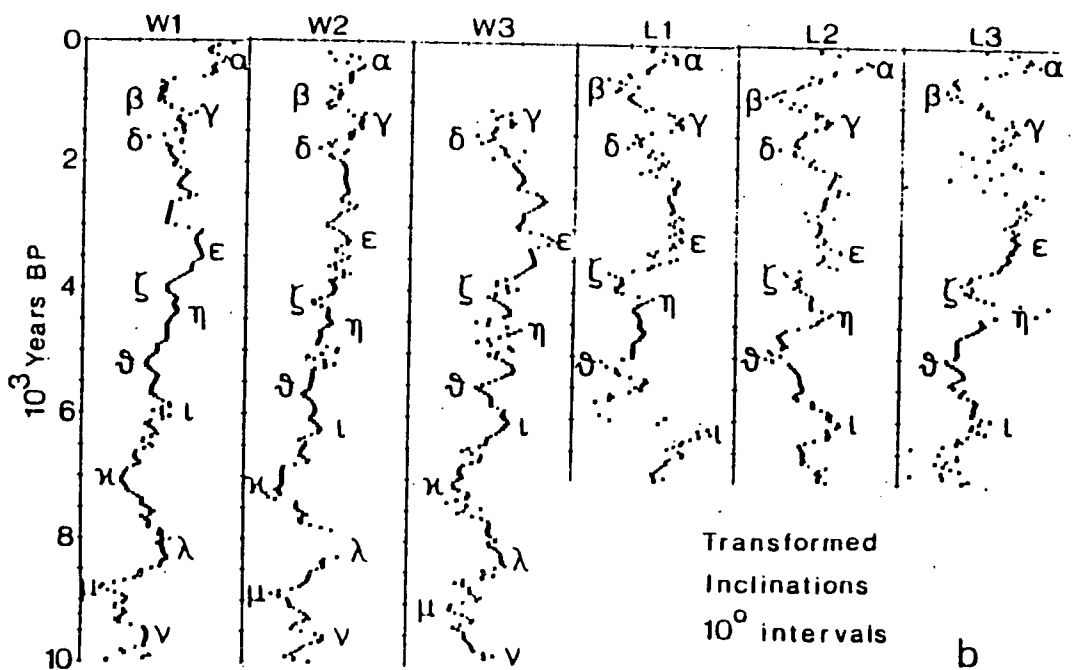
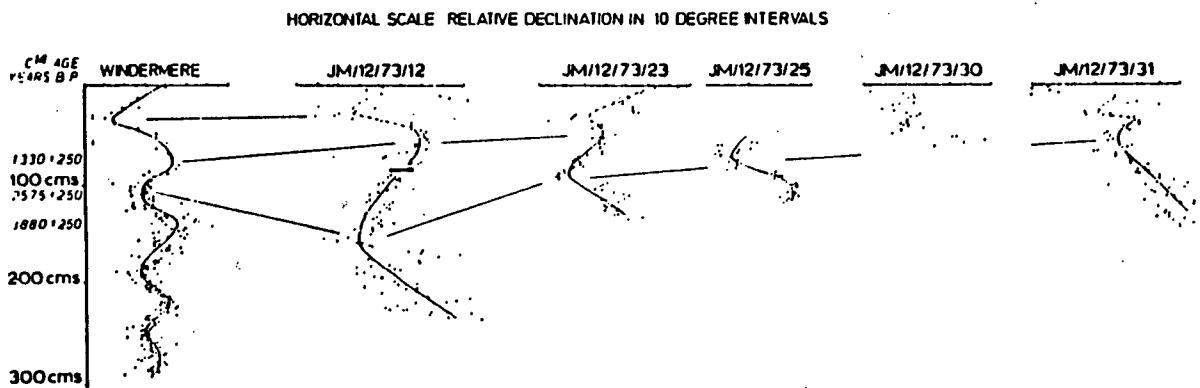


Fig. 1b. Transformed inclinations for the same six cores as Fig. 1a and the same time scale.

- Fig 1.2 Typical lake sediment secular variation records fitted to a time scale derived from radiocarbon and pollen dates. (Thompson and Turner, 1979).



- Fig 1.3 Declination values for five cores obtained from the Inner Sound of The Firth of Clyde compared to results from Lake Windermere, (Bishop 1975).

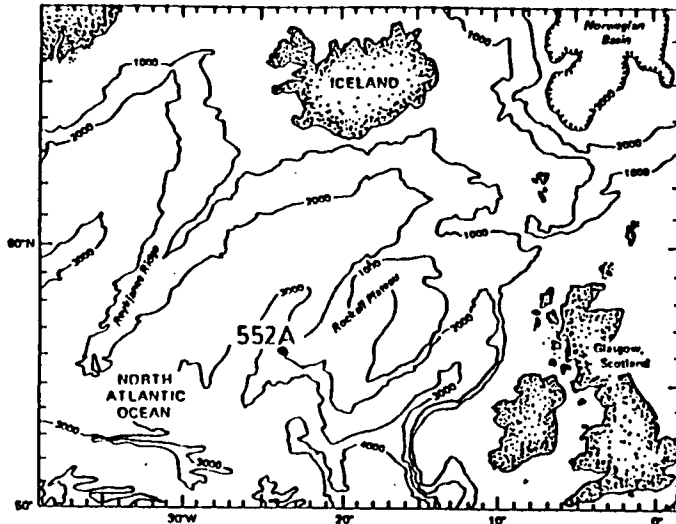


Fig. 1 Location map for Site 552A (56°02.56' N, 23°13.38' W, 2,311 m water depth).

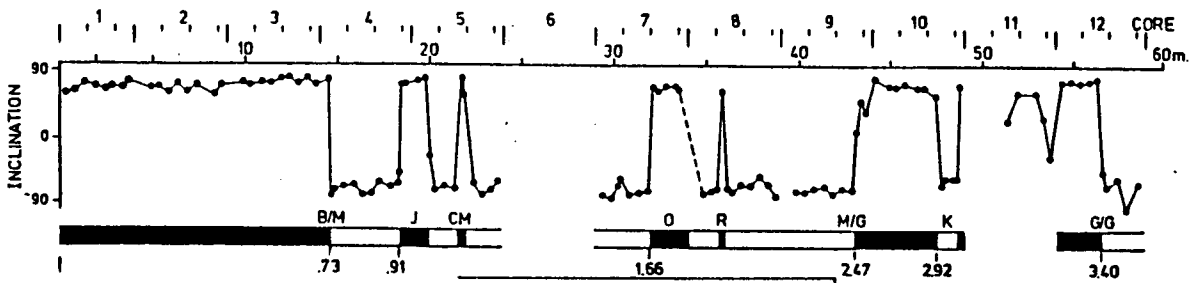
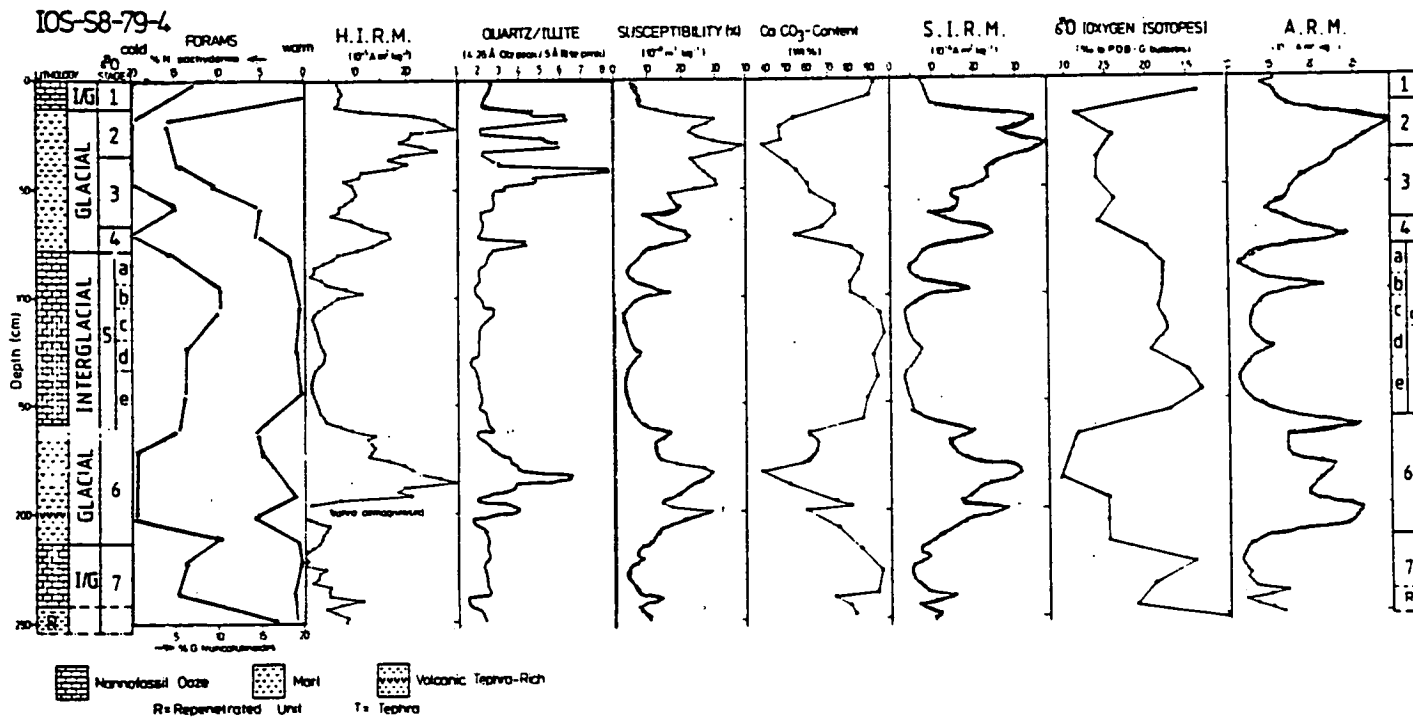


Fig. 2 Magnetic record for Site 552A. Demagnetized inclinations are shown only for apparently undisturbed parts of the cores (the data from core 11 suggest that some unrecognized disturbance may be present).

- Fig 1.4 Figure showing location of, and palaeomagnetic reversal stratigraphy obtained for DSDP site 552A, Shackleton et al, 1984.



- Fig 1.5 Comparison of the concentration dependent mineral-magnetic properties of IOS core S8-79-4 with its record of late Pleistocene palaeoclimate variations indicated by oxygen isotopes, quartz/illite ratios, CaCO₃ content and planktonic foraminifera. (Robinson 1986).

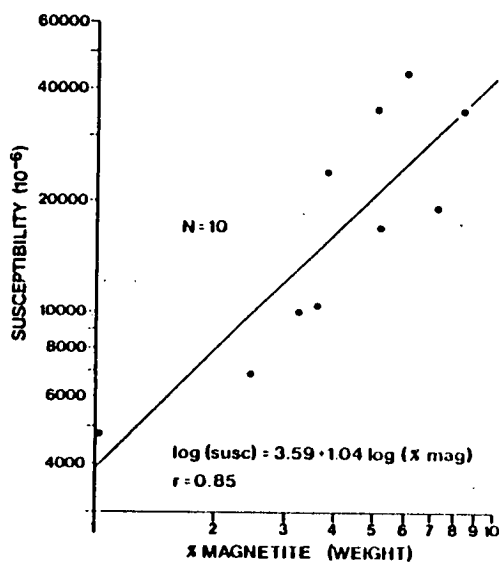
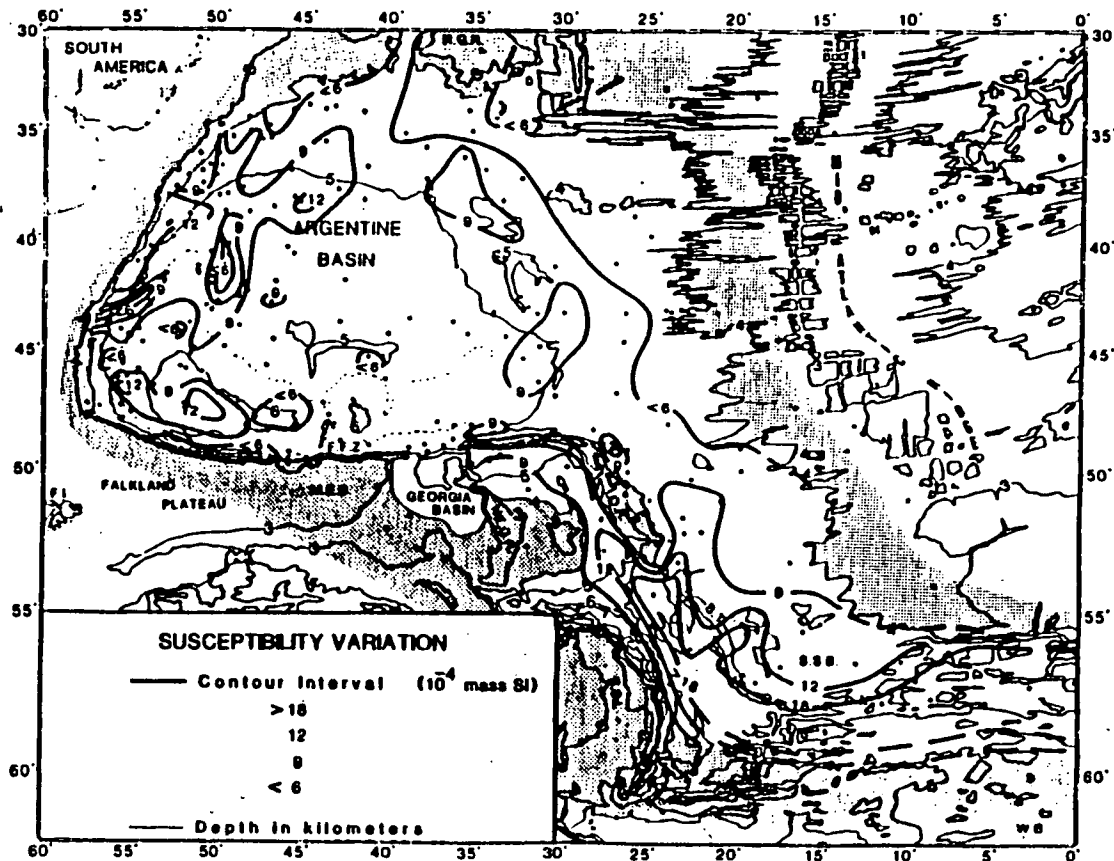


Fig.2. Magnetic susceptibility vs. magnetite content of 10 samples.

- Fig 1.6 The relationship of magnetic susceptibility and magnetite content in 10 grab samples from the Canadian continental shelf. (Currie and Bornhold (1983)).



- Fig 1.7 Contour map of susceptibility variation of core-top samples in the Argentine Basin and vicinity. Shaded areas are $< 4000\text{m}$ water depth. (Sachs and Ellwood 1988).

CHAPTER 2 TECHNIQUES AND INSTRUMENTATION

2.1 BGS/IGS Sampling Techniques

The BGS employs a range of modern geophysical and geological equipment, much of it developed 'in-house'. Details of this equipment are contained in BGS information sheets enclosed in Appendix A. During the course of my work I had access to raw and interpreted data from BGS, gathered by a variety of techniques. The majority of my magnetic analyses were undertaken on vibrocores, gravity cores and shipex grab material. 'Pinger' geophysical data was widely used as appropriate background information.

Both vibrocore and gravity cores were originally recovered in 6m long, 10cm diameter plastic liners. The core and liner were extruded from the steel barrel by a combination of a hydraulic ram and manual labour. An orientation line was then marked along the length of the 6m liner before it was cut into 1m sections. These 1m sections were then longitudinally split into two equal D-shaped halves to enable thorough examination. Halved, the cores were preserved in flexible lay-flat polythene tubing which was heat sealed at each end to prevent moisture loss.

2.2 Subsampling for magnetic analysis

Subsampling of cores was undertaken as soon as possible after core recovery for fresh cores. The time interval between recovery and sampling varied from 5 minutes to 48 hours. In the case of stored material, care was taken during subsampling to ensure a minimal amount of drying out.

To obtain a subsample, small plastic boxes (20x20x20mm) were inserted into the sediment. Each box had a small hole in its base to allow air to escape during the insertion process. All boxes were carefully aligned parallel with the core sides and adjacent to the previous sample in the sequence if a contiguous series of samples were being taken. Orientation relative to the core vertical was achieved by small arrows marked on the base of each box with appropriate sample numbering. Once removed, each subsample box was lidded, the air hole sealed with tape and stored in a refrigerator. The remainder of the

core was then resealed in 'lay-flat' tubing and returned to store.

In the case of grab samples and some dried core material, plastic cylinders were used instead of cubes. Sediment was packed into the cylinder by means of a simple mechanical press and plastic foam used to fill any void in order to prevent subsequent movement of the sample within the container.

2.3 Palaeomagnetic and Mineral magnetic techniques and terminology.

The following list provides a brief summary of the terminology used in this study in relation to palaeomagnetism and mineral magnetism. It is largely based on information and definitions found in Thompson and Oldfield (1986) and Tarling (1983), both of which provide a comprehensive review of the available literature.

'Magnetic Terms and Parameters'

- **Anhyseretic Remanent Magnetisation, 'ARM'**...see Remanence.
- **Anisotropy of Susceptibility**...is the variation of magnetic susceptibility depending upon the direction of measurement. Dominated by the shape of ferrimagnetic grains, and often indicative of a sedimentological fabric.
- **Antiferromagnetism**...magnetic behaviour resulting from crystals having lattices in which adjacent atoms have antiparallel spins. Symptoms are a low susceptibility and zero remanence.
- **Canted antiferromagnetism**...similar to antiferromagnetism, but with adjacent atoms which have 'not quite' antiparallel spins, resulting in the ability to retain a weak remanence, eg haematite.
- **Chemical Remanent Magnetisation, 'CRM'**....see remanence section.
- **Coercivity or coercive force**... $(B_0)_C$...is the 'reverse' field required to reduce the magnetisation to zero from saturation, which is assumed as the 'forward' direction. Also known as **coercivity of remanence**... $(B_0)_{CR}$...where a remanent magnetisation is involved.
- **Demagnetisation**....as its name suggests, removing magnetisation from a specimen by means of an alternating field for recent sediments.

- **Detrital Remanent Magnetisation.....'DRM'...see remanence section.**
- **Diamagnetism...occurs due to a change in orbital motion of electrons about the nucleus in an applied field. Symptoms are (an often masked) weak negative susceptibility, as exhibited by water, quartz, calcite.**
- **Ferrimagnetism....a phenomenon of some crystalline substances and spinel structured minerals (eg magnetite, maghaemite) resulting from 'exchange interactions' (these forces are due to unbalanced electron spins combined with an ionic spacing**
- **Ferromagnetism** A phenomenon of some crystalline substances due to unbalanced electron spins combined with an ionic spacing such that very large forces called exchange interactions, cause coupling and alignment of all the individual magnetic moments of millions of atoms to give highly magnetic domains. This results in large susceptibilities, remanence and hysteresis. eg metallic iron.
- **HIRM, - High field Isothermal Remanent Magnetisation.** This is the difference between isothermal remanence induced by fields of 1T and 0.1T (ie, $IRM_{1T} - IRM_{0.1T}$). In practice this gives the remanence due to imperfect antiferromagnets such as haematite and goethite, the ferrimagnets such as magnetite having effectively saturated by 0.1T.
- **Isothermal Remanent Magnetisation,....IRM....see Remanence**
- **Natural Remanent Magnetisation,....NRM....see Remanence**
- **Paramagnetism... a small (positive) susceptibility arising from the alignment of the magnetic moment of individual atoms of the substance in an applied field. Often seen in clays, pyroxenes, amphiboles and other substances with rare earth or transition series members.**
- **Q ratio** Ratio of NRM intensity to susceptibility. Interpreted by some as an indication of the strength of the geomagnetic field causing the NRM.
- **Remanence/remanent magnetisation....The magnetisation remaining when external fields are removed. There are several types of remanence commonly referred to:**
 1. Natural Remanent Magnetisation...'NRM'...summation of all components of remanence acquired by natural processes.
 2. Detrital Remanent Magnetisation...'DRM'...acquired by the physical rotation of magnetic particles during deposition as a sediment.
 3. Chemical Remanent Magnetisation...'CRM'...acquired as a magnetic mineral nucleates and grows in a magnetic field.

4. Isothermal Remanent Magnetisation... 'IRM'... grown by the application and subsequent removal of magnetic field... usually induced in laboratory conditions, but can occur naturally due to lightning strikes.
5. Anhyseretic Remanent Magnetisation... 'ARM'... acquired when a ferromagnetic particle is subjected simultaneously to alternating and direct magnetic fields... usually grown deliberately by smoothly reducing an AC field in the presence of a weak DC field, but they are often accidentally grown during demagnetisation at high fields (poorer quality demagnetisers often suffer from a spurious DC component at higher fields ie 40+ mT).
6. Viscous Remanent Magnetisation... 'VRM'... produced by a weak field applied over a long period of time. A VRM is often seen due to sample storage in non-zero field conditions, but the remanence is weak and is usually easily removed by 48 hours storage in zero field conditions for recent sediments although older material may require a 20 mT demagnetisation to clear this unwanted component.

- **S ratio.** The ratio of a 0.1T backfield IRM to a 1T forward IRM. Originally defined by Thompson and Stober (1979) and used for samples with unusual haematite to magnetite ratios. It is based on the fact that, in practice, most ferrimagnets will saturate below 0.1T. Any difference in high field remanence will be due to the imperfect antiferromagnets such as haematite and goethite (Thompson and Oldfield 1986).
- **SIRM, Saturation Isothermal Remanent Magnetisation.** In this study this is taken as the remanent magnetisation acquired after exposure of the sample to a 1T field. In practice, this was the largest field continuously available. Other studies may utilise a saturating field from 0.8T to 5T, depending on equipment availability. 0.8T and 1.0T are the most commonly used fields.
- **SIRM/ χ ratio.** The features and function of this ratio are best defined by reference to plots of SIRM to χ such as figs 2.1 and 2.2 (from Thompson and Oldfield 1986). In natural samples (eg fig 2.1), there is a correlation coefficient between SIRM and χ of 0.86 with an average SIRM/ χ ratio of 10 kAm⁻¹. Samples with unusually high haematite to magnetite ratios plot to the right of the main grouping, giving SIRM/ χ values of approximately 1000kAm⁻¹. Low SIRM but moderate χ samples plot to the left of the main group, the χ value being influenced by paramagnetic contributions. Fig 2.2 shows the use of SIRM/ χ to determine particle size in situations where magnetite effectively the sole contributor to the remanance.
- **Superparamagnetism...**The phenomenon of rapid decay of remanence in magnetic grains. For example very small grains (haematite < 0.03 μ m diameter and magnetite < 0.05 μ m diameter) which show a strong susceptibility when placed in a magnetic field, but have this alignment destroyed by thermal vibrations upon removal of the field.
- **Susceptibility...**two distinct parameters are often quoted:

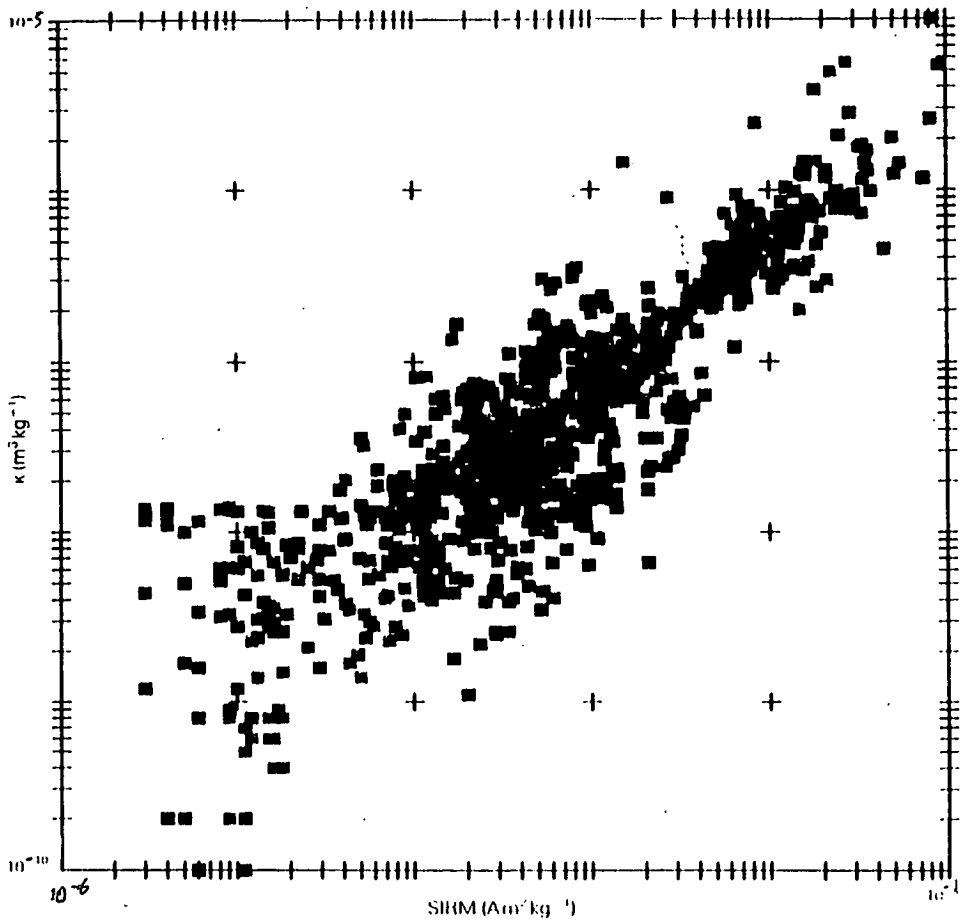
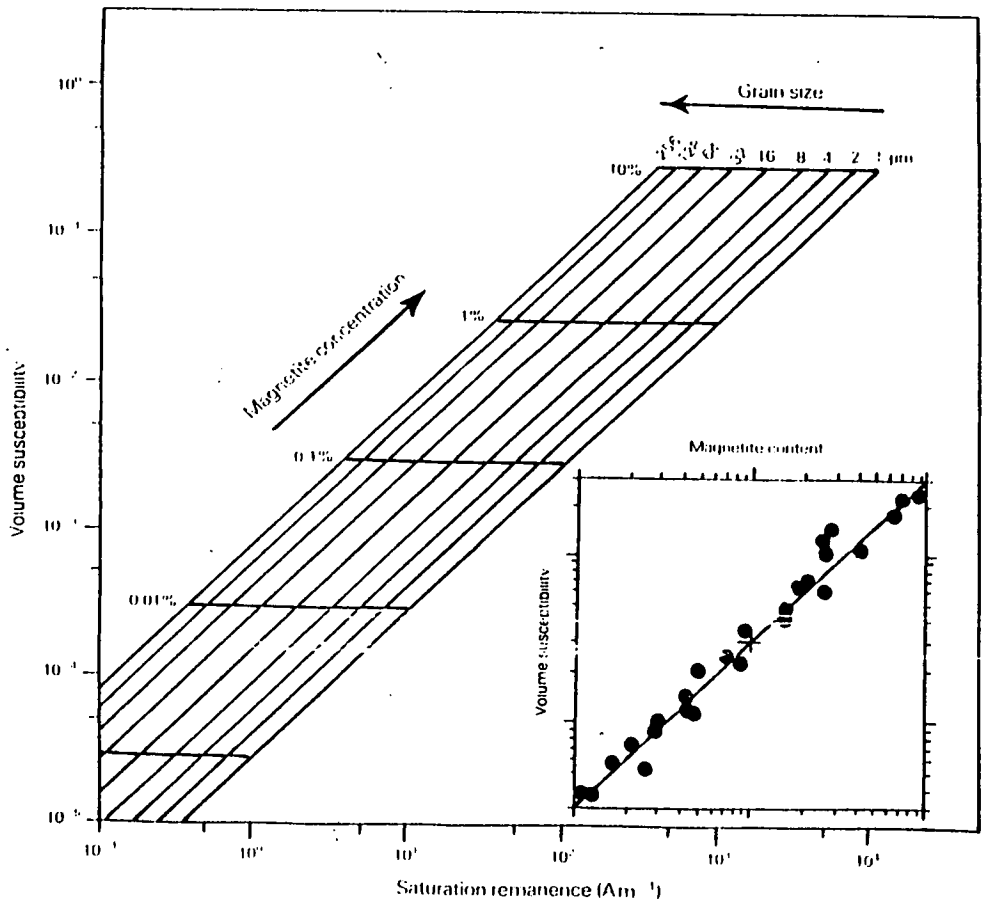


Fig 2.1 Log. SIRM ($\text{Am}^2\text{kg}^{-1}$) vs log. χ (m^3kg^{-1}) for 1000 natural samples. High magnetite concentrations plot towards the top right and low concentrations towards the bottom left corners of the diagram. Specimens lying below and to the right of the main group tend to have ^{high} haematite to magnetite ratios. Low SIRM, but moderate χ specimens, plotting to the far left have relatively high susceptibilities on account of paramagnetic contributions. Multidomain magnetites and assemblages with high concentrations of superparamagnetic magnetite plot on the upper side of the main group. (Thompson and Oldfield, 1986).



- Fig 2.2 Log. SIRM ($A m^{-1}$) vs log. K (dimensionless). The concentration/ grain size grid is for pure magnetite. Inset illustrates the linear relationship commonly observed, in sets of natural samples, between magnetite and susceptibility concentration. Taken from Thompson and Oldfield (1986). Based on data from Parry (1965) and Dankers (1978).

1. Susceptibility...' κ '...A measurement of the degree to which a substance can be magnetised... $\kappa = M/H$ where M is the magnetisation and H is the intensity of the applied field.
2. Specific Susceptibility...' χ '...magnetic susceptibility on a mass specific basis.....ie expressed in $\text{m}^3 \text{kg}^{-1}$.

- **Viscous Remanent Magnetisation...'**VRM'**...see 'remanence'.**

1 Magnetic Susceptibility Measurements

The two instruments used for magnetic susceptibility measurement in this study were:

(a) *Digico* susceptibility equipment. The standard sensor head on this instrument was not large enough to accommodate sample cubes supplied by BGS, so a larger version was constructed by the author (fig 2.3). Calibration was by means of chemical salt standards, fig. 2.4. Noise levels for this instrument were found to be low, at less than 1×10^{-6} S.I. units. The operating principle of this type of AC susceptibility bridge is described in Molyneux and Thompson (1973).

(b) *Bartington* susceptibility equipment. This equipment differs from the AC type bridge in that it interprets frequency change in a tuned oscillator circuit in terms of susceptibility as described by Lancaster (1966). In this study, several variations of Bartington equipment were used. An MS2C meter (interfaced to a BBC microcomputer by the author) coupled to an MS1B 25mm sensor head was employed for subsamples. An MS2C 125mm dual frequency loop sensor was used for whole core measurements. Noise levels were below 1×10^{-6} S.I. units. Calibration was by means of chemical salt standards (see fig 2.4). Separate standards were made for the different sensor heads and a cross-calibration between whole core and subsample measurements carried out (fig 2.5). However, as all core material obtained from BGS had the same diameter (100mm), an arbitrary volume susceptibility K scale consisting of readings taken directly from the Bartington equipment was adopted for whole core measurements. This arbitrary K scale proved effective for comparison between cores. Mass specific susceptibility, χ , measurements were obtained for subsamples and are reported in units of $10^{-6} \text{m}^3 \text{kg}^{-1}$ or $\mu\text{m}^3 \text{kg}^{-1}$.

The actual technique of susceptibility measurement for subsamples was very straightforward. Either the Bartington or Digico instruments would be calibrated and then the sample inserted for the measure cycle. If the sample was of known mass, a mass specific (χ) susceptibility could be easily calculated.

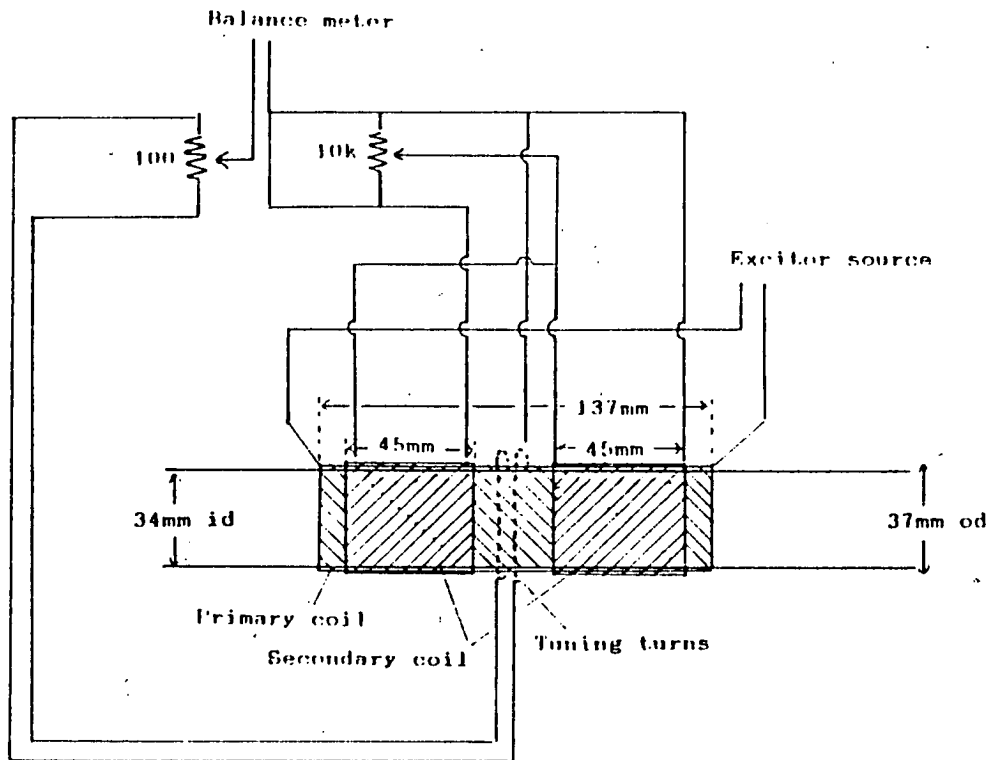
The wholecore susceptibility technique proved a rapid and effective way to investigate cores. Measurements were taken at 5cm intervals downcore with the instrument calibration being checked between each 1m section of core. Fig 2.6 shows how measurements based on 1m core sections were built up into a whole core susceptibility profile for an entire 5m core. The transitions between 1m sections were always found to be smooth. These smooth transitions demonstrate the constant, drift-free calibration achieved with the Bartington equipment. An experienced operator could measure whole core susceptibility on approximately 1m of core a minute.

2 NRM measurement

Two instruments were used for the measurement of NRM, a *Molspin* spinner magnetometer and a *CCL Cryogenic magnetometer*.

The Molspin is a portable fluxgate magnetometer based on well proven designs (Thompson and Oldfield 1986). The instrument was interfaced to a BBC micro-computer enabling semi-automatic operation and data logging. Calibration was by means of a magnetic tape standard with known intensity and direction of magnetisation. Noise levels were found to be in the order of $1 \times 10^{-6} \text{ Am}^2$. Each measurement of NRM required 6 different spin sequences in three mutually perpendicular axes in both upright and inverted positions. This instrument provided the bulk of the directional data in this project.

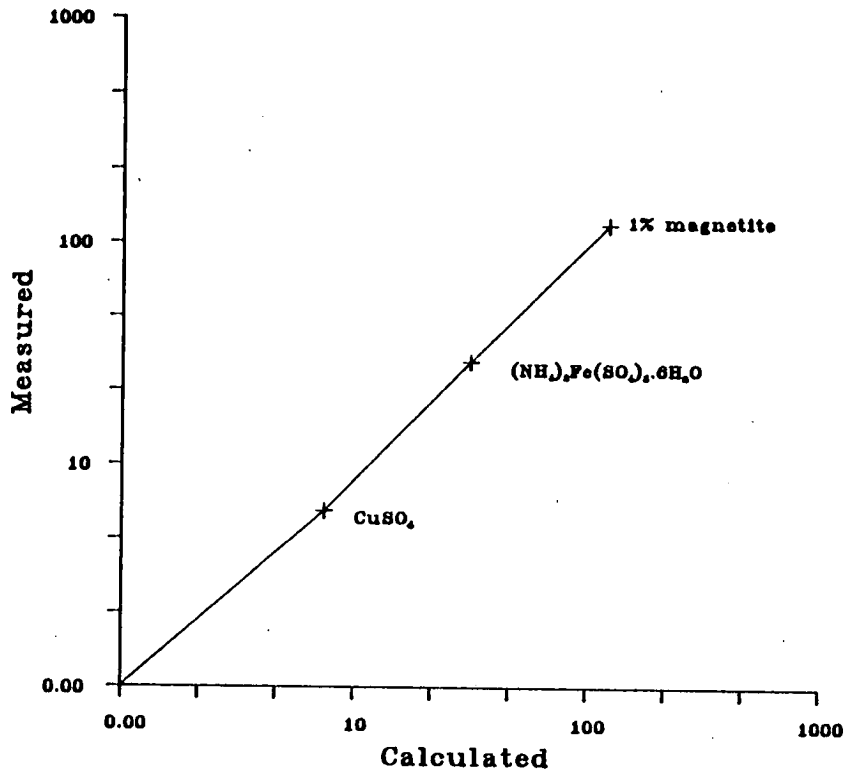
The cryogenic magnetometer is based on SQUID (super-conducting quantum interference device) technology. The basic principals are described by Goree and Fuller (1976), the main advantage over other magnetometers being speed and sensitivity (in the order of 10^3 times more sensitive than the Molspin). Control and data acquisition was semi-automatic via a Sirius micro-computer. The principal disadvantages were reliability and availability due to the high cost of helium consumption. Calibration was again by means of magnetic tape standard of known intensity and orientation.



All coils 24 turns per 10mm

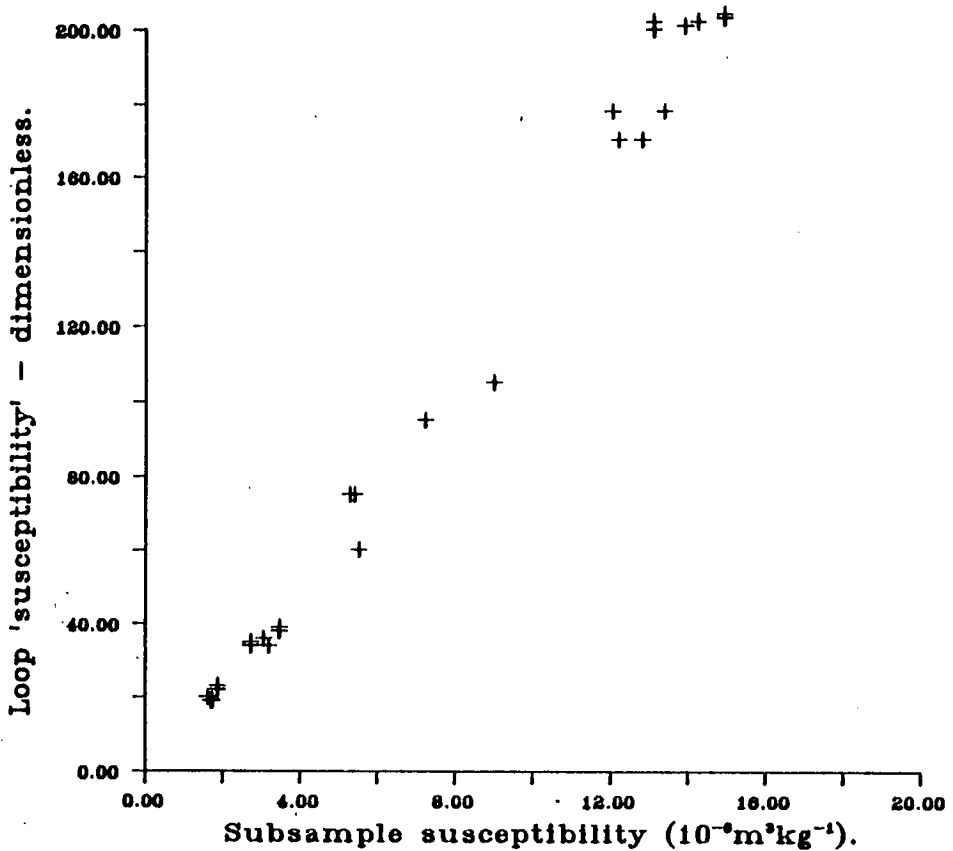
- Fig 2.3 Diagram showing principal coil design features and local tuning circuits for a 'Digico' susceptibility bridge. This unit was constructed to take samples up to 34 mm diameter and accommodate standard BGS palaeomagnetic subsamples.

**Chemical Calibration
of Susceptibility**
Units: $10^{-8} \text{m}^3 \text{kg}^{-1}$

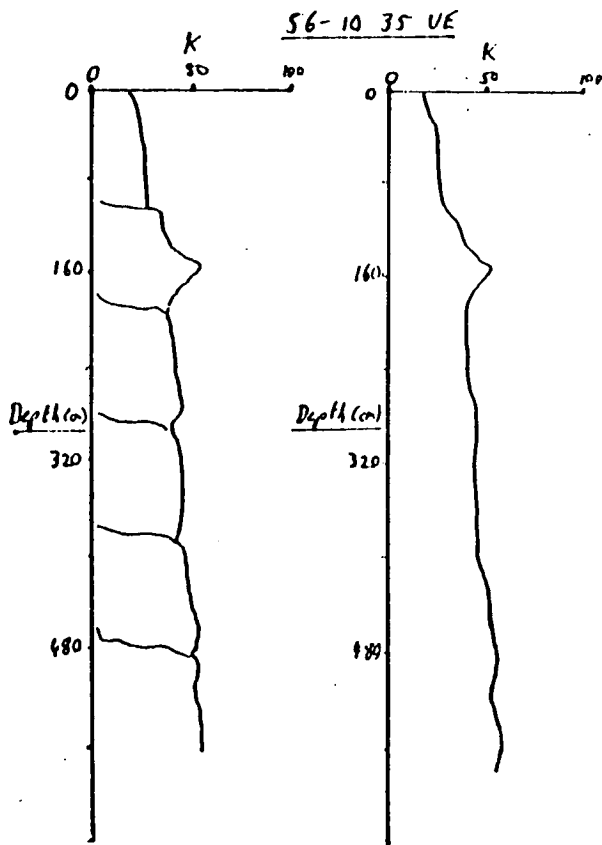


- Fig 2.4 Chemical calibration of Bartington susceptibility equipment against chemical standards. The expected susceptibility was calculated from reference tables (Tennent 1971). Three materials were used to provide a comprehensive range of susceptibility values.

Bartington Loop/Subsample cross-calibration



- Fig 2.5 Cross-calibration of values obtained from Bartington susceptibility equipment. The loop sensor provided a dimensionless value, whereas mass-specific data could be obtained for subsamples. Core values were obtained using measurements from positions which exhibited little variation in K over 25 cm each side of the sensor. Subsamples were then taken from these areas and a mass-specific χ value obtained.



- Fig 2.6 Data obtained using Bartington loop on core 56-10 35VE. The left hand profile shows the effect of the ends of 1m sections. The right hand profile shows end effects removed and data concatted. The simple technique of ignoring data obtained from within 5 cm of the section boundary and substituting the previous value was employed.

It should be noted that declination data in this study is relative to the individual core in question, no absolute determination being available due to lack of orientation control during coring.

3 Alternating Field Demagnetisation

Two different instruments were used during this project. The majority of work was undertaken using a motorised variac type unit constructed by Dr L. Molyneux. This gave a peak field of 99.5 mT adjustable in a range 0.00 to 99.5 mT using 0.5 mT steps. The second instrument was manufactured by Highmoor instruments and gave a peak field of 80 mT adjustable in steps of 0.1 mT. The operating principles of AF demagnetisers are well covered by As (1967).

Both instruments were used in the manner outlined by Snape (1971), which was designed to reduce the effect of spurious ARMs. However, in some circumstances, a spurious ARM was still generated with our equipment at peak alternating fields of over 40 mT. In practice however, the spurious ARM at high fields did not represent too significant a problem, as in the unconsolidated sediments being studied, any secondary remanence components were revealed by 40 mT.

In this study, AF demagnetisation was carried out on pilot samples from each core to assess the influence of secondary magnetisations. Typical increasing peak field steps were 5mT, 10mT, 20mT, 40mT, and 80mT.

Before AF demagnetisation, samples were stored in a zero magnetic field environment for at least 48 hours, in order to eliminate any viscous components.

4 IRM acquisition

The external fields necessary for producing IRMs were generated either by high powered electromagnet or pulse-magnetiser. An electromagnet was used to provide magnetic fields up to 1T. Higher fields were generated using a 'Trilec' pulse magnetiser fitted with a 37mm diameter coil (sample aperture 31mm diameter). The Trilec system gave fields in the range of 0.1T to 4.7T. However, 2.5T was the maximum continuously repeatable field obtainable. A comparison of SIRM acquisition as produced by a pulse-magnetiser and an

electromagnet using identical subsamples is shown in fig 2.7. As can be seen from fig 2.7 the IRMs grown by the pulse magnetiser and the electromagnet were very similar. Consequently, it was possible to combine the results from the two instruments to build up an IRM acquisition curve from 0T to 4T without reduction in the quality of data at the change-over field between instruments. In practice, a 1T field was found to saturate most of the material studied in this thesis with higher fields only being used when a large high-coercivity component of remanence was present.

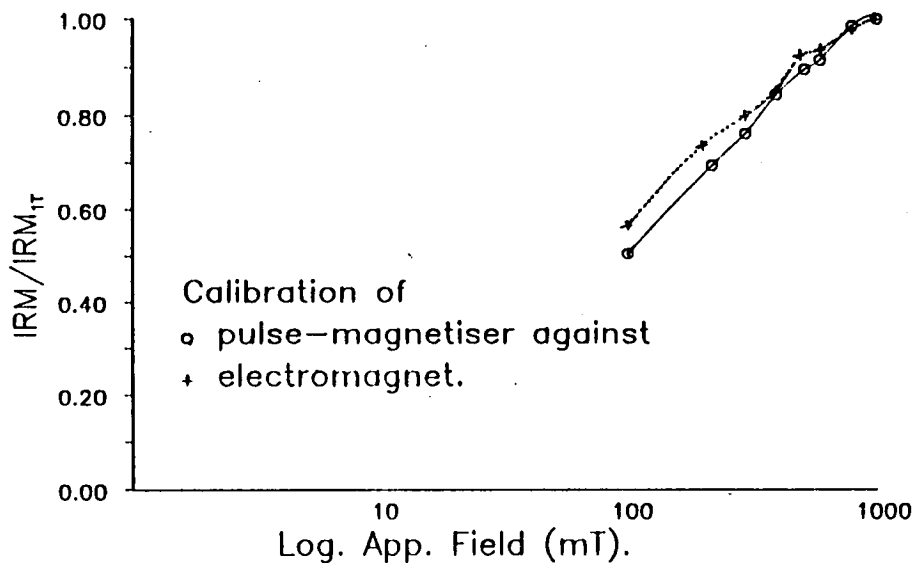
During the course of this study, the IRM acquisition technique was applied in three ways. For pilot studies, full forward IRM curves were grown using applied fields of 5, 10, 20, 40, 100, 200, 400, 800 and 1000mT. In contrast if a large number of samples had to be examined then only three fields of 100, 1000, and -100mT were used in order to give enough information to derive S and HIRM parameters. Finally if it proved necessary to obtain further IRM data, backfield IRMs were grown in the same field increments as for forward IRMs but with the incremental field applied in the opposite direction to the saturating field.

5 IRM measurement

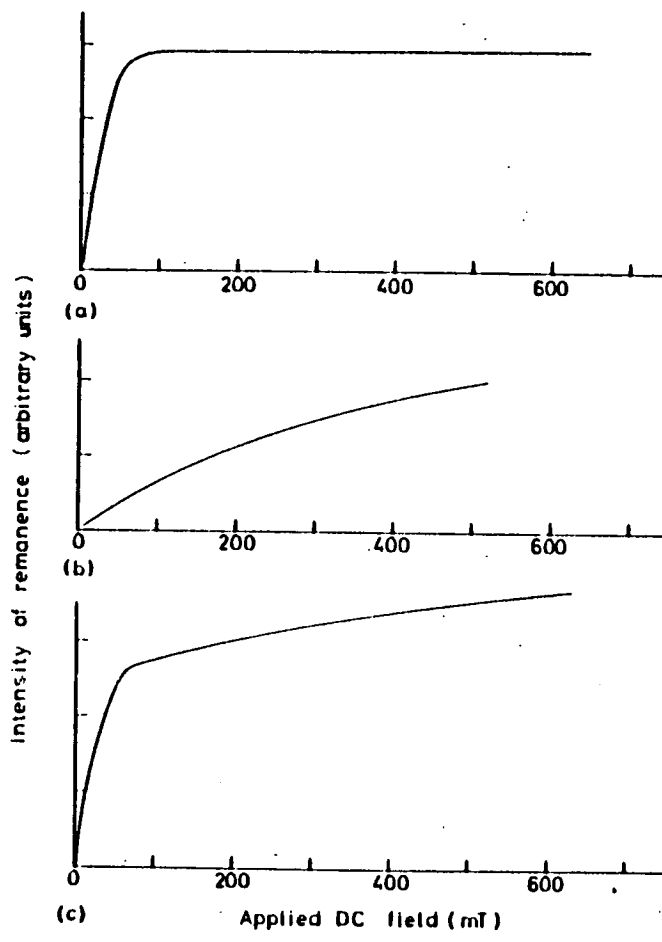
IRM measurement was carried out using the Molspin fluxgate magnetometer. Following exposure to each field, samples were measured in one orientation in the Molspin. Data from the Molspin could then be used in several ways. For plotting IRM acquisition curves, all data was normalised with respect to the saturation value, generally taken as 1T. When using the data from the Molspin to calculate SIRM or HIRM, the instrument reading (sample moment) was divided by the mass of the sample to give mass specific results reported in $\text{mAm}^2\text{kg}^{-1}$.

6 IRM interpretation

Several examples of IRM acquisition work are shown in figs 3.9 and 4.6. Fig 2.8 taken from Tarling, (1983) shows the forward IRM acquisition curves for three different samples. Each sample differs in composition, sample (a) showing characteristic IRM growth for magnetite with saturation occurring well before 100 mT; sample (b) showing the IRM curve for haematite with saturation not being reached even at 500 mT and sample (c) for a magnetite haematite mixture. The three examples from Tarling are for simple mineralogies.



- Fig 2.7 A cross-calibration performed between a Newport Instruments electromagnet and a Trilec CDM 1600 pulse-magnetiser. Direct comparison was possible between 100 and 1000mT where the instrument ranges overlapped. To effect a comparison, a homogeneous sample of high coercivity was split into two smaller samples. Both were then exposed to magnetic fields, one by the magnets, the other by the pulse-magnetiser. Intensity of IRM was then compared using a Molspin spinner magnetometer.



- Fig 2.8 Forward IRM curves illustrating the different responses of (a) magnetite, (b) haematite, (c) a mixed assemblage of magnetite and haematite to an externally applied field. Taken from Tarling (1983).

The magnetic properties of magnetite and haematite however also depend on grain size. Fig 2.9 shows the IRM acquisition curves based on empirically derived data for a range of magnetite and haematite grain sizes. Both haematite and magnetite display decreasing coercivity with increasing grain size. Better estimates of the concentration of magnetite and haematite in samples can therefore be made if the magnetic grain sizes can be established.

When SIRM data is used in conjunction with χ , the resulting SIRM/ χ ratio provides a means of numerically assessing the dominant mineralogy in any sample. Magnetite and haematite are easily distinguishable by SIRM/ χ ratios by virtue of their differing ferrimagnetic and antiferromagnetic properties. Typical values of SIRM/ χ for varying grain sizes of magnetite and haematite are given in fig 2.9. In the case of magnetite dominated mineralogies, SIRM/ χ can be used as a grain size discriminator. Austin (1987) preferred to use the inverse ratio χ /SIRM, named 'G' ratio for the same purpose.

Magnetite and haematite are the two most commonly encountered magnetic minerals. However, other less common minerals are sometimes found, usually contributing a minor, but nevertheless significant part of the magnetic properties. Table 2.1 lists some of these additional magnetic minerals and their magnetic characteristics.

By using several magnetic parameters in biplot form, grids representing expected magnetic mineralogies can be established. Fig. 2.10 shows such a grid constructed using coercivity and SIRM/ χ ratio data for samples. The choice of parameters depends on selecting data which will give the greatest differentiation between samples for a particular sample set.

Fig 2.11 shows a hysteresis loop and illustrates the origin of some of the magnetic terminology used in this thesis.

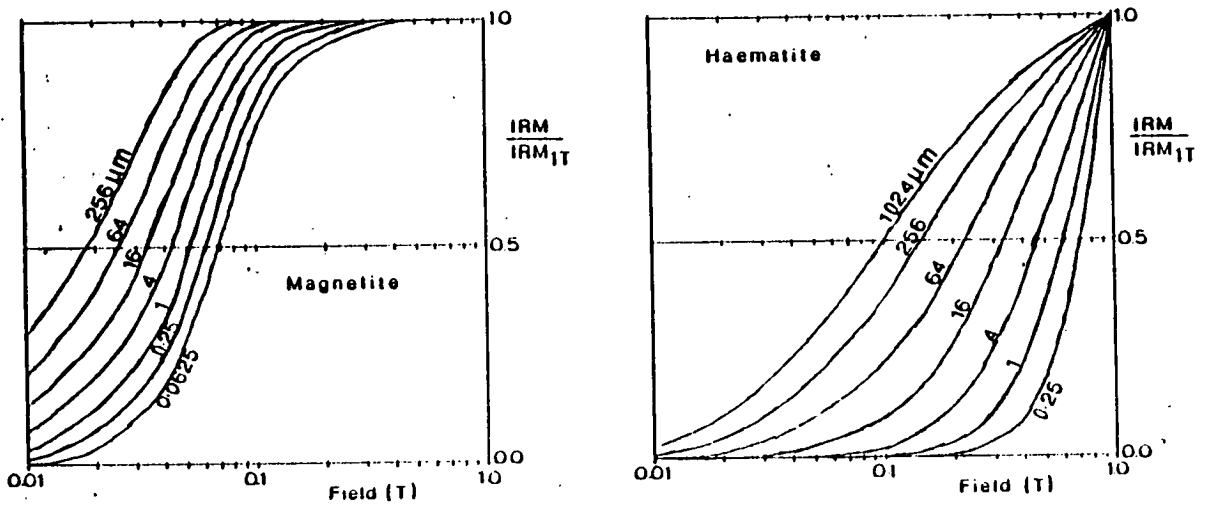
2.4 Magnetic Mineral Extraction Equipment

In order to carry out XRD and Curie point analysis on samples, it was necessary to extract a sample of the magnetic minerals contained in the sediment. Various methods were attempted based on equipment (fig 2.12) described by Von Dobeneck¹ (1985; pers. comm.). The Von Dobeneck system consisted of a soft iron needle covered with a fine plastic sheath. This needle

1. based on previous work by Papamarinopoulos (1978).

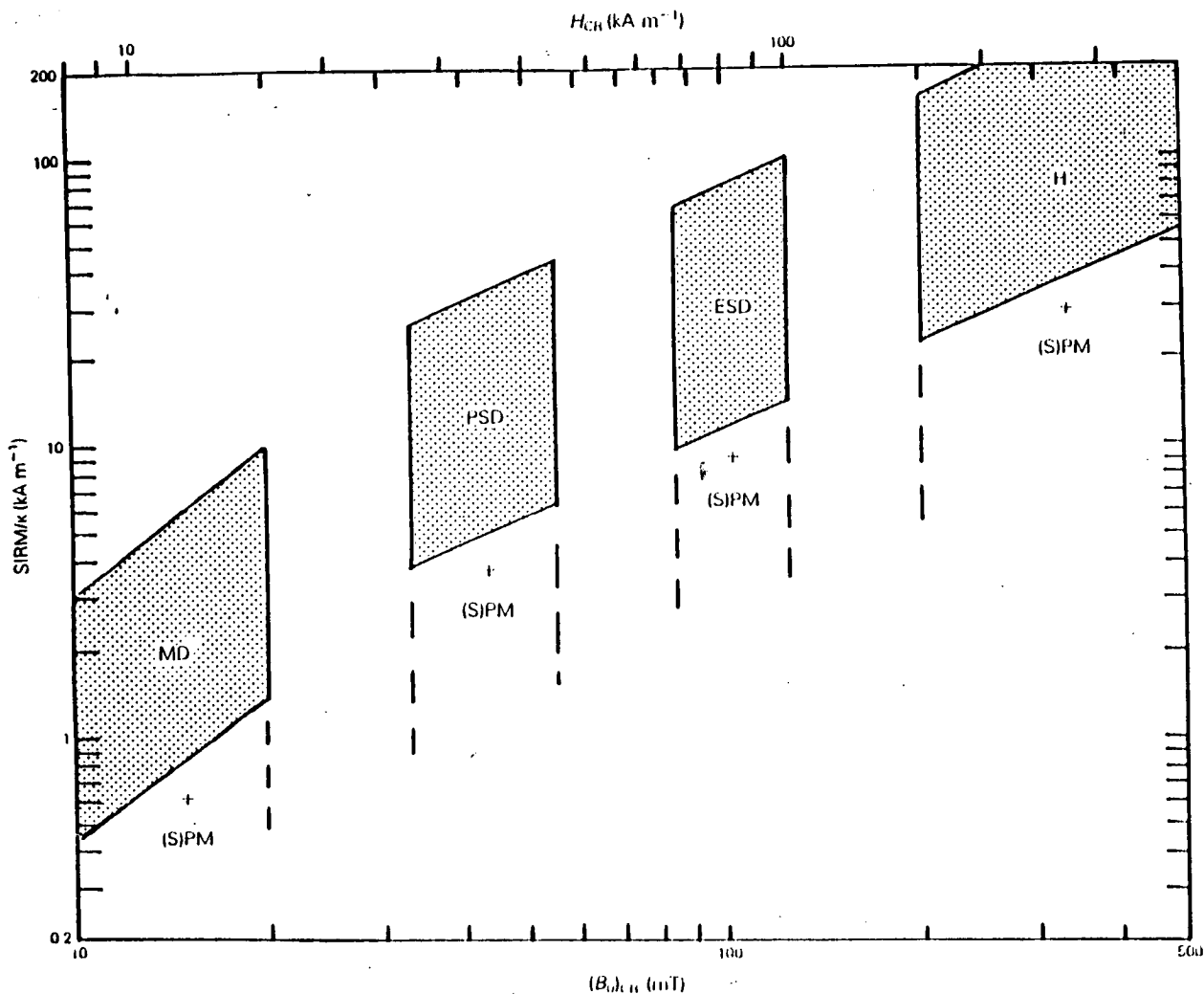
Mineral	Curie Temp.	Saturation Magnetisation	Susceptibility
magnetite	585	93	5×10^4
haematite	675	0.5	60
ilmenite	-218		200
maghaemite	740		4×10^4
pyrrhotite	300	20	5×10^3
iron	780	200	2×10^7
goethite	120	1	70
lepidocrocite	-196		70

Table 2.1 - Magnetic properties of various remanence magnetic minerals. Units: Temperature ($^{\circ}\text{C}$), Room temperature saturation magnetisation ($\text{Am}^2\text{kg}^{-1}$), specific susceptibility ($10^{-8}\text{m}^3\text{kg}^{-1}$).

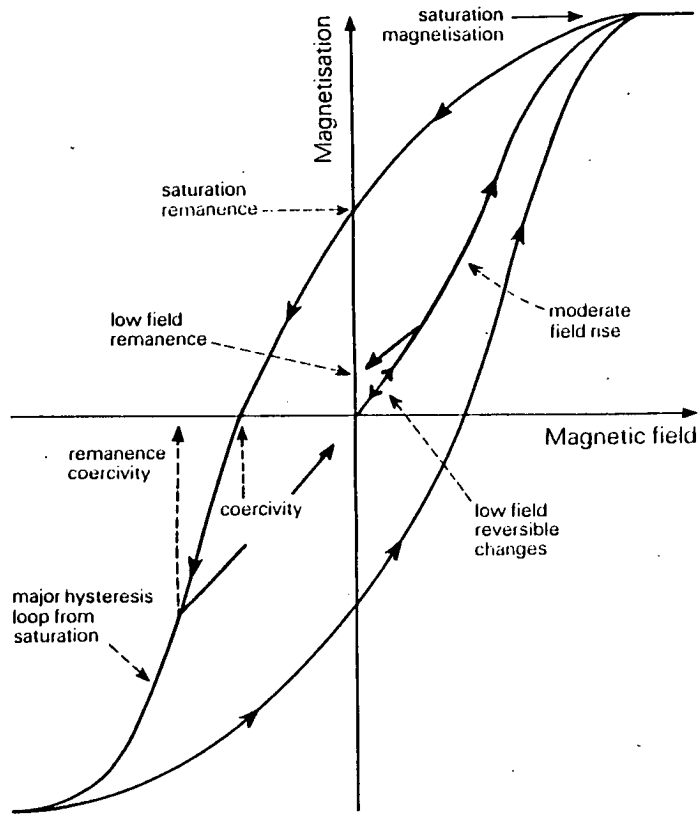


Grain size (μm)	SIRM/ χ	
	Magnetite	Haematite
0.0625	80	/
0.250	55	492
1.000	35	447
4.000	18	405
16.00	7.2	373
64.00	3.33	360
256.0	1.59	352
1024.	/	345

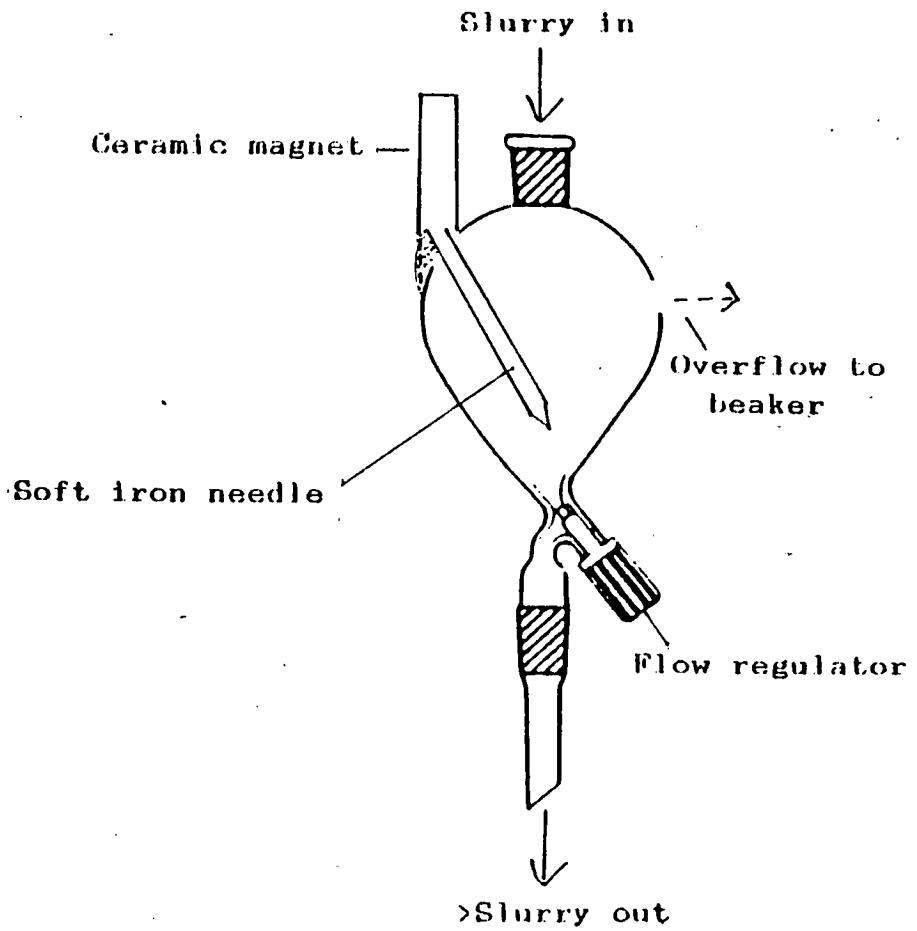
- Fig 2.9 Empirically derived normalised IRM acquisition curves for (a) magnetite of grain diameters 0.0625, 0.25, 1, 4, 16, 64, and 256 μm ; and (b) haematite of grain diameters 0.25, 1, 4, 16, 64 and 1024 μm . The attached table shows the SIRM/ χ ratio for each grain size. (From Thompson 1986).



- Fig 2.10 $SIRM/\chi$ vs $(B_0)_{CR}$ diagram. The grid schematically divides the diagram into magnetisation states. Multidomain (MD), pseudo single domain (PSD) and elongated single domain (ESD) magnetites fall into the upper left to centre of the diagram. Haematite (H) lies in the upper right curve, mixtures containing (super) paramagnetic grains lie further towards the lower right (Thompson and Oldfield (1986)).



- Fig 2.11 Diagram illustrating the principal features of a hysteresis loop from Thompson and Oldfield (1986).



- Fig 2.12 The central extraction vessel of the magnetic extraction equipment designed by von Dobeneck (1985 pers. comm.)

was magnetised by means of a strong ceramic magnet placed on its base thus creating a high magnetic gradient at the sharp tip. The needle was positioned in a glass vessel such that a sediment suspension could be pumped past it at various speeds. Magnetic material from the sediment accumulated at the tip of the needle. To recover the magnetic material, the needle was withdrawn from the glass vessel, demagnetised by simply removing the ceramic magnet and the extract washed off into a separate container. The sediment slurry was continuously cycled past the needle until an adequate extract was obtained. The Von Dobeneck system was found to be too sensitive for use on continental shelf material, tending to clog rapidly as magnetic particles built up around the extraction needle. As a result it needed hourly attention and was not suitable for continuous running. A more effective method was found to be a strong bar magnet wrapped in a latex sheath, suspended in a stirred suspension of sediment in water. The magnetic fraction tended to stick to the sheath from which it could be collected once the magnet was withdrawn. Several sheaths were experimented with, the best was found to be 'finger gloves' or individual fingers of surgical gloves. Yields of 80% of magnetic minerals were easily obtained after 24 hours of operation with minimum attention necessary. It was found that the more sensitive equipment designed by Von. Dobeneck could be used on the residual slurry to extract up to a further 5% of weakly magnetic material. The extract yield was calculated on mass specific susceptibility measurements before and after extraction. SIRM was also used to assess yield in circumstances where canted antiferromagnets were expected to be present.

2.5 Curie temperature analysis

Curie temperature analysis was carried out on extracts using a horizontal Curie force balance constructed by Humphrey Instruments and N. Petersen.

The balance was interfaced to a BBC microcomputer which served as a data logger by Heath (1988). An external DC field was supplied by an Oxford Instruments electromagnet.

Discussion of the operating details, and result interpretation from Curie balances are found in Tarling, (1983), Collinson, (1983), Thompson and Oldfield, (1986) and Housden et al, (1988). The essential point for basic interpretation is

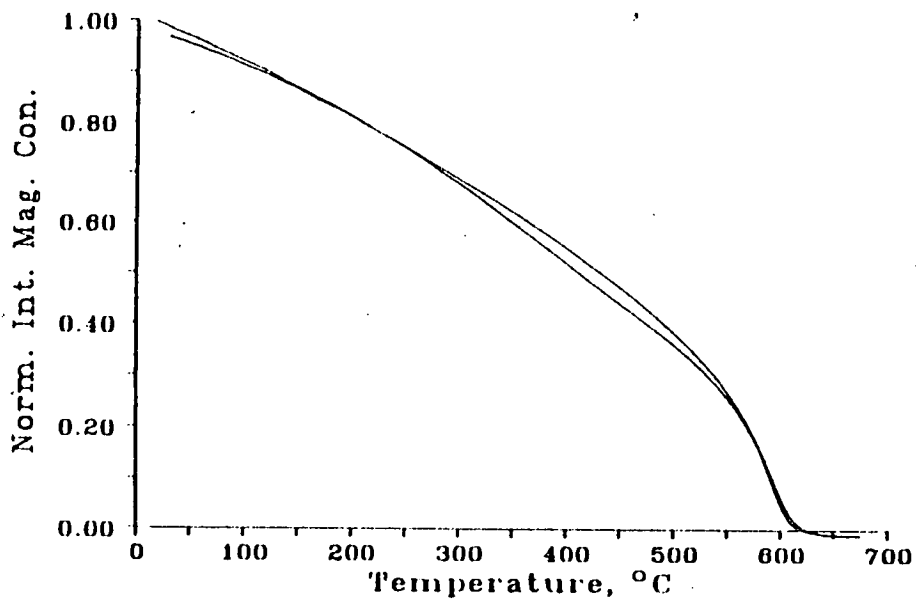
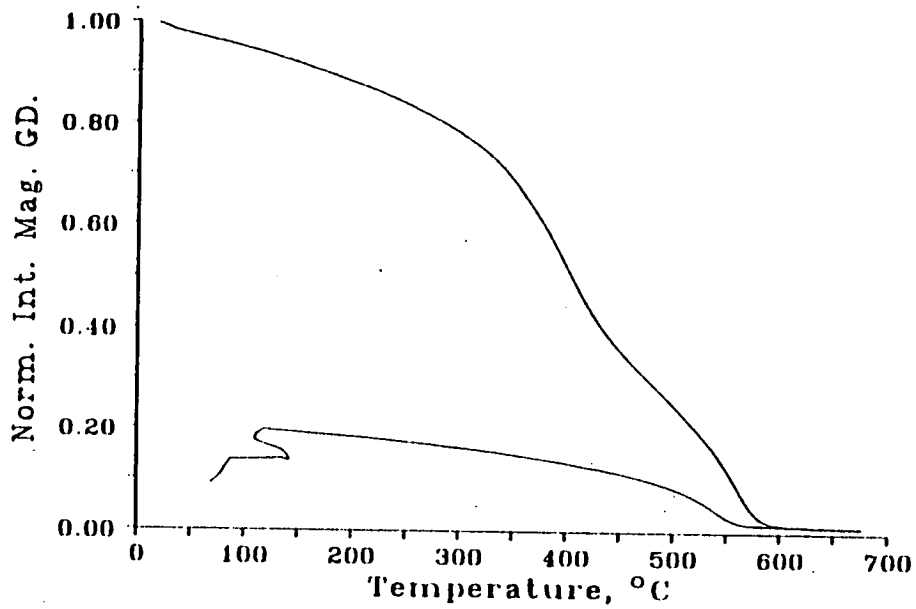


Fig. 2.13 Data acquired from the Curie balance for two magnetite standards. The intensity of magnetisation is normalised with respect to the initial intensity.

that magnetic minerals lose their magnetisation at individually characteristic temperatures, as seen in fig. 2.13. This figure shows the characteristic loss of magnetisation at approximately 580°C for magnetite standards provided by Dr B. Maher. Haematite would be expected to lose its magnetisation at 680°C. A summary of Curie temperatures for common magnetic minerals is shown in table 2.1.

2.6 Geological Techniques

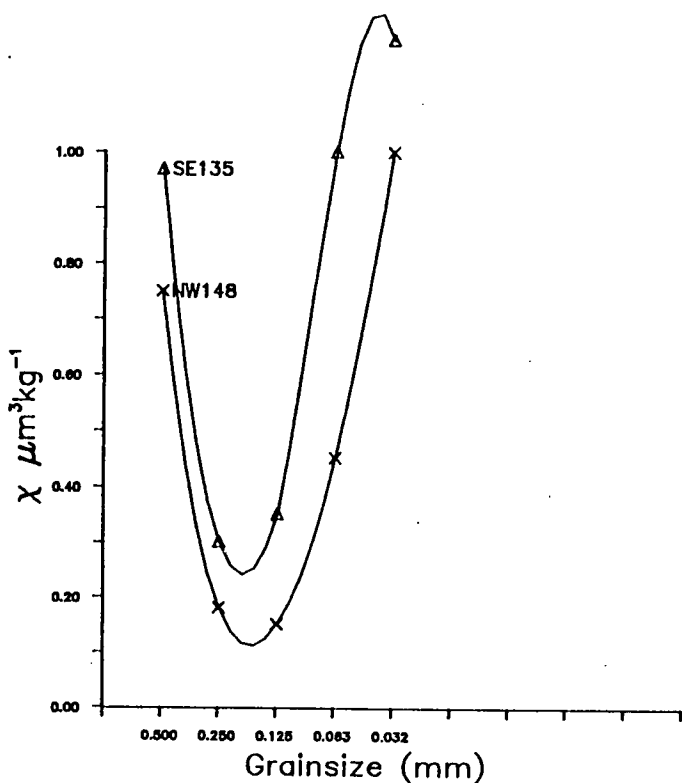
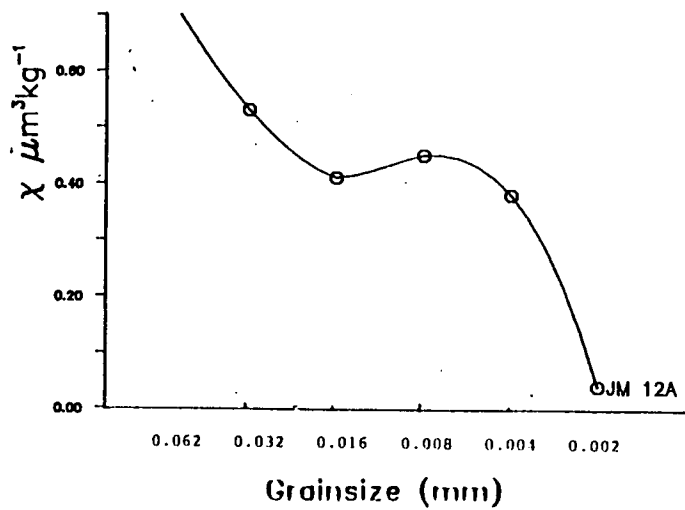
Although the bulk of geological data concerning samples for this study had been gathered as part of BGS routine examinations, occasional further work was required, consisting of:

1 Particle size work

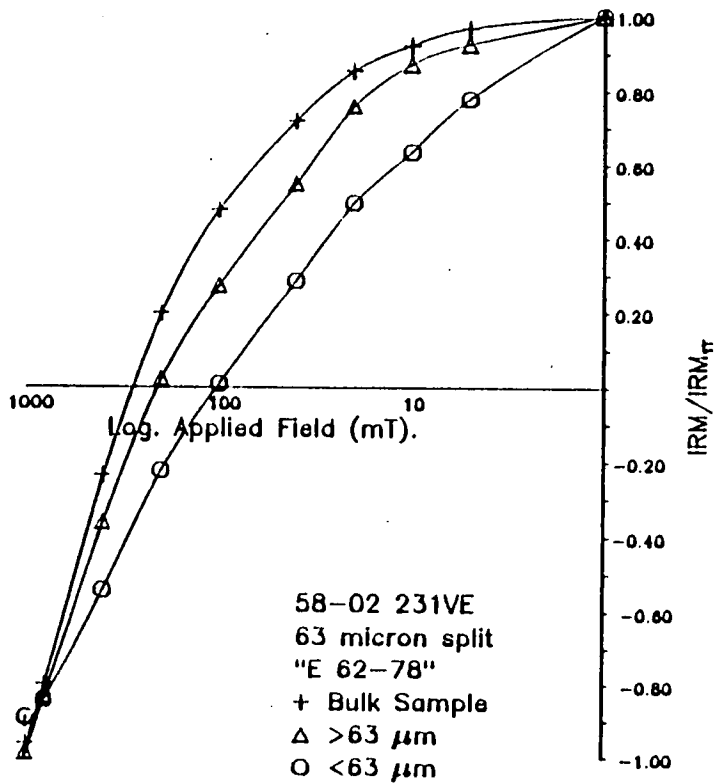
Initially, all samples were sieved through a 2mm mesh to remove drop-stones. Once the latter had been removed, the <2mm sediment was split into sand and mud fractions using a 63µm mesh. The >63µm fraction could then be further subdivided by sieving through a range of meshes. The <63µm fraction could be split by controlled settling through a water column with timed removal at certain depths, the times being calculated by reference to Stokes' Law. IRM acquisition curves were then grown on the sieved fractions to identify the magnetic mineralogy associated with particular particle sizes, see for example figs. 2.14. and 2.15.

2 Heavy Liquid Separation

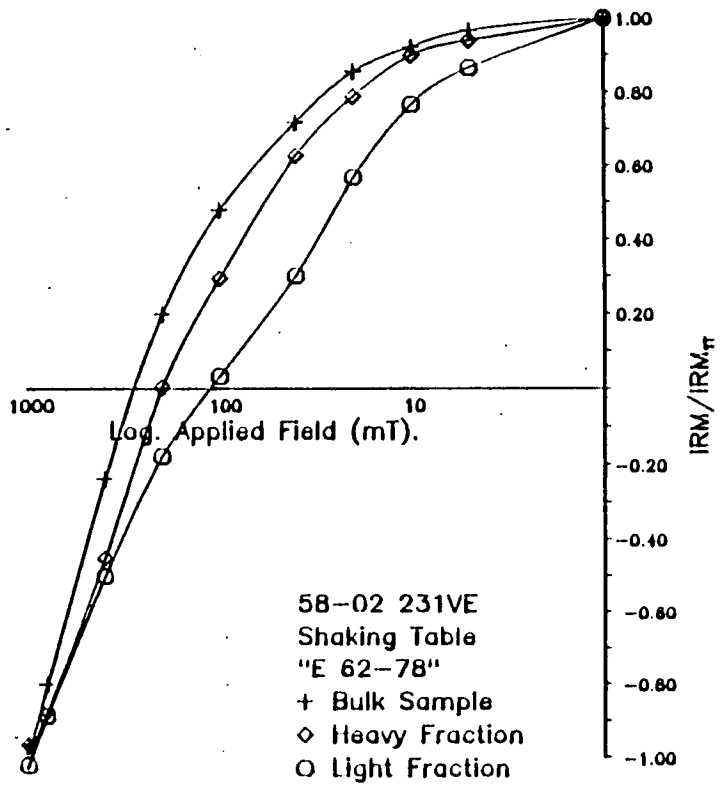
Heavy liquid separation techniques were employed on several samples in an attempt to remove the heavy mineral fraction. This extraction work was undertaken at the Applied Geology Department, University of Strathclyde under the guidance of Mr A. Beg. A synthetic heavy liquid, *sodium polytungstate*, $3\text{Na}_2\text{WO}_4 \cdot 9\text{WO}_3 \cdot \text{H}_2\text{O}$ was used. This synthetic medium gave a density of 3.1 gcm^{-3} , comparable to ordinary organic heavy liquids, for example bromoform and having none of the problems associated with toxicity. A standard approach of filtration through sintered glass filters was employed to recover the heavy mineral fraction.



- Fig. 2.14 Results illustrating the relationship of particle size and χ in sediments from the Clyde. A full account of these results is given in chapter 6.



- Fig 2.15 IRM curves obtained for splits after sieving bulk sample through 63µm mesh. Sample material derived from core 58-02 231VE. 'Bulk' = original sample, 'Sand' = >63µm, 'Fines' = <63µm.



- Fig 2.16 IRM curves obtained for splits after use of a 'shaking table'. 'Bulk' = entire original sample, 'Heavy' = material retained on table, 'Lights' = light material washed from table.

3 Shaking Table

The shaking table is effectively an automated panning technique. It was useful for splitting up large quantities of sample into light and heavy fractions. The machine used in this project was a *Mozley Laboratory Mineral Separator Mk II*. The shaking table was operated under the supervision of Mr A. Beg at the Department of Applied Geology, University of Strathclyde. Due to the scale of the operation relatively large subsamples from cores were needed, with 500g being a common sample size. Large amounts of various size fractions were obtained, facilitating later magnetic measurements on individual fractions. IRM acquisition and backfield curves were grown for each particle size fraction, see for example fig. 2.16.

4 XRF

XRF was carried out at Wolverhampton Polytechnic under the supervision of Mr Brian Bucknall and Dr J.P Smith. The equipment consisted of a Philips PW 140 X-ray spectrometer with automatic scan control under a software package developed by Dr J.P. Smith. The automated scan gave both raw data and processed results in terms of 15 major elements and oxides. Sample preparation was as follows:

Approximately 20 g of sample were heated overnight at 550° to burn off any organic material. The samples were weighed before and after heating so that a loss on ignition and percentage organic content could be calculated. After heating, the material was ground to a fine powder using a Tema mill. 8.500g of the ground sample powder was then mixed with 1.500g of *Hoechst* wax, to provide an inert matrix. Mixing was by means of plastic ball pestles in an automated shaker to ensure a homogeneous end product. The mixture was then compressed into a pellet using 17 tonne pressure from a hydraulic press. The sample was then ready for use.

A carbonate bomb was used to determine a percentage carbonate figure for each sample.

CHAPTER 3 PEACH AREA

3.1 Background

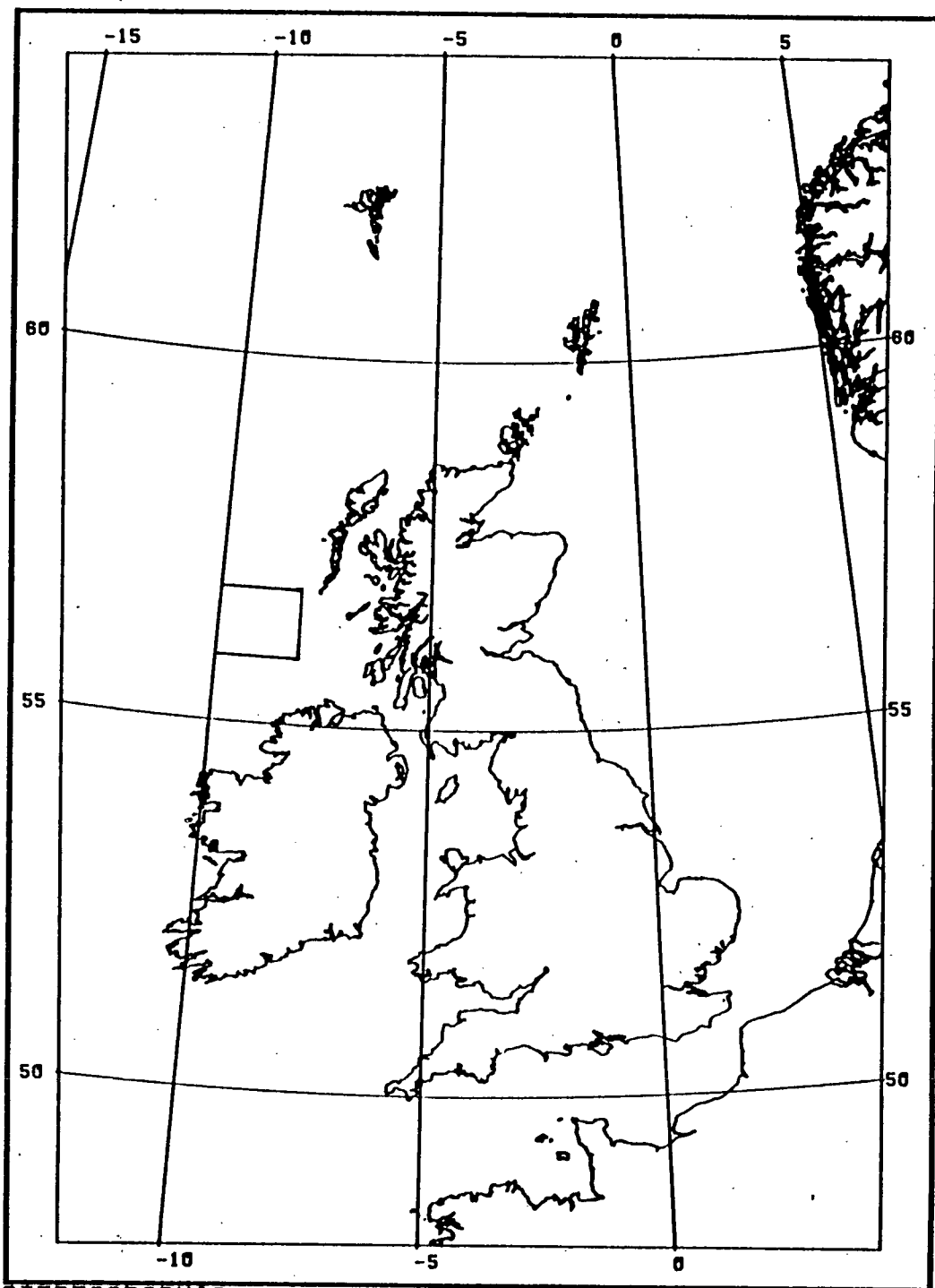
The Peach Area lies towards the western edge of the UK Continental Shelf (fig 3.1), approaching the limits of the continental slope. Water depth in the region of the shelf covered by the Peach area can be up to 2000m and approaches the operating limits for BGS sample recovery equipment. The Pinger results shown in fig. 3.2 gives a good indication of the sea-bed conditions in The Peach area. The most prominent feature seen in fig 3.2 is the edge of the continental shelf and associated slumped sedimentary sequences. To the east of the shelf edge the sea-bed consists of large hollows with varying types of sediment infill punctuated by outcropping boulders. To the west of the shelf edge, the dominant features on the sea-bed are slumped sediments associated with the steep edge of the shelf. These slumped sediments are followed westwards by layered sediments which in turn give way to hummocky sediments.

M.V. British Magnus, under charter to BGS, was surveying the Peach area area during November 1985. This gave me an opportunity to undertake measurements and sampling in a shipboard environment. It also provided the opportunity to obtain samples for magnetic analysis from core material fresh from the sea bed. There was also ample opportunity to observe BGS deck crew practices whilst participating in the cruise and assess the possibility of handling effects upon subsequent palaeomagnetic measurements. Sample station positions for the Peach area are shown in fig. 3.3.

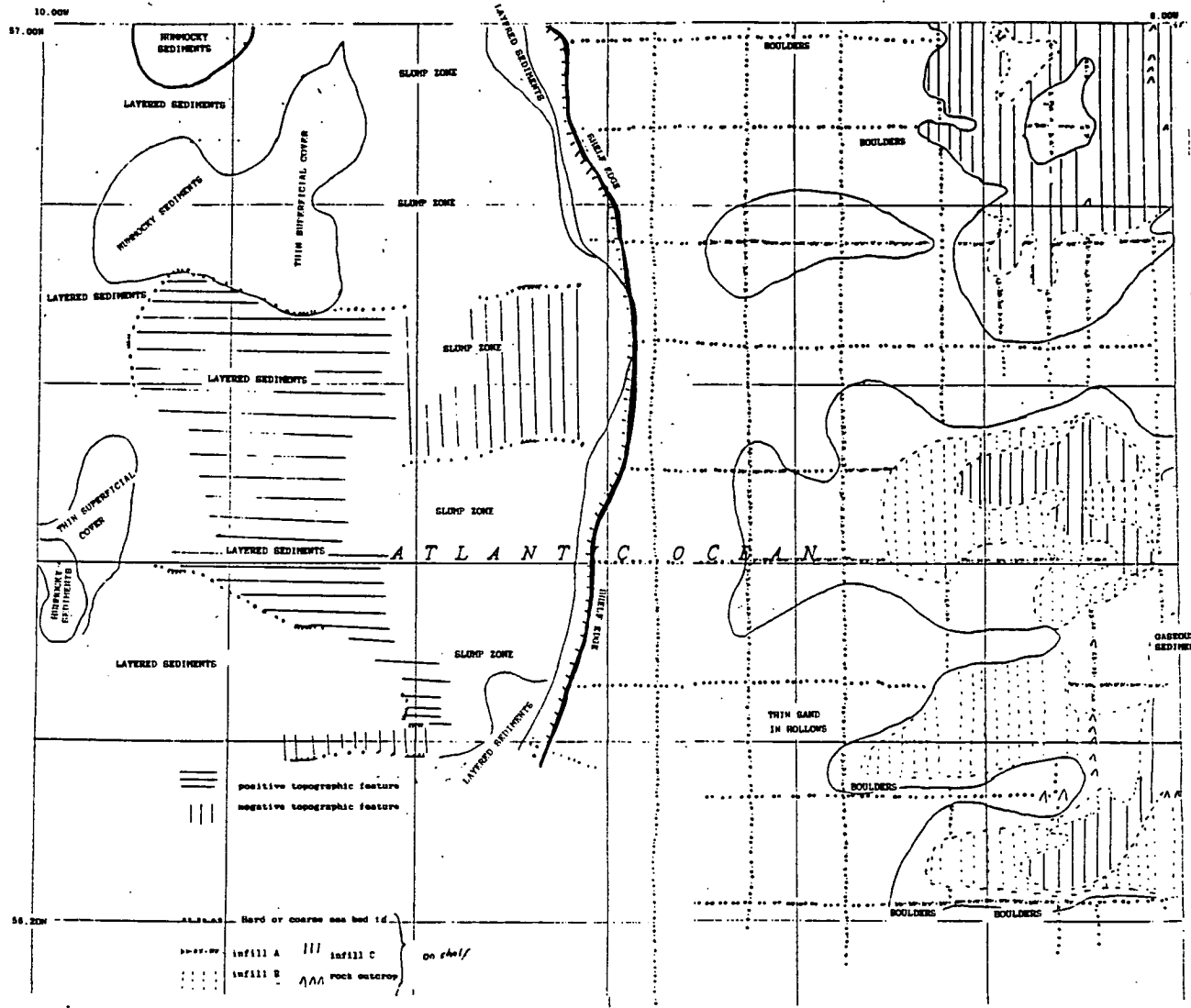
3.2 Ship board sampling and magnetic measurement procedures

Work undertaken at sea principally consisted of intensive subsampling of selected cores as they became available. Subsamples were obtained from vibrocores and gravity cores, the subsamples were placed in refrigerated storage until disembarkation.

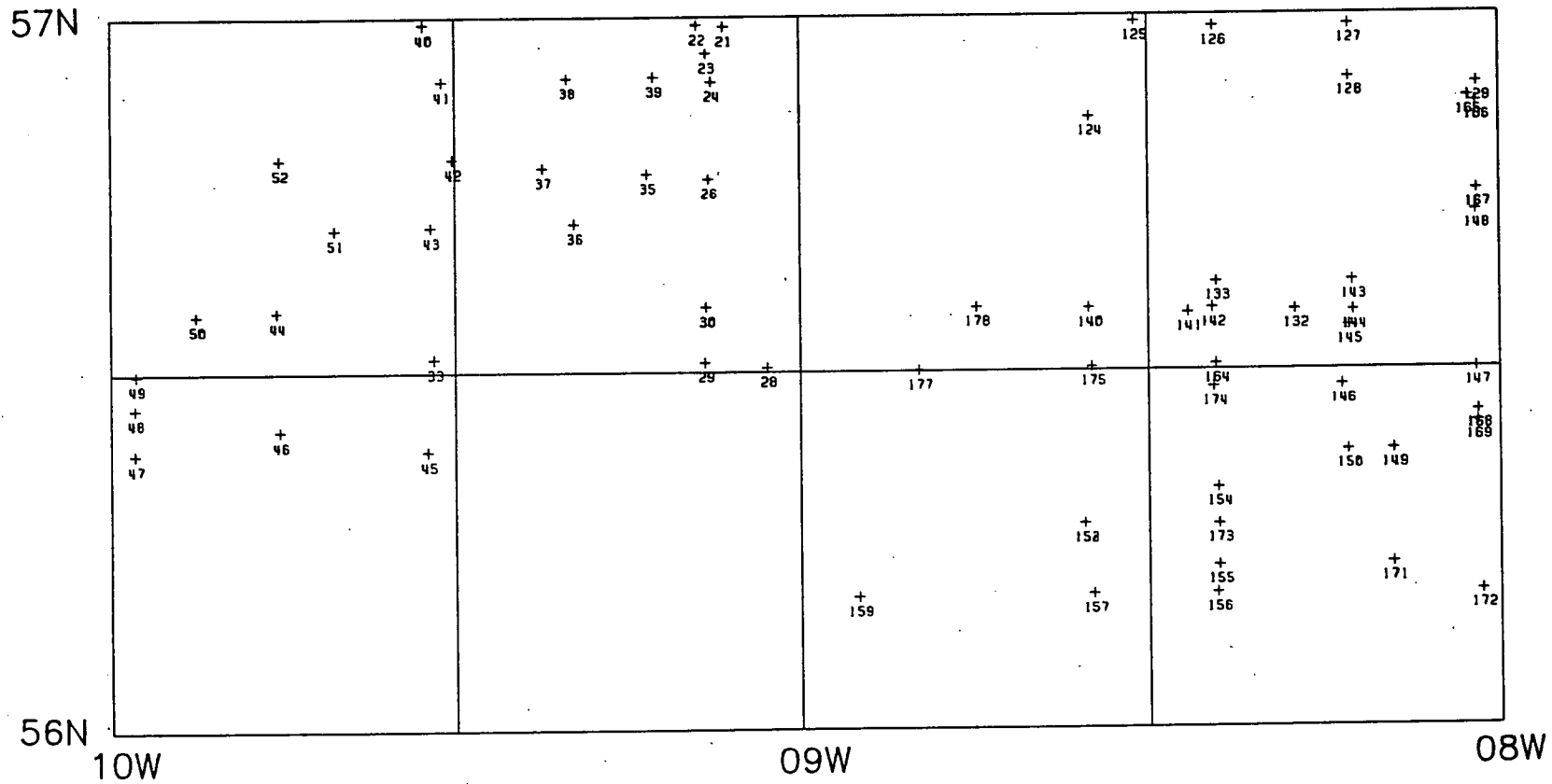
Bartington subsample susceptibility equipment was available for use on



- Fig 3.1 The position of the Peach sea area with respect to the British Isles.



- Fig 3.2 Pinger data interpretation showing the characteristics of the sea floor sediments in the Peach area.



- Fig 3.3 Position of sample stations in the Peach area.

board *M.V. British Magnus*. All subsamples taken were subjected to volume susceptibility measurement. Chemical salt standards were also measured to check for any discrepancy in instrument calibration due to the environment of the ship's laboratory.

3.3 Laboratory sampling and magnetic measurement procedures

The subsamples taken on the ship were supplemented by additional subsamples taken on land. In many instances, these additional subsamples were taken from the same position downcore as at sea with a view for checking for consistency between ship and shore measurements.

All subsamples were subjected to NRM measurement using the CCL cryogenic magnetometer. Using these NRM measurements it was then possible to select a range of representative pilot samples for A.F. demagnetisation studies. Mass-specific susceptibility measurements were also undertaken on subsamples at this stage.

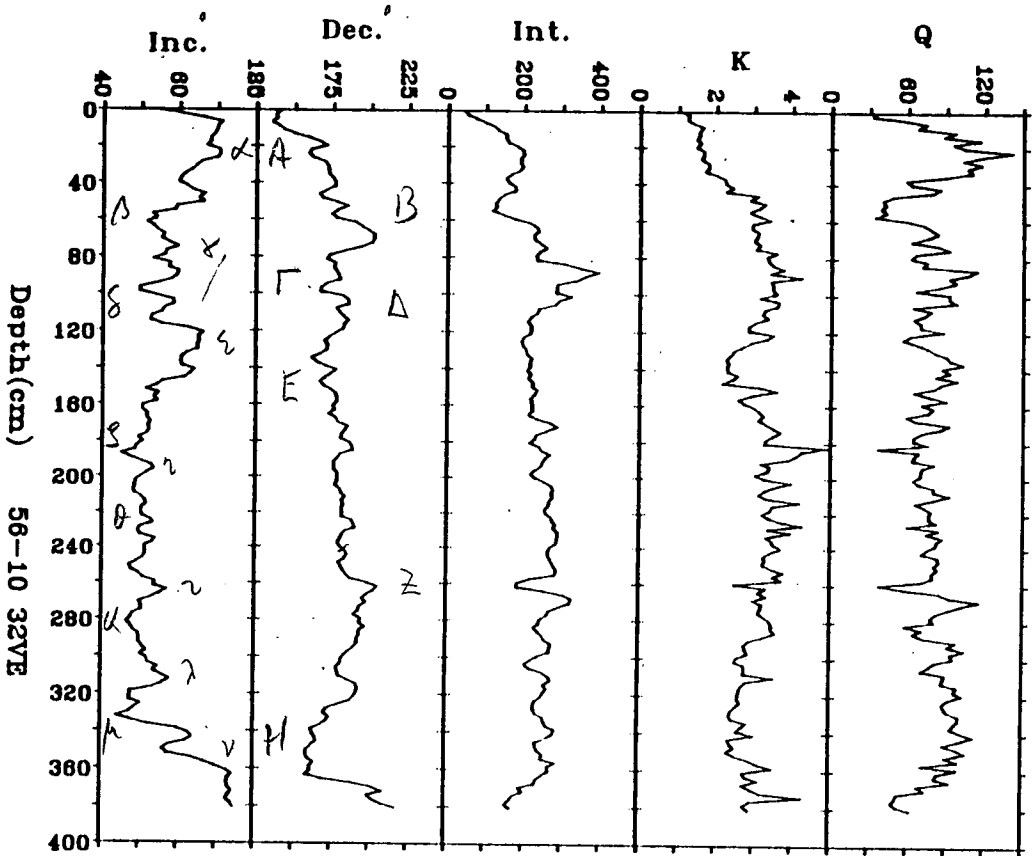
A whole core sensor for the Bartington susceptibility equipment became available early in 1986. This sensor was used to provide whole core susceptibility profiles for 70 vibrocores and gravity cores from the Peach area.

IRM acquisition curves were grown for 60 pilot samples taken from a range of cores to give an indication of the magnetic remanence carriers. Further confirmation of NRM carrier was sought using Curie point analysis on magnetic extracts obtained using equipment designed by Von Dobeneck (pers. comm. 1985), and simple magnetic gradient methods described in chapter 2.

3.4 Results

1 Palaeomagnetic Results

NRM results for contiguous subsamples from cores 56-10 32VE are shown in fig 3.4. All subsamples exhibited a normal polarity. Inclination data for core 56-10 32VE varies between 45° and 70° with an average value of approximately 60° . Relative declination is seen to vary downcore by $\pm 60^\circ$. Intensity is seen to rise downcore from a minimum of 25 mAm^{-1} in the top



- Fig 3.4 Downcore palaeomagnetic data for core 56-10 32VE. Results based on data obtained from contiguous subsampling. Units: Intensity, μAm^{-1} ; K - volume susceptibility, arbitrary units; Q ratio, Am^{-1} .

5cm to 400 mAm^{-1} by 100cm, before decreasing to 210 mAm^{-1} for the lower reaches of the core.

Demagnetisation results for pilot samples taken from various depths down core 56-10 32VE are shown in fig 3.5. For each sample, an orthogonal projection, normalised intensity plot and stereographic projection of the palaeomagnetic data are shown. The scales on the orthogonal plots are normalised with respect to maximum intensity. On the orthogonal plot a single dominant component of NRM can be seen for all subsamples. There is evidence of a minor secondary component in subsamples 22 and 172. The slight secondary component shows up clearly on the stereographic projection, distracting from an otherwise tight data grouping. A median destructive field in the range 21-23 mT is seen for all subsamples.

2 Mineral magnetic data

Whole core susceptibility

Whole core susceptibility profiles for all 66 cores from the Peach area are shown in figs 3.6a to 3.6i. Three cores have been picked out as examples illustrate the range of data and are shown in fig 3.7. Whole core susceptibility values are seen to range from a low of 3 instrument units in core 56-09 168VE to over 2000 arbitrary units in core 56-09 159VE. Many cores exhibit 'spikes' in their susceptibility profiles. Within core variation in susceptibility patterns downcore differ widely between cores. Most cores, eg core 56-09 129VE exhibit little change in susceptibility downcore, but others exhibit considerable change, eg core 56-09 155VE.

Mean values for whole core susceptibility are shown superimposed on a map of Pinger derived sedimentary data from part of the Peach area (fig 3.8). A wide range of mean whole core susceptibility values (from less than 10 instrument units to over 200 instrument units) are observed.

Subsample Susceptibility

A comparison of ship and land based measurements of volume susceptibility is shown in table 3.1.

- Fig 3.5 Examples of alternating field demagnetisation data for pilot samples taken from core 56-10 32VE. In each case plots are marked with sample number (corresponding to depth down core in cm), NRM intensity ($\text{mAm}^2\text{kg}^{-1}$), medium destructive field (mT). For each pilot sample an orthogonal projection, normalised intensity plot and stereographic projection of the palaeomagnetic data are shown. The scales on the orthogonal plot are normalised with respect to maximum intensity.

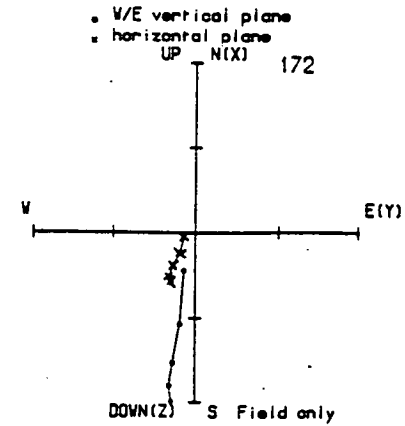
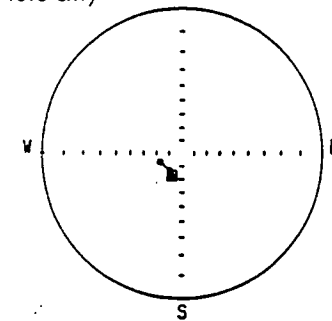
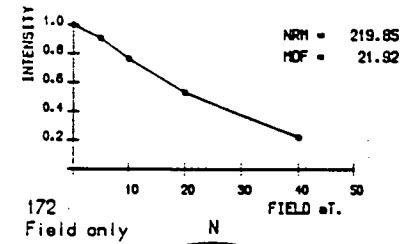
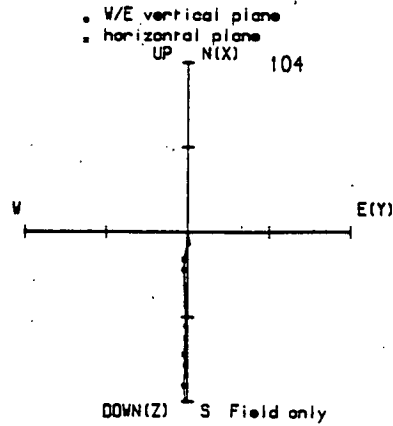
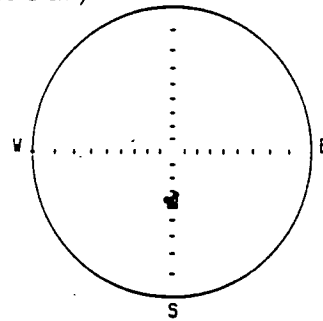
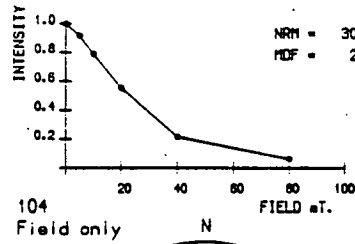
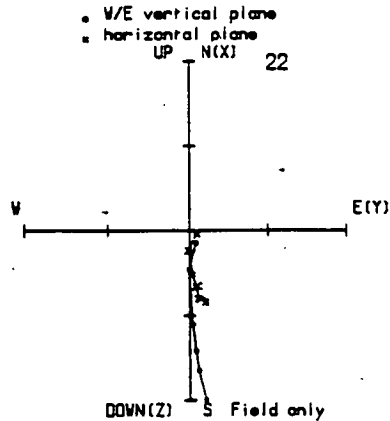
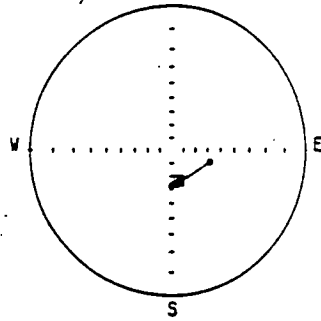
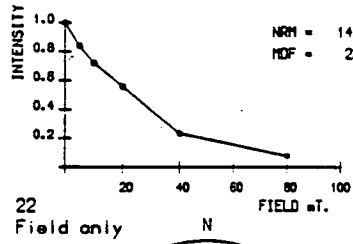
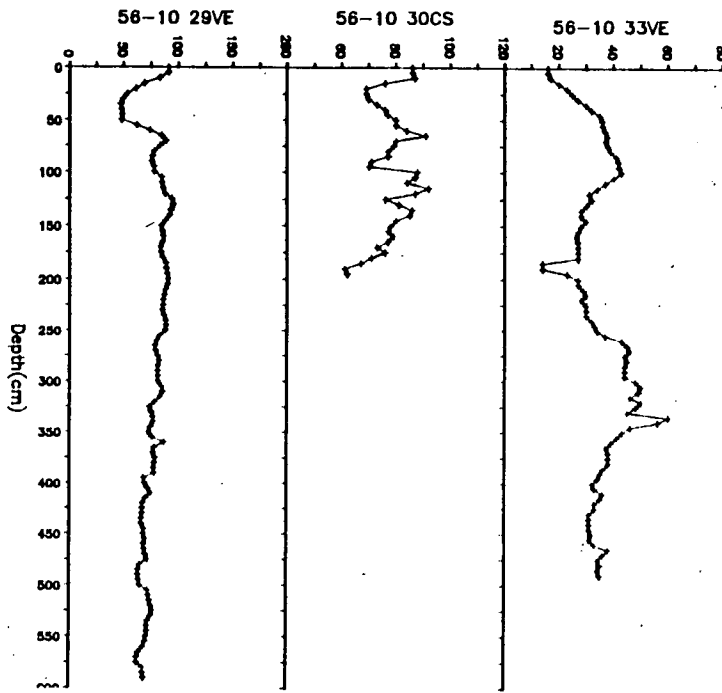


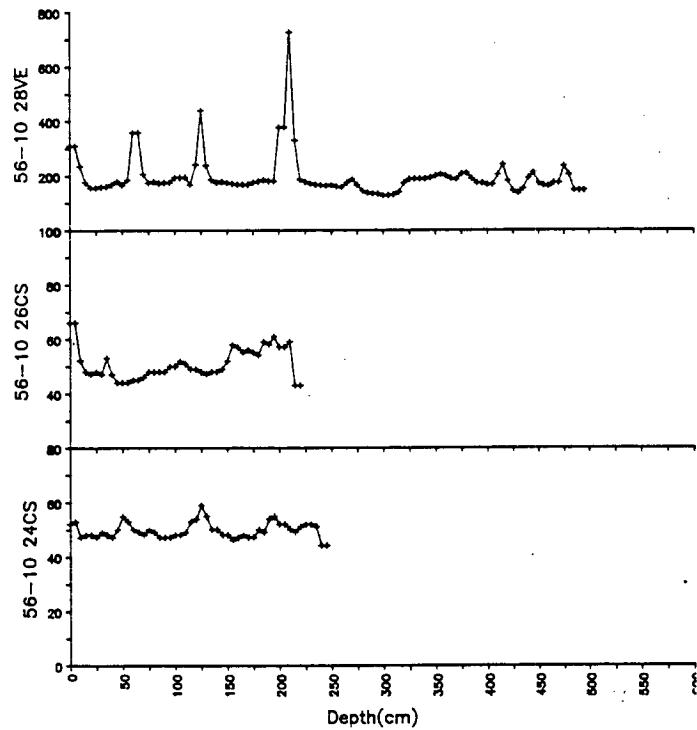
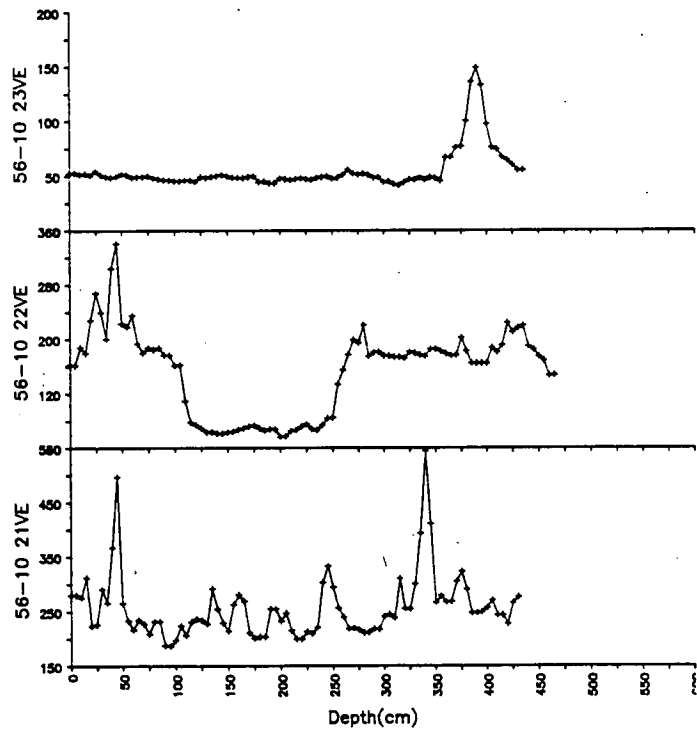
Table 3.1 Comparison of susceptibility values for ammonium ferrous sulphate standards between ship and shore based measurements.

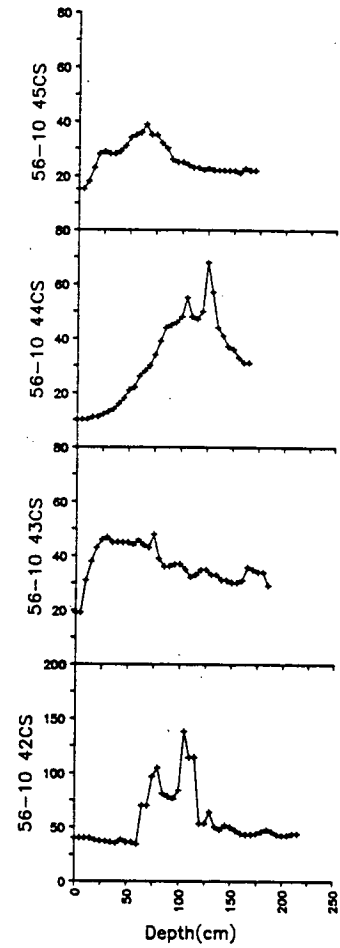
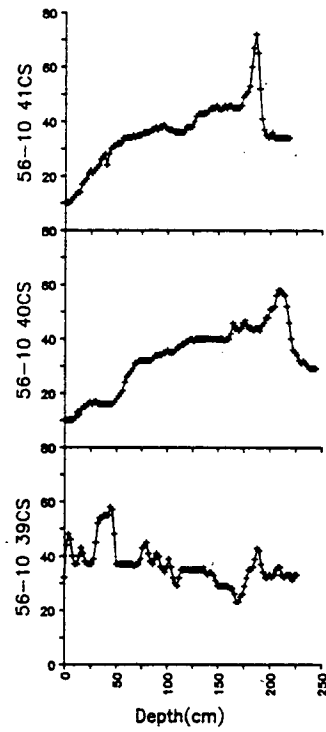
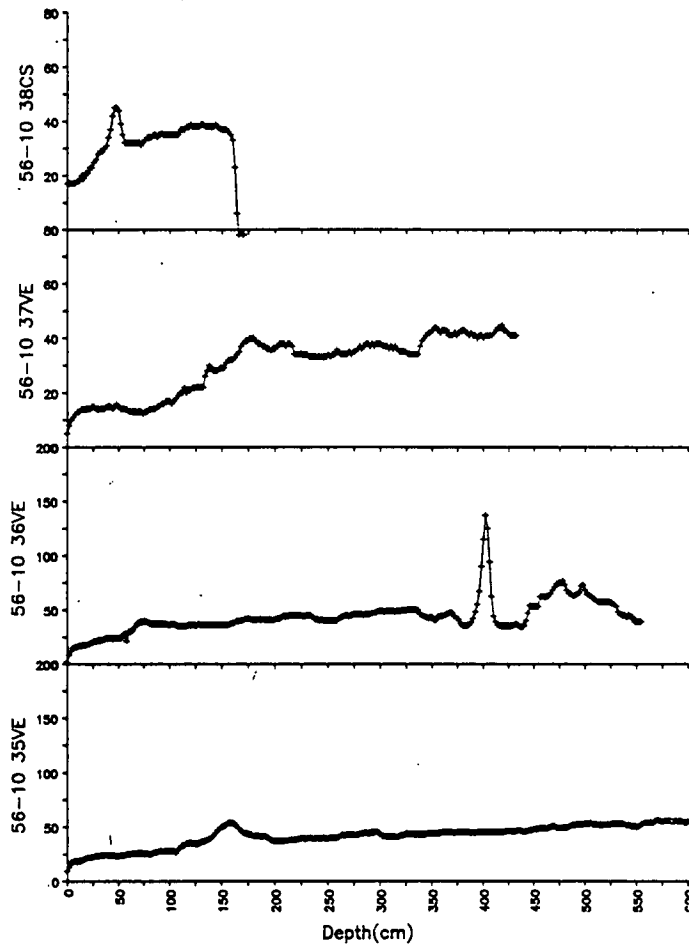
Standard	'Shipboard'	'Shore'
2.2 cm cube	2.31-2.43	2.35-2.45
10 cc cylinder	5.6-5.9	5.6-5.8

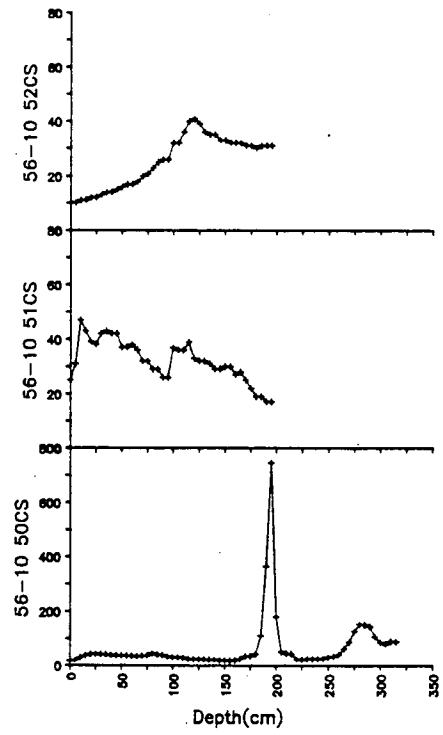
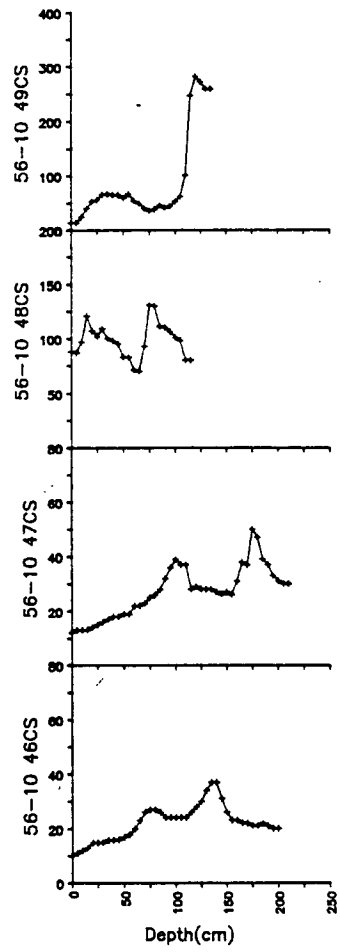


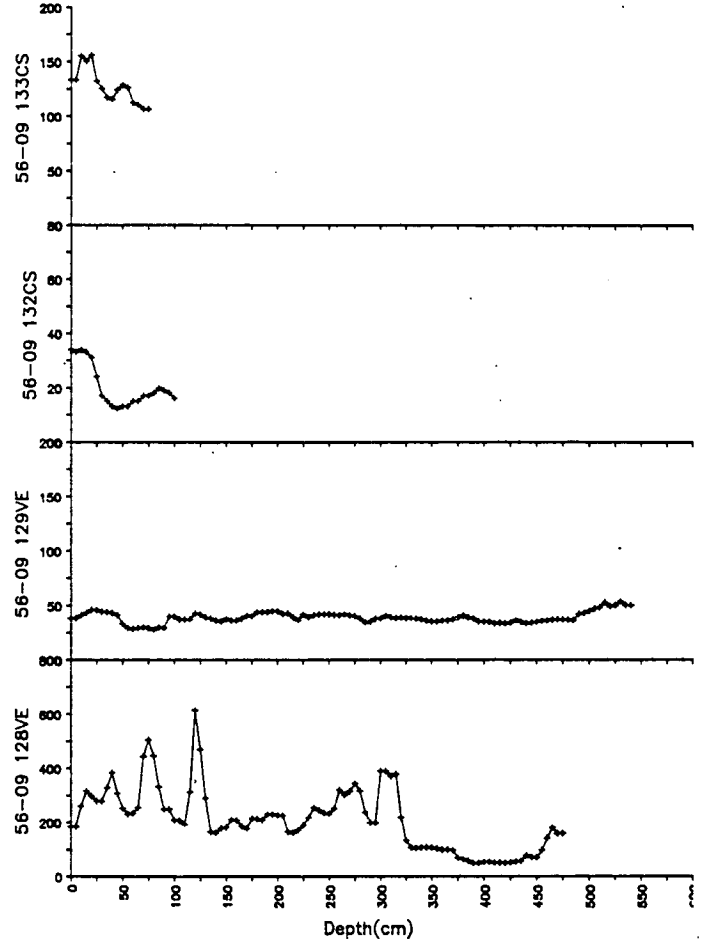
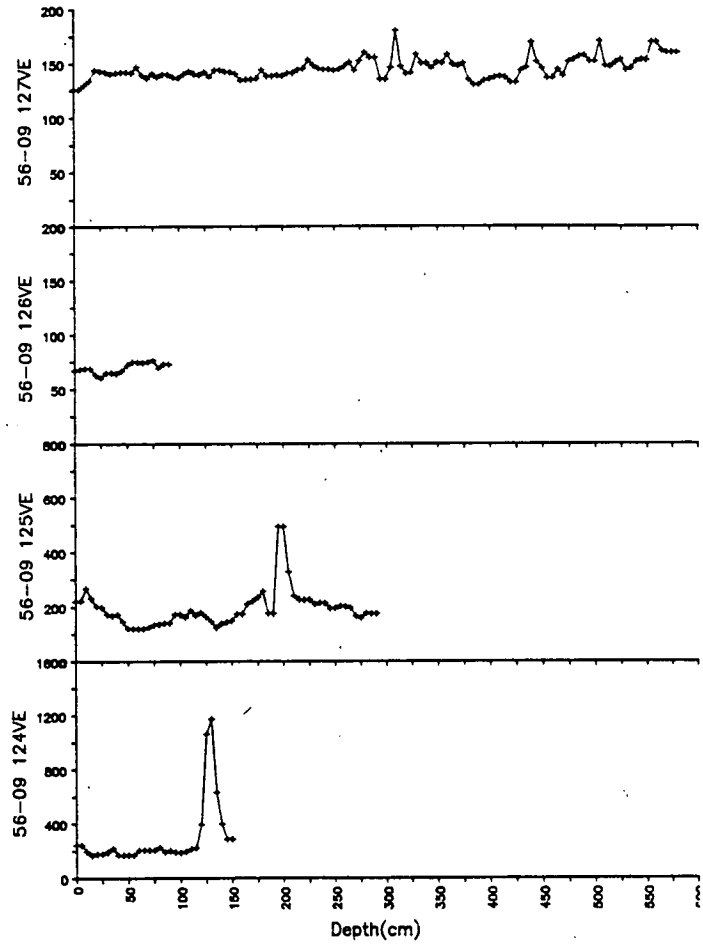


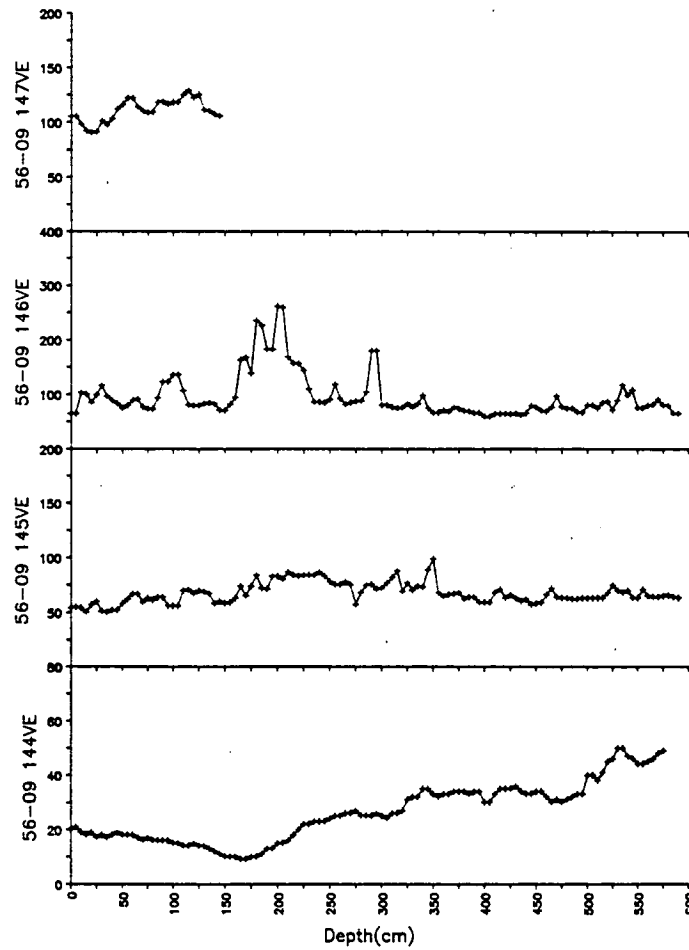
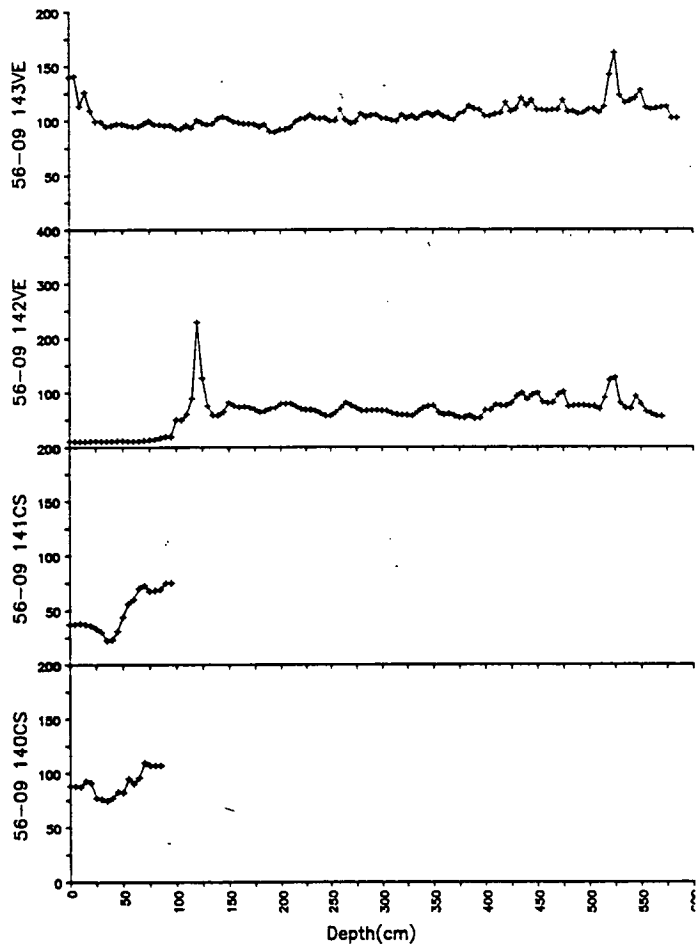
- Fig 3.6a-i Whole core susceptibility profiles for cores from the Peach area. Susceptibility is in arbitrary units.

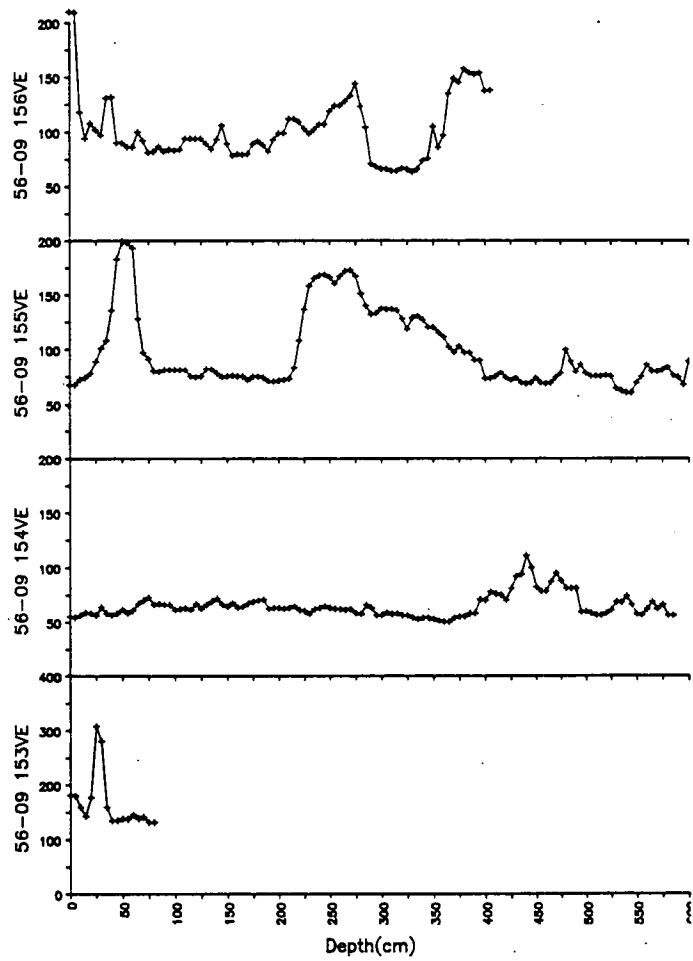
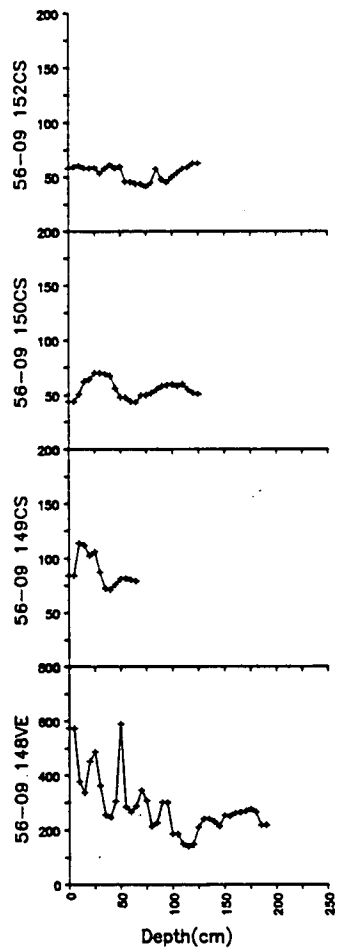


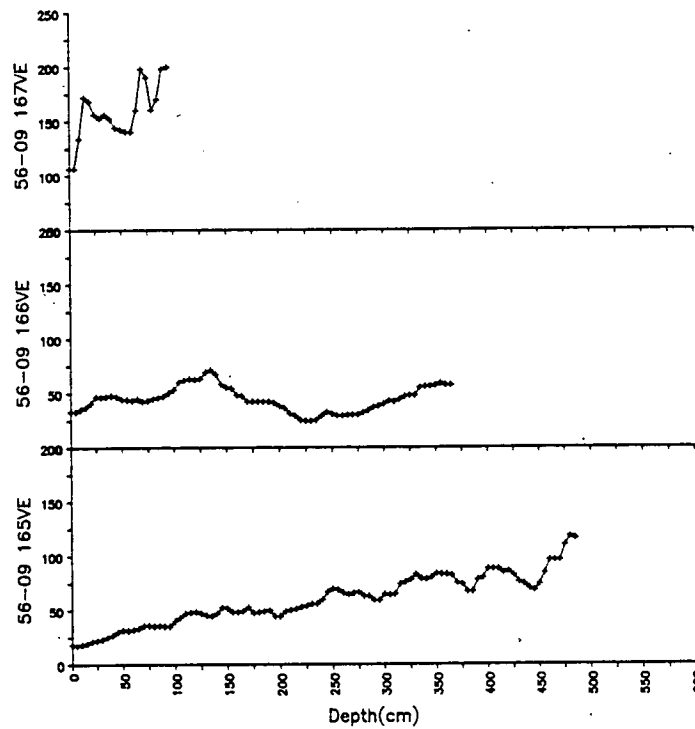
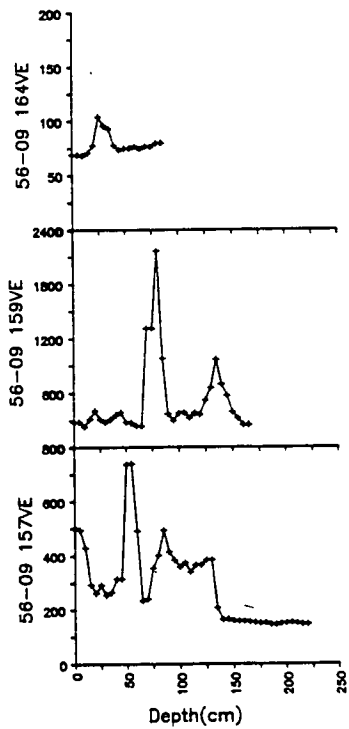


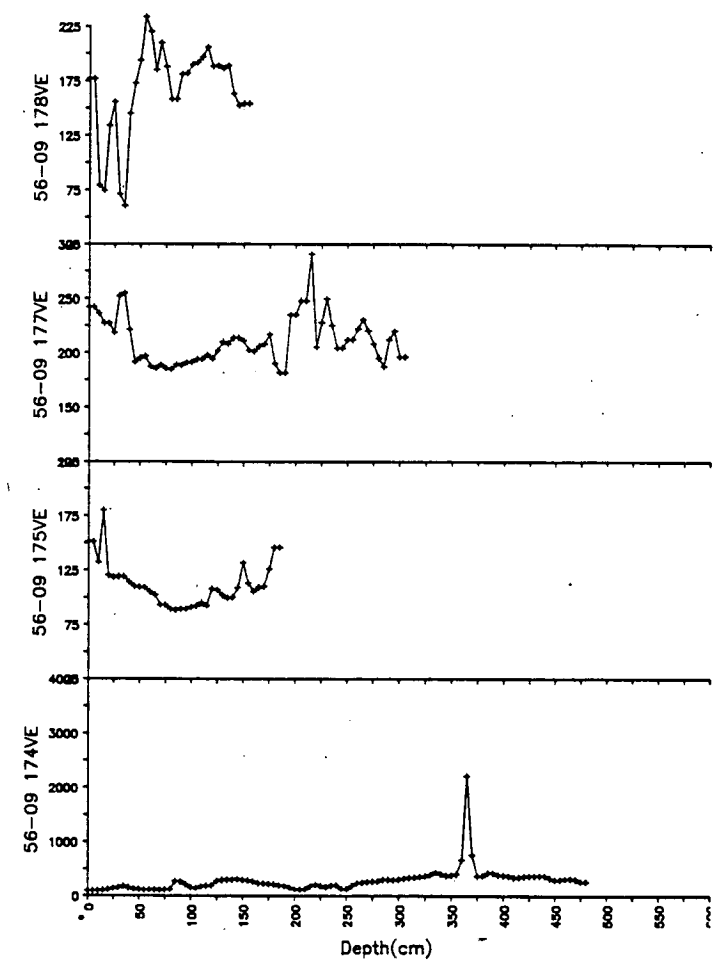
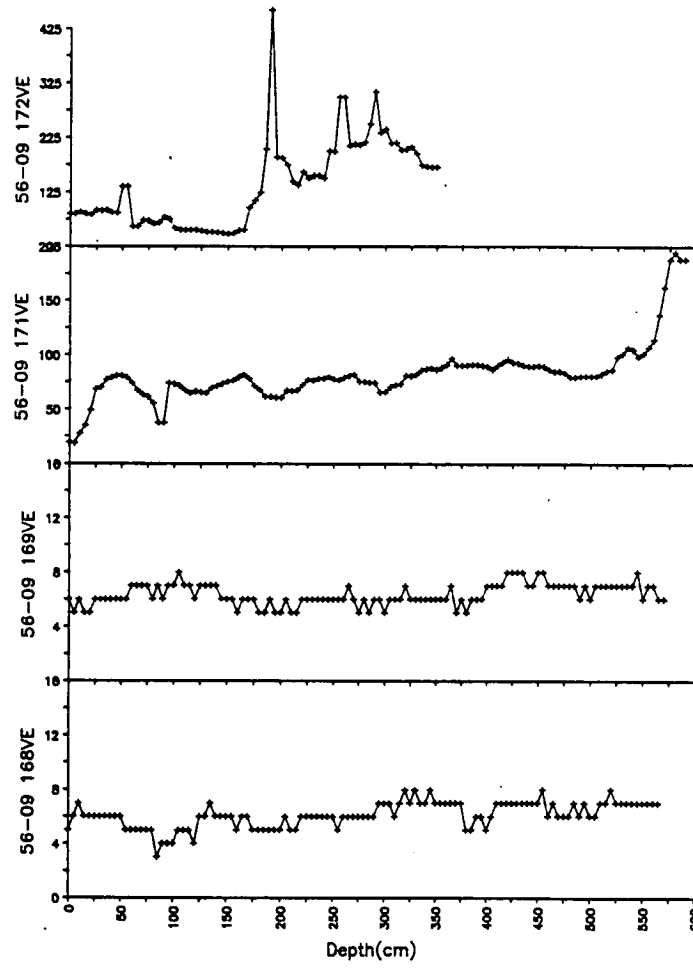


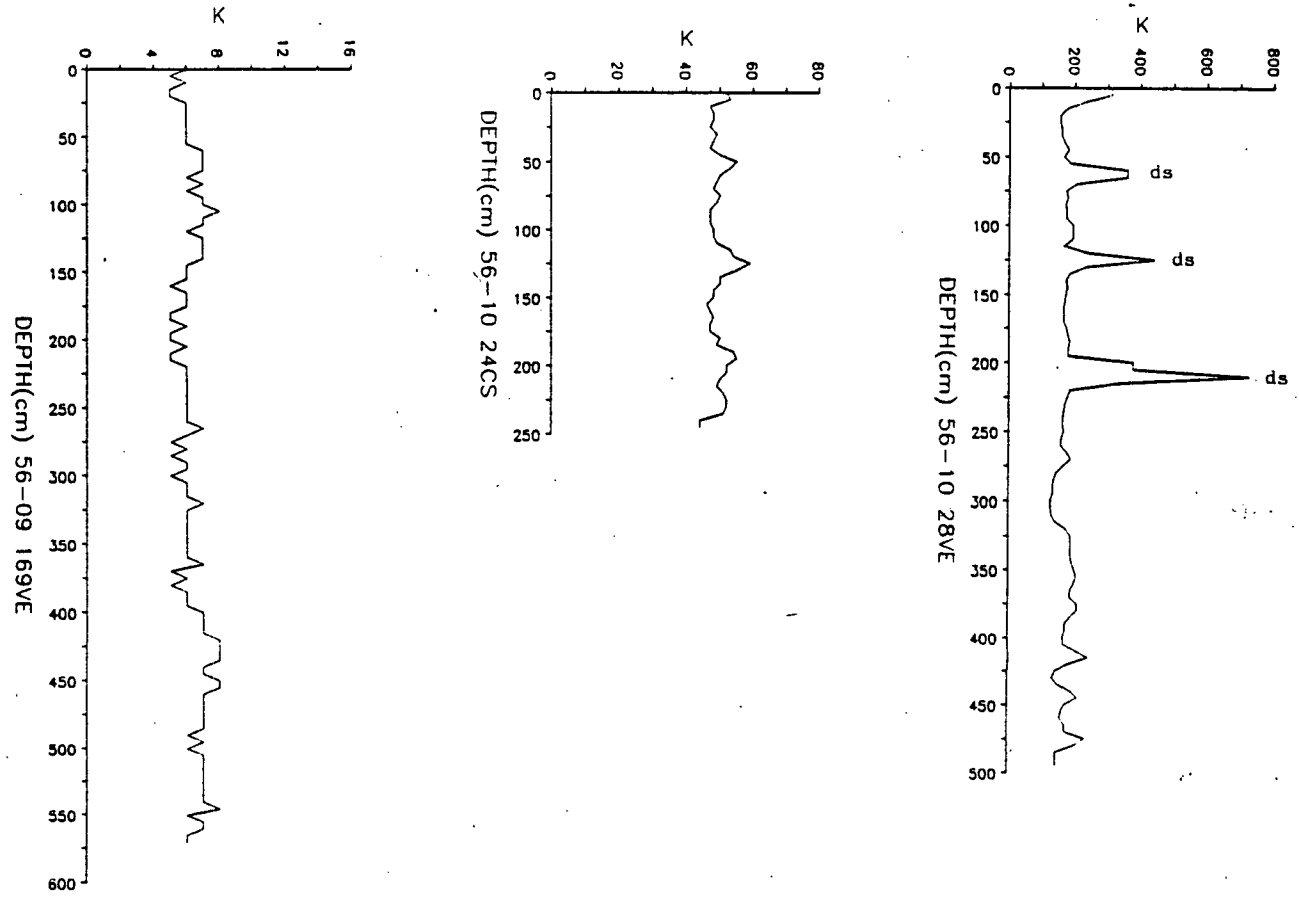












- Fig 3.7 Whole core susceptibility (K) profiles for cores cores 56-09 169VE, 56-10 42CS and 56-10 28VE. These represent the range of data seen across the Peach area. Susceptibility features associated with observed drop-stones are labelled 'ds'.

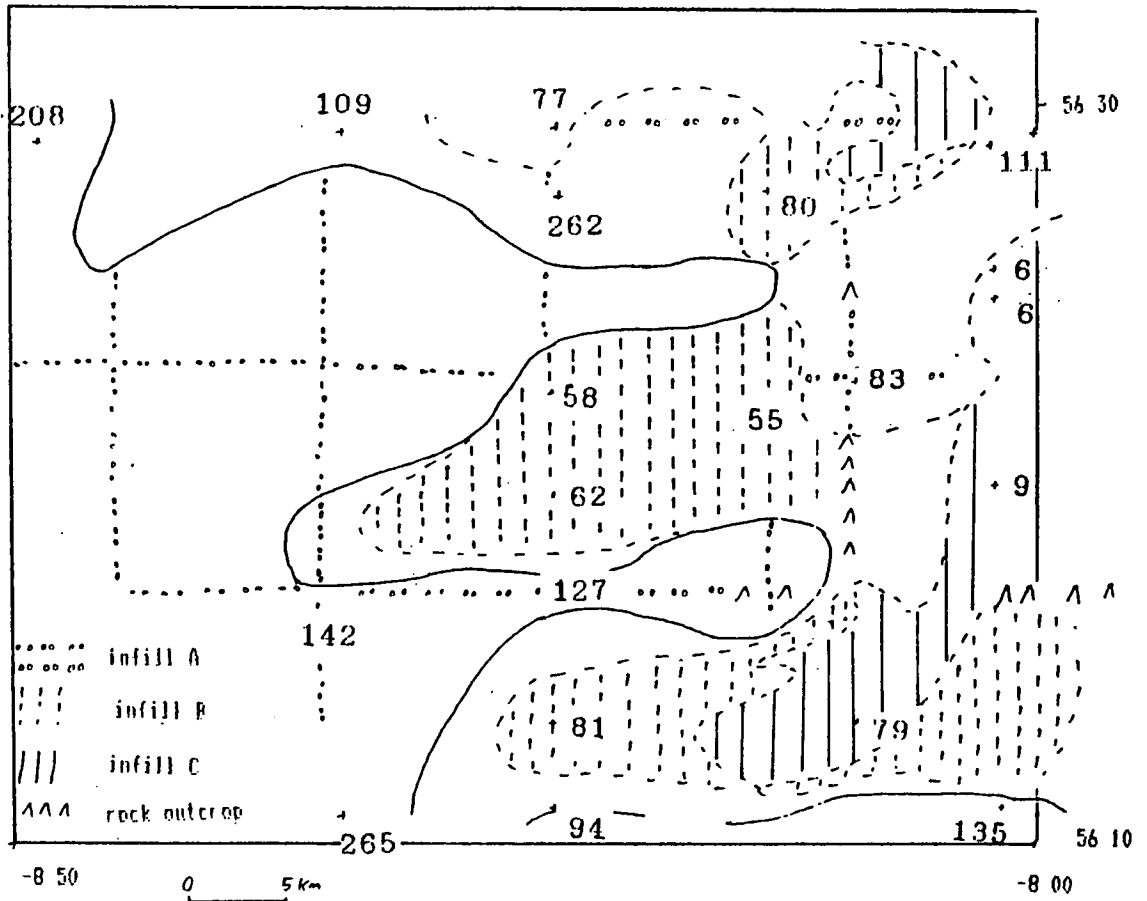


Fig 3.8 Composite map of median values of whole core susceptibility (K) superimposed on sedimentary types defined by BGS 'pinger' data. The whole core median K values were obtained after manually removing the 'spikes' attributed to the effects of dropstones. After this, a median value for the top 3m of core were obtained. This value was then shown as a single data point in its appropriate geographical position. The key to pinger derived sediment types is shown on the figure.

IRM acquisition data

IRM acquisition curves were grown for approximately 60 subsamples from the Peach cores. Fig. 3.9 shows four examples taken from varying depths down core 56-10 32VE. Coercivity varies from 40 to 60 mT and increases with depth. SIRM/ χ ratios also increase with depth from 12.8 kAm⁻¹ at 112cm to 21.1 kAm⁻¹ at 343cm.

Curie Point Analysis

Curie point analysis for a typical sample from the Peach area is shown in fig 3.10. The extract from core 56-10 28VE shows a loss of magnetisation at 580°C, characteristic of magnetite.

3 Geological core logs

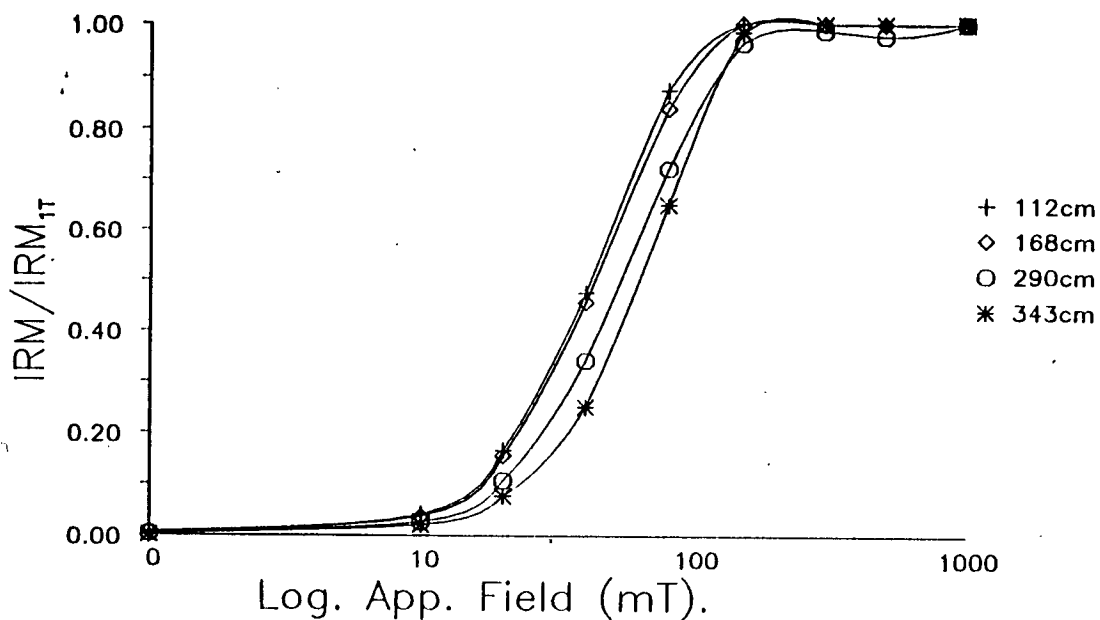
These logs were compiled from observations made by the duty geologists on board the sampling vessel that recovered the cores. Where appropriate, more detail has been added by the author based on laboratory observations. An example of a geological core log is shown in fig 3.11.

3.5 Discussion

1 Palaeomagnetic Parameters

The palaeomagnetic data shown in fig 3.4 for core 56-10 32VE is typical for cores studied in the Peach area. There is a clearly measurable and consistent signal downcore. The record is too recent to record a change in magnetic polarity and lacks sufficient features for a satisfactory match to a secular variation master curve, for example that of Turner and Thompson (1981). Interpretation is further complicated by a slight alignment mismatch as seen in the declination data between core sections. Core 56-10 32VE suffered less from misalignment between 1m sections than other cores studied. Alignment problems of this nature were found to be present to varying degrees in all BGS cores.

The absolute value of the palaeomagnetic inclinations is low for the latitude of the sample sites. An inclination of 71° would be expected for a latitude of 56° in the Peach area using a geocentric axial dipole field model. For such a



Depth (cm)	SIRM/ χ (kAm^{-1})	S
112	12.8	+0.81
168	12.0	+0.78
290	16.9	+0.74
343	21.1	+0.75

- Fig 3.9 Normalised IRM acquisition data for subsamples taken from various horizons in core 56-10 32VE. SIRM/ χ values are also included.

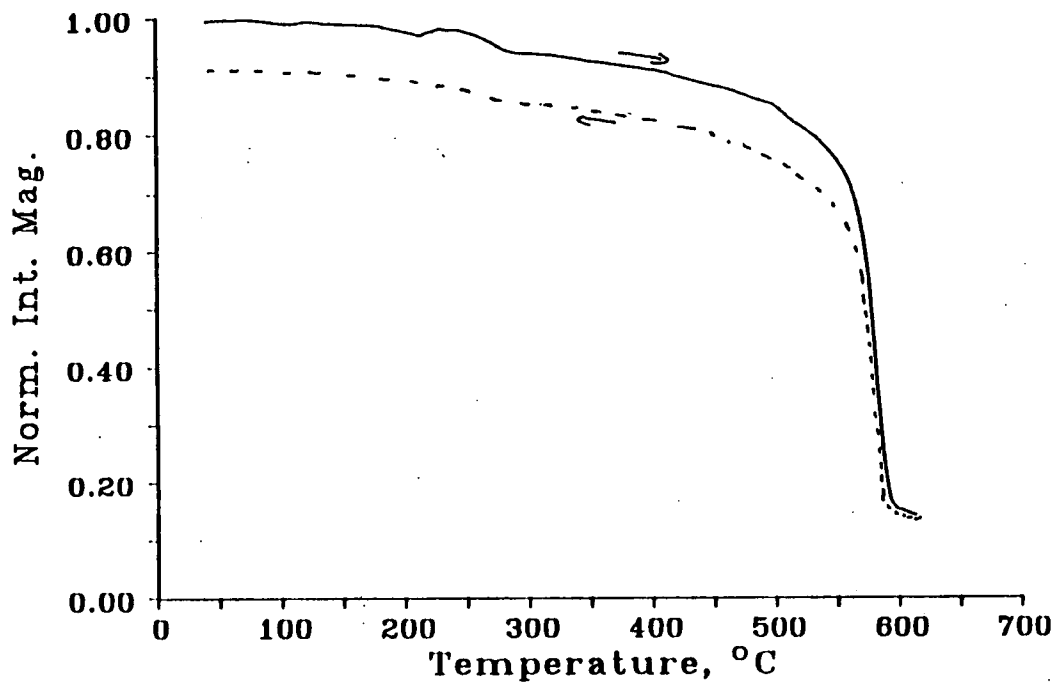
model the simple equation $\tan I = 2 \tan \lambda$ where I is the inclination and λ the latitude, provides the approximate inclination value.

Demagnetisation data for pilot samples from core 56-10 32VE (fig 3.5) reveal an NRM dominated by one component. There are signs in some samples of a minor secondary component, suggesting some slight realignment of magnetic remanence carriers after their initial acquisition of a DRM. The presence of multiple components of magnetisation was considered very likely in samples from vibrocores as the vibration that provided the energy for core penetration into the sediment could also be expected to realign magnetic grains in the present magnetic field at the coring site. The fact that secondary components are only seen in some and not all subsamples suggests that realignment depends on varying downcore lithology. One possibility could be that the sedimentary horizons which provided the greatest resistance to penetration would be subjected to a vibration longer so resulting in a greater chance for grain realignment. In all cases where a secondary component was found, the primary component still contributed over 90% of the natural magnetic remanence.

2 Mineral Magnetic Parameters

IRM acquisition curves were grown on pilot samples in order to determine the magnetic mineralogy of the cores. Four examples of IRM acquisition curves are shown in fig 3.9. In the 60 subsamples examined, saturation was seen to occur in fields of approximately 100 to 120mT, with 90% of the saturation IRM occurring before 100 mT. Saturation at these fields indicates a magnetite dominated magnetic mineralogy. The remaining 10% of the saturation remanence can be accounted for by high coercivity minerals, for example haematite. Variation in the shape of IRM curve below 100mT are associated with changes in magnetite grain sizes. The IRM curves for the four samples from core 56-10 28VE show a trend towards slightly increasing coercivity with core depth.

Curie point analysis on extracts from the IRM subsamples (fig 3.10) shows a loss in magnetisation at approximately 580°C, as would be expected for magnetite. (table 2.2) The shape of the curve is that of pure magnetite (see fig 2.13), with no evidence of an initial decay or regaining of magnetisation caused by the presence of titamagnetites. The minority high coercivity component



- Fig 3.10 Example of curie point analysis on magnetic extracts from core 56-10 28VE. Extraction was by magnetic methods (see chap 2).

was not evident in the Curie balance results, either being masked by the dominant magnetite component or more likely being difficult to extract with the permanent magnet technique.

Whole core susceptibility data provided information for all cores available from the Peach area. The examples shown in fig 3.7 illustrate some of the principal susceptibility patterns seen. Values of whole core susceptibility varied both within and between cores. The variation between cores was much greater than the variation downcore, and these between core differences could be used as a basis for identifying different surface sediment types, as shown in fig 3.8. By taking a median value for each core, it was possible to produce point data to compare with sedimentary types defined by other methods. This susceptibility mapping approach was found to be effective as long as downcore fluctuation in susceptibility was limited compared to the between cores susceptibility changes. Variation in susceptibility between cores was several orders of magnitude in the Peach area. For example, there is a marked contrast in susceptibility between cores 56-09 169VE (susceptibility approximately 6 instrument units), 56-10 24CS (susceptibility approximately 50 to 60 instrument units) and 56-10 28VE (susceptibilities in the range 180 to 700 instrument units).

Superimposed upon the whole core susceptibility profiles of many cores were spikes associated with the presence of glacial dropstones. Such features are shown on the profile for core 56-10 28VE in fig 3.7. Dropstones were easy to detect, magnetically, visually and by X-Ray. The dropstone effects were manually removed when calculating median susceptibility values for the sediment.

Mass specific susceptibility was found to be the same for subsamples from both ship and shore measurements. This consistency is shown by table 3.1 for two chemical standards, confirming the validity of comparing ship-based and land measurements.

Conventional heavy mineral (heavy liquid, panning) separation techniques proved inadequate for use on the Peach area materials on account of to the particle size distribution. As the majority of the Peach sediment was less than 63 μm in size, clogging occurred during filtration. Dispersal of these small particles also proved difficult and rendered the separation techniques

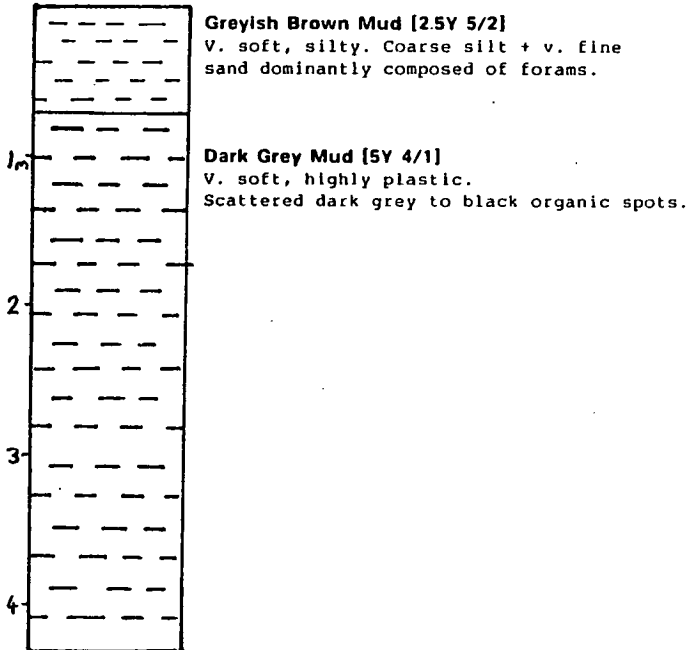
impractical.

Susceptibility horizons coincided well with changes in lithology (as recorded by the ship's duty geologist) once the effects of dropstones had been manually filtered out. On account of the limited down core variation in lithology in the Peach cores, the downcore changes in susceptibility are not as immediately obvious as in for example cores taken in the Witch Ground Basin (see chapter 5). Nevertheless, some general susceptibility trends with depth are still clearly visible. For instance, in core 56-10 32VE (fig 3.11) a change at approx 70cm from very soft, silty greyish brown mud to very soft, highly plastic dark-grey mud is reflected in both susceptibility (fig 3.6) and palaeomagnetic intensity (fig 3.4). Both the latter sets of magnetic data show a graded change occurring over a zone from the top of the core to about 50cm down core. In many respects the magnetic results are superior to the geological observations as they can show a gradual but significant change without being restricted to an exact changeover horizon.

IRM acquisition data for the two sediment types in core 56-10 32VE illustrated a similar magnetite dominated mineralogy to each other but with different total concentrations of magnetic minerals, reflected in the differing mass specific susceptibility and SIRM data for each sediment type.

3 Deck Operations

Actual observations of BGS sample ship deck operating procedures provided an insight into practices which could have an influence on the magnetic properties of the samples recovered. Alignment of 1m sections of cores tended to be not as rigidly applied as would be the case in a study specifically designed for palaeomagnetism. The core cutting process provided the greatest hazard for core contamination, a rusty hack-saw being the standard cutting tool. To avoid any undue interference from this process, any magnetic measurements taken within 5cm of the end of a core section have been treated as unreliable. Another problematical aspect of core recovery is the tendency for core material to expand when recovered from deep water (over 1600m). This remains a somewhat unquantifiable aspect of continental shelf sampling operations.



- Fig 3.11 Geological log of core 56-10 32VE based on observations on board MV British Magnus.

3.6 Significant Points

1) A measurable NRM can be obtained from a vibrocore.

2) The Peach area palaeomagnetic records were of insufficient length to show a magnetic reversal stratigraphy.

3) The recorded inclination is shallow for the latitude.

4) The secular variation pattern is clear, but does not have sufficient features for a match to a master-curve.

5) The magnetic mineral assemblage appears to be dominated by low coercivity magnetite, with some evidence of minor amounts of a high coercivity mineral.

6) Due to the simple magnetic mineral assemblage in the Peach area, susceptibility measurements offer a means of mapping sediment type.

CHAPTER 4 FLETT AREA

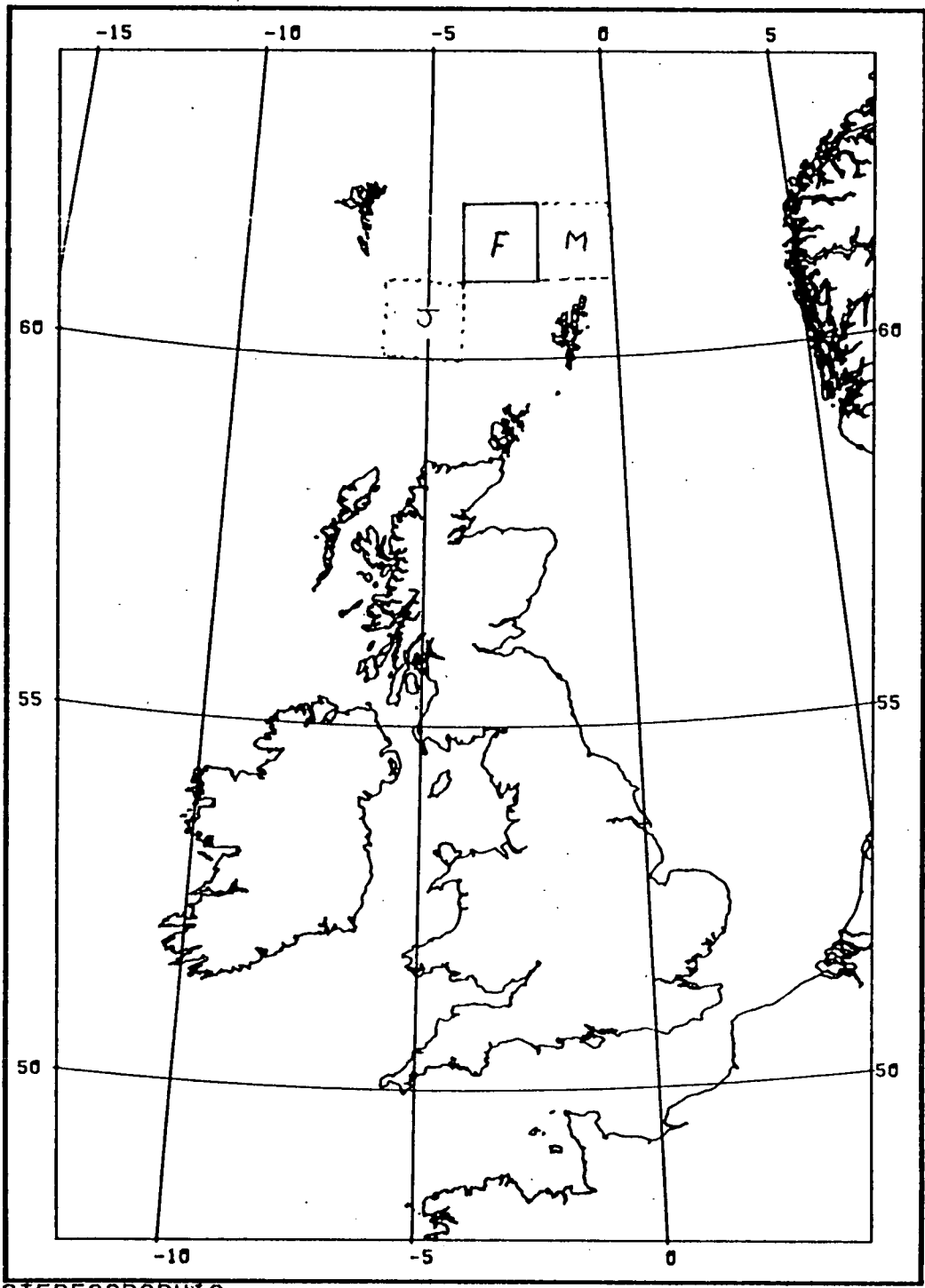
4.1 Background

Core material from the Flett area (fig 4.1) was obtained using the survey ship *M.V. Kommander Subsea* during October 1988. The *Kommander Subsea* cruise was arranged by BGS to complete geological survey work previously undertaken in the Miller, Flett and Judd regions. The cruise gave the author an opportunity to test the newly acquired Bartington whole core susceptibility equipment whilst participating as a crew member on board the *M.V. Kommander Subsea*.

A selection of fresh material from a range of locations was recovered. The majority of core sites fell within the Flett area, with occasional cores being taken in the Miller and Judd regions. Sampling station positions are shown in fig. 4.2. At several sample stations, duplicate cores were recovered and are marked in fig 4.3 by suffixes 'i' and 'ii'. Whole core susceptibility profiles were taken on all duplicates to compare the consistency of both the coring technique and whole core susceptibility measurements.

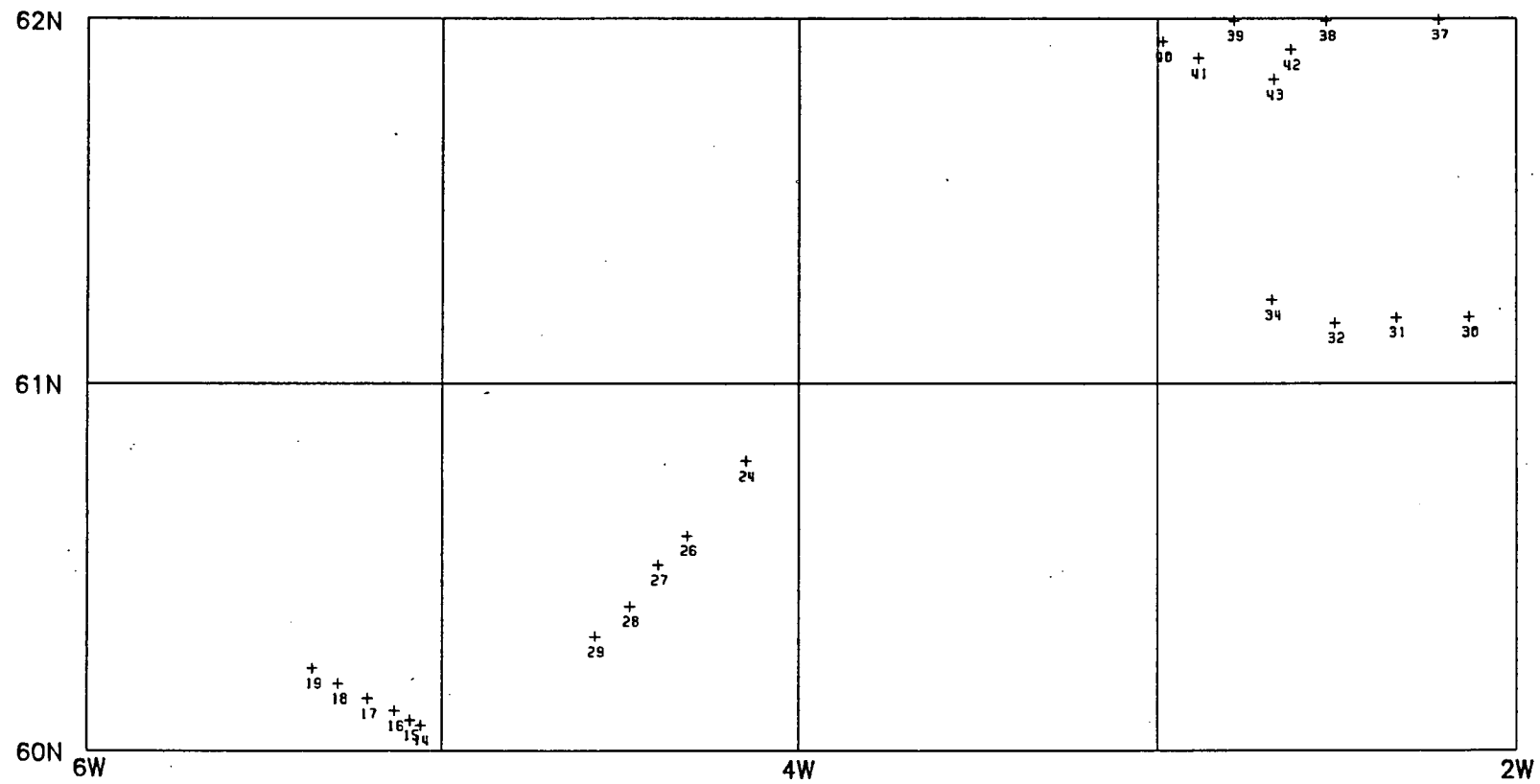
Following retrieval from the sea bed, most cores were split on board the *Kommander Subsea*. Split cores could then be subsampled. The subsamples were retained for fuller magnetic analysis on shore.

After the return of the *M.V. Kommander Subsea* to port, cores were transferred to BGS core stores. From here, they were easily accessible to the author for the subsequent two years (1986-1988). Ready access to the core store gave an opportunity to carry out regular repeat whole core susceptibility measurements on several cores. The results from the repeat measurements gave an indication of any change in magnetic properties of the cores during storage.



STEREOGRAPHIC
 SCALE = 1 : 10000000

- Fig 4.1 The position of the Flett sea area with respect to the British Isles. The adjacent Miller and Judd areas are also shown.



- Fig 4.2 Sample station positions in the Flett area.

4.2 Sampling and Measurement Procedures

1 Shipboard Procedures

The sampling and measurement routine on *M.V. Kommander Subsea* consisted of two principal operations.

a) The whole core susceptibility equipment was used to measure as many cores as possible whilst complying with BGS deck operations. 36 gravity cores were measured in total.

b) Subsamples were taken from various sedimentary horizons within the cores. The subsample positions were selected on the basis of whole core susceptibility measurements and geological logs of the core material.

Before using the whole core susceptibility equipment, it was necessary to establish an operating position with the minimum possible background electromagnetic interference. A straight-forward noise monitoring exercise was conducted in various locations physically suitable for operating the Bartington equipment. This exercise consisted of continuous free-air measurements with a note being made of the characteristics of any drift seen. It was found that there were two categories of electromagnetic noise.

(i) On a large scale, electro-mechanical plant operation associated with the ships diesel electric propulsion systems was found to cause occasional disruption in the Bartington equipment wherever it was sited on the ship. The occasional disturbance was usually associated with sudden changes in the power state of the ships thruster motors. Such changes occurred most frequently whilst the ship was maintaining position at a sample station. Consequently whole core susceptibility measurements were best taken while the ship was cruising steadily between sampling positions.

Disruptions caused by the ships power units were short lived and were identified as sudden jumps in calibration value. The magnitude of disturbance was up to 20% of the value of the calibration standard, some 5 instrument units on the arbitrary susceptibility scale as defined in chapter 2. A disturbance of this magnitude was relatively insignificant in the case of Flett cores which generally had arbitrary susceptibility values of 100 to 200.

However, such a disturbance would represent a considerable source of error in areas with low susceptibility sediments, for example parts of the Peach area (chapter 3) where whole core susceptibility values averaged less than 10 instrument units.

(ii) On a smaller scale, electromagnetic interference was found to come from local electrical appliances and fittings. The worst interference was found to be associated with operational VDUs which completely disabled the Bartington meter. Once the Bartington Bridge was positioned clear of local interference sources, an instrument drift level of less than 1 instrument unit per minute was maintained. Constant calibration checks against a chemical standard before and after measuring every metre core section were carried out.

2 Shore based procedures and measurements

The following sampling and measurement techniques were employed on shore.

(a) Whole core susceptibility measurements.

As a follow up to the whole core susceptibility measurements undertaken on M.V. Kommander Subsea, two cores previously measured for whole core susceptibility at sea were selected for repeat whole core susceptibility measurement on shore. The repeat measurements were carried out at 6 monthly intervals for the period 1986-1988 on cores 61-03 42CS and 61-03 30CS. Both cores had been split onboard ship and then stored in protective lay-flat polythene tubing.

(b) Additional subsampling.

Additional subsamples were taken from cores to supplement those taken at sea. During subsampling, a note was made of any samples came from sedimentary horizons that showed signs of disturbance. Core 61-03 42CS was subsampled contiguously.

(c) Palaeomagnetic analysis.

Palaeomagnetic measurements for NRM were undertaken on all subsamples using either a Molspin fluxgate magnetometer or a cryogenic magnetometer. A.F. demagnetisation studies were undertaken for approximately 8 samples from

each core.

(d) Mineral magnetic measurements.

Mineral magnetic analysis was carried out on subsamples from 9 cores. There were approximately 8 subsamples from each core except for 61-03 42CS where a contiguous set of subsamples were available. χ and IRM acquisition measurements were taken for each subsample.

(e) Magnetic extraction.

Magnetic extracts were obtained from samples which showed the highest SIRM. The extracts were then used for Curie point analysis.

(g) Geological and Geotechnical work.

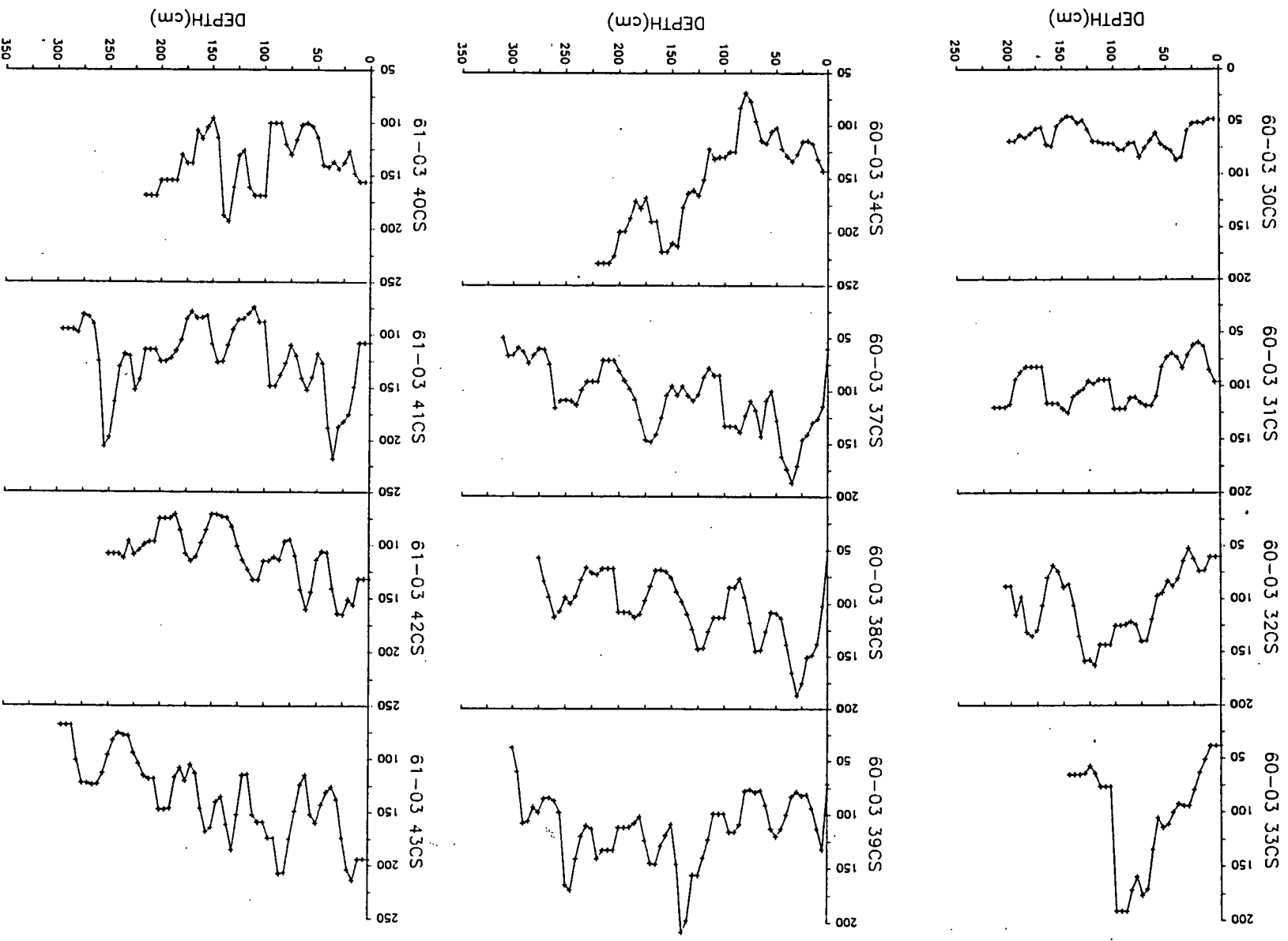
Geological logs and geological data for Flett cores were obtained from Dr A. Stevenson of the BGS. These data sets were then compared to whole core susceptibility profiles and used in the interpretation of changes on magnetic properties of subsamples.

4.3 Results

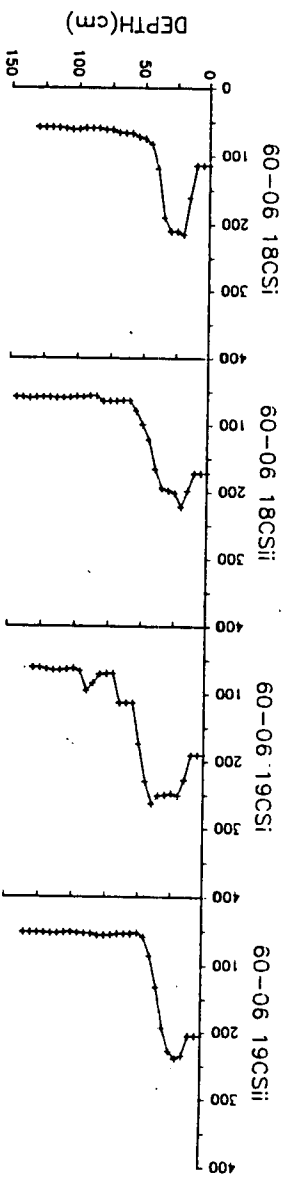
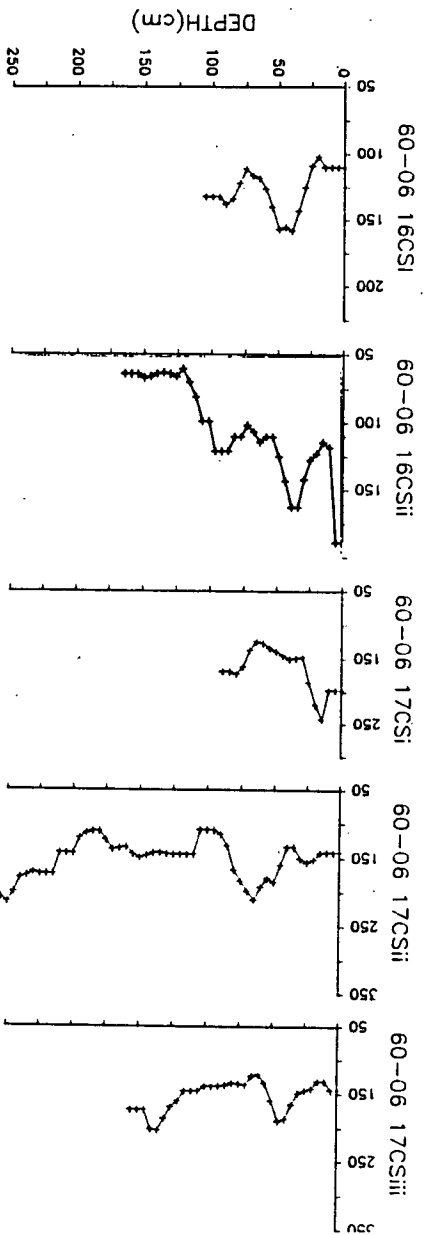
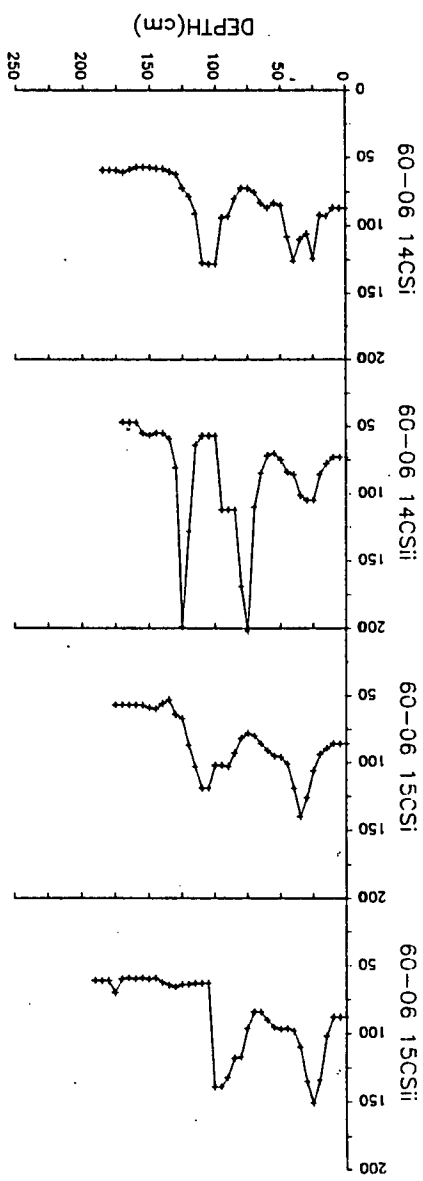
1 Whole core susceptibility results

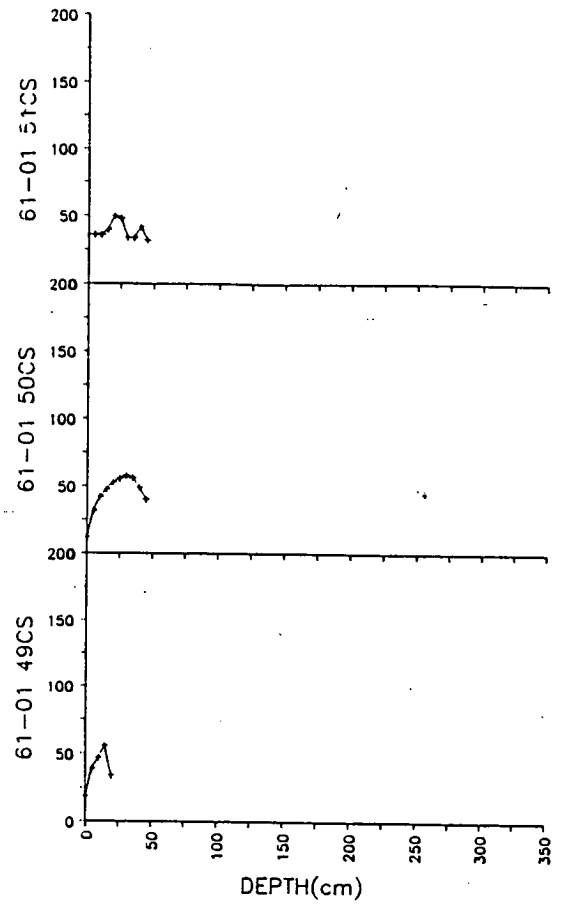
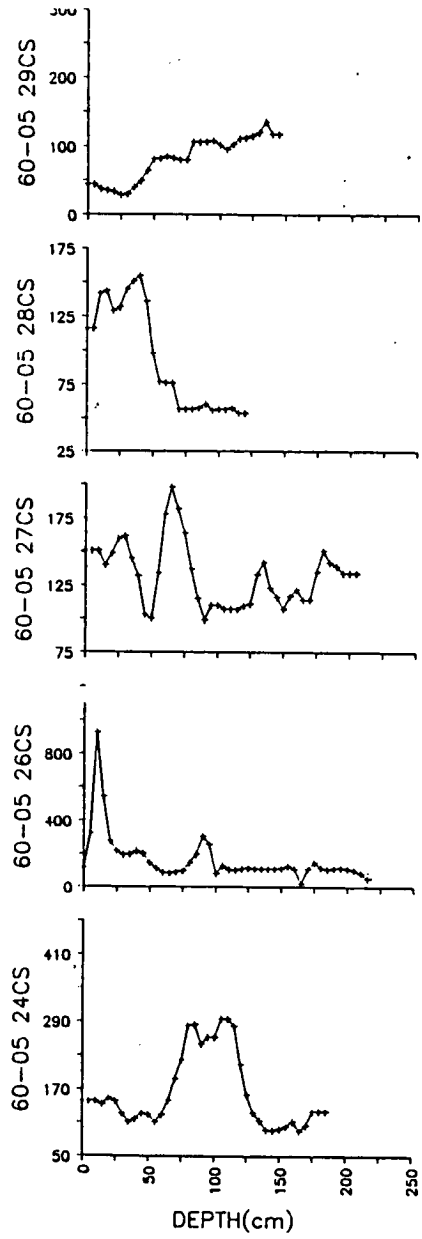
Whole core susceptibility results for 34 cores are shown in figs 4.3a, 4.3b and 4.3c. These whole core susceptibility profiles are all based on measurements obtained whilst onboard *M.V. Kommander Subsea*. The length of core varied between 25cm (core 61-01 49CS) and 300cm (core 60-03 37CS). Whole core susceptibility values ranged from a low of 23 instrument units for 61-01 49CS to a high of over 800 instrument units for 60-05 26CS. The majority of the cores from the Flett area showed considerable downcore variation in whole core susceptibility. The exceptions to this variation were 61-01 49CS, 61-01 50CS and 61-01 51CS which were physically too short to record much variation.

Of the duplicate cores (suffixes i and ii), nearly all have very similar patterns of downcore variation in susceptibility. The three triplicate cores for site 60-06 17 show dissimilar susceptibility patterns due to different amounts of sediment



- Fig 4.3a-c, Whole core susceptibility profiles for cores from the Flett area. Susceptibility units are arbitrary.





recovered.

The downcore variation patterns are generally graded over several data points. However, some cores show abrupt changes in susceptibility warranting individual mention. Core 60-03 33CS has a rapid drop in susceptibility from 200 to 50 instrument units at a depth of 125cm. A similar feature is seen in 60-06 15CSii at 125cm. Cores 60-06 14CSii and 60-05 26CS exhibit sudden spikes in their susceptibility profiles. In the case of 60-03 26CS there is a sudden jump from 50 to over 800 instrument units in the top 25cm.

2 Repeat whole core susceptibility results

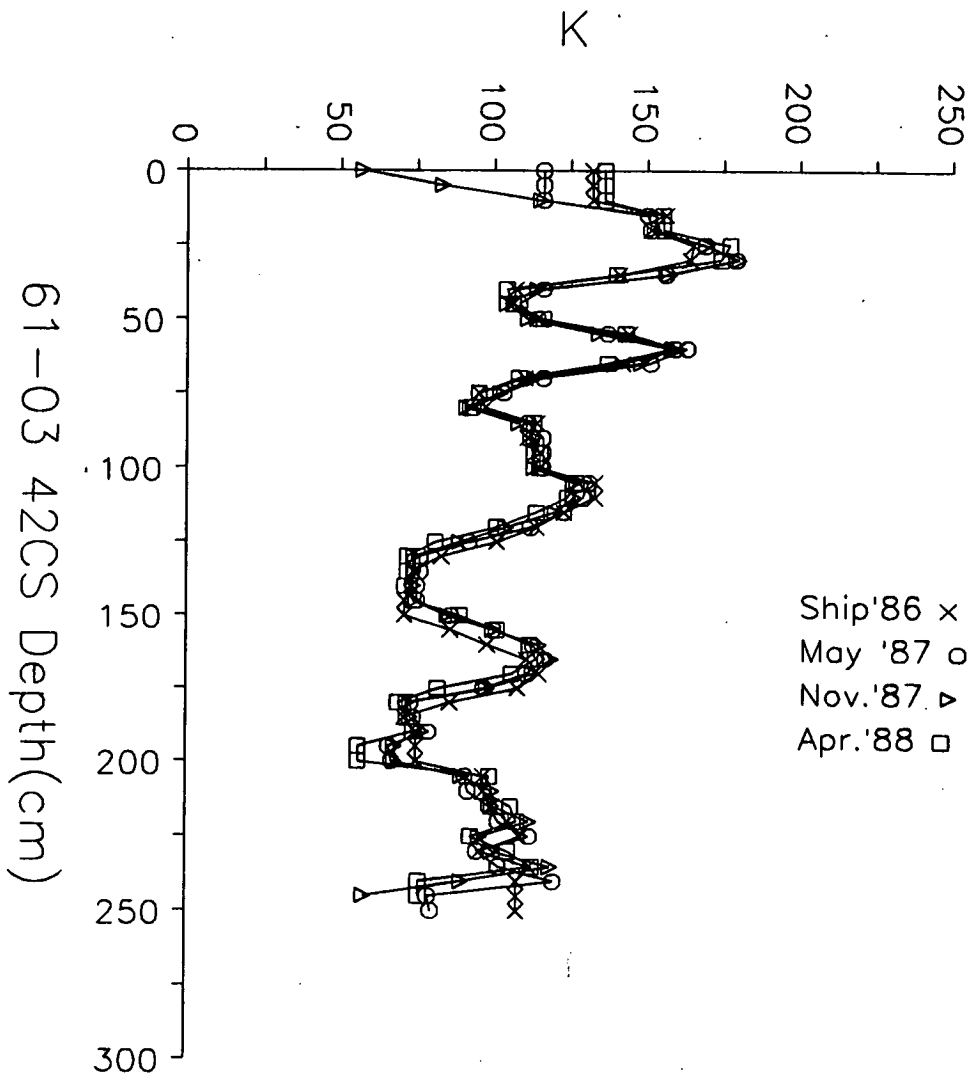
Figs 4.4a and 4.4b show the whole core susceptibility profiles for cores 61-03 42CS and 61-03 30CS repeatedly measured between 1986 and 1988. In the case of 61-03 42CS, all the susceptibility profiles follow a near identical pattern, steadily fluctuating between 50 and 175 instrument units. The whole core susceptibility profiles for 61-03 30CS show a similar consistency but with a slight offset in the profiles at 100cm coincident with the ends of a core section..

3 Repeat subsample measurements.

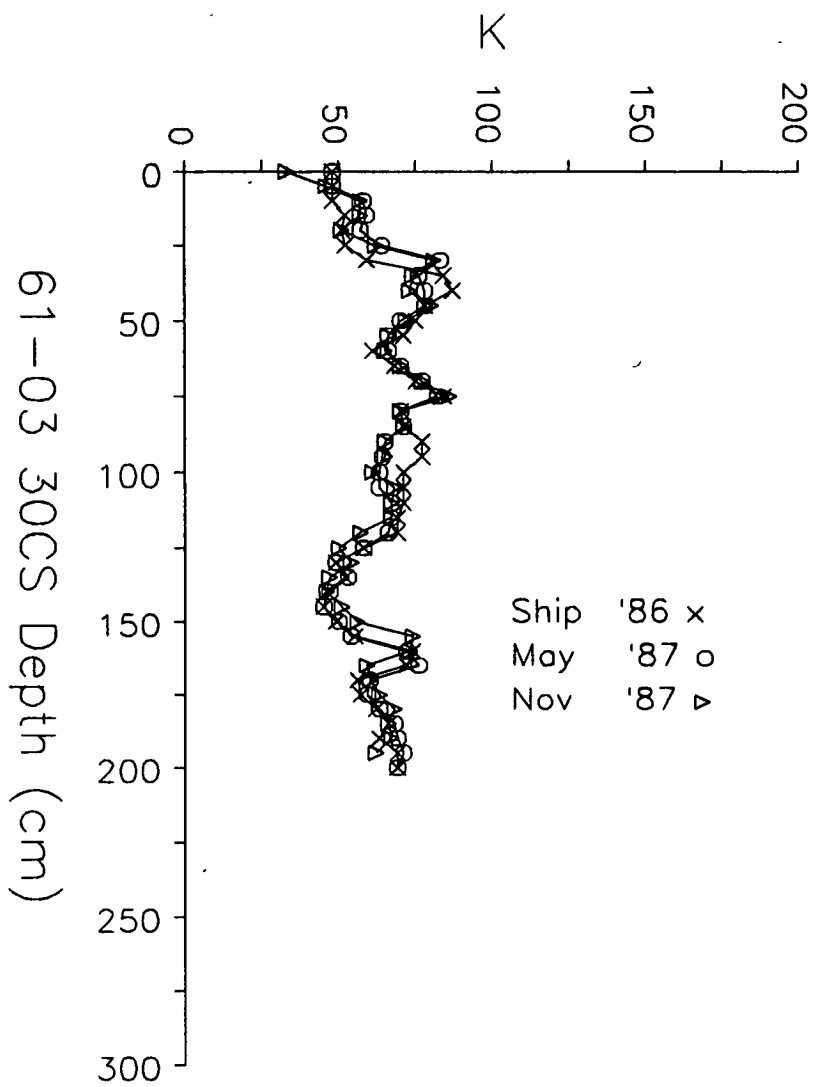
Data for repeated measurements of subsamples from core 61-03 42CS are shown in table 4.1. Volume susceptibility shows little evidence of a change between 1986 and 1988, the maximum change being approximately 9% in samples from the top 5cm of the core. The average change in susceptibility downcore is less than 3%. SIRM data in table 4.1 exhibits greater change than susceptibility, the minimum change being 4% with one sample showing a 16% increase. The average change in SIRM is approximately 10%. SIRM/ χ ratio data for the 1986-88 period shows the cumulative effects of changes in susceptibility and SIRM. Samples from the top 10cm of core 61-03 42CS show changes in SIRM/ χ ratio of 17%. However, the average change in SIRM/ χ ratio is approximately 7%.

4 Mineral Magnetic Data from subsamples

Mineral magnetic data were available for 9 cores from the Flett area. The ranges in χ and SIRM/ χ ratio values for each core subsampled are shown in table 4.2. Subsamples from core 61-03 42CS showed the greatest range of χ



- Fig 4.4a Whole core susceptibility profiles for core 61-03 42CS. The measurements were repeated every 6 months from October 1986 (Ship) to April 1988 giving a series of four measurements.



- Fig 4.4b Whole core susceptibility profiles for core 61-03 30CS. The measurements were repeated every 6 months from October 1896 (Ship) to November 1987 giving a series of three measurements.

and SIRM/ χ ratio values and it was consequently selected for continuous subsampling .

Fig. 4.5 shows the mineral magnetic data for a contiguous set of subsamples from core 61-03 42CS. This data consists of whole core susceptibility, χ , SIRM, SIRM/ χ , S ratio and HIRM. The whole core susceptibility data shows a gentle but continuous fluctuation downcore between a maximum 160 and minimum 60 instrument units. χ data shows a higher frequency of variation than whole core susceptibility. χ values peak at just over $3 \mu\text{m}^3\text{kg}^{-1}$ in the top 50cm, decreasing to an average of $1.25 \mu\text{m}^3\text{kg}^{-1}$ in the lower reaches of the core. SIRM data has a very similar pattern to χ with peak values of $100 \text{mAm}^2\text{kg}^{-1}$ in the top 25cm steadily decreasing to fluctuate between 20 and $40 \text{mAm}^2\text{kg}^{-1}$ further downcore. In contrast to the whole core susceptibility, χ and SIRM data, the SIRM/ χ ratio remains virtually constant downcore at approximately 20kAm^{-1} . The only deviation from this value are peaks to about 30kAm^{-1} seen in the top 25cm and at a depth of 160cm. The S ratio varies inversely with the SIRM/ χ ratio and shows two dips in value, one in the top 25 cm and the other at 160 cm. HIRM data reflects the pattern seen in SIRM, but with less amplitude of variation. A peak value for HIRM of $35 \text{mAm}^2\text{kg}^{-1}$ is seen in the top 25cm, reducing to an average value of $7 \text{mAm}^2\text{kg}^{-1}$ further downcore. Occasional peaks in HIRM are seen at 160cm ($12 \text{mAm}^2\text{kg}^{-1}$) and 240cm ($10 \text{mAm}^2\text{kg}^{-1}$), similar to the peaks seen in χ and SIRM at these depths.

5 IRM acquisition curves

Two IRM curves representing the extreme range of data from 61-03 42CS are shown in fig 4.6. The curve drawn from a subsample taken from 4.5cm does not reach saturation until approximately 120mT whereas the sample from 130cm has saturated by 100mT.

6 Thermomagnetic Analysis

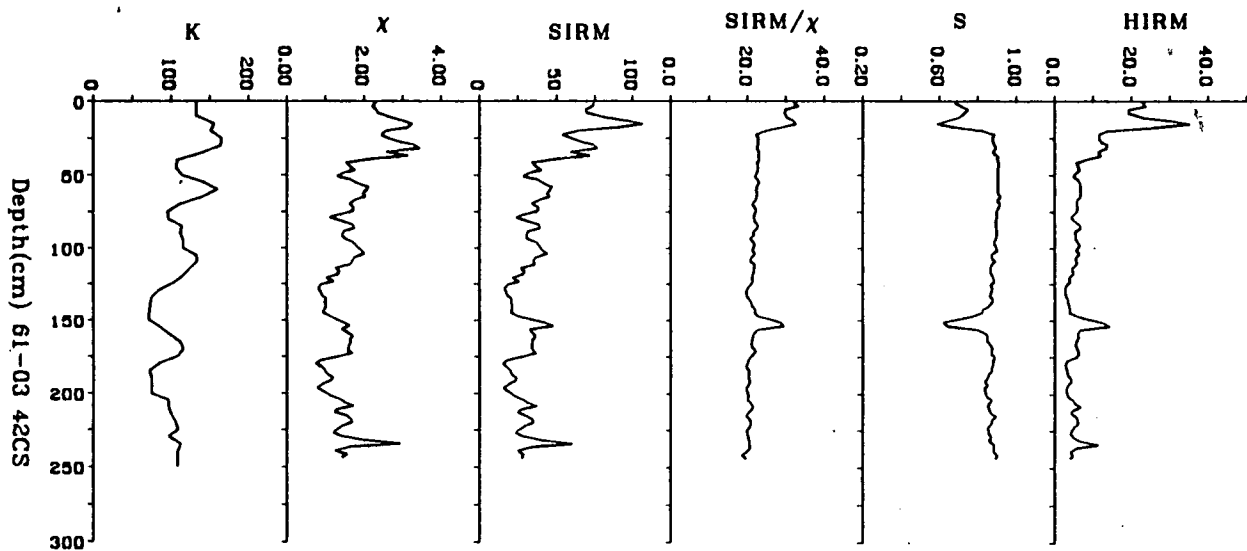
Fig 4.7 shows the thermomagnetic analysis results from an extract taken from core 61-03 42CS. A loss of magnetisation is seen at approximately 580°C . Both heating and cooling curves are very similar, the magnetisation following the same path during heating and cooling cycles.

Sample depth	Vol. Susc.			SIRM/ χ kAm ⁻¹			SIRM mAm ² kg ⁻¹		
	1986	1988	% change	1986	1988	% change	1986	1988	% change
2.5	6.79	7.37	+9	36	30	-17	244	221	-9
4.5	7.23	7.88	+9	36	31	-16	260	244	-6
10.0	9.97	9.99	+3	30	35	+17	299	350	+16
22.5	14.16	14.49	+2	24	22	-8	339	319	-6
35.0	14.81	14.94	+1	23	20	-13	340	299	-12
43.5	9.12	9.03	-1	23	21	-9	210	190	-10
57.5	14.31	14.21	-1	22	21	-4	315	298	-5
66.5	10.40	10.37	-1	21	20	-5	218	207	-5
83.5	9.50	9.76	+3	24	21	-13	228	205	-10
104.5	12.02	12.33	+3	23	21	-9	276	259	-6
130.0	5.77	5.79	00	21	20	-5	121	116	-4
170.0	8.07	8.19	+1	23	21	-9	186	172	-7
212.0	7.53	7.75	+3	21	19	-10	158	147	-7
232.0	9.50	9.91	+4	22	19	-14	209	188	-10

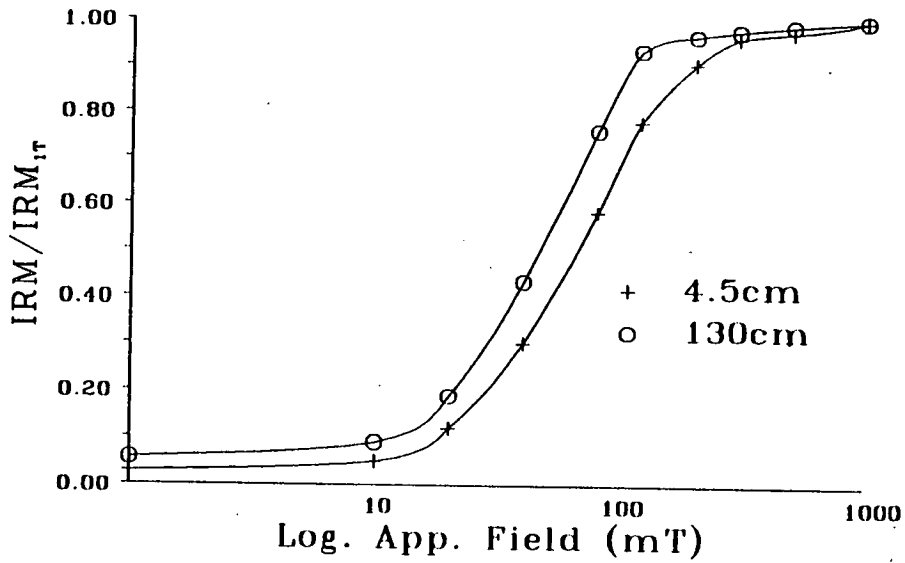
Table 4.1 - Comparison of volume susceptibility and SIRM/ χ data for subsamples from 61-03 42CS. The 1986 data set was obtained just after sample recovery. The 1988 data set shows measurements taken on the same samples as 1986, but after two years in storage.

Core Number		χ	SIRM	SIRM/ χ
60-05 22CS	min	0.18	2.9	15.5
	max	0.19	3.0	15.6
60-05 24CS	min	0.785	15.0	20.2
	max	2.713	62.0	23.1
60-05 28CS	min	0.318	5.0	5.5
	max	1.419	32.0	32.0
60-05 29CS	min	0.35	7.1	19.7
	max	1.17	27.7	23.9
61-03 30CS	min	0.29	5.3	17.5
	max	1.96	71.0	36.0
61-03 31CS	min	0.45	9.0	20.2
	max	1.16	25.0	21.7
61-03 32CS	min	0.80	18.0	17.7
	max	1.67	46.0	27.5
61-03 42CS	min	0.80	17.0	21.2
	max	2.60	62.0	36.6

Table 4.2 The range of mineral magnetic data for subsamples from 9 Flett cores. Units: χ ($\mu\text{m}^3\text{kg}^{-1}$); SIRM ($\text{mAm}^2\text{kg}^{-1}$); SIRM/ χ (kAm^{-1}).



- Fig 4.5 Mineral magnetic data for core 61-03 42CS. Data based on results from contiguous subsample set. Units: K dimensionless, χ $\mu\text{m}^3\text{kg}^{-1}$, SIRM $\text{mAm}^2\text{kg}^{-1}$, SIRM/ χ kAm^{-1} , 'S' dimensionless ratio, HIRM $\text{mAm}^2\text{kg}^{-1}$.



Depth (cm)	SIRM/ χ kAm ⁻¹	S
4.5	36.64	0.71
130.0	21.56	0.83

- Fig 4.6 IRM acquisition curves for subsamples from core 61-03 42CS. The two examples shown represent the extremes of coercivity found downcore. The depths show the position of the sample downcore. SIRM/ χ and S values are also included.

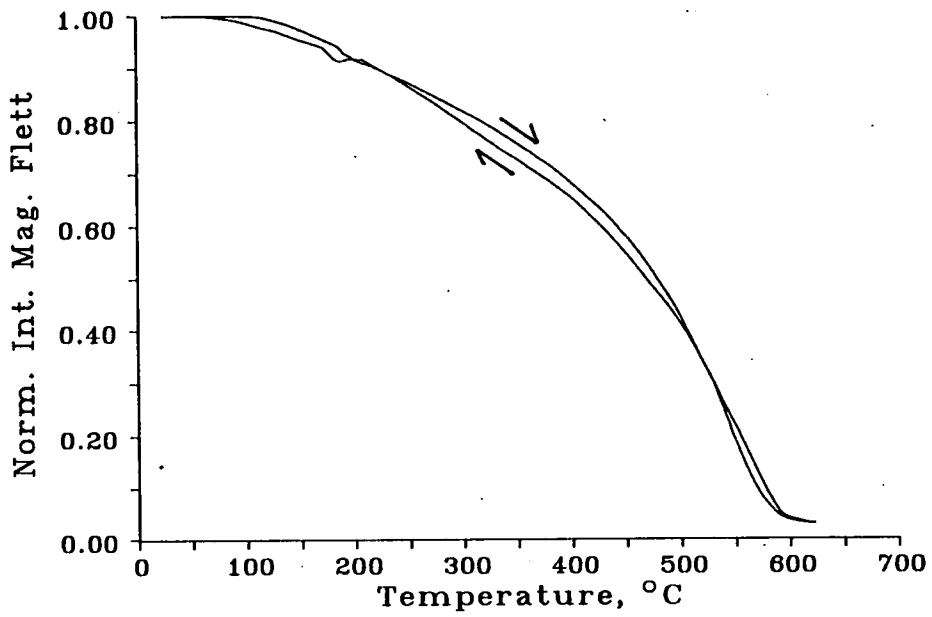
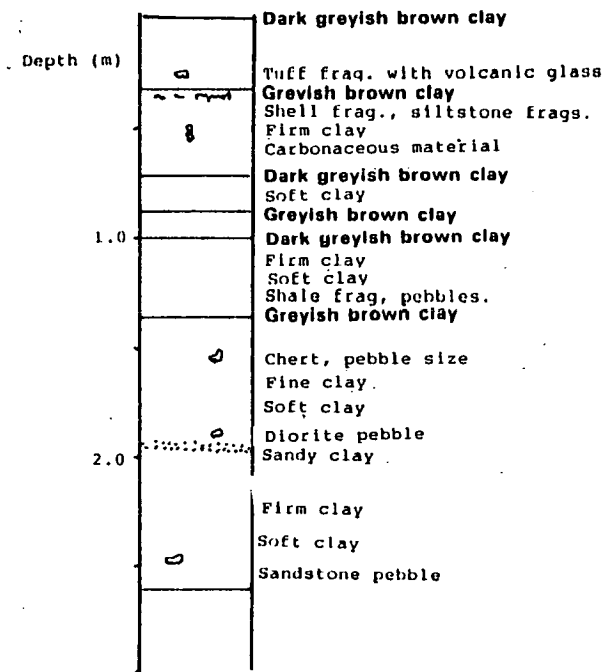
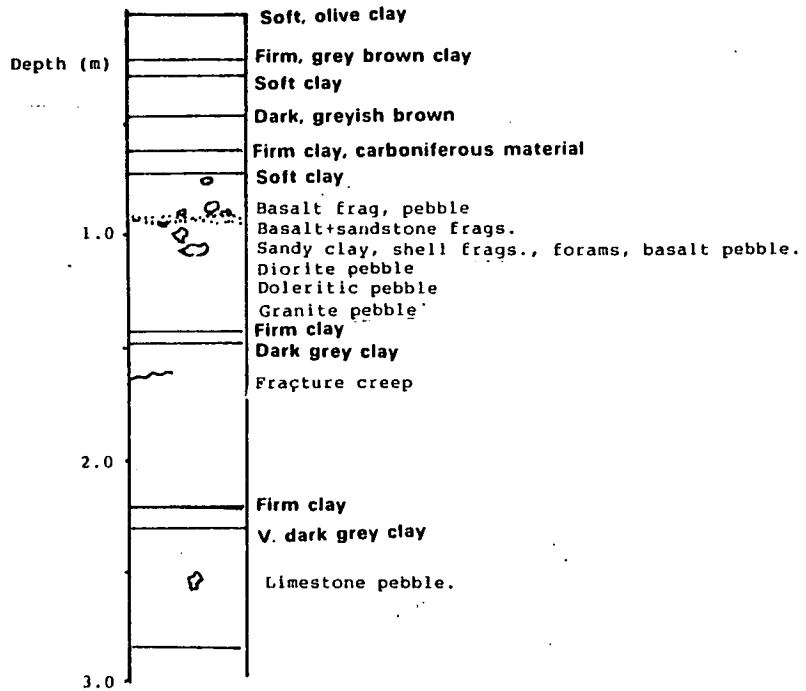
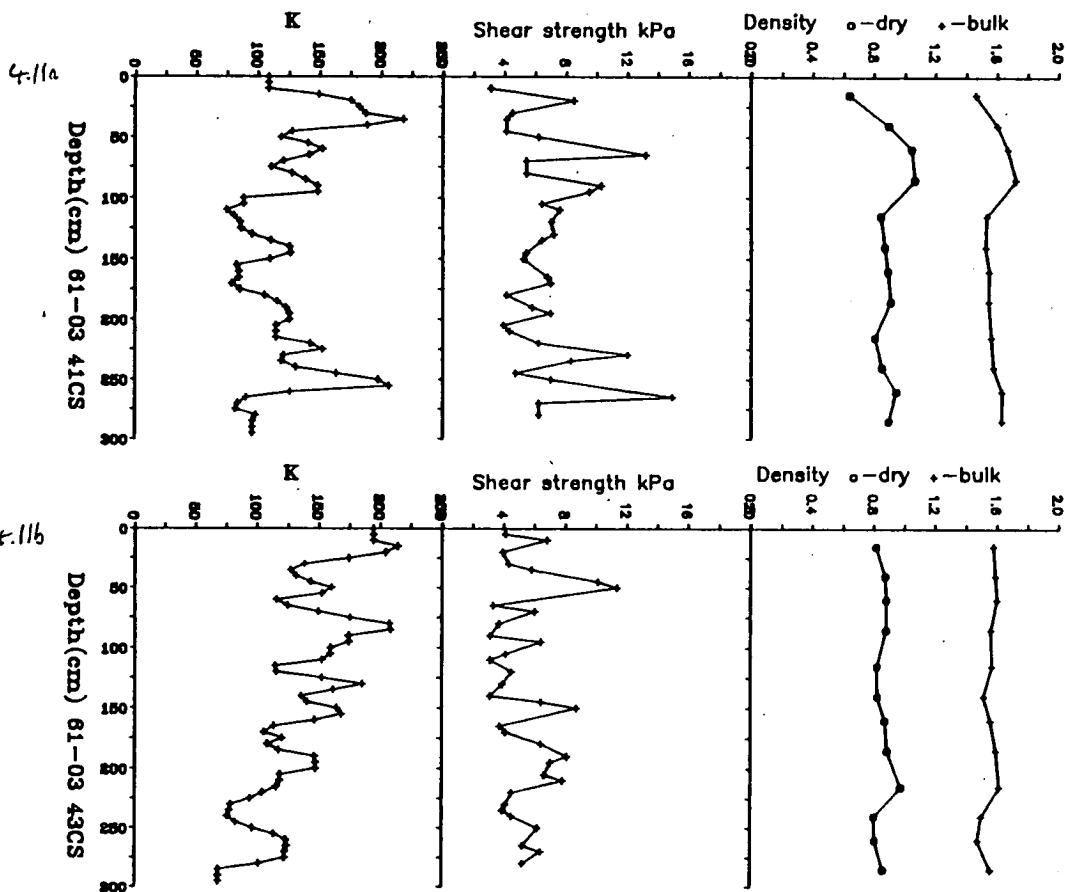


Fig 4.7 Curie point analysis data for an extract from core 60-05 24CS. Extraction was by magnetic means (see chapter 2).



- Fig 4.10a and b Geological logs of cores 61-03 41CS and 61-03 43CS prepared by A. Stevenson.



- Fig 4.11a Geotechnical data for core 61-03 41CS with K included for comparative purposes. Units: K- dimensionless, shear strength- kPa, density- mgm⁻³. Geotechnical data provided by A. Stevenson.

- Fig 4.11b Geotechnical data for core 61-03 43CS with K included for comparative purposes. Units: K- dimensionless, shear strength- kPa, density- mgm⁻³. Geotechnical data provided by A. Stevenson.

in bands ranging from 1cm to 10cm in thickness. Geotechnical data (fig 4.11) shows considerable fluctuation downcore with data in the ranges 2–16 kPa. Conversely, both wet and dry densities are relatively constant downcore.

4.4 Discussion

1 Whole core susceptibility

The downcore variation in wholecore susceptibility in all Flett cores can largely be attributed to changes in lithology. Taking a comparison of the whole core susceptibility profile and geological log of core 61-03 41CS (fig 4.10) as an example, several trends can be picked out. The large clay bands provide a general background variation, over distances in the order of tens of centimetres. Superimposed on this low frequency variation was high frequency change due to local features. A typical example of a local feature is the peak in susceptibility in the top 25cm of core 61-03 43CS due to the presence of a tuff and volcanic glass.

Features from whole core susceptibility profiles (fig 4.3) provide a useful insight into the quality of both whole core susceptibility measurement and the coring technique itself. Sudden changes in susceptibility, for example at 100cm in core 61-03 33CS are sometimes coincident with the division of the core into 1m sections. These coincidences suggested the possibility of recalibration problems with the Bartington Bridge in between 1m sections. However, examination of sudden change features in duplicate cores relieves the recalibration doubt. For example, cores 60-06 15CSi and 60-06 15CSii both exhibit a sharp drop in susceptibility, occurring at 100 cm in 60-06 15CSii but spread over 100 to 125cm in 60-06 15CSi. If the core 60-06 CSii result had been examined in isolation, miscalibration would have been expected as the sudden change in susceptibility is coincident with a core section ending. Taking the core 60-06 CSi result into account where the same sudden change seen in core 60-06CSii is spread across some 25cm of core suggests that there is a lithology controlled change in susceptibility that just happens to be coincident with a core end in core 60-06 CSii.

Examination of the susceptibility profiles from all duplicate cores gives an indication of the quality of the coring technique. The profiles for sites 60-06 18 and 60-06 19 show excellent correlation between duplicates. However, the

triplicate data for site 60-06 17 shows significant differences in the amount of core recovered, whilst the profiles for site 60-06 14 show quite different susceptibility patterns. The fact that in the case of some duplicates, for example 60-06 17CS cores, there are widely differing amounts of core recovery suggests that the gravity coring process is prone to inconsistent recovery. As well as achieving varying amounts of penetration, the gravity corer may also bounce on the sea bed, leading to a spurious core being collected.

2 Repeat Measurements

Repeat whole core susceptibility results for cores 61-03 42CS and 61-03 30CS (fig. 4.4a and 4.4b) show excellent consistency with time. The lack of change is an excellent result especially considering that both cores had been split and subsampled with consequent risk of oxidation.

The stability during storage is quite different to results obtained by other workers. For example Snowball and Thompson (1988) record large changes in susceptibility in Loch Lomond sediments due to the oxidation of the iron sulphide, greigite (Fe_3S_4).

Repeat measurements on subsamples (table 4.1) from core 61-03 42CS revealed a greater change in storage than seen for the whole core susceptibility. Subsample susceptibility changes were acceptably low with less than 4% being the norm. However samples with high SIRM/ χ ratio values (36 kAm^{-1}) showed changes of nearly 10% in susceptibility and 17% in SIRM/ χ ratio after two years, compared to an average 8% for samples with SIRM/ χ ratio values initially in the order of 20 to 24 kAm^{-1} . All samples showed a drop in SIRM/ χ ratio value after two years. The greater percentage drop in SIRM/ χ values for material with initially high SIRM/ χ ratios than that in material with initially low SIRM/ χ ratios points to a possible sulphide oxidation (Ian Snowball, pers comm). It should also be noted that the higher SIRM/ χ ratios occurred near the top of the core. Here one would expect a more unstable chemical situation with the various constituents of the core yet to reach a chemical equilibrium.

3 Palaeomagnetic data

The palaeomagnetic data obtained from Flett cores (fig 4.8) is of good quality in that the NRM direction and intensities and direction are stable under demagnetisation (fig 4.9). The small secondary component in the Zijderveld plots could be attributed to magnetisation picked up during coring or storage. It may also reflect the presence of a slight post-depositional CRM, and there was also the possibility of error from subsampling as described by Stump *et al* (1986). However, whatever its cause, the intensity of the secondary component is small compared to that of the principal component.

Despite the quality of the NRM retained by individual subsamples, the downcore NRM data is of limited value. There are rapid fluctuations in direction between adjacent subsamples making overall features difficult to identify. The situation is further complicated by the mismatch in declination results at 100cm. This mismatch is due to poor orientation control during core cutting on ship. One overall feature of the downcore palaeomagnetic record that can be identified is the shallow average inclination. The inclination based on a geocentric axial dipole model ($\tan I = 2 \tan \lambda$ where I is the inclination and λ the latitude) should be 74° . The data for core 61-03 42CS shows an average of 60° . Inclination errors are commonly found in continental shelf and estuarine situations (eg Bjorck and Sandgren, 1987). Defining the cause of inclination error has proved difficult. Several possible mechanisms are presented by King (1966) and Griffiths and King (1960). These explanations generally involve the physical realignment of sediment grains following deposition and depend very much on the characteristics of certain sediment types. A much more mundane explanation of the shallow inclinations could be the persistent non-vertical entry of the gravity corer. As cores were being recovered from depths of several hundred metres, it is easy to visualise a situation where a slight movement of the ship or drag of the current on the corer cable could cause a few degrees of tilt.

4 Mineral Magnetic Results

Varying concentrations of magnetic minerals are reflected in χ , SIRM, and HIRM parameters for core 61-03 42CS (fig. 4.5). Despite the frequent fluctuations in concentration, the proportion of high to low coercivity components remains steady as reflected by near constant S ratio and SIRM/ χ ratio values. The only exceptions to the near constant downcore values are

found in the top 25cm and at a depth of 150cm. At these depths a slight increase in SIRM/ χ ratio from 20 to 32 kAm⁻¹ and drop in S ratio value from 0.9 to 0.6 reflects an increase in high coercivity components. IRM acquisition curves for subsamples (fig 4.6) from 25 and 150 cm emphasise the difference in coercivities. The relatively high coercivity sample from 4.5cm is only 80% saturated by 100mT whilst a typical coercivity sample from 130cm is 95% saturated by 100mT. The coercivity data suggests a magnetic mineral assemblage dominated by magnetites but with a minority high coercivity component, probably haematite present. Comparison of coercivity data from Flett to that obtained from the Peach area (fig 3.9) shows little difference between a normal coercivity Flett sample and a normal Peach sample. If the coercivity values for Flett material are used in conjunction with the SIRM/ χ ratio as in fig 2.10, it can be seen that the value for samples from the Flett area fall well within a magnetite classification.

Thermomagnetic analysis of magnetic extracts (fig 4.7) gave a Curie temperature of 580°C, suggesting magnetite as the dominant magnetic mineral. There was no sign of any significant fluctuation in magnetisation before the Curie temperature either during heating or cooling cycles suggesting a relatively pure extract devoid of clay minerals that could increase the magnetisation during the measurement run as iron bearing minerals oxidised to form magnetic oxides.

4.5 Significant Points

1) The Bartington whole core susceptibility equipment can operate successfully onboard survey vessels.

2) Whole core susceptibility profiles correlate with geological horizons in cores from the Flett area.

3) No variation in magnetic susceptibility was found during core storage for a period of up to two years.

4) Mineral magnetic composition showed little variation downcore and was dominated by magnetite.

5) A strong stable palaeomagnetic signal of normal polarity was seen. The average inclination values were shallower than would be expected from a dipole field model. The secular variation pattern lacked sufficient features to be matched to a palaeomagnetic master curve.

CHAPTER 5 CENTRAL NORTH SEA

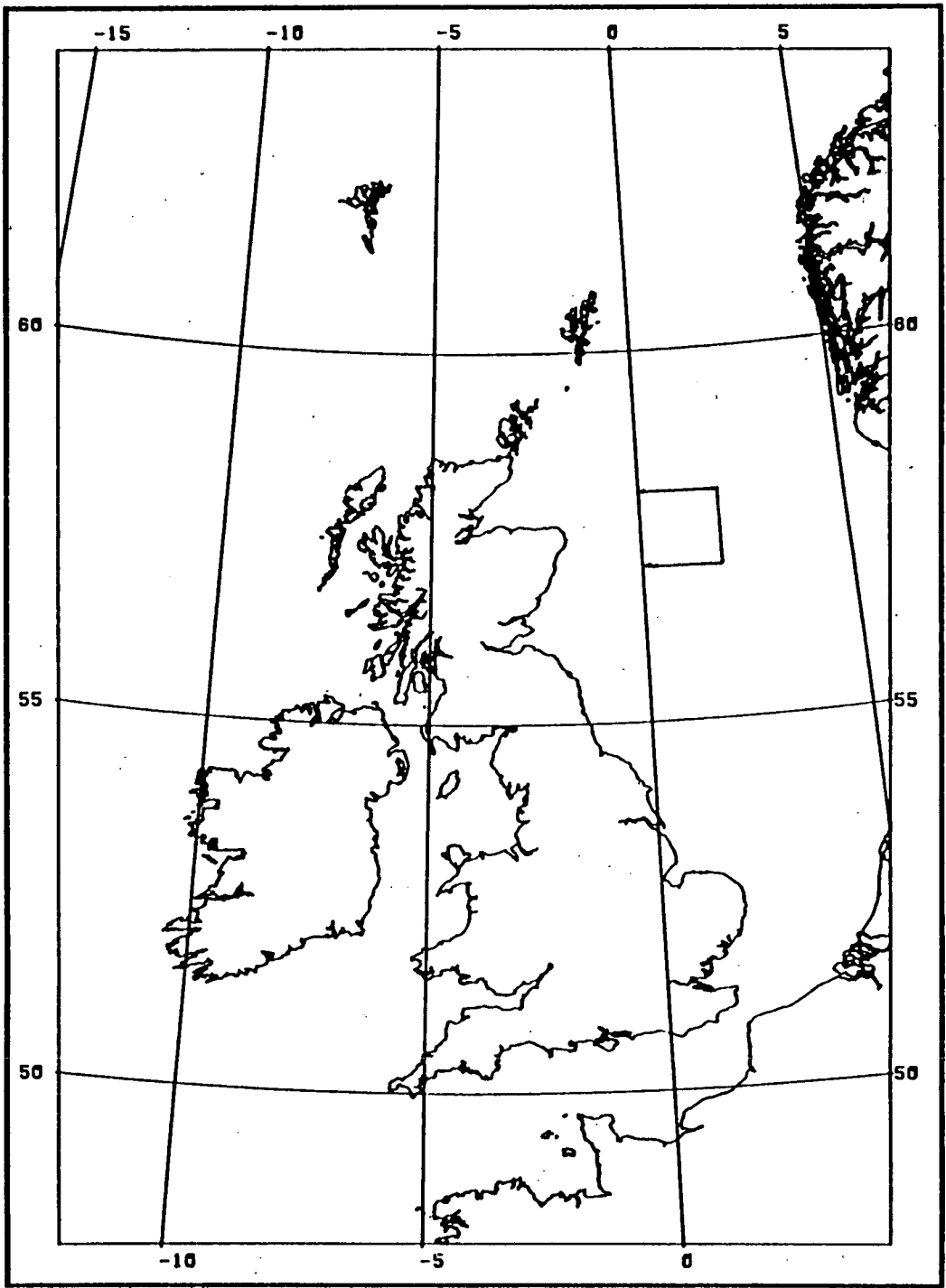
5.1 Introduction

The Central North Sea was subjected to extensive geophysical survey and geological sampling during the 1970s by BGS. In addition to routine BGS reports and analysis considerable further work was carried out by Bent (1987). He provided a Quaternary stratigraphic framework for the sea bed in grid squares 58N 00W, 58N 01W and 58N 02W (see fig 5.1). Detailed geological descriptions of several suites of cores are included in his thesis against which magnetic data obtained during my study could be compared. Positions of the cores used in the latter are shown in fig. 5.1b. Palaeomagnetic work on borehole material from the Central North Sea had been successfully undertaken by Stoker et al (1983). Some of their results are shown in figs 5.2 and 5.3. Unfortunately, material from the BGS boreholes used by Stoker et al was no longer available for further analysis. However, virtually all the core material examined by Bent (1987) were still available for use from BGS stores.

5.2 Core Selection and Magnetic Measurement Procedures

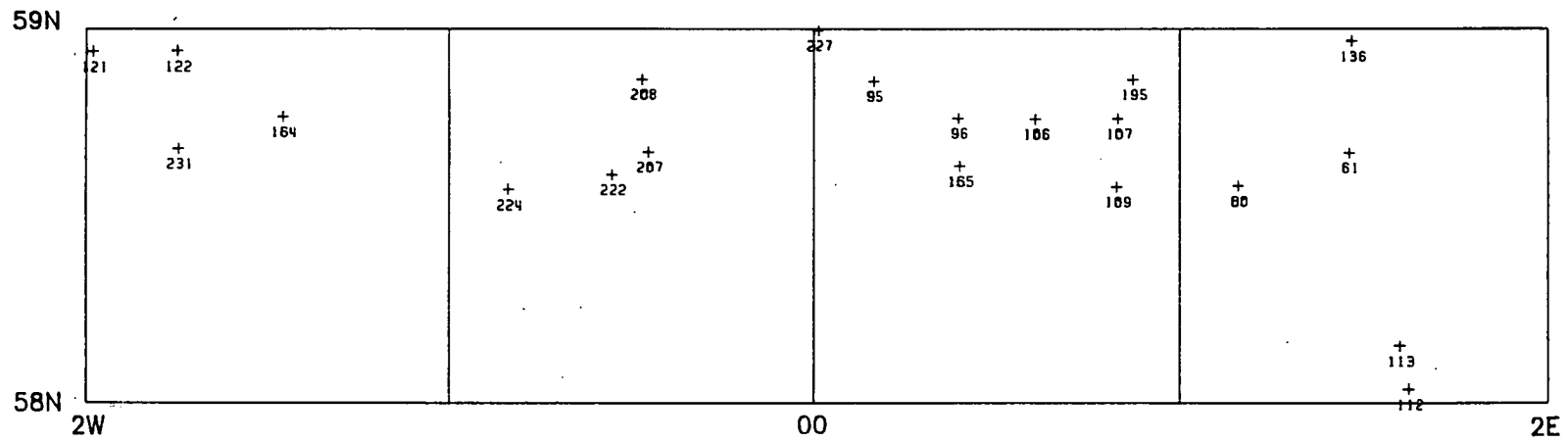
Cores were selected for whole core susceptibility measurement on the basis of their varied lithology. The whole core susceptibility profile for each core was used in conjunction with the geological log and state of preservation of each core to decide on a programme of further magnetic, particle size and heavy mineral analysis.

Of the 22 cores originally used for whole core susceptibility measurements in the Central North Sea area, two were found to be of particular interest for further study: cores 58-02 231VE and 58-02 122VE. Visual examination of the original 22 cores revealed that only one core, 58-02 122VE was in a good enough state of preservation to warrant subsampling for palaeomagnetic purposes. Other cores had dried out to such an extent that their sedimentary fabric had visually altered with widespread cracking apparent. Palaeomagnetic work on core 58-02 122VE was undertaken by W. Suttie as an undergraduate project under the supervision of the author. Contiguous subsamples were taken from core 58-02 122VE and measured for NRM in the cryogenic magnetometer.

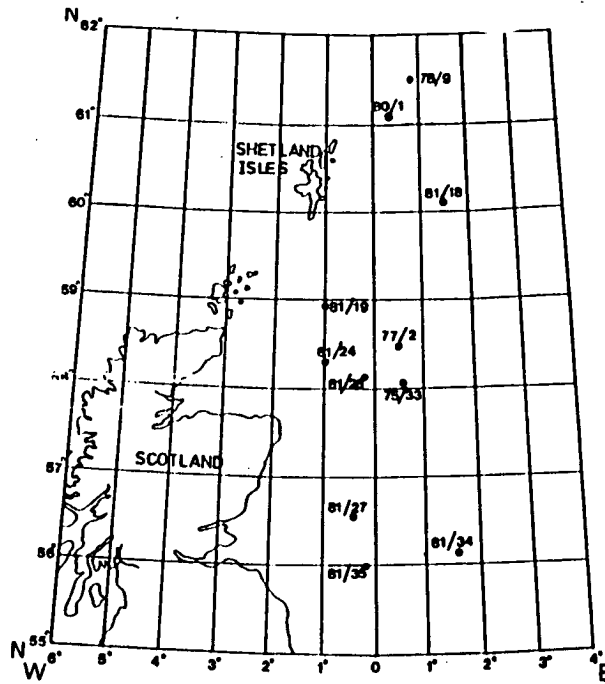


STEREOGRAPHIC
SCALE = 1 : 10000000

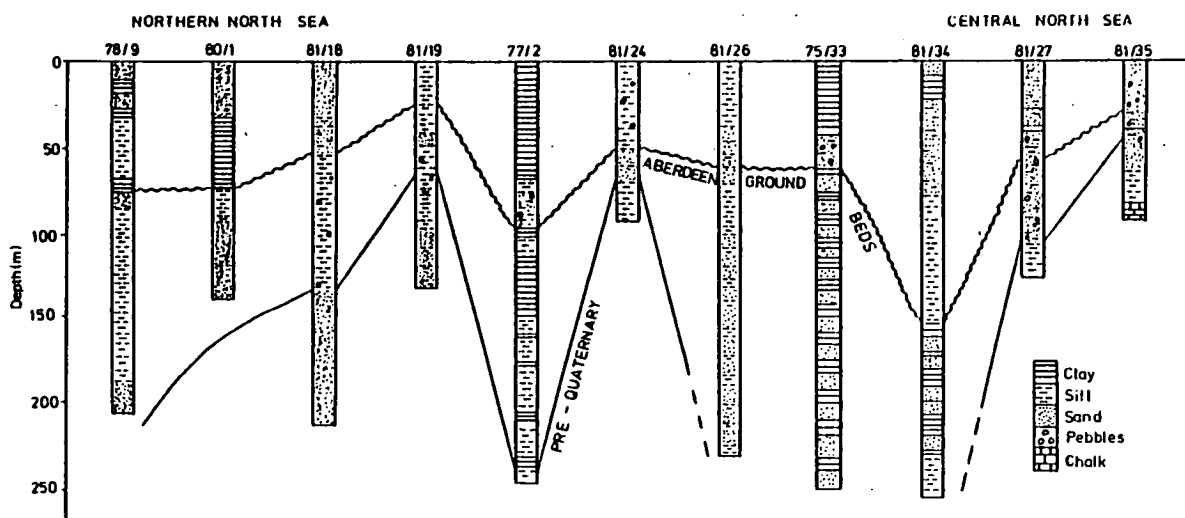
- Fig 5.1 The position of the Central North Sea site studied with respect to the British Isles.



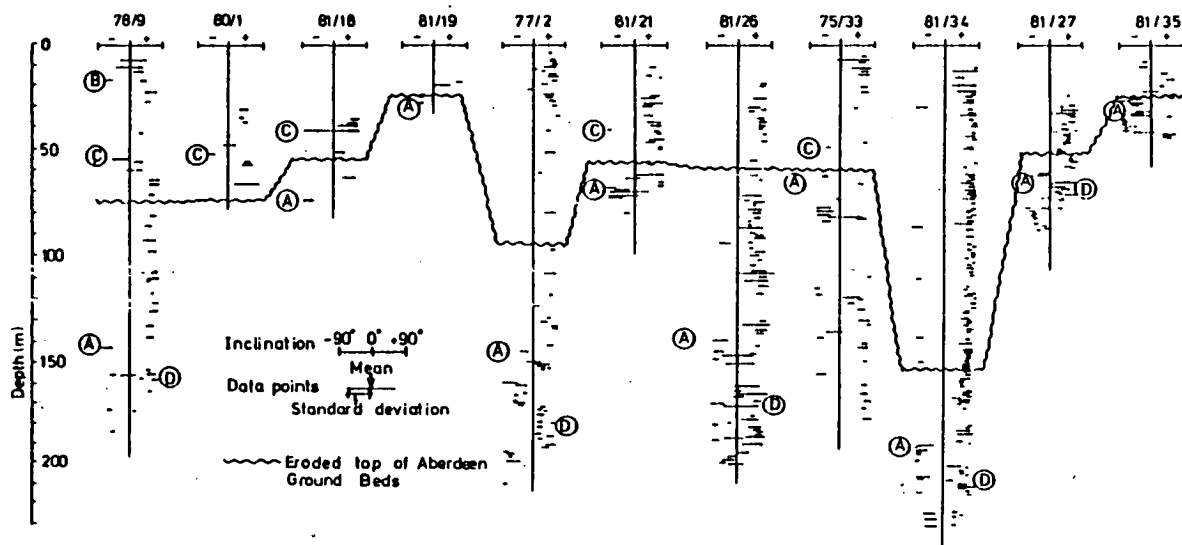
- Fig 5.1b Sample stations for the Central North Sea.



- Fig 5.2 Location map showing sites of previous palaeomagnetic work in the North Sea (from Stoker at al 1983). Position codings refer to BGS borehole numbers.



Correlation of IGS boreholes using seismic stratigraphy derived from IGS seismic profiles. The correlation lines shown indicate major seismic reflectors which are visible on records over the entire area of survey.



- Fig 5.3 Results from Stoker et al (1983) showing seismic stratigraphy data and palaeomagnetic correlations for IGS boreholes 78/9, 80/1, 81/18, 81/19, 77/2, 81/24, 21/26, 75/33, 81/34, 81/27, 81/35. The upper diagram shows the correlation of boreholes based on IGS seismic profiles. Correlation lines indicate major seismic reflectors which are visible on records across the entire survey area. The lower diagram shows correlation of palaeomagnetic results with annotation as follows: A - Brunhes-Matuyama boundary (~790 kyr BP); B - Lashamp and Olby excursion (~36-42 kyr BP); C - Blake event (~108-114 or 104-117 kyr BP); D - Jarmillo event (~890-950 kyr BP).

24 of the subsamples were used in pilot AF demagnetisation studies.

Core 58-02 231VE was too dried out to be considered for palaeomagnetic analysis. However, it possessed a varied lithology and produced the most varied whole core susceptibility profile of the original 22 cores examined. It was consequently an ideal candidate for additional mineral magnetic investigation. Subsamples were taken at 5cm intervals. These subsamples were then used for a standard set of mineral magnetic measurements with χ , SIRM, SIRM/ χ , S and HIRM being derived for all subsamples. Backfield IRM curves were also obtained for pilot samples.

The patterns seen in the mineral magnetic data for core 58-02 231VE were then used to decide where to take further large samples for heavy mineral work. The large samples (500 g) were necessary for use in the shaking table heavy mineral extraction technique. Additional small samples (20 g each) were taken at the same horizons as the large samples for use in magnetic extraction studies.

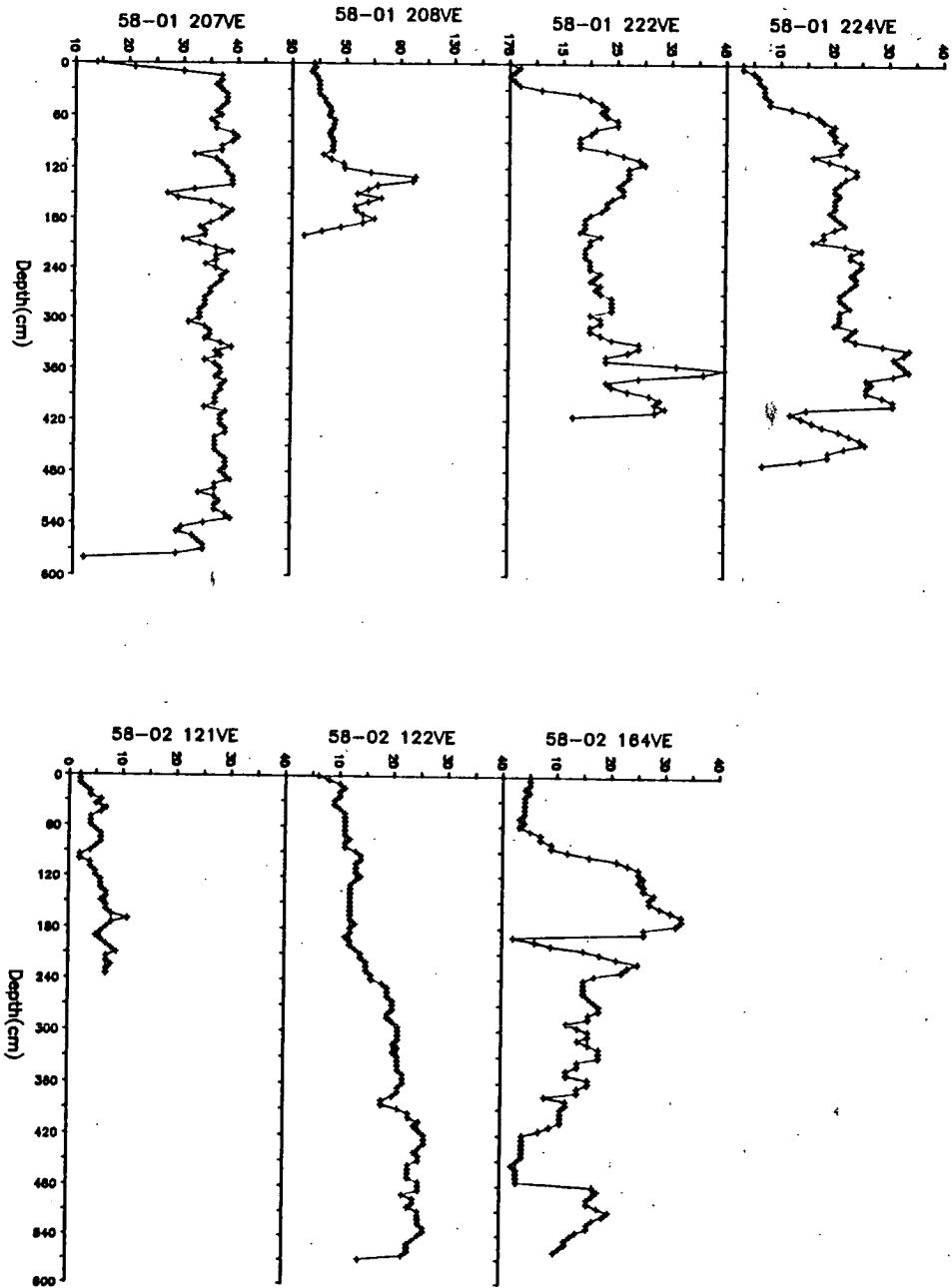
Due to the large quantities of sample used by the shaking table, the splits obtained from it were of sufficient size to be used for backfield IRM analysis. The much smaller but more concentrated extracts obtained by magnetic techniques were used for thermomagnetic analysis.

Approximately 50g of each large subsample was retained for particle size analysis. This analysis was carried out using a 63 μ m mesh sieve to give sand (>63 μ m) and mud/silt (<63 μ m) fractions.

5.3 Results

1 Whole Core Susceptibility

Fig 5.4a, 5.4b and 5.4c show the whole core susceptibility profiles for the 22 cores selected from the central North Sea. The length of core varied between a minimum of 180cm in the case of core 58+00 195VE to a maximum of 570cm in the case of core 58-01 207VE. Whole core susceptibility values ranged from a low of 2 instrument units at the top of core 58-02 121VE to a high of over 70 instrument units at the top of core 58+01 61VE. The pattern of downcore variation in whole core susceptibility differed between cores, but the majority



- Fig 5.4 Whole core susceptibility profiles for 22 cores from the Central North Sea. Susceptibility is in arbitrary units.

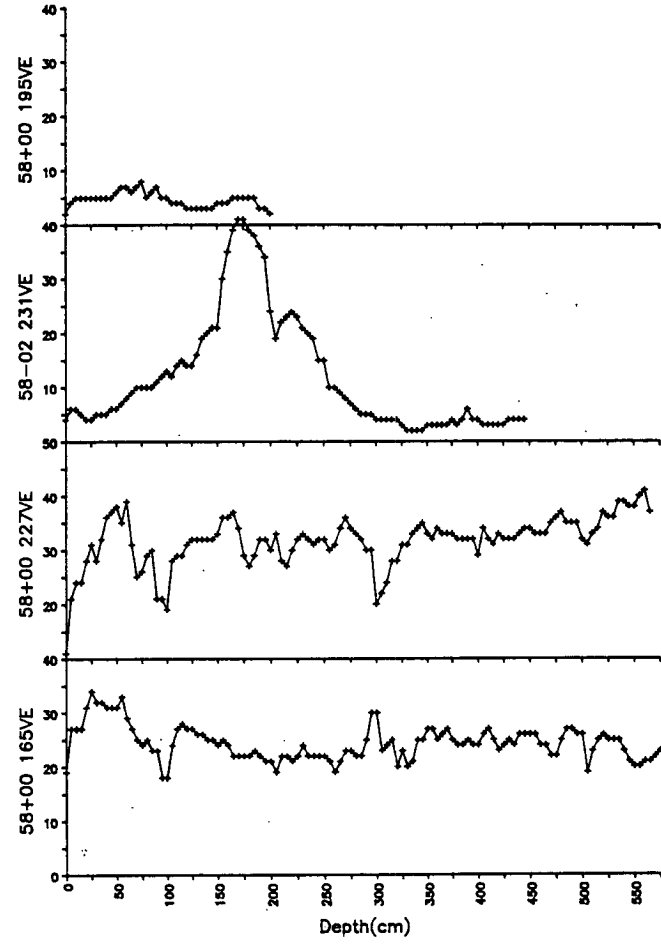
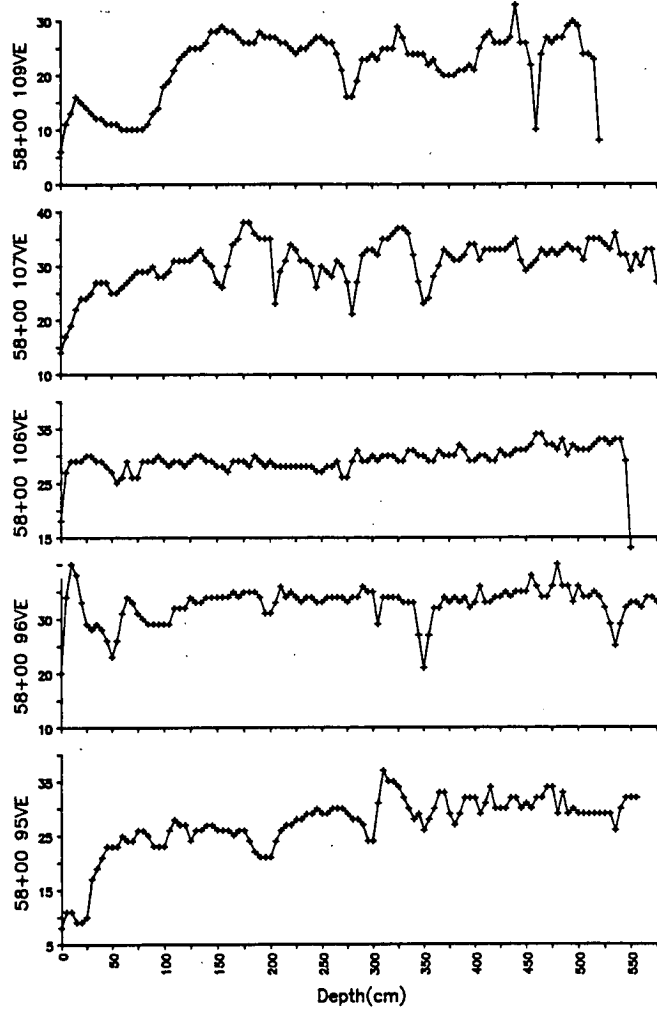


Fig 5.4b

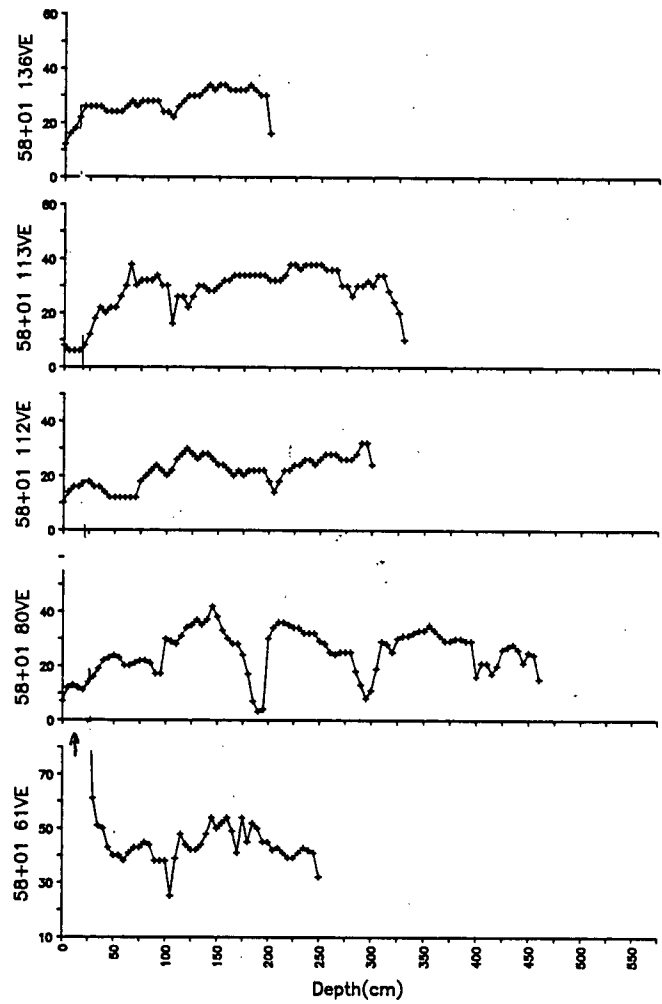
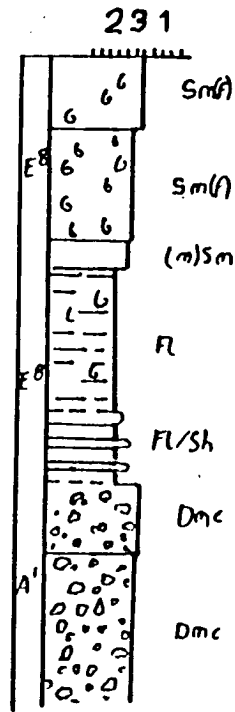
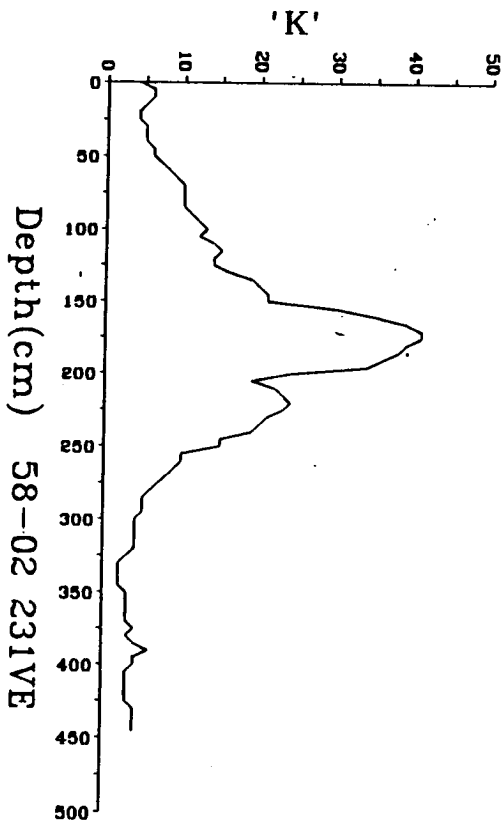


Fig 5.4c



- Fig 5.5a Whole core susceptibility data for core 58-02 231VE based on measurements every 5cm with Bartington MS2C loop.
- Fig 5.5b Lithological description of core 58-02 231VE from Bent (1987). Abbreviations as follows: Sm(f) - Sand, massive, >5% shell material. (m)Sm - muddy sand massive. Fl - Fine grained mud, horizontal laminations. Fl/Sh - interlaminated mud/sand. DmC - Diamict, massive, >5% clasts.

had a near constant susceptibility downcore. The most obvious exception to this was core 58-02 231VE which exhibited quite marked changes in susceptibility downcore apparently due to its varied lithology (fig 5.5). These downcore changes are explained in conjunction with other mineral magnetic data for core 58-02 231VE in the next section. A frequently occurring feature in many cores was an occasional dip in the susceptibility log, for example at 200cm in core 58-02 164VE and at 200cm in core 58+01 80VE. These susceptibility dips are attributable to gaps in the core caused by either cracking or previous subsampling.

2 Mineral Magnetic Data - Core 58-02 231VE

Downcore mineral magnetic data for core 58-02 231VE is shown in fig 5.6. Whole core susceptibility, χ , SIRM, SIRM/ χ ratio, HIRM and S ratio all show considerable variation downcore.

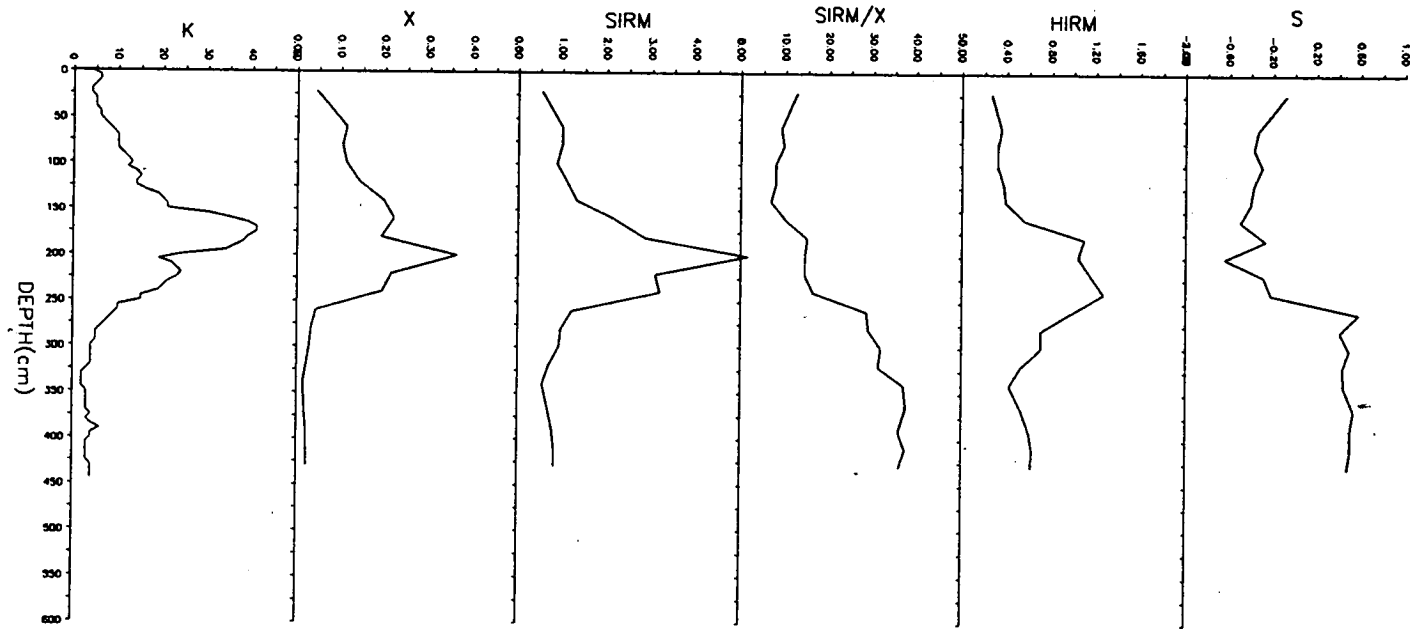
The whole core susceptibility starts from an initial value of 5 instrument units at 5cm, then gradually increases with depth until reaching a broad peak of 40 instrument units at 175cm, before dropping back to about 5 instrument units by 300cm.

χ shows a similar pattern to whole core susceptibility, starting low at 0.05 $\text{mAm}^2\text{kg}^{-1}$ in the top few cm and steadily to a broad peak of 0.35 $\text{mAm}^2\text{kg}^{-1}$ by 180cm. This peak value is then followed by a decline to approximately 0.02 $\text{mAm}^2\text{kg}^{-1}$ by 270cm.

The SIRM pattern is similar to that seen in χ , starting low at 0.5 $\text{mAm}^2\text{kg}^{-1}$ in the top few cm of core, gradually increasing to 5 $\text{mAm}^2\text{kg}^{-1}$ at 200cm before decreasing to approximately 1 $\text{mAm}^2\text{kg}^{-1}$ by 270cm.

The SIRM/ χ ratio, unlike whole core susceptibility, χ and SIRM does not show a continuous variation downcore. Instead, SIRM/ χ ratio values fluctuate slightly between 10 and 14 kAm^{-1} for the top 230cm of core. From 230cm to 280 cm there is a rapid increase from 14 kAm^{-1} to 30-35 kAm^{-1} followed by a gentle increase to nearly 40 kAm^{-1} by the bottom of the core.

HIRM data shows a similar pattern to χ , SIRM, but with a plateau value of 1.2 $\text{mAm}^2\text{kg}^{-1}$ between 180 cm and 240 cm instead of a clearly defined peak. Values either side of the plateau are in the range 0.2 to 0.3



- Fig 5.6 Mineral magnetic parameters for core 58-02 231VE. Results based on data from subsamples at 5cm intervals. Units: K - dimensionless; χ - $\mu\text{m}^3\text{kg}^{-1}$, SIRM - $\text{mAm}^2\text{kg}^{-1}$; SIRM/ χ - Am^{-1} ; 'S' - dimensionless ratio; HIRM - $\text{mAm}^2\text{kg}^{-1}$.

$\text{mAm}^2\text{kg}^{-1}$.

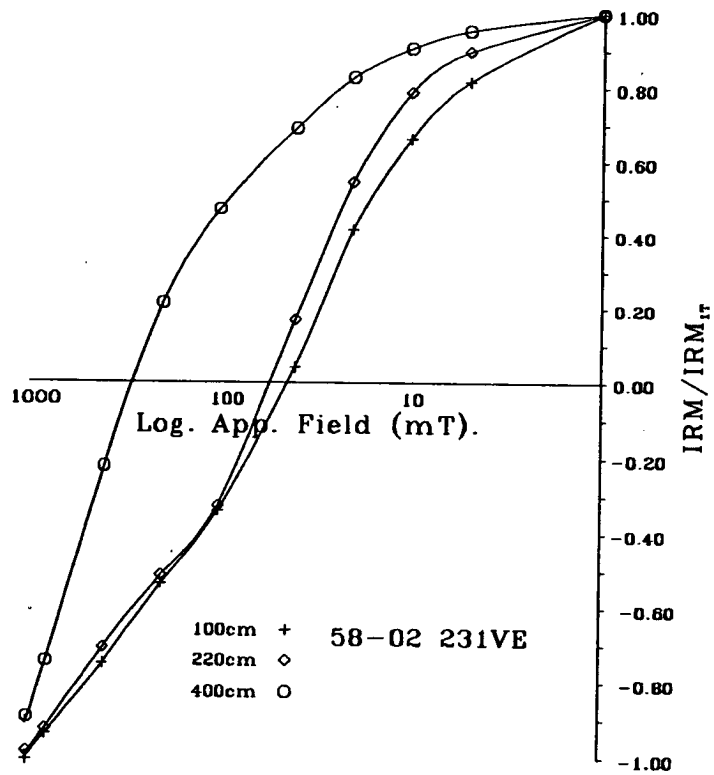
The S ratio shows a similar pattern to SIRM/χ , steady in the top 225cm of core with a value of about -0.2, then a rapid increase to +0.8 by 270cm retaining the latter value until the base of the core.

Backfield IRM curves for 3 pilot samples taken from three different sedimentary horizons down core 58-02 231VE are shown in fig 5.7. These horizons corresponded to depths of 100 cm, 220 cm and 400 cm. The IRM curves for samples from 100 cm and 220 cm are very similar in both pattern and magnitude of coercivity whereas the IRM curve for the sample from 400 cm differs both in pattern and magnitude of coercivity. The curves for samples from 100 cm and 220 cm consist of two sections. In the first section, up to an applied field of 100mT, the IRM data curves smoothly. However, from 100 mT onwards, the curve becomes almost linear. Both the samples from 100cm and 220 cm give a coercivity of approximately 45 to 60 mT. The IRM curve for the sample from 400 cm consists of one smooth convex curve with a coercivity in the order of 290 mT. There is no sign of the secondary linear feature seen in samples from 100cm and 220 cm.

3 Shaking Table and Particle Size Results

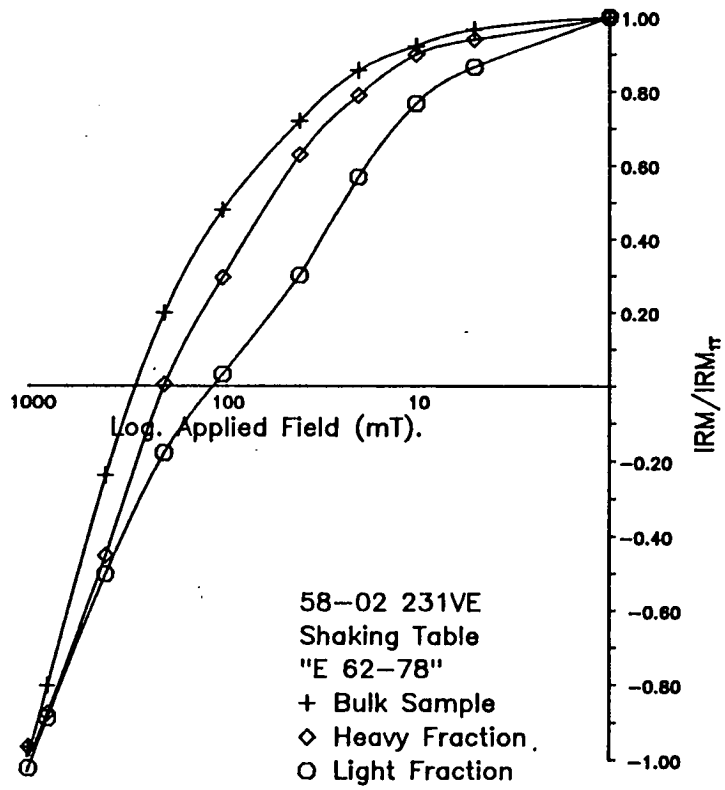
The results of shaking table separation on a subsample from a depth of 400cm are shown in fig 5.8. IRM curves for the bulk sample and heavy and light fractions are shown. The bulk sample has a coercivity of over 300mT, the heavy fraction a coercivity of 200mT and the light fraction a coercivity of 100-120 mT. The curves for bulk sample and heavy fraction appear to be smooth, unlike the curve for the light fraction which appears to consist of two parts.

The results for particle size work are shown in fig 5.9. IRM curves have been done for the original samples and for both the $>63\mu\text{m}$ and $<63\mu\text{m}$ splits. The bulk sample has a coercivity of about 200mT, the $<63\mu\text{m}$ split a coercivity of 100mT, and the $>63\mu\text{m}$ split a coercivity of 160 mT.



Depth (cm)	SIRM/ χ (kAm ⁻¹)	S
100	10	-0.25
220	15	-0.30
400	38	-0.56

- Fig 5.7 IRM curves for pilot samples from core 58-02 231VE. Data normalised to IRM at 1T. SIRM/ χ and S ratio are also listed.



- Fig 5.8 Results obtained from use of the 'Shaking Table' on a subsample from core 56-02 231VE (section E, 62-78 cm). Bulk - entire original sample; 'Heavy fraction' = material retained on table; 'Light fraction' - material washed from table.

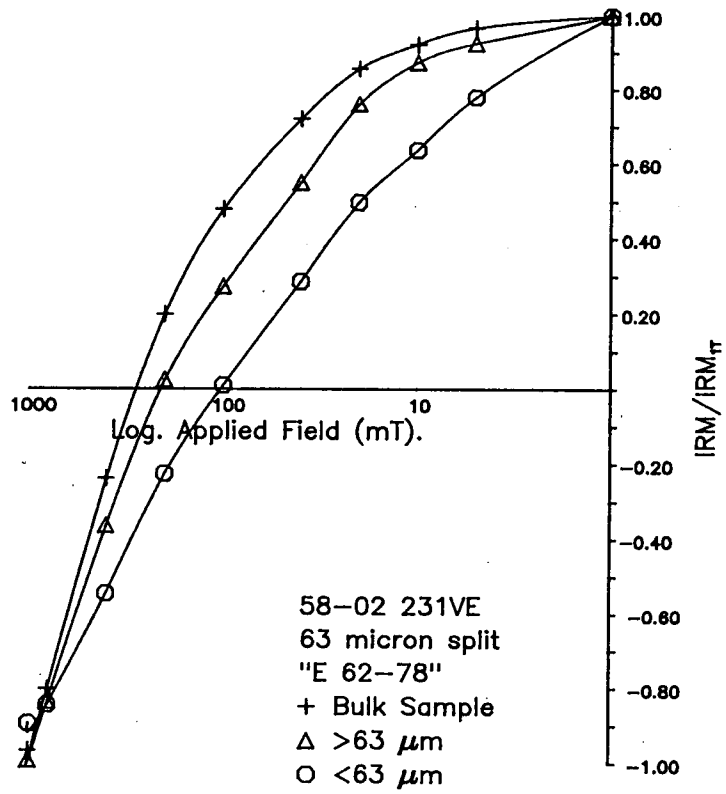


Fig 5.9 IRM curves for particle sizes obtained by sieving bulk samples through a 63μm mesh. Sample material derived from core 58-02 231VE, section E, 62-78cm. Bulk = original sample; 'Sand' = >63μm; 'Fines' = <63μm.

4 Thermomagnetic Results

The Curie balance analysis data for two magnetic extracts from core 58-02 231VE are shown in fig 5.10. The B extract came from 110 cm downcore and exhibited a Curie temperature of about 580°C. The E extract came from 400cm downcore and exhibited a Curie temperature of 680°C. The 110 extract gave a smooth curve with magnetisation reaching 20% of its room temperature value at 600°C. The 400 extract gave a rougher curve, with approximately 40% of its room temperature magnetisation remaining at 700°C.

5 Palaeomagnetic Results

Downcore NRM results for a contiguous set of subsamples from core 58-02 122VE are shown in fig 5.11. The inclination, declination and intensity data all show differing characteristics. The inclination has a low value of 40° in the top 5cm of core, rising to a steady 80° in the band 50-150cm. From 175cm downwards inclination values drop to a steady 55°. The inclination pattern is very erratic in the top 50cm with 20° jumps between adjacent data points, but becomes much more stable further downcore. The declination data for core 58-02 122VE is very erratic in the top 100cm, but stabilises to a value of approximately 220° by 110cm. Intensity data shows a near constant value of 0.01 $\mu\text{Am}^2\text{kg}^{-1}$ in the top 225cm. Between 225cm and 240cm intensity rises to 0.2 $\mu\text{Am}^2\text{kg}^{-1}$ where it remains for the rest of the core.

Demagnetisation results for three typical pilot samples for core 58-02 122VE are shown in fig 5.12. The pilot samples taken from 37cm, 204.5cm and 552cm represent the main demagnetisation characteristics seen in all pilot samples from core 58-02 122VE. The sample from 37cm shows erratic directional behaviour under demagnetisation. The Zijderveld plot shows at least three components present with no overall dominant component visible. The erratic directional data results in scattered data on the stereographic projection.

The sample from 204.5cm shows more stable directional behaviour under demagnetisation. The Zijderveld plot shows the presence of several components but an overall direction is clearly visible and the data grouping on the stereographic projection much tighter than for the 37cm sample. The sample from 552cm has a single clear directional component visible in the Zeigerfeld plots and a consequently tight grouping of points on the stereographic projection.

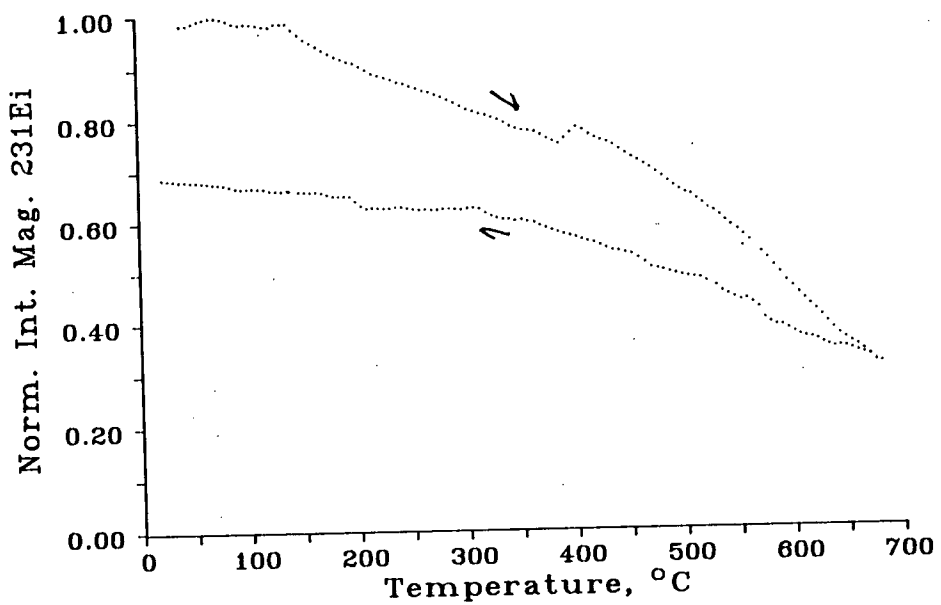
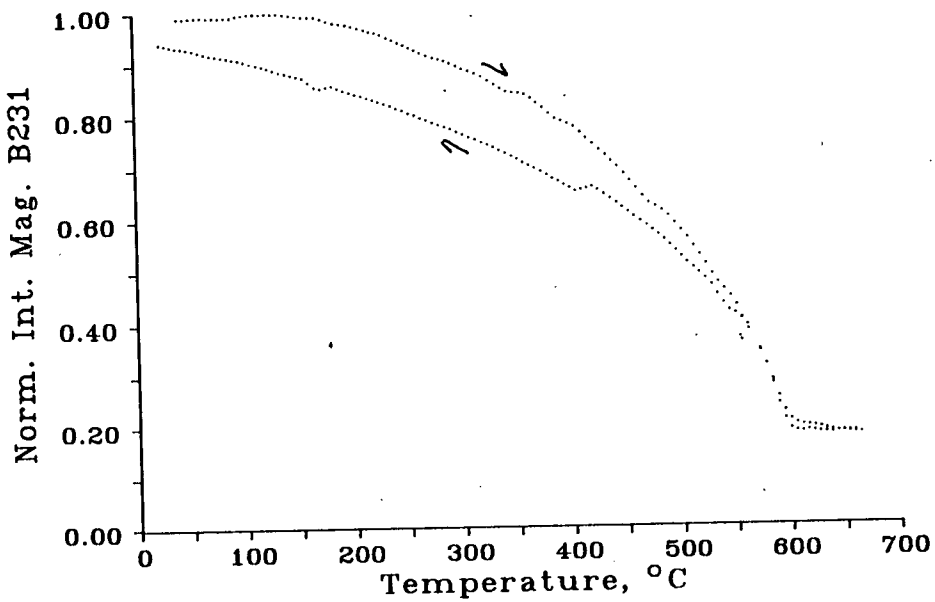
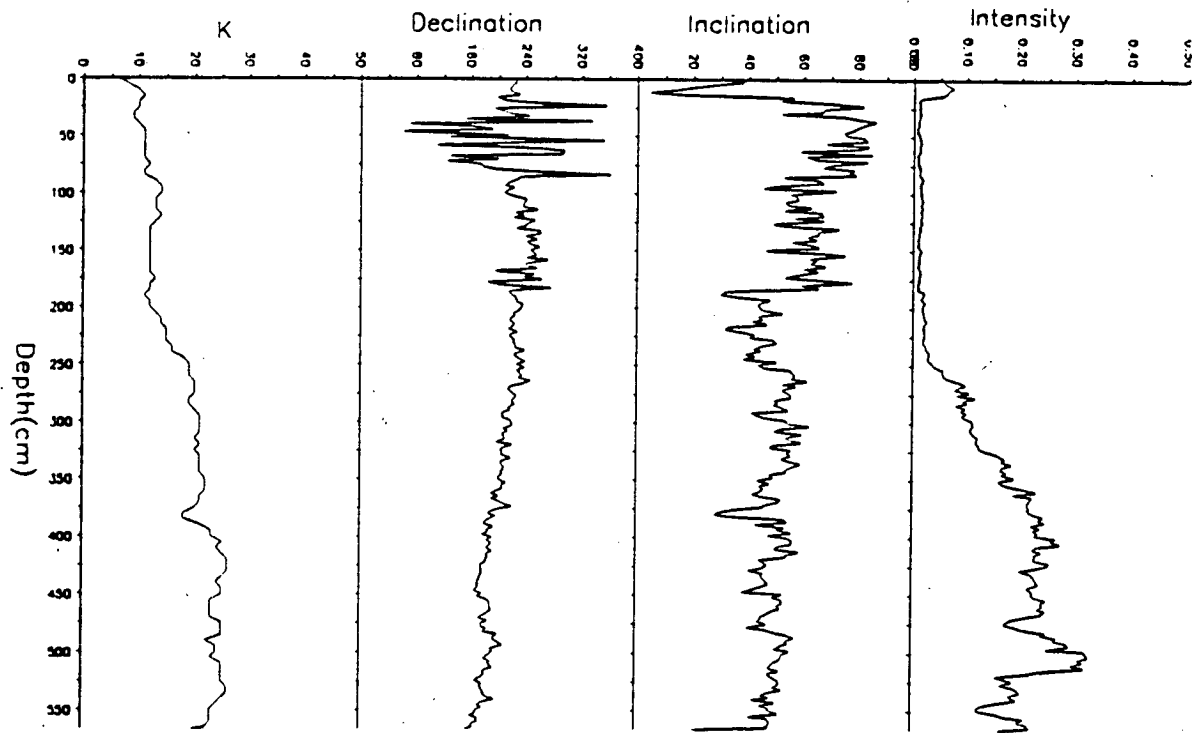
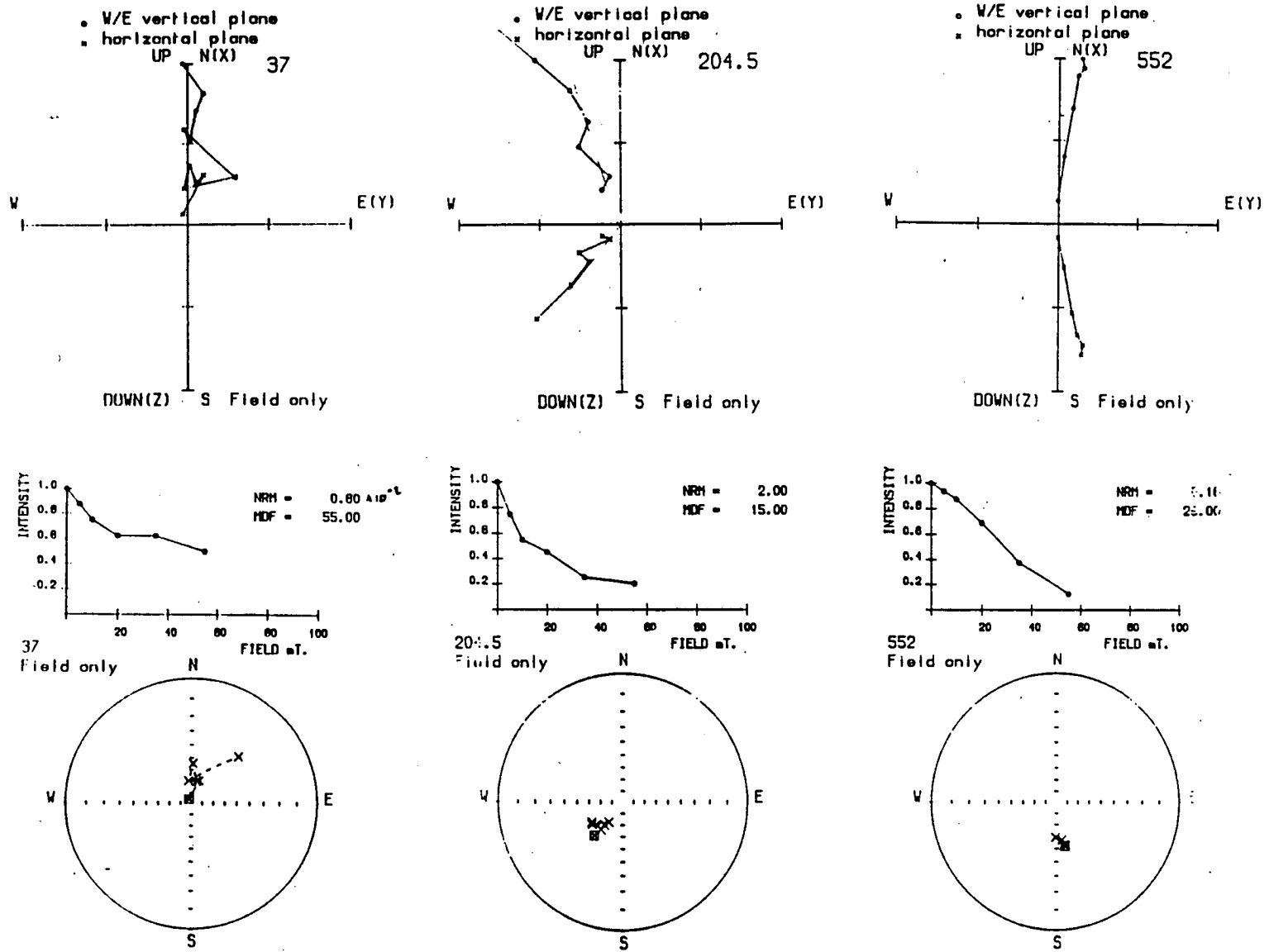


Fig 5.10 The result of thermomagnetic analysis for two magnetic extracts from core 58-02 231VE. The B231 extract came from 110 cm downcore and the 231Ei extract from 400 cm downcore.



- Fig 5.11 Downcore palaeomagnetic results for core 58-02 122VE. Based on data obtained for a contiguous subsample set. Units: NRM intensity - $\mu\text{Am}^2\text{kg}^{-1}$; K = whole core susceptibility, arbitrary units.



- Fig 5.12 Alternating field demagnetisation data for pilot samples from core 58-02 122VE. Labels refer to depth of sample within the core. Units: NRM intensity - $\mu\text{Am}^2\text{kg}^{-1}$; MDF - mT.

5.4 Discussion

1 Whole Core Susceptibility

Whole core susceptibility profiles for cores from the Central North Sea reflects the variations in lithology seen in the cores. Core 58-02 231VE shows the most distinct susceptibility changes with lithology as shown by comparing the original geological log drawn by Bent (1987) and the whole core susceptibility profile in fig 5.5. The downcore lithology of core 58-02 231VE consists of a gradual change from sands, to muds, and then a rapid change to diamict material. The various lithological changes are easily seen in the susceptibility profile, with values peaking in the fine mud section. The gradual increase in whole core susceptibility with increasing proportion of mud seen in the top 175cm of the core suggest that particle size has a strong influence on susceptibility.

2 Mineral magnetic Data

The mineral magnetic data in fig 5.6 for core 58-02 231VE shows two distinct trends. Concentration dependent parameters, K , χ , SIRM and HIRM all reflect the same trend of a peak at about 175–200cm, reflecting a change in dominant particle size from sand to mud. However, SIRM/ χ ratio and S ratio reflect the rapid change to diamict material at 270cm by a rapid swing in their values. Reference to the IRM curves further underlines the distinct difference in magnetic mineral assemblages between the upper and lower core sections, with a much greater proportion of high coercivity material in the lower sections.

3 Extraction

Attempts at extracting minerals by shaking table and magnetic methods provided quite differing results. If the results for the shaking table (fig 5.8) had been examined in isolation, it would have appeared that the shaking table had successfully split high coercivity and low coercivity mineralogies. However, a quick comparison with the particle size results in fig 5.9 suggests that the shaking table has merely split the original sample on a particle size basis rather than specific gravity. Higher coercivity material appears to be dominant in the $>63\mu\text{m}$ fraction and low coercivity in the $<63\mu\text{m}$ fraction.

Magnetic extraction procedures produced much smaller but purer extracts. Thermomagnetic analysis (fig 5.10) showed a Curie temperature of 580°C, suggesting a magnetite dominant in the upper part of core 58-02 231VE. A Curie point of 680°C was seen for an extract from the lower diamict section of the core (extract E) suggesting haematite dominant in the diamict section. If HIRM data is examined, it can be seen that there is a similar concentration of haematite in the upper (HIRM = 0.35 mAm²kg⁻¹) and lower (HIRM = 0.4 mAm²kg⁻¹) parts of core 58-02 231VE. However, there was no evidence of haematite in the thermomagnetic analysis of the upper extract. It would appear that the magnetite has dominated the haematite in the Curie analysis of the upper extract. However, in extract E from the lower sections of the core, the proportion of magnetite to haematite as shown by an S ratio of 0.8 is much lower than in the top section of core. Hence, despite the similar concentrations of haematite in the lower and upper parts of the core, it can only be seen in extracts from the lower half due to the near complete absence of magnetically dominant magnetite.

The intensity of magnetisation seen for the E extract in thermomagnetic analysis is in the same order of magnitude as the magnetisation of the sample holder. Consequently the magnetisation seen for the E extract in fig 5.10 does not reach zero, the glass sample holder contributing some 40% of the total signal strength. If magnetite had been present in the E extract, even in minor amounts, the weak haematite signal would have been easily swamped.

4 Palaeomagnetic Results

The palaeomagnetic results for 58-02 122VE (fig 5.11, 5.12) were disappointing. The wildly fluctuating declination and inclination records for the upper part of the core suggest considerable disturbance in this area. Beyond the disturbed top meter, there are no significant features in declination and inclination suitable for a match to other secular variation data. The cores are also too short to record any reversal that could be matched to Stokers work.

The demagnetisation data for pilot samples from core 58-02 122VE show the changing quality of the palaeomagnetic data with increasing depth. The sample from 37cm showed the disturbed and confused NRM in the upper regions of the core with multiple components seen in the Zijdeveld plot. The NRM quality improves by 204 cm becoming good by 552 cm. This

improvement in quality downcore supports the idea of excessive disturbance in the top meter of sediment.

5.5 Significant Points

1) There is a good relationship between whole core susceptibility and the lithology of the sediment.

2) There are a wide range of magnetic minerals present in Central North Sea sediments with coercivities varying between 20 and 300 mT.

3) Both the concentration of magnetic minerals and magnetic stability varies with the sediment particle size. High coercivity minerals tend to be associated with the sands and low coercivity minerals with the $<63\mu\text{m}$ fractions.

4) Both haematite and magnetite can be removed by magnetic extraction techniques.

5) Palaeomagnetic data from cores that have been stored for several years in non-refrigerated conditions are not reliable.

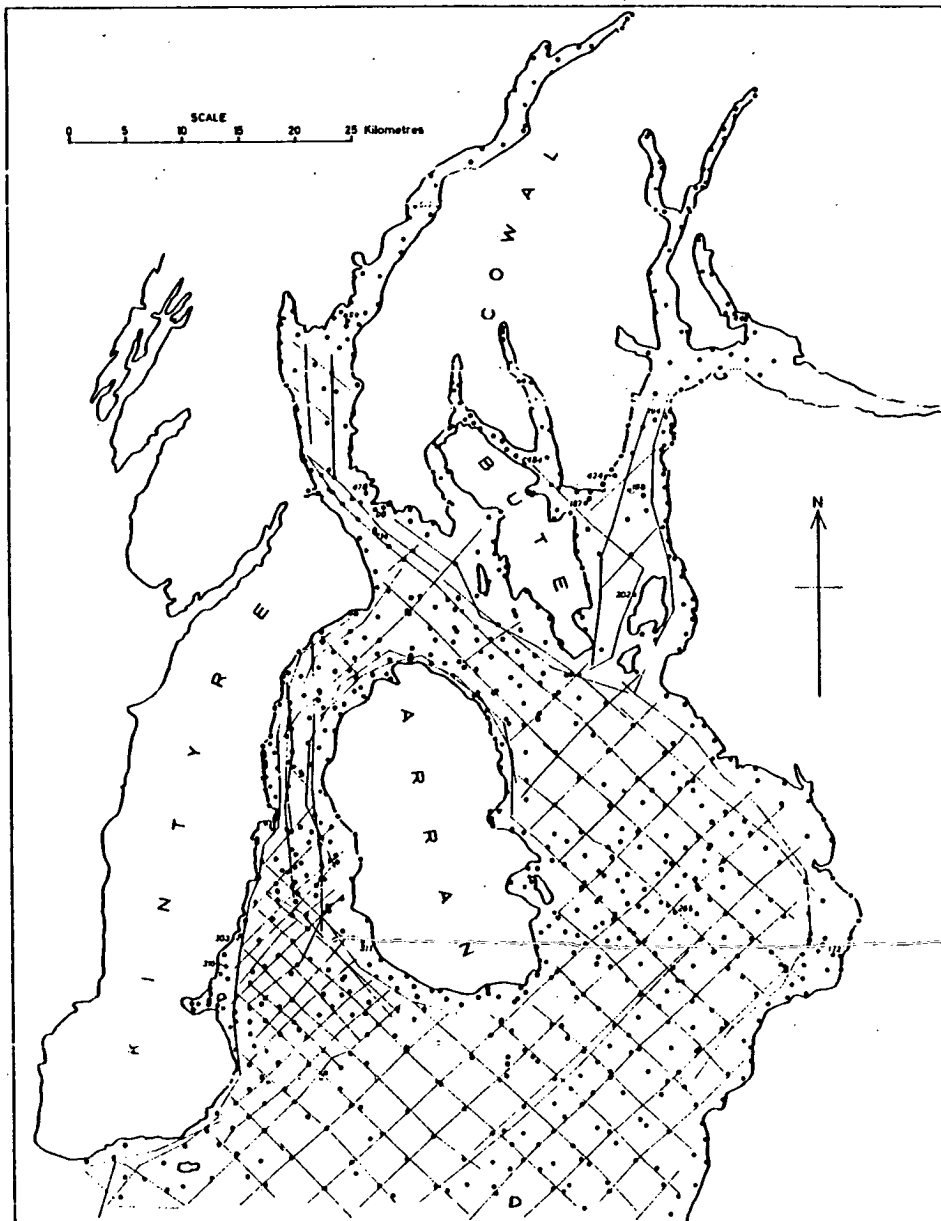
CHAPTER 6 FIRTH OF CLYDE

6.1 Background

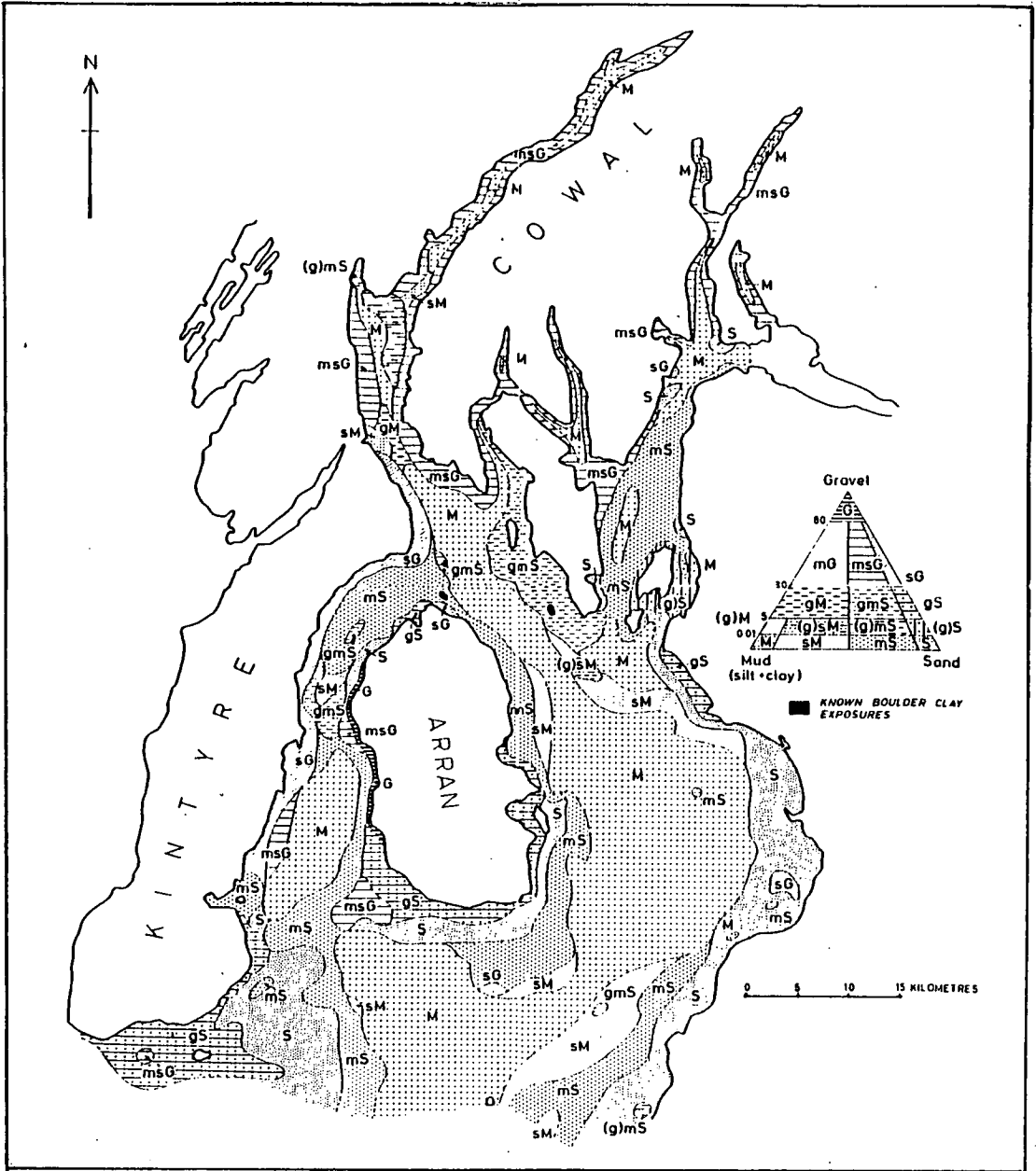
The Clyde Estuary and waters adjacent to the Isle of Arran were extensively surveyed by The Institute of Geological Sciences (IGS) in five phases between 1969 and 1971. A large volume of geophysical and geological data was gathered and interpreted in an IGS report published in 1973 (Deegan, 1973). The information contained in the latter is summarized in Fig 6.1 (sample distribution), Fig. 6.2 (onshore geology), Fig. 6.3 (surface sediment classification by particle size) and Fig. 6.4 (manganese distribution).

Magnetic analysis in the Clyde area marked a move away from the exclusive use of core material in this thesis. Work was instead centred around the mineral magnetic analysis of superficial surface sediments that had been recovered using a Shipex Grab sampler. It was hoped to apply the technique of mapping sediment types through susceptibility properties developed in the Peach area to samples from the Clyde. However, in the case of the grab samples from the Clyde, mass specific susceptibility, (χ) was used instead of whole core susceptibility. Palaeomagnetic techniques were not relevant in the study of surface sediments. Emphasis was placed on using χ , and other mineral magnetic parameters as rapid sediment mapping tools.

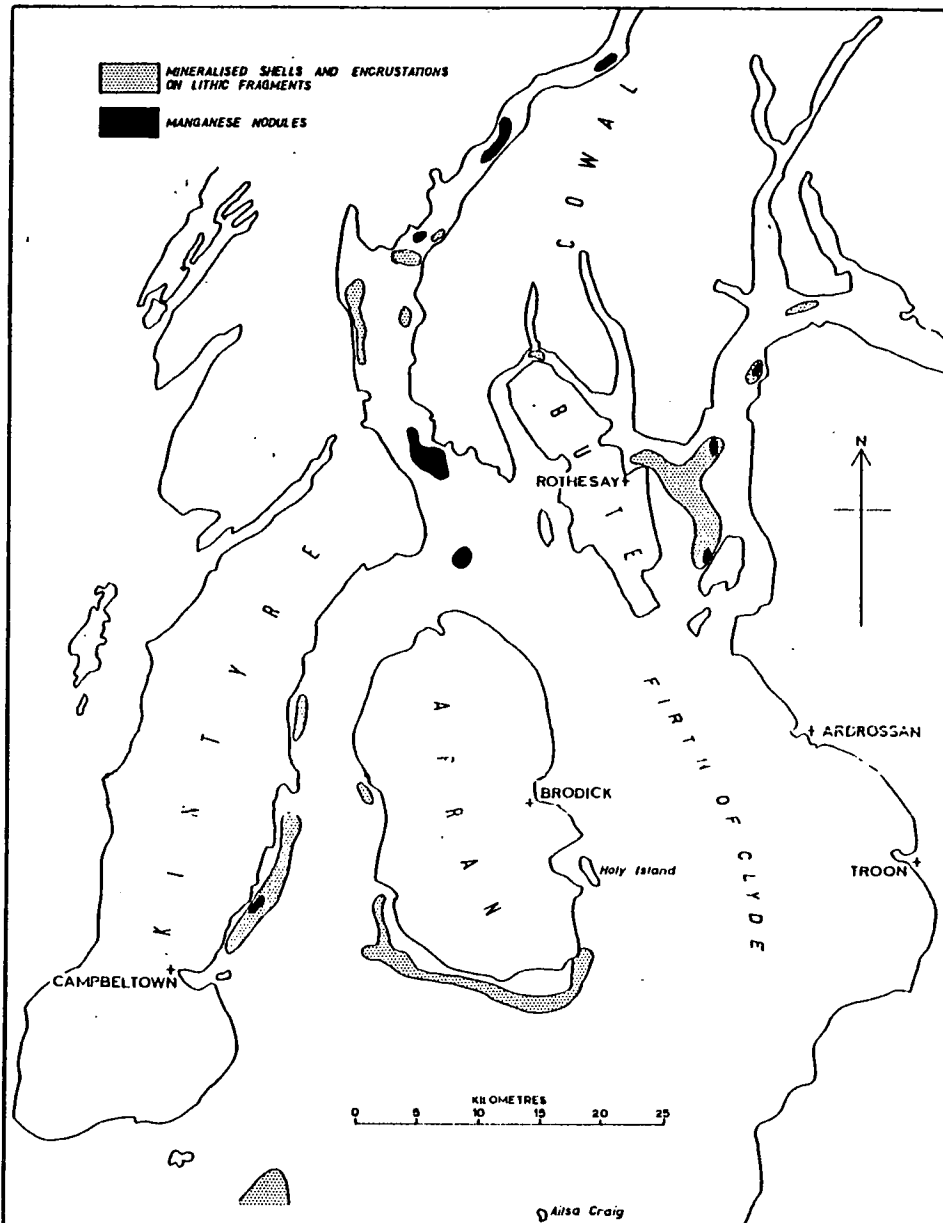
In addition to having a large sample set readily available, the Firth of Clyde had other attractions as a study area. There are a large number of possible sediment source areas, ranging from local reworked beaches to catchments feeding the connecting sea-lochs (Deegan, 1973). Recent anthropogenic inputs, associated with approximately 300 years of heavy industrial activity centred around the Clyde and Ayrshire coasts are superimposed upon the sedimentation pattern created by the natural environment. Another factor taken into account in the choice of survey sites was the documented evidence of diagenesis within recent sediments and the associated formation of manganese concentrations, recorded as far back as 1878 (Buchanan, 1891). It was hoped that some grab samples might show signs of manganese concentrations in their magnetic properties.



- Fig 6.1 Map showing density of sample stations and geophysical data lines in the Firth of Clyde (Deegan 1973). Based on data obtained from *M.v. Moray Firth IV* 17-30 May 1969 (Geophysics), *R.v. Strathclyde* 8-23 April, 6-25 June 1969 (reconnaissance geological sampling), *M.v. Maria W.* 21-24 July 1969 (vibrocoring), *M.v. Stella Maris* 8-19 Dec 1969 (supplementary shallow seismic profiling), *M.v. Whitethorn* 24 Nov- 21 Dec 1970, 2 Feb.- 2 Mar 1971 (Over the side drilling).



- Fig 6.3 Distribution of sediments in Firth of Clyde based on Folk classification (Deegan 1973).



- Fig 6.4 Areas of manganese mineralisation in Firth of Clyde (Deegan 1983).

1 Sample Distribution

Fig. 6.1 shows all the BGS sample stations in the Clyde area. The intensity of sampling is considerable, extending from the upper reaches of the associated Lochs to beyond Ailsa Craig. Sampling was carried out to within close proximity of the shore lines. The resulting sample set is one of the most comprehensive available for a UK continental shelf location. As the majority of work previously undertaken by BGS on samples from the Clyde region was non-destructive, grab samples from virtually all the sampling stations in fig 6.1 were available from BGS stores for magnetic analysis.

2 Onshore Geology

The solid geology of the coastal areas adjoining the Firth of Clyde is very varied. As can be seen in fig 6.2, the coastlines of Kintyre, Cowal and Bute consist of Dalradian material. The southern tip of Kintyre features local bodies of Upper Palaeozoic lavas and Lower Old Red Sandstones. The coastlines of the Irvine and Ayr Bays consist principally of Carboniferous material with Palaeozoic lavas set some distance inshore. South of Ayr Bay, the coast around Culzean Bay is dominated by Lower Old Red Sandstones. Situated slightly off the mainland, the Isle of Arran has its own peculiar geology. Dominating the north of the Island is a large body of Tertiary Granite, set within a thin belt of Dalradian material. The southern half of the island consists of a large mass of New Red Sandstone.

3 Surface Deposits

Fig. 6.3 illustrates the surface sediment distribution for the Clyde area. It is based on 124 complete particle size analyses combined with rapid microscopic examination of all other samples as they were recovered. (Deegan, 1983). Deegan identified three principal facies on the basis of particle size and mineralogy.

- a) Course Littoral Facies - Defined by 80% of the sample being greater than 62.5 μ m. These course facies can contain 'manganese nodules' eg in the lower Loch Fyne area. Magnetite is recorded as a common accessory mineral.
- b) Transitional Facies - the mS and SM divisions of fig 3. This facies often shows evidence of pea-sized manganese nodules and mineralised shell debris.
- c) Deep silty-clay Facies - Cohesive silty clays, not more than 1% bigger than

62.5 μ m. Where sand is present, magnetite is found as an accessory mineral.

4 Manganese Distribution

Fig 6.4 shows the areas of manganese distribution in the Firth of Clyde. The main manganese concentrations are of limited extent. Areas of mineralised shells and encrusted lithogenic fragments are seen close to the coasts of Arran, Kintyre and Bute. Much smaller zones of manganese nodules are found in Loch Fyne and the upper reaches of the river Clyde. The zones of manganese mineralisation located by Buchanan (1891) proved difficult to relocate in the 1970s surveys, suggesting that manganese mineralisation may be a transient feature in particular areas (Deegan, 1983).

6.2 Measurements

Magnetic measurements on the Clyde grab samples were carried out in three stages. Each stage consisted of an individual undergraduate project with the author providing overall supervision. Initial work was undertaken by Matthews (1986) working on a geographically representative set of 158 grab samples covering the upper Firth of Clyde region. Measurements consisted of χ and SIRM on all 158 samples, plus the growth of IRM acquisition curves (up to an applied field of 1T) for selected pilot samples. Matthews (1986) worked on the mud fraction, <63 μ m, from each grab sample.

Using Matthews (1986) work as a guide, Sommerville (1987) performed similar work on the sand fraction of the same set of grab samples. Investigation of the relationship between particle size and χ was also undertaken by Sommerville.

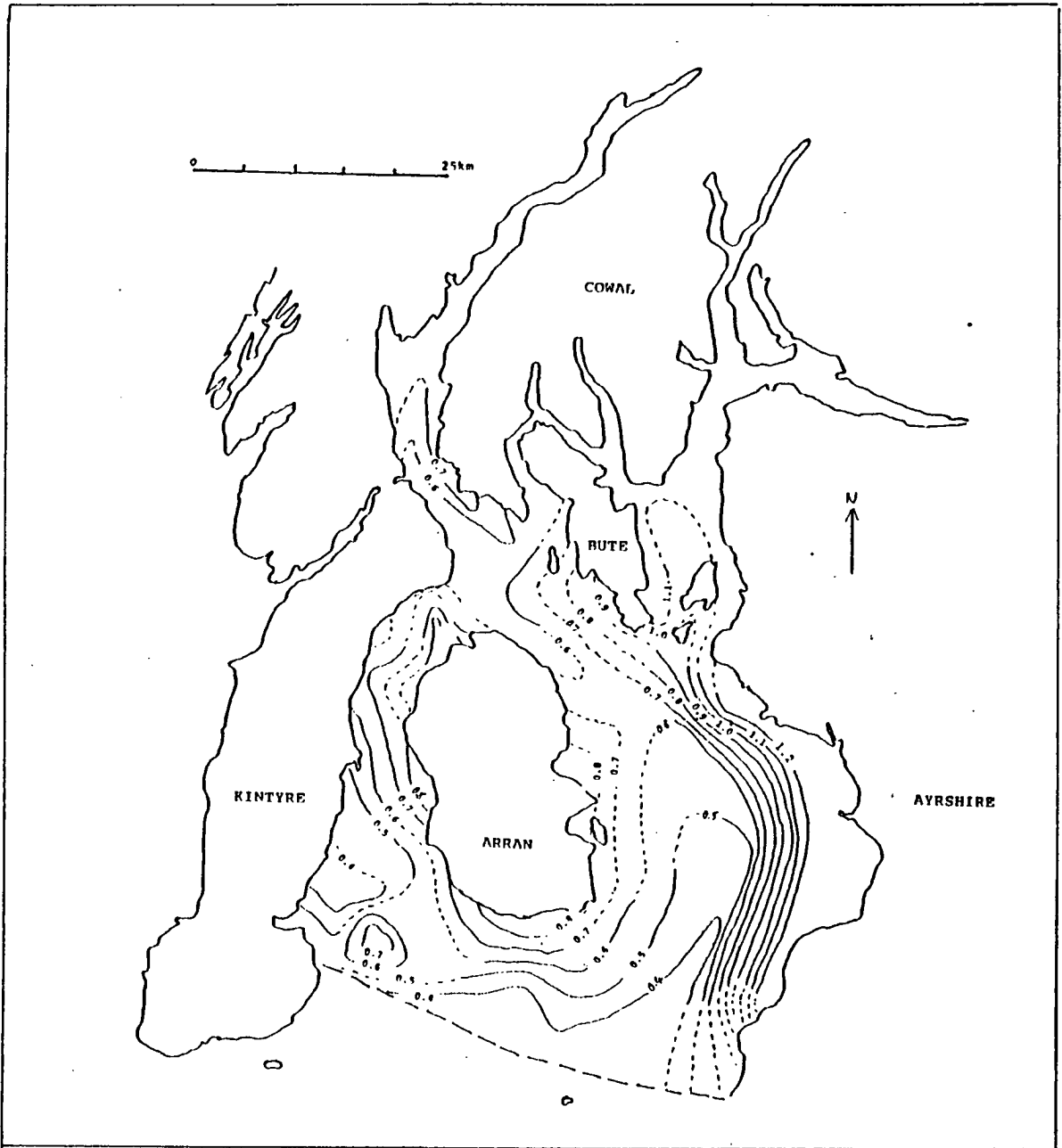
The final phase of work was carried out by Anderson (1988) who took 150 additional grab samples for χ and SIRM analysis, and made 25 further backfield IRM analyses to complete the coverage of the southern Clyde past the tip of Kintyre and Ailsa Craig. Dr R. Thompson also provided some unpublished data on particle size and χ measurements obtained for cores taken from the Clyde (Turner, 1978).

6.3 Results

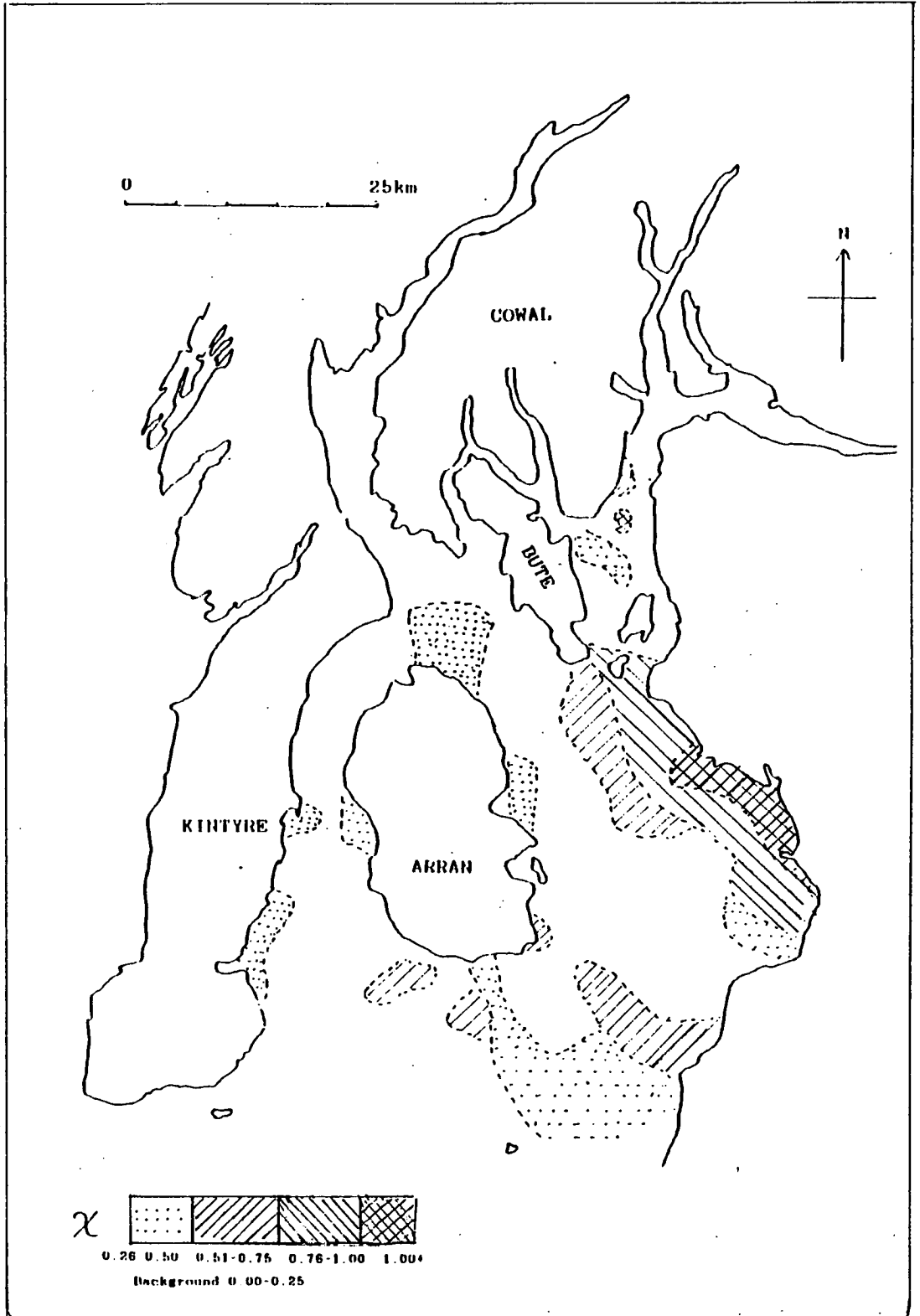
1 Susceptibility Results

Fig. 6.5 shows χ distribution in the mud fraction as originally contoured by Matthews (1986). The mud χ data contoured easily revealing a number of features in the distribution of χ across the Firth of Clyde. The dominant feature of this distribution is the increase in χ with proximity to the Ayrshire coast. χ values of $>1.2 \mu\text{m}^3\text{kg}^{-1}$ were common in the Ayrshire Bay. Similar high values were found in the vicinity of Bute, whilst lesser values ($0.8 \mu\text{m}^3\text{kg}^{-1}$) were found in pockets around the Isle of Arran. χ lows were found in the vicinity of the eastern coast of Kintyre, χ grading from $0.8 \mu\text{m}^3\text{kg}^{-1}$ off the West of Arran to as low as $0.4 \mu\text{m}^3\text{kg}^{-1}$ off the east of Kintyre. χ was also seen to generally decrease in a southerly direction down the Firth of Clyde, dropping to $0.4 \mu\text{m}^3\text{kg}^{-1}$ in the southern reaches of the study area. One notable exception to the trend of southerly decreasing χ was an isolated high of $0.7 \mu\text{m}^3\text{kg}^{-1}$ in the vicinity of the south east tip of Kintyre.

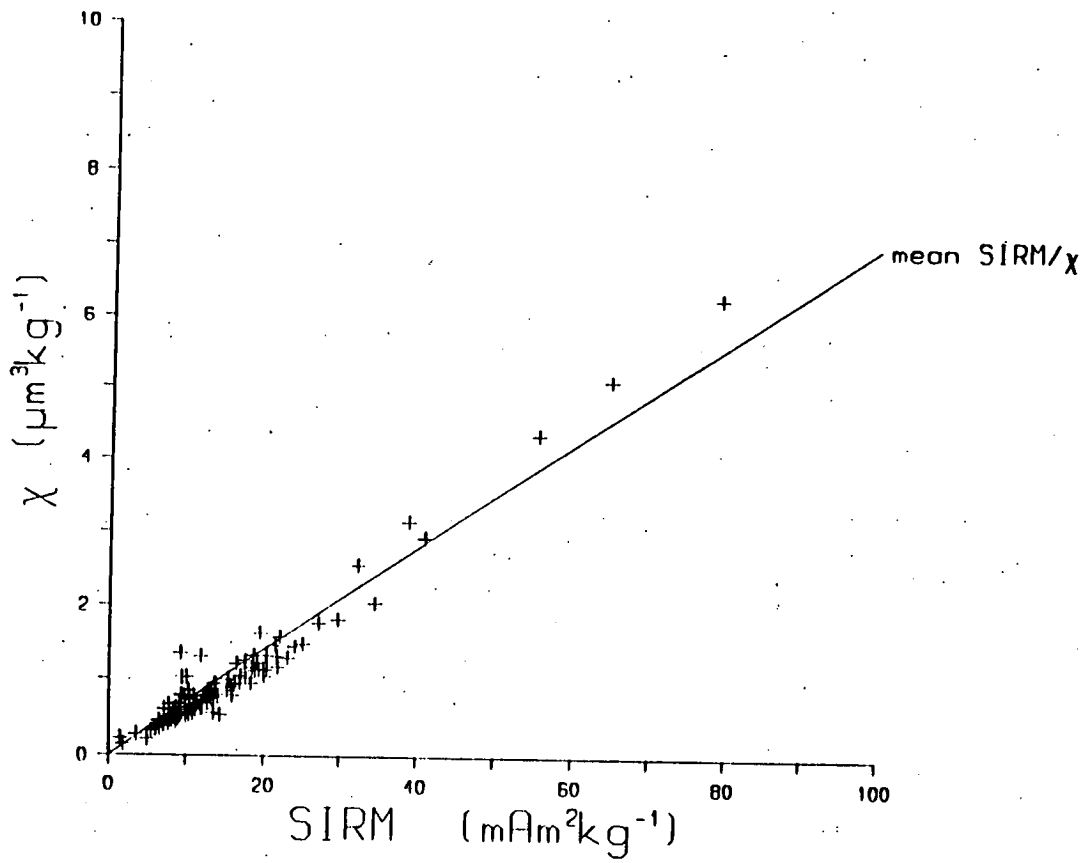
Fig. 6.6 incorporates the two data sets from Sommerville (1987) and Anderson (1988) for the sand fraction. In the case of the sand χ values, the data has been displayed in terms of zones of varying susceptibility by the author as the nature of the data distribution did not suit contouring. The use of computer based contouring packages proved impractical due to the large areas of coastline and islands giving rise to numerous edge effects. These edge effects would require manual interpretation, defeating the nature of using an automated contouring package. The sporadic distribution of the sand fraction data also meant that the use of a computerised plotting package was inappropriate. The dominant feature of the χ distribution in the sands is the generally low χ value in the range 0.00 to $0.25 \mu\text{m}^3\text{kg}^{-1}$ found for the majority of samples. Superimposed on this low background are small pockets of higher χ . The highest values of χ are in the range 0.76 to $1.00 \mu\text{m}^3\text{kg}^{-1}$ found in the Ayrshire bay. Other lesser highs are found in pockets around the coast of Arran, the east coast of Kintyre, off Bute and in a band stretching from the southern tip of Arran to Culzean Bay.



- Fig 6.5 Magnetic susceptibility, χ ($\mu\text{m}^3\text{kg}^{-1}$) distribution in Firth of Clyde grab samples, mud fraction, (Matthews 1987).



- Fig 6.6 Magnetic susceptibility, χ distribution in the sand fraction of grab samples. Compiled using data from Sommerville (1987) and Anderson (1988).



- Fig 6.7 Relationship of SIRM to χ in Firth of Clyde grab samples , mud fraction, (Matthews 1986).

2 SIRM/ χ Results

The relationship between SIRM and χ for the mud fraction of grab samples is shown in fig 6.7 (Matthews 1986). The SIRM/ χ ratios for the muds varied between 12 and 19 kAm^{-1} , but the majority were tightly grouped around an average of 16.5 kAm^{-1} . SIRM/ χ ratios for the sand fractions varied in the range 14 to 24 kAm^{-1} .

3 IRM Results

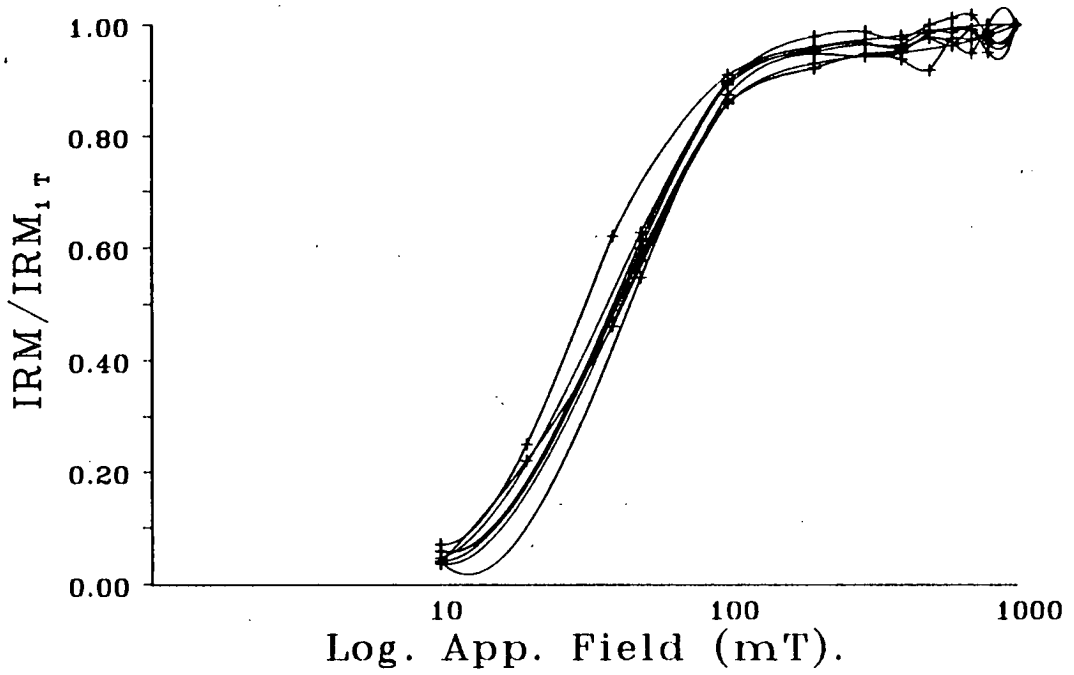
Forward IRM data derived by Matthews (1986) for the mud fraction of grab samples is shown in Fig. 6.8. The IRM data has been replotted on a logarithmic scale. All the IRM curves are tightly grouped, with coercivity of approximately 40 to 50mT, all samples reaching 90% of saturation by 100mT. Backfield IRM data for the sand fraction of selected samples derived by Anderson (1988) is shown in fig 6.9. The IRM curves are spread over a wide range with coercivities falling within a broad range of 25 to 90 mT. Both Figs 6.8 and 6.9 have been chosen to show a representative range of the total data set.

4 Particle Size Results

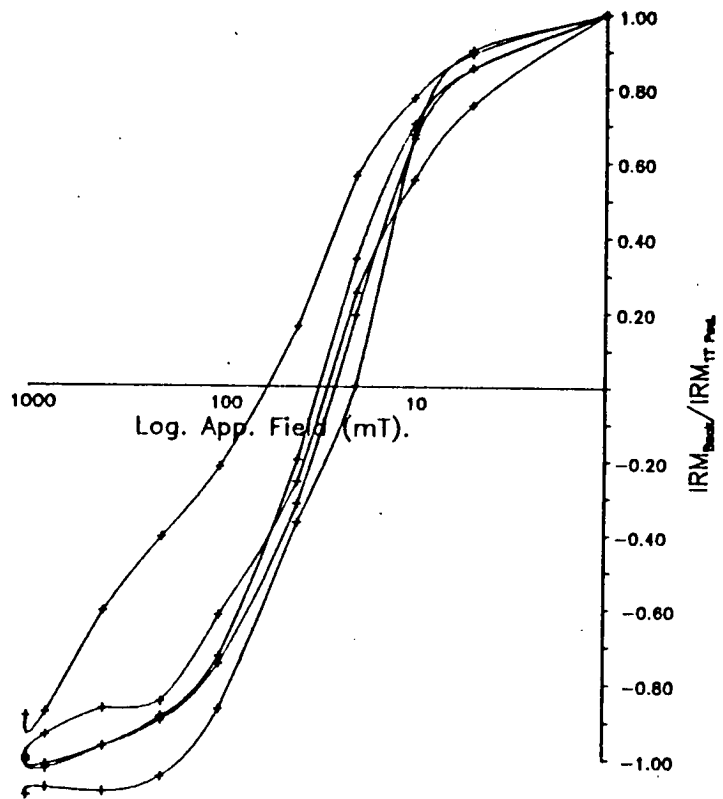
Figure 6.10 shows the distribution of χ with particle size for two examples taken from Sommerville (1987). Sommervilles work is supplemented by data provided by Dr. R.Thompson for the finer fractions. When these two data sets are taken together, a double peaked relationship of χ to particle size is seen. χ peak values of 1 and 1.2 $\mu\text{m}^3\text{kg}^{-1}$ are seen in the 0.063 to 0.032mm and >0.5 mm fractions.

6.4 Discussion

The susceptibility data for for the Clyde is summarized in the maps of χ distribution for muds, fig. 6.6, and for sands, fig 6.7. These figures show several common features, for example high values of χ off the Ayrshire coast, but differ considerably in the spread of data. Fig. 6.6 showing data from the mud fraction has smoothly grading data which contours readily, whereas fig. 6.7, with data from the sands has abrupt changes around pockets of extreme high and low susceptibilities. Consequently the sand χ data does not contour easily. Instead, it was found that defining zones of certain χ ranges worked



- Fig 6.8 Forward IRM curves illustrating the range of magnetic mineralogies encountered in the mud fraction of grab samples from the Firth of Clyde. Compiled from data obtained from Matthews (1986).



- Fig 6.9 'Back-field' IRM curves illustrating typical magnetic mineralogies encountered in the sand fraction of grab samples from the Firth of Clyde. Compiled using data from Anderson (1988),

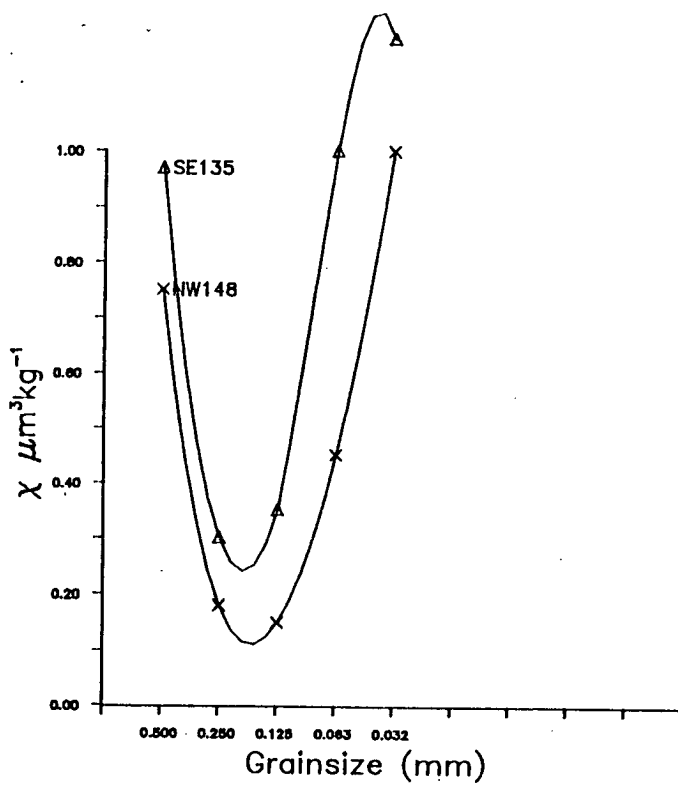
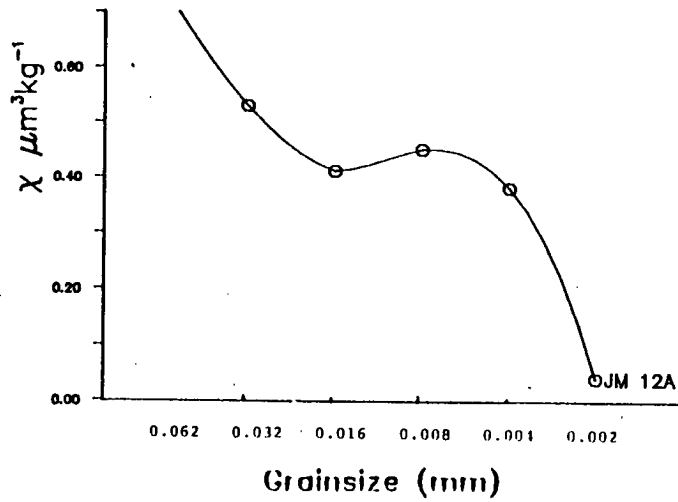
acceptably well for the sands.

The difference in nature of the mud and sand data sets can largely be explained by reference to Stoke's Law. The lighter mud fraction would remain in suspension longer, being transported further than the sand fraction originating from the same source. The differential in ease of transport between sand and mud would result in a more homogenous distribution for the muds. Conversely, the sands can be expected to remain nearer to source, leading to localized highs and lows.

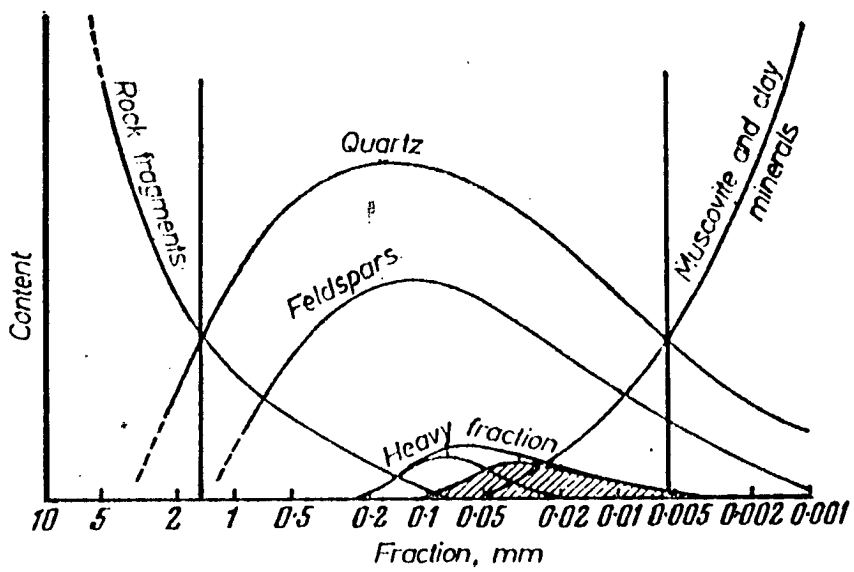
If Stokes Law is taken as the dominant control on sediment distribution, it would be expected that the magnetic properties of the sand fraction would reflect local geology to a greater extent than than the muds. However, other factors have to be considered. Superimposed on the Stokes Law effect are possible diagenetic effects, as supported by the manganese concentrations (fig 6.4, Deegan 1973). Reference also has to be made to the variation of magnetic mineral concentration with particle size. For example, one would expect high coercivity components to be more closely associated with sands where haematite is likely to be cemented to the quartz grains. As a result of such competing factors, some magnetic characteristics of a sediment source may be found in one particle size fraction only.

The relationship of χ to particle size is shown in fig 6.10 (Sommerville 1987 and Thompson, unpublished data). The double peak distribution featuring χ highs in the 0.5mm+ and 0.063-0.032mm fractions can be explained in terms of the general distribution expected for clastic material in the grain size spectrum of as sediments outlined by Strakhov (1969), fig 6.11. High χ in the 0.5mm+ fraction is likely to be due to the presence of locally derived highly magnetic rock fragments while the magnetic minerals derived from the breakdown of rock fragments would tend to concentrate in the 0.063 to 0.032 mm heavy mineral particle size range, leading to a second χ high.

Examining the χ distribution in greater detail shows that there are several zones that warrant individual comment. The Ayrshire Bay area is characterized by increasing χ towards the coast. The χ increase is common to both the mud and sand fractions, and can be attributed to the local Carboniferous shore geology combined with the possible effects of heavy industry along the Ayrshire coast. The gravel composition data (fig 6.14) shows material with a



- Fig 6.10 Particle size vs χ for Clyde material. Compiled from Sommerville (1987)-grainsizes 0.032-0.5mm and Thompson (1988 unpublished data) grainsizes 0.002 to 0.062 mm.



- Fig 6.11 Distribution of clastic material in the grain-size spectrum of sediments (Strakhov 1969).

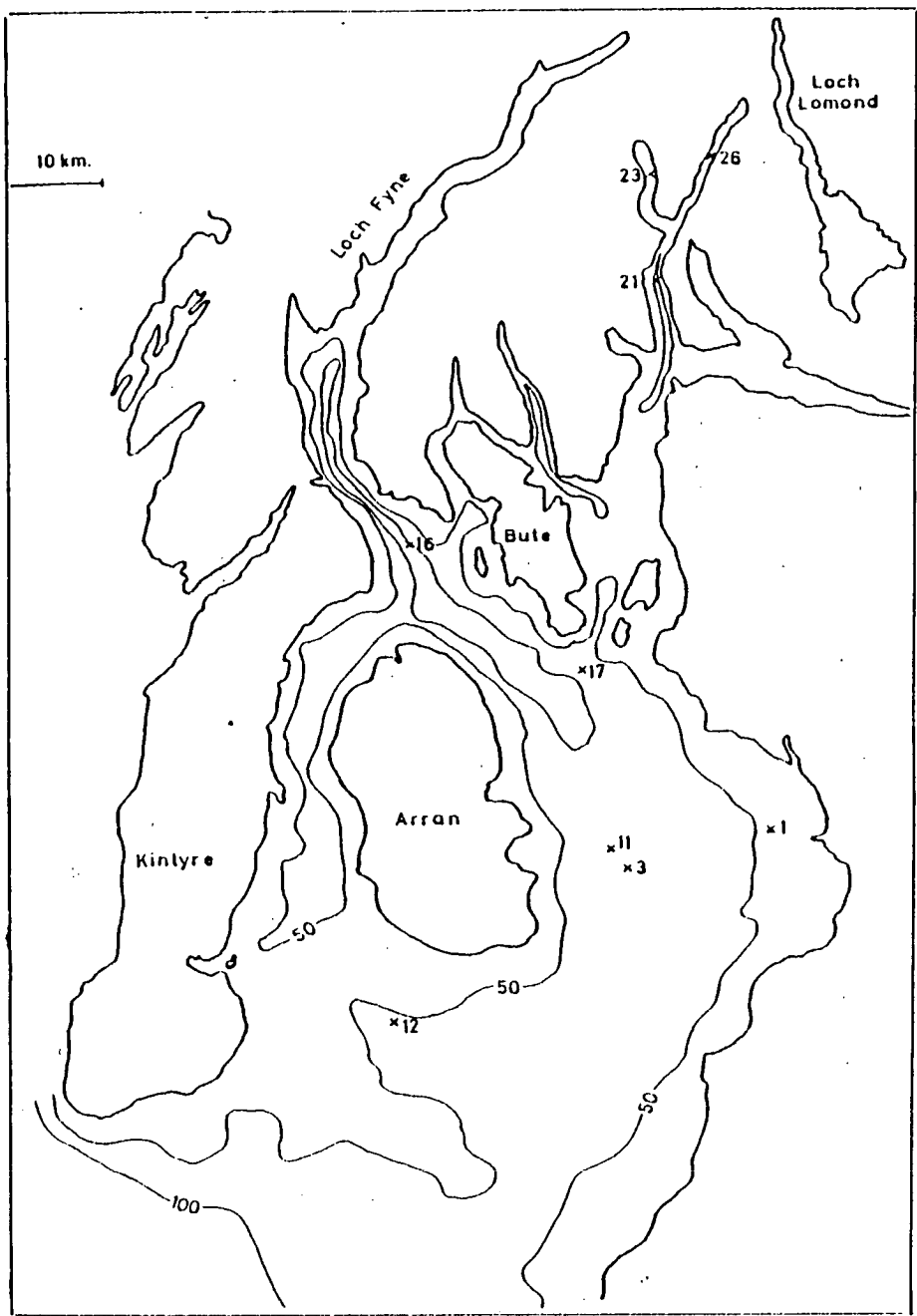
significant basic component which is reflected in a χ high. According to Deegan (1973), Ayrshire Bay is also an active sedimentary environment leading to the selective sorting of material culminating in a higher proportion of heavy components. Deegan (1973) also proposed a closed environment of sedimentation, with little external input. Consequently reworking of old beaches along the Ayrshire coast provides a large proportion of the sedimentary material within the Ayrshire Bay.

To the east of the Isle of Bute, high manganese concentrations are found in the same area as a χ high. A similar situation is also seen off the southern tip of Arran. The close relationship between iron, χ and manganese is shown in chapter 9.

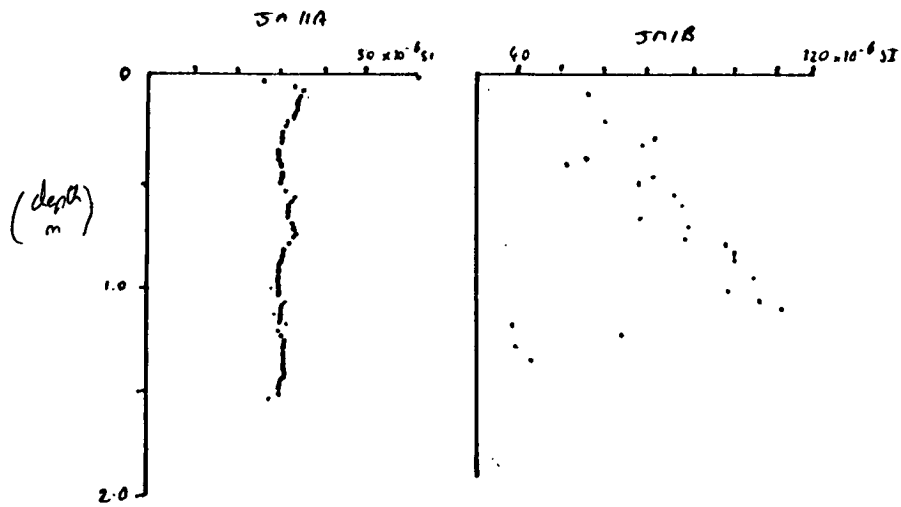
There is little evidence of high coercivity components in grab samples from the the Clyde region. The presence of large bodies of sandstones on Arran, Kintyre, and Culzan Bay (fig 6.2) would suggest a source rich in haematite for the sediments adjacent to these bodies. However the IRM data for mud fractions (fig 6.8), indicates that magnetite is the dominant magnetic mineral, most samples saturating well before 100mT and with SIRM/ χ ratios in the range 12–19 kAm⁻¹. The range of SIRM/ χ ratios in the sands is much more varied than in the mud fraction. There is some evidence of high coercivity material in the sands off the southern tip of Kintyre. Samples from the latter position gave an SIRM/ χ ratio of 24 kAm⁻¹, the highest of any in the Clyde area. However, the χ value for these samples was low (0.08 $\mu\text{m}^3\text{kg}^{-1}$), suggesting that the high coercivity component is more visible in these sample due to a relative magnetite deficiency. Off the south coast of Arran, SIRM/ χ values of 14 kAm⁻¹ were typical, suggesting a mineralogy totally dominated by magnetites. The absence of a haematite component is surprising, considering that sandstones constitute half the land mass of Arran. It would appear that haematite is not transported to deposition sites local to the sources.

The influence of basic components within the course sands and gravels on χ can be seen off the Eastern Kintyre coast. Here, basic material is mostly absent leading to a low (relative to Arran and Ayrshire coasts) χ despite increasing particle size.

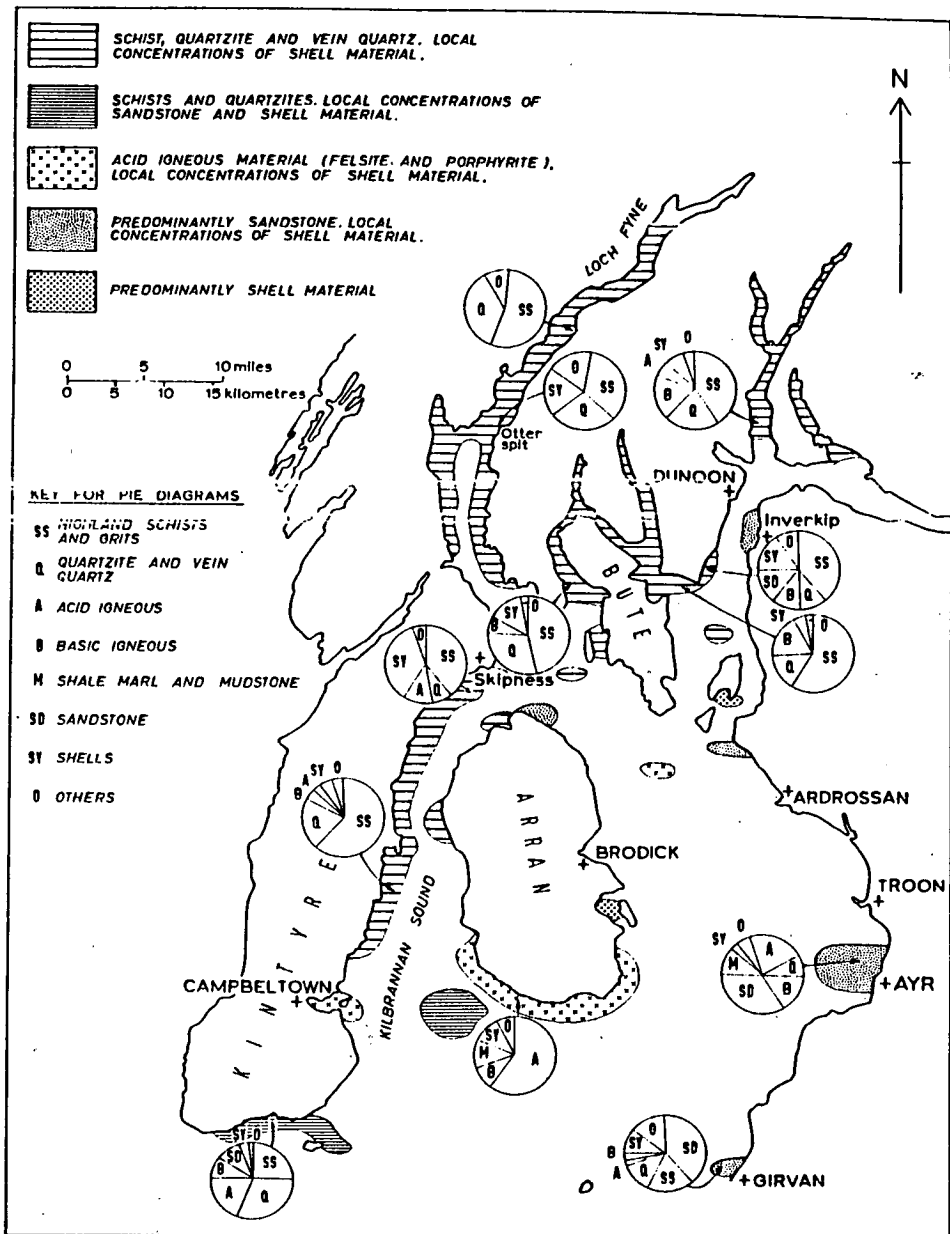
Earlier work by Turner (1979) on cores from the Clyde area (fig 6.12) gives an indication of the effects of diagenetic change. Most of the cores in Turner's



- Fig 6.12 Coring sites on the Firth of Clyde. Coring undertaken by *M.V. John Murray*. (Turner 1979).



- Fig 6.13 Whole core susceptibility data for cores 11A and 1B from the Firth of Clyde, (Turner 1979).



- Fig 6.14 Composition of gravel samples from the Clyde (Deegan 1973).

study showed whole core susceptibility patterns similar to that of core JM6.12 and 6.13A (fig 6.13). In these cases there is little variation through time suggesting a stable depositional and chemical environment. An exception to this stability is core JM1B which shows considerable fluctuation. This fluctuation reflects the likely reworking of old beach material in the Ayrshire Bay area (Deegan 1973) and the possible varying influx of material from the Ayrshire coast. Another interesting feature of cores 11A and 1B is a ratio of mean susceptibilities between the cores, of approximately 4:1 which is very similar to that obtained from surface χ data (3.5:1) from comparable positions. Such comparisons suggest a continuity in depositional conditions through time.

An additional unknown in the Clyde study is the condition of the samples compared to their in situ state. 15 years of storage in a dry state may have led to chemical change. However work on Flett material (chapter 4) comparing fresh and post-storage cores suggests little change occurs on wet stored material.

6.5 Significant Points

1) Susceptibility data can be successfully contoured within the Firth of Clyde area.

2) Magnetite is the dominant magnetic mineral in all samples studied, masking the presence of small quantities of haematite.

3) Susceptibility distribution is controlled by a combination of particle size, diagenetic change associated with manganese concentrations and basic igneous components.

4) Core susceptibility data indicates stable deposition in respect of susceptibility and particle size through time, except in areas of beach reworking.

CHAPTER 7 THE MORAY FIRTH

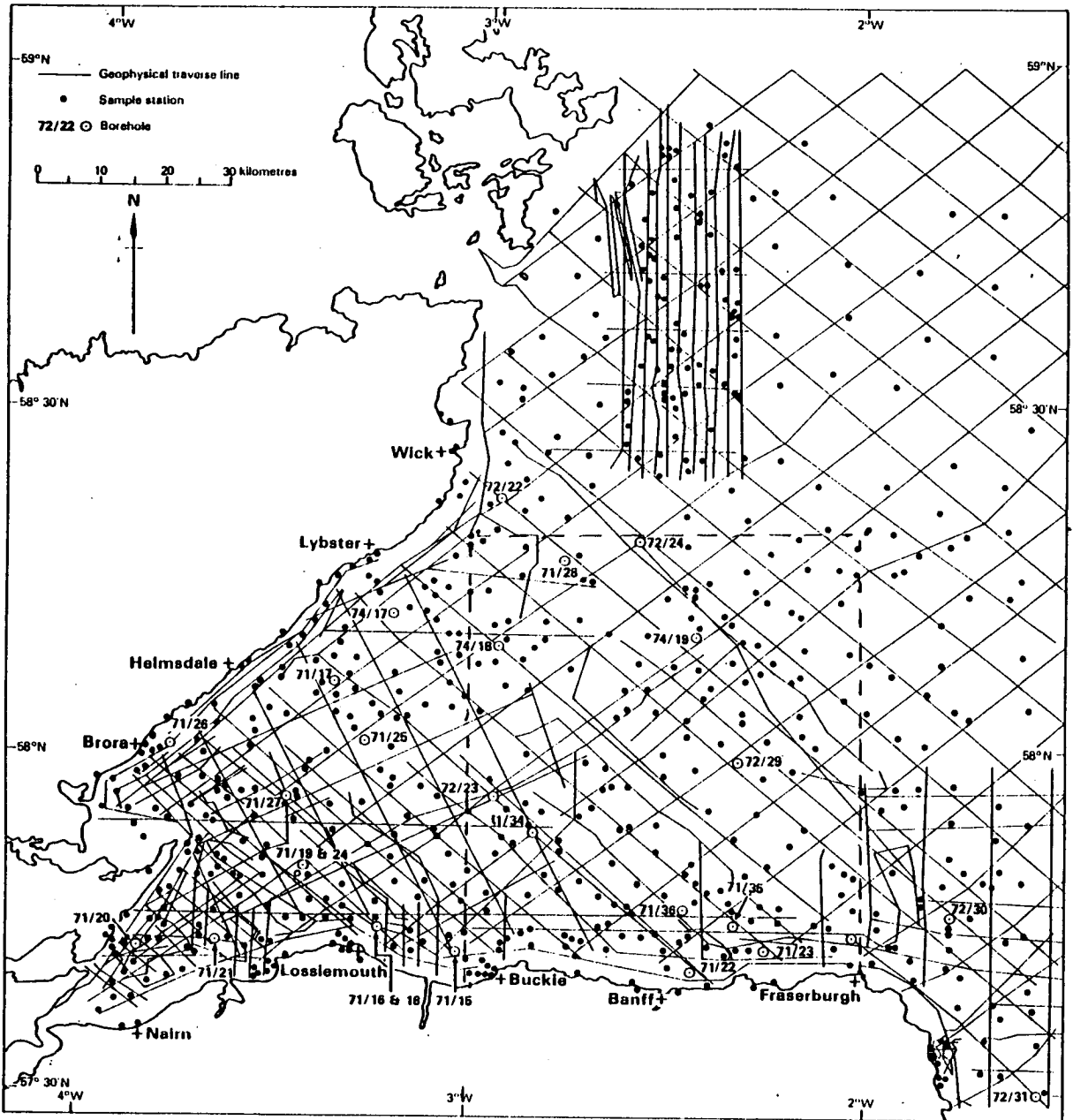
7.1 Introduction

Following the study of magnetic properties of surface sediments of The Firth of Clyde (chapter 6), The Moray Firth was selected as another site for investigation based on surface grab samples. It was hoped to apply the sea bed susceptibility mapping developed in the Clyde study to this second area. Given the varied geology of the coastlines of the Moray Firth it was also hoped to use mineral magnetic parameters to provide sediment source linkages. The situation in The Firth of Clyde had been complicated by possible industrial pollutants and manganese concentrations. The Moray Firth is in contrast relatively free of such influences.

The Moray Firth area was extensively surveyed by The Institute of Geological Sciences/British Geological Survey during the period 1966 to 1974. A large amount of geophysical data and geological sample material was gathered and has been well summarized by Chesher (1983). Fig. 7.1 shows the intensity of the sampling program undertaken by BGS. Shipex grab samples were available to the author for virtually all the sample stations shown in fig. 7.1.

In addition to the IGS/BGS sample sets, Reid and McManus (1987) collected information on current and suspended sediment distribution for the Moray Firth from a variety of sources. Their work provided an integrated picture of sediment sources, transport paths and sinks. Extensive particle size analysis was also carried out by Reid and McManus (1987). Particle size splits from their work were still available for use in this study.

Due to the size of the area and the volume of material available, a pilot study area was selected (see fig 7.1). Initial magnetic analysis was carried out by Howe (1988) as an undergraduate project. He further divided the pilot study area into a northern zone (58 20N to 58 00N) and a southern zone (57 40N to 58 00N).



- Fig 7.1 - BGS geophysical survey lines and geological sample station coverage in The Moray Firth including borehole sites (Chesher and Lawson 1983).

7.2 Geological Background

The local onshore/offshore geology is described in detail by Chesher and Lawson (1983). The coastlines of the area vary in geological nature (fig 7.2), particularly in terms of physical stability. Probert and Mitchell (1980) categorized the coastline into two types; outer 'hard' coastlines and inner 'soft' coastline coincident with the division of the offshore zone into the Inner Moray Firth and Outer Moray Firth.

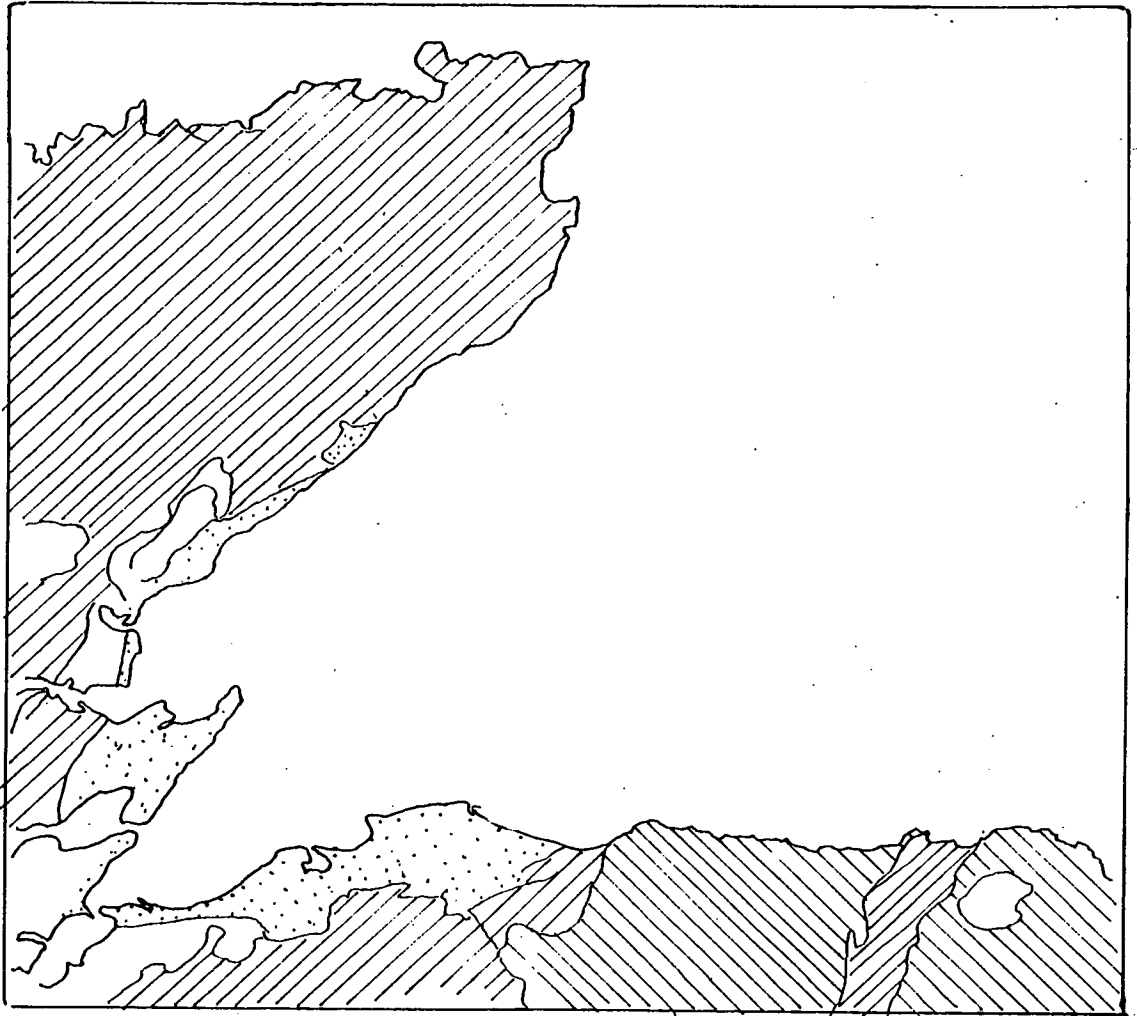
The 'hard' outer coastlines are generally cliff-girt and rocky with Old Red Sandstones dominating the Caithness coasts. The Banffshire coast, another 'hard' coastline consists principally of Dalradian metamorphic rocks.

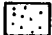
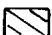

In contrast the inner 'soft' coastlines are characterized by large post-glacial accumulations of sediment with a wide particle size range but principally consisting of sand and mud. The sands tend to occur in large wind blown deposits whilst the muds commonly accumulate in the middle and upper reaches of the inner Firth. The post-glacial deposits may exceed 80m in thickness (Chesher and Lawson 1983).

The distribution of surface sediments within the Moray Firth is shown in fig. 7.3. This figure shows the dominance of sand size sediment over the northern central part of the Moray Firth. However, the southern coast shows a much more complex assemblage of grain sizes.

7.3 Sample Selection and Measurement Procedures

73 *Shipex Grab* samples were taken from the study area (fig 7.1). Two or three subsamples were selected at random from each 10 minute by 10 minute grid square within the study area. The sand fraction from each was selected for use on the basis that sand samples for the Firth of Clyde had shown greatest variation in mineral magnetic assemblages. It was hoped that such variation could be exploited in a sediment-source linkage model. All 73 samples were initially used for χ measurement. From these 73 samples, twelve samples were selected for IRM analysis. In each case IRMs were grown in pre-selected steps from 5mT to 1T applied field. Particle size splits remaining from Reids (1988) work were also subjected to χ measurement to assess the distribution of χ with particle size.

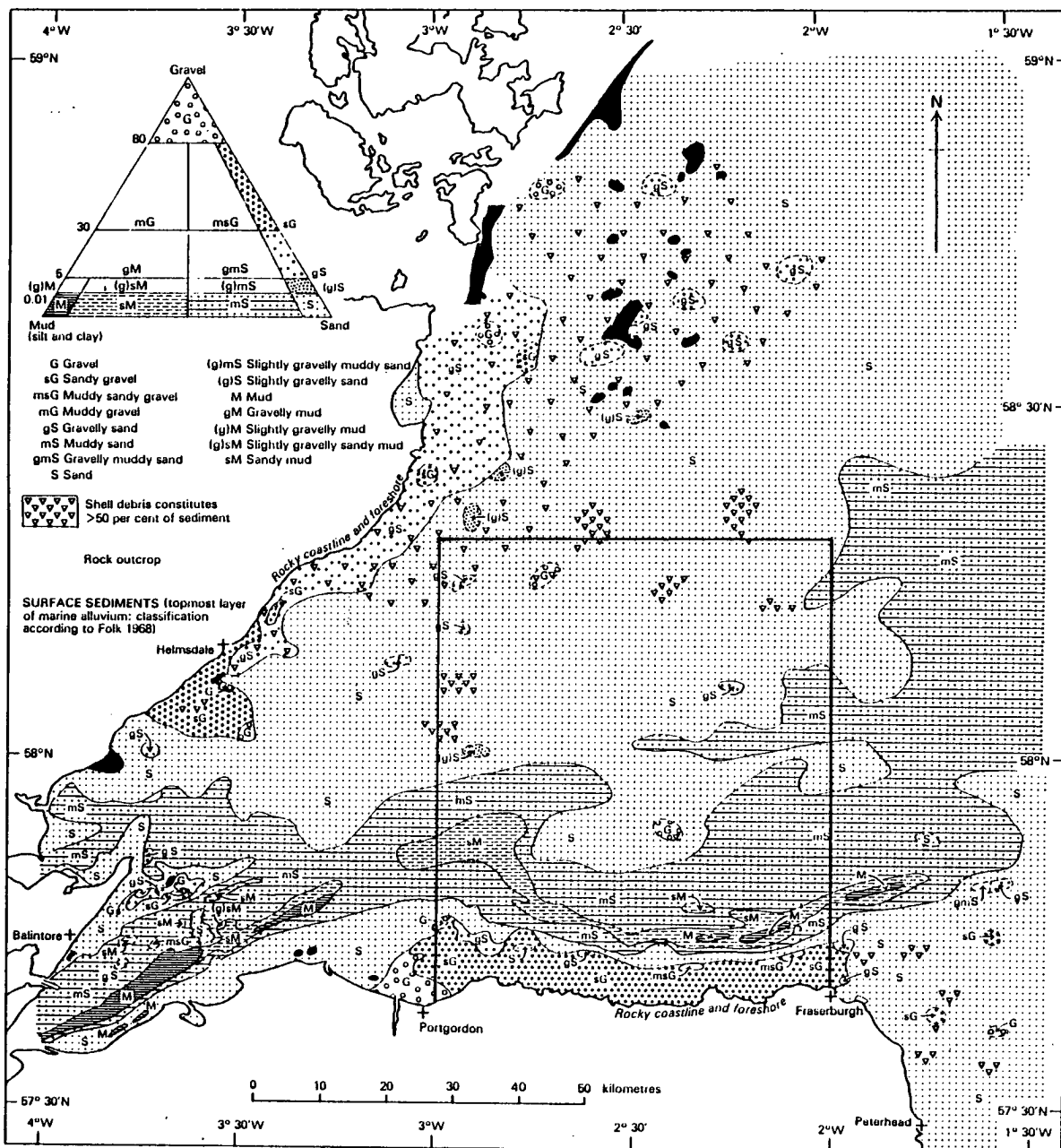


-  Post-glacial sediment
-  Dalradian metamorphics
-  Middle Old Red Sandstone

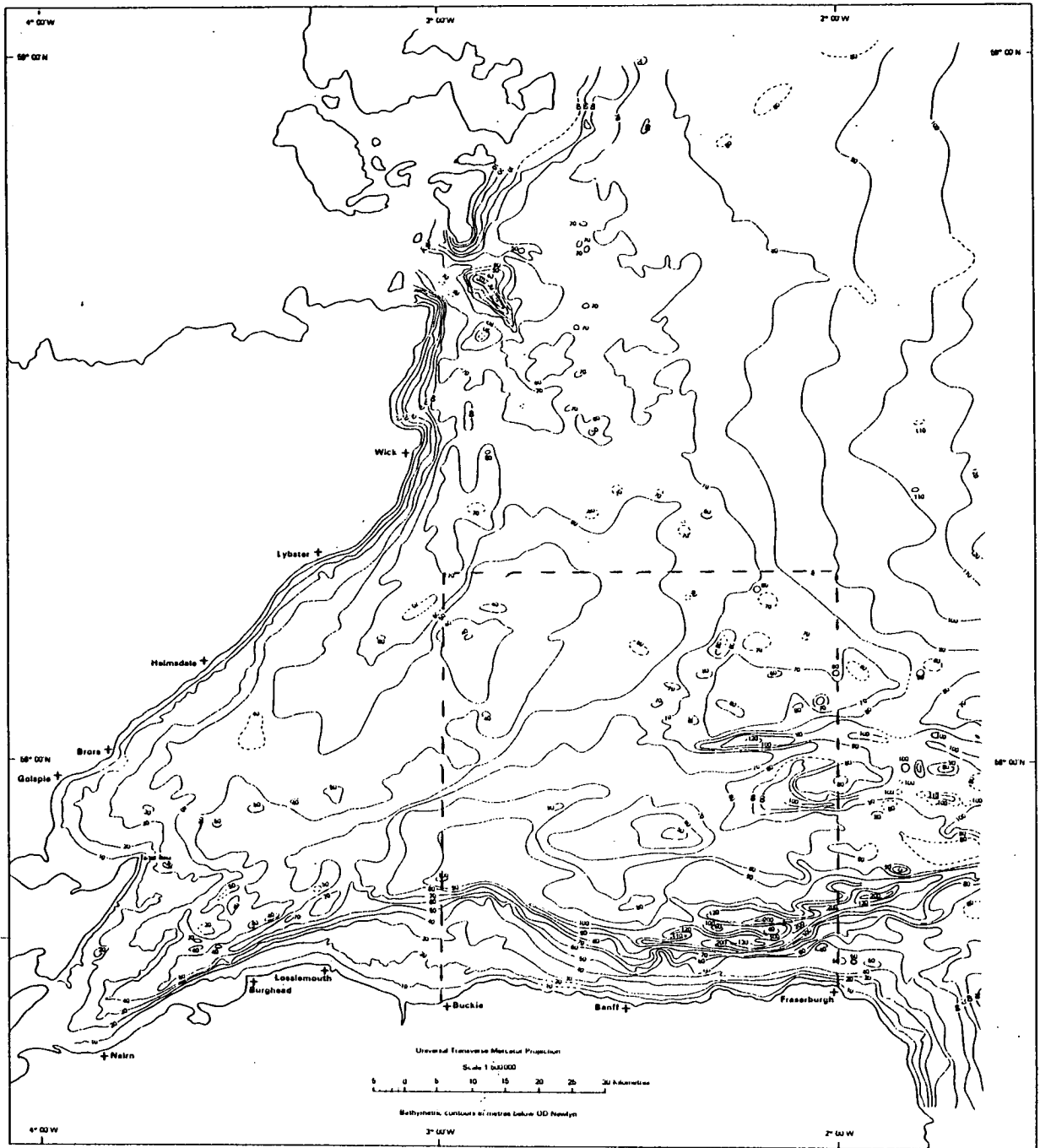
0 25km



Fig 7.2 A sketch map of the geology of the Moray Firth.



- Fig 7.3 - Particle size distribution of surface sediments in The Moray Firth based on Folk (1968) classifications (Chesher and Lawson 1983). Note the study area outline (Howe 1988).



- Fig 7.4 - Bathymetry of The Moray Firth, depth in metres below O.D. Newlyn (Chesher and Lawson 1983).

7.4 Results

1 Susceptibility Data

χ measurements were obtained for 73 samples from the Moray Firth. A wide range of χ values were found, the lowest being $0.011 \mu\text{m}^3\text{kg}^{-1}$, the highest $0.104 \mu\text{m}^3\text{kg}^{-1}$. The average χ value for the 73 samples was $0.048 \mu\text{m}^3\text{kg}^{-1}$. The average χ value for the northern area was $0.037 \mu\text{m}^3\text{kg}^{-1}$, and for the southern area $0.055 \mu\text{m}^3\text{kg}^{-1}$. Typical χ measurements for particular sediment classifications are shown in tab 7.1

Folk classification	Typical sample	χ	SIRM/ χ	HIRM
Sandy gravel	MF447	0.051	10.4	0.176
Sand	MF429	0.011	18.5	0.0508
Muddy sand	MF177	0.100	8.0	0.179

Table 7.1:

Table of χ ($\mu\text{m}^3\text{kg}^{-1}$), SIRM/ χ ratio (kAm^{-1}) and HIRM ($\text{mAm}^2\text{kg}^{-1}$) for samples representing the principal particle size groupings in the Moray Firth.

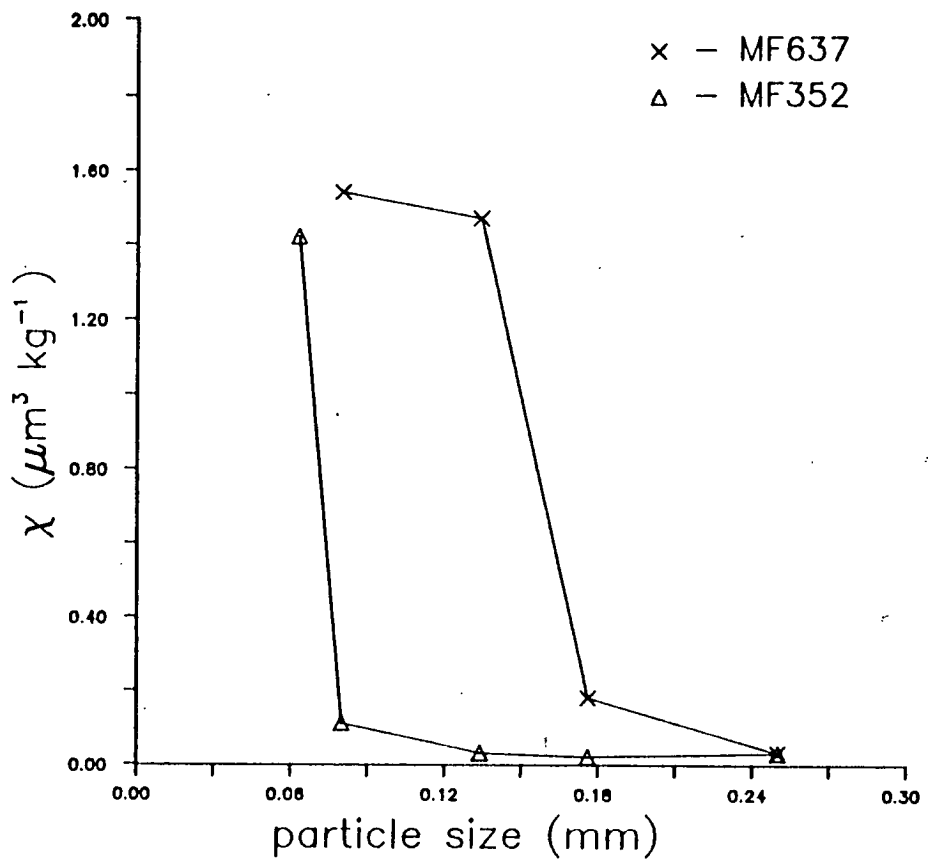
The relationship between particle size analysis and χ in two typical samples, MF637 and MF352 is shown in fig 7.5. χ is seen to peak towards the finer fractions (0.063 to 0.075mm split).

2 IRM analysis

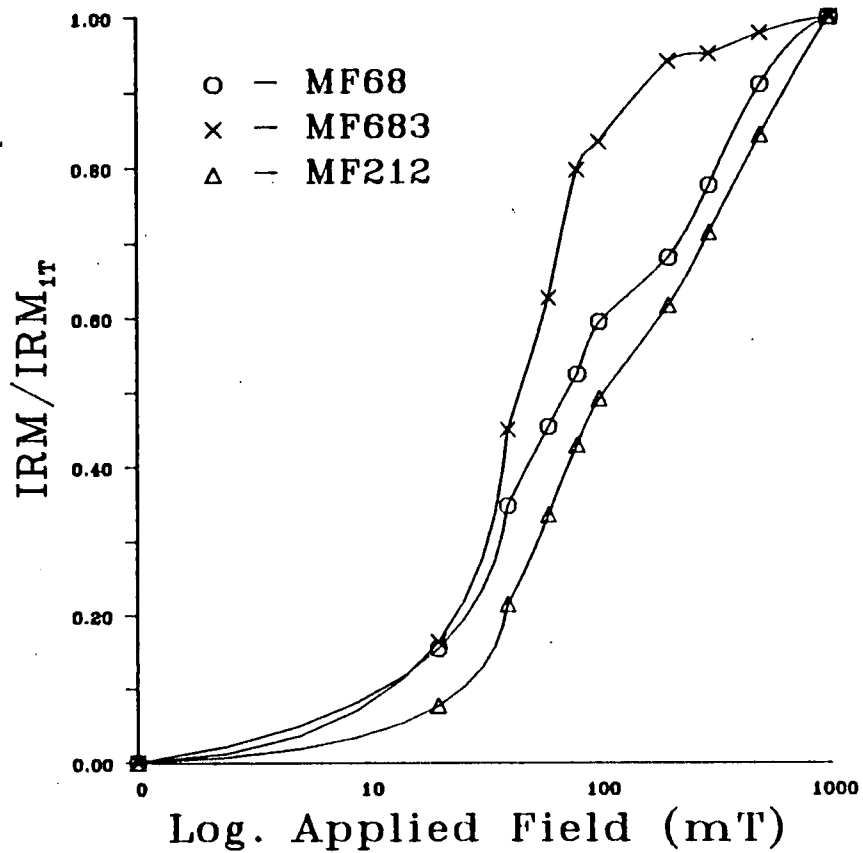
Example IRM acquisition curves for three samples representing the range of data seen in the pilot samples are shown in fig 7.6. Coercivity varies between 40 and 90 mT. All three samples exhibit a dual component IRM curve consisting of an initial curve from 0 to 100mT followed by a linear component from 100 to 1000 mT. In the case of sample MF683, there is arguably a third component between 100 and 200 mT.

3 SIRM/ χ and coercivity results

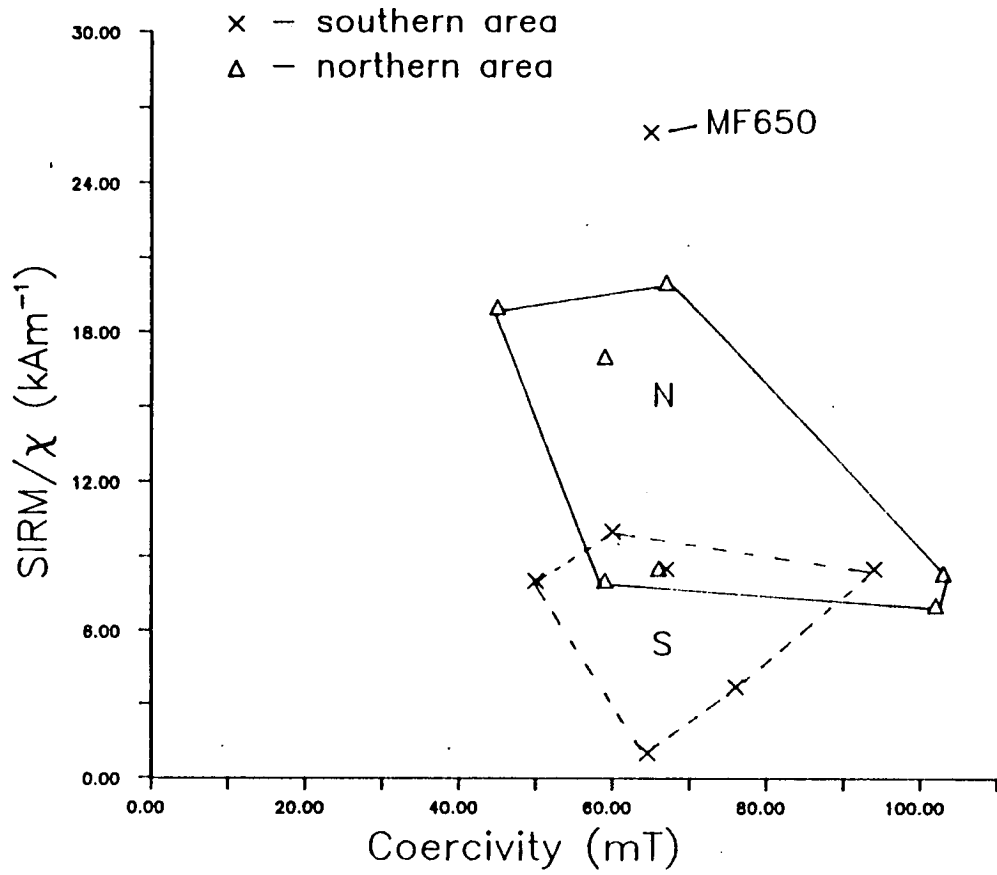
Fig. 7.7 shows the SIRM/ χ and coercivity values for 14 pilot samples from the Moray Firth. SIRM/ χ varies from 0.7 to 26.4kAm^{-1} , whilst coercivity varies from 52 to 101mT. With convex hull analysis applied, two slightly overlapping groups representing the northern and southern zones of the pilot study area



- Fig 7.5 - Examples of trend towards increased χ with decreasing particle size for samples from The Moray Firth (Howe 1988). Particle size splits provided by Reid (1988).



- Fig 7.6 - Acquisition IRM curves showing the range of magnetic mineralogies found in Moray Firth *Shipex* grab samples.



- Fig 7.7 - Coercivity vs SIRM/χ for pilot samples from The Moray Firth. Groupings based on convex hull analysis .

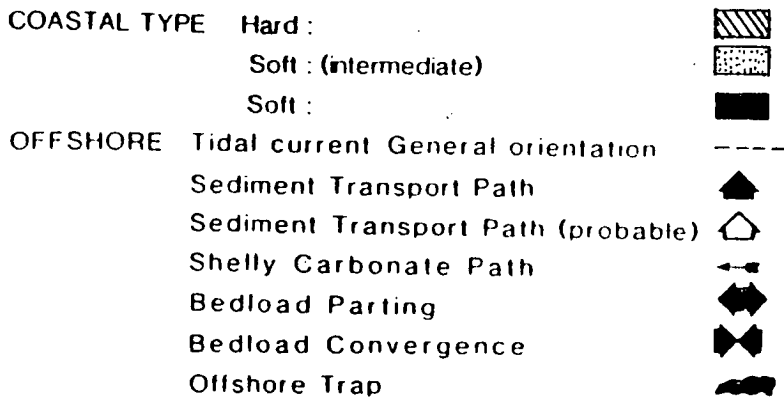
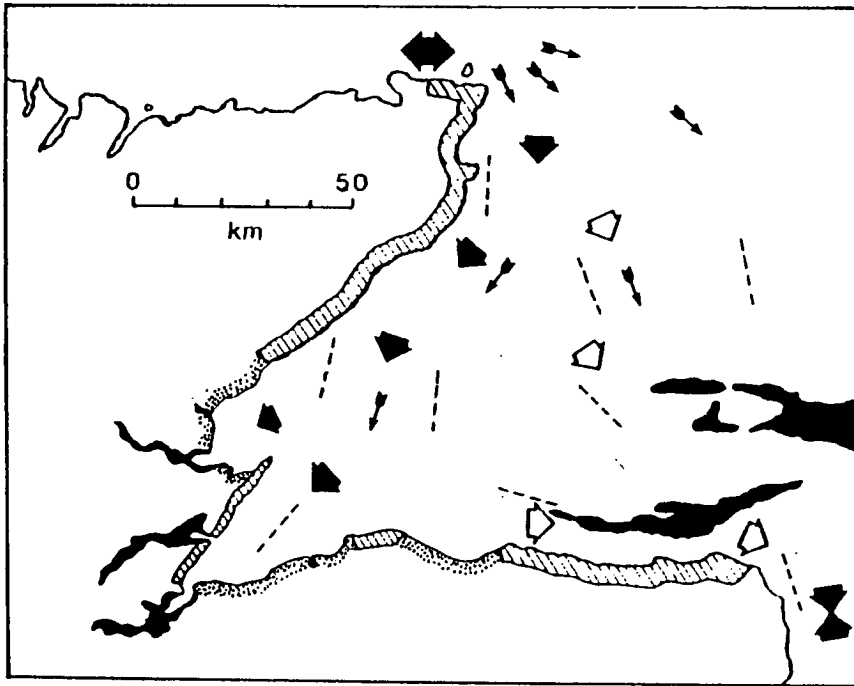
are seen. Coercivity for both sample groups falls within a similar range, 40 to 105 mT, but SIRM/ χ ratio distinguishes between them, typically 1 to 11 kAm⁻¹ for the southern zone and 9 to 20 kAm⁻¹ for the northern zone.

7.5 Discussion

From fig 7.5, it can be seen that χ is strongly related to particle size, but lacks the double peak seen in the Clyde (fig 6.10). Instead there is a single χ peak and as in the case of the Clyde, χ peaks at the sand/silt boundary. This peak of χ in <63 μ m particle sizes is reflected in 'typical values' of χ for the varying grain size fractions across the Moray Firth seen in table 7.1, with muds having higher χ values than sands or gravelly sands. The χ values for differing particle size sediment assemblages can be substituted on the particle size distribution key to provide a zoning of χ . Interpretation of χ distribution becomes problematical in close proximity to the southern shore of the Moray Firth as gravel fractions are encountered in sporadic concentrations.

The SIRM/ χ data shown in table 7.1 does not show as clear cut a peak as χ , but instead reveals high ratios in the sand fraction. This high ratio could be a reflection of the sediment input from Old Red Sandstone areas (Caithness) with haematite bound to the quartz/sand grains. However, when taking into account the relatively low HIRM in the sands compared to the muds, it would seem that the high SIRM/ χ ratio in the sands reflects an increased proportion of high coercivity components due to a decrease in the contribution of magnetite dominated coastal sediments to the overall sedimentary composition. A similar situation was seen in the Clyde grab samples, with magnetically stronger magnetite masking any haematite contributions.

Using a biplot of SIRM/ χ ratio against coercivity for the pilot samples (fig 7.7) it can be seen using simple convex hull analysis (R. Thompson pers comm) that there are two overlapping groupings of data. Samples from the north of the study area have a higher proportion of high coercivity and high SIRM/ χ components relative to the overall values of the entire study area. The overlap of the southern and northern areas supports the idea of reworked coastal material dominating the southern area but having less influence in the north of the study area. Attempts at magnetically extracting the haematite using the techniques outlined in chapter 2 were unsuccessful with only the magnetite



- Fig 7.8 Diagram of principal transport paths and sediment sinks in the Moray Firth area (Reid and McManus 1987).

fraction being readily removed from the sediment. The selective removal of magnetite suggests that the haematite is either relatively inaccessible to extraction, existing within or cemented to the quartz sand grains, or magnetite is masking the haematite.

IRM acquisition data for pilot samples (fig 7.6) showed a varied magnetic mineralogy. As in the case of the Clyde, magnetite is the dominant magnetic mineral, but in the case of The Moray Firth there is a much harder and significant haematite component superimposed. The resulting mixed magnetic mineral assemblage is the product of high coercivity components derived from the Caithness sandstones being transported into the Moray Firth where they become trapped. Using evidence obtained from surface and suspended sediment analysis, plus current data, Reid and McManus (1987) suggested a sediment transport pattern (fig 7.8) that is in agreement with the latter hypothesis, of Caithness sandstones entering the Moray Firth. Reworked glacial deposits and fluvial inputs however constitute 70% of the sediment trapped in the Moray Firth (Reid and McManus 1987).

7.6 Significant Points

1) Susceptibility is strongly influenced by particle size in the Moray Firth surface sediments.

2) Although magnetite is the dominant magnetic mineral, but there are significant harder stability magnetic components present throughout the Moray Firth area.

3) The sediment source linkage of Caithness sandstone entering The Moray Firth proposed on the basis of high coercivity components fits with the sedimentary regimes proposed by McManus and Reid (1987).

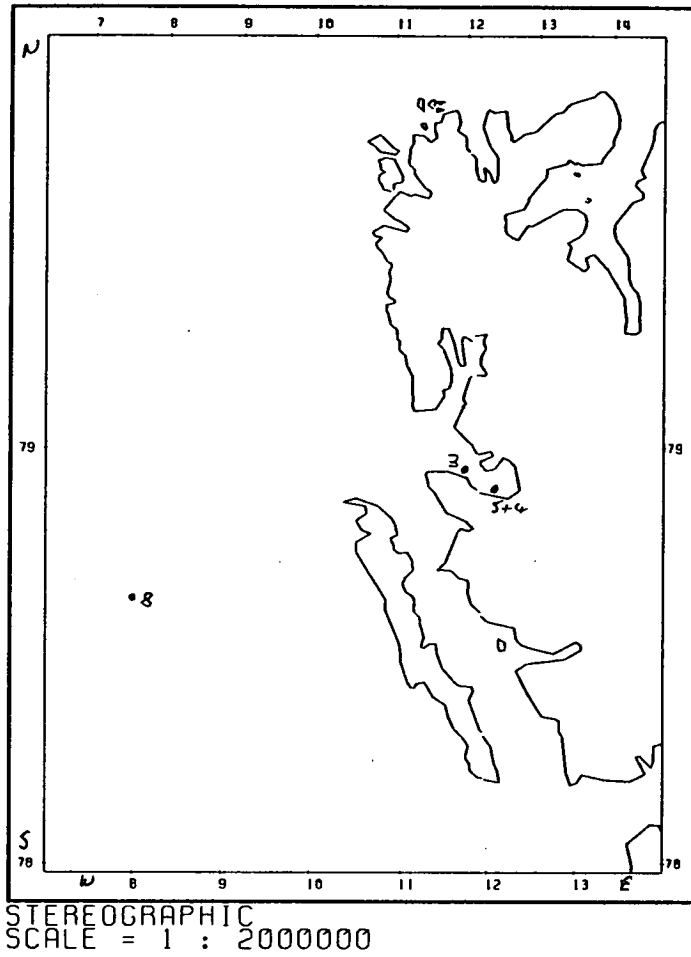
CHAPTER 8 SPITSBERGEN

8.1 Background

During 1987, sediment cores collected from the Spitsbergen area were made available for palaeomagnetic analysis by Prof G. Boulton. The core site positions are shown in fig. 8.1. The cores were recovered using a large section (28cm by 28cm) box corer. This provided a large yield of high quality sediment as relatively small amounts of disturbance were produced by the coring action on account of the low ratio of cutting edge to overall cross section of the corer. The sample sites were in a geomagnetically interesting area. In particular previous palaeomagnetic work on cores from the Spitsbergen area (fig 8.2) had produced evidence of unusually shallow inclinations. From a mineral magnetic viewpoint, there was also the potential for identifying the magnetic mineral characteristics of a wide variety of sediment types and comparing these to the magnetic mineral assemblages found in UK continental shelf sediments.

1 The Geology of Spitsbergen

The geology of Spitsbergen is complicated. Fig 8.3 taken from Alder (1980) shows the main geological features, while more detailed descriptions can be found in Harland (1961). The most extensive group of rocks found on Spitsbergen are the Hecla Hoek Group. Rocks of this group range in age from Precambrian to Ordovician and outcrop over a large area in Nordaustlandet, in the north and west of the main island of Vestspitsbergen and on Prince Charles Foreland in the West (Ager 1980). The Hecla Hoek group is essentially a large sedimentary pile. It commences with a succession of dominantly argillaceous sediments but with some volcanic material. This is followed by a series of dominantly quartzitic sediments with basic volcanics and with evidence of glacial horizons. The clastic sedimentation is replaced by limestones, including oolites and dolomites. Moving away from the Hecla Hoek series, other features of the geology of Spitsbergen worth individual mention are:- (i) a thick body of Old Red Sandstone found in north and central Spitsbergen. (ii) the Triassic deposits of east Spitsbergen, which consist mainly of sandstones and marine beds passing through to continental deposits with coal seams. (iii) Carboniferous and Permian rocks which consist of a basal sandstone followed



- Fig 8.1 Map showing location of core sites used in this study. (Boulton, pers. comm. 1988).

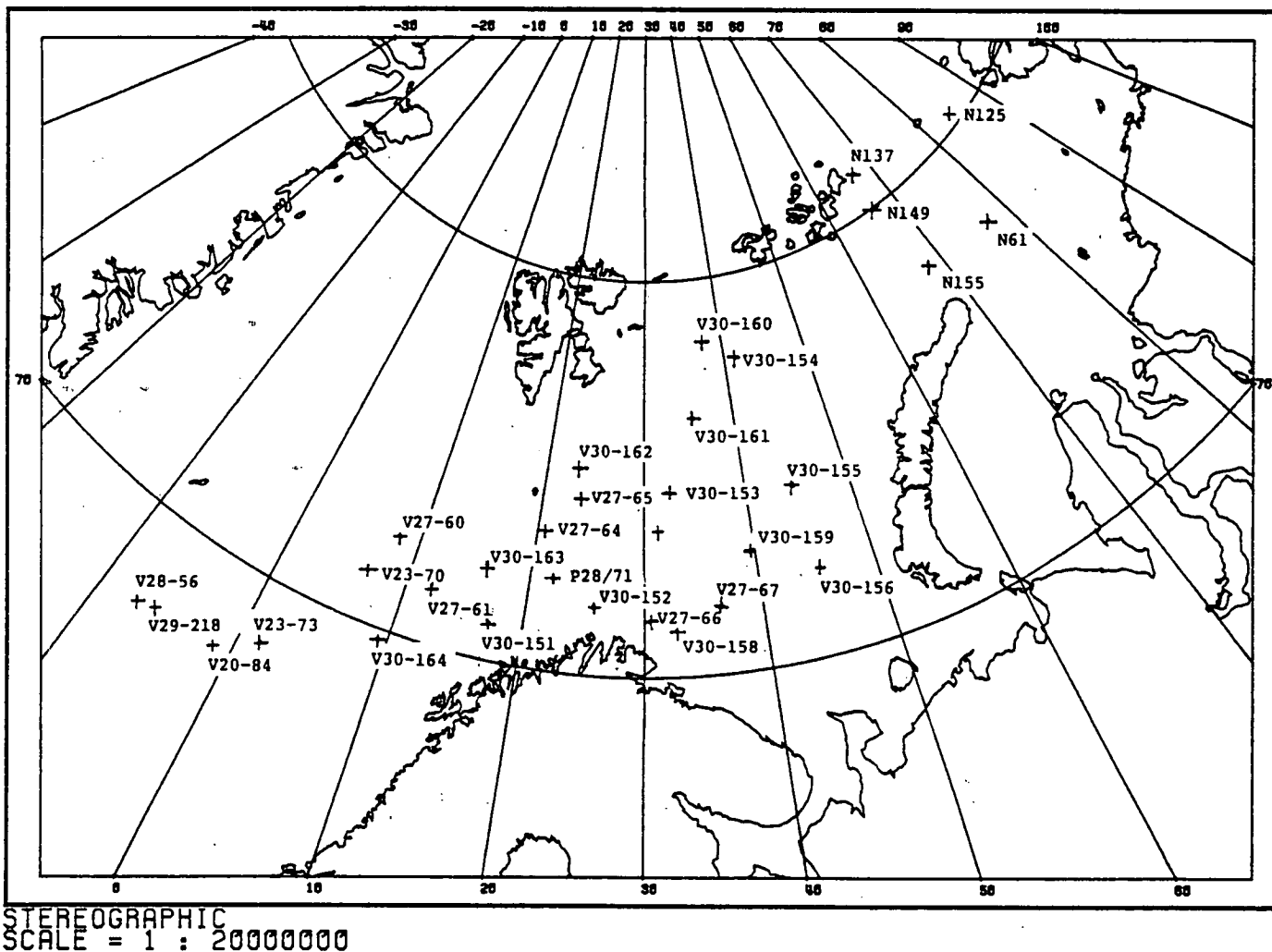
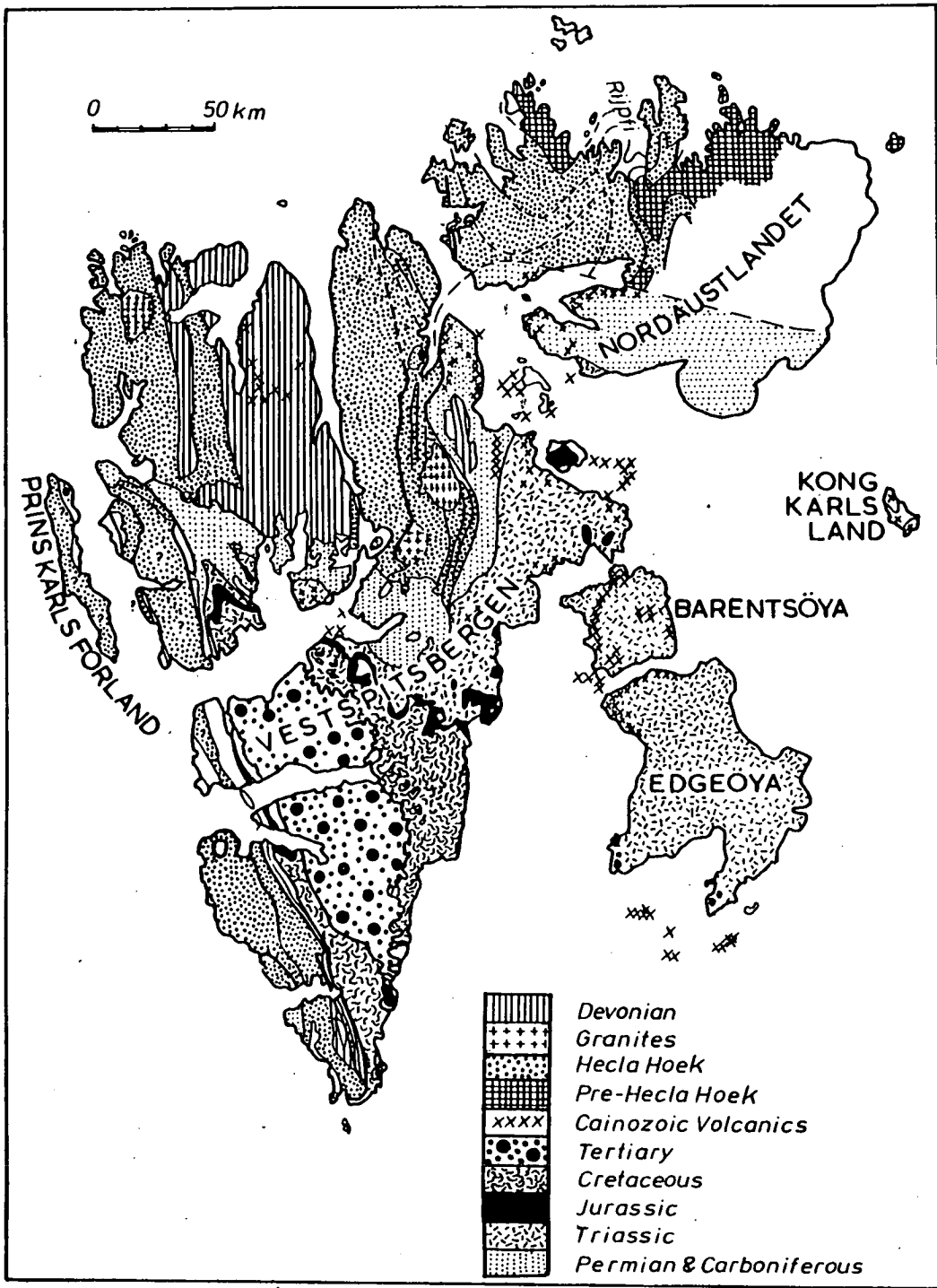


Fig 8.2 Map showing location of coring sites for palaeomagnetic purposes in the Kara Sea, Norwegian Sea and Barents Shelf. (from Austin 1987).



- Fig 8.3 Geological sketch map of Spitsbergen (from Ager 1980).

by a mainly marine succession which transgresses upwards to gypsiferous deposits and limestones. The Carboniferous and Permian rocks are widespread in central and north east Vestspitsbergen and in the southern part of Nordaustlandet.

2 Previous palaeomagnetic work in the Spitsbergen area

Previous palaeomagnetic data for the Spitsbergen shelf area was collated by Austin (1987). This work largely consisted of establishing secular variation records for suites of cores from the Barents Shelf (figs 8.4), Kara Sea (figs 8.5) and the Norwegian Sea (figs 8.6). Austin's work was not limited to palaeomagnetic directional data, he also placed considerable emphasis on the mineral carrier of the remanence. For example fig 8.7. taken from Austin (1987) shows how his G-ratio can be used to illustrate varying magnetite mineralogies.

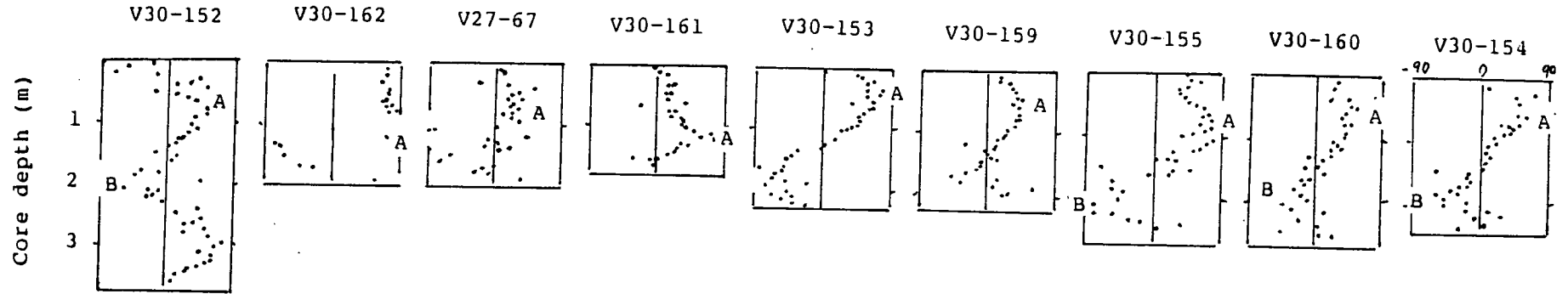
8.2 Sampling

Palaeomagnetic subsampling was undertaken on board the survey vessel as soon as possible after core recovery by Dr. L. Jobson. The subsampling interval employed was approximately 10cm. Upon disembarkation, the cores were moved to cold store at The British Geological Survey, Edinburgh. Further contiguous subsampling was undertaken by Dr B. Maher and the author on four cores for sites 3,4,5, and 8 (see fig. 8.1).

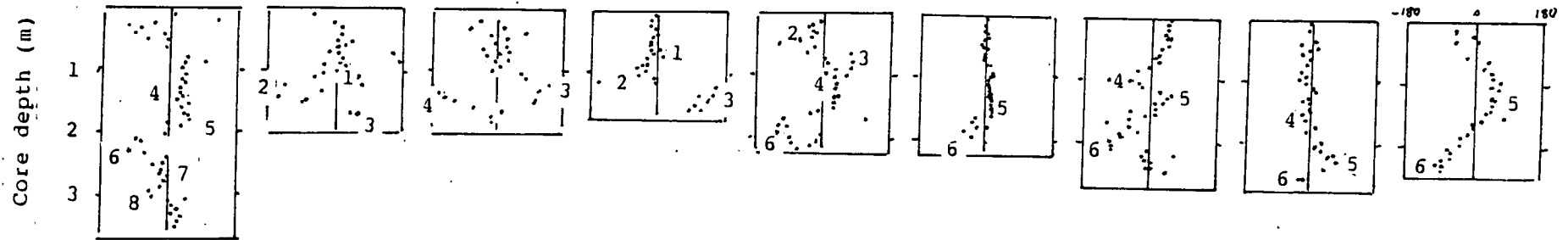
8.3 Measurement

Both the ship-board and shore-laboratory sample sets were subjected to basic palaeomagnetic directional measurement using a Cryogenic Magnetometer. Once NRM measurement was complete, mineral magnetic measurements were carried out on all subsamples. These mineral magnetic studies consisted of susceptibility measurement, followed by the measurement of remanence after each subsample had been exposed to D.C. fields of 0.1T, 1.0T and -0.1T. Using these four measurements in conjunction with sample mass, it was possible to derive HIRM, S ratio, SIRM/ χ ratio and χ as defined in chapter 2.

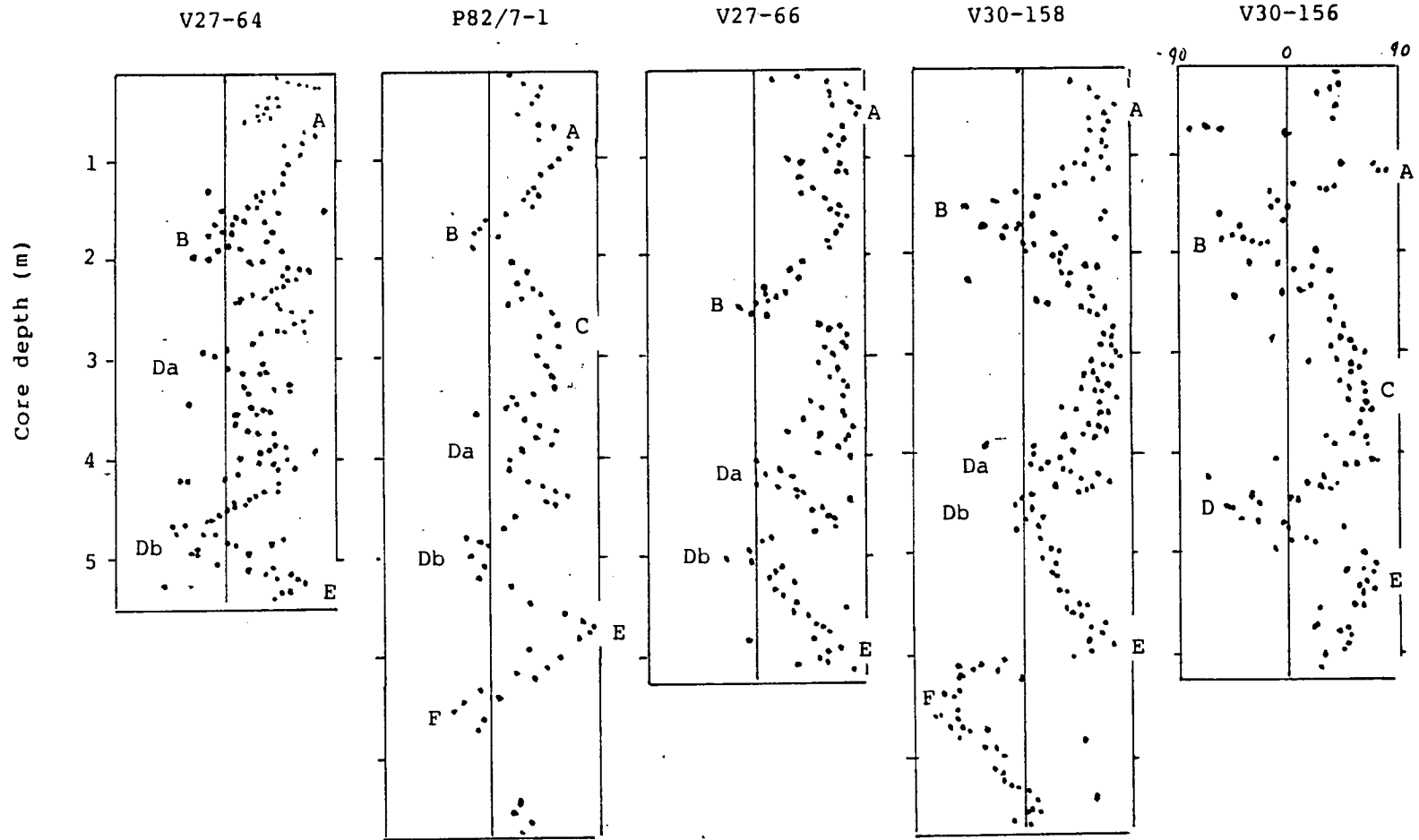
(a) Inclination



(b) Declination



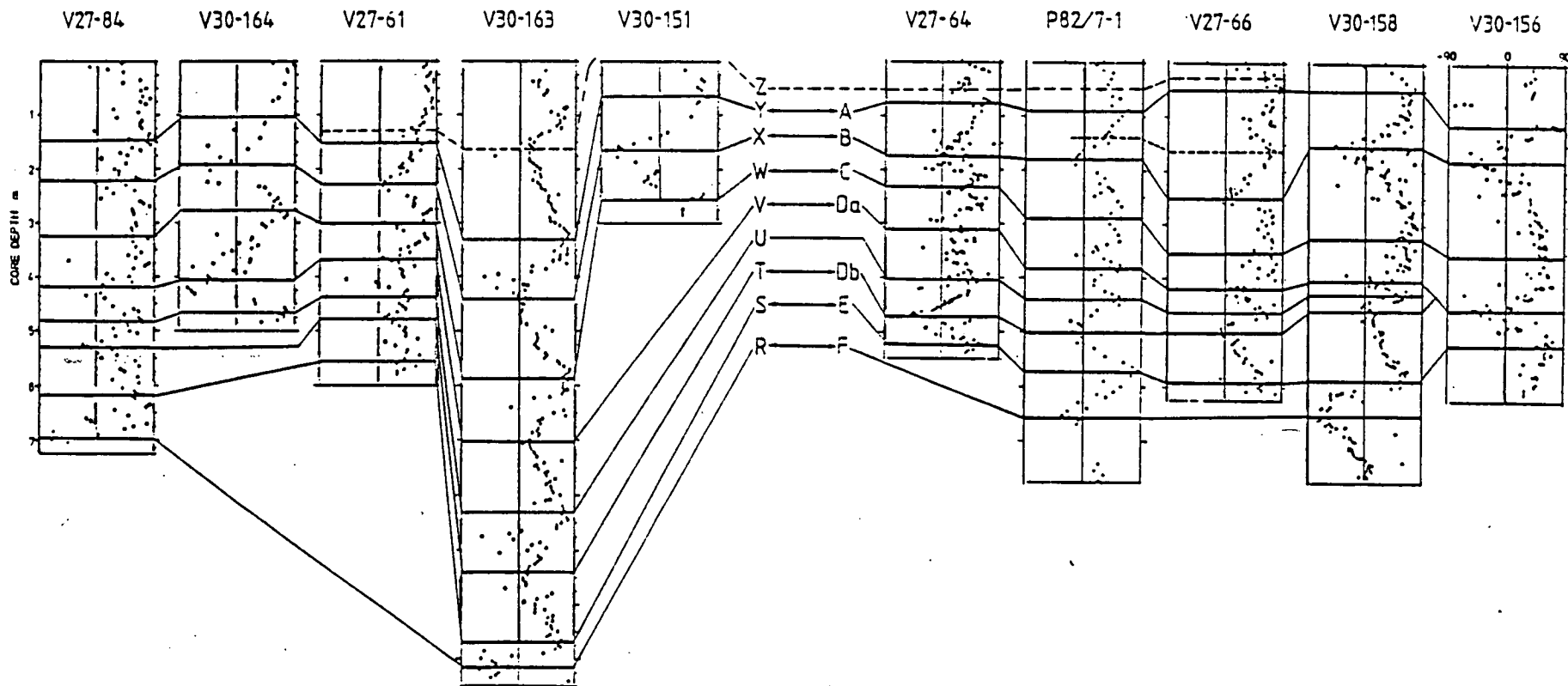
- Fig 8.4 Examples of inclination and declination data from short cores taken off the Barents Shelf. Correlation is by visual comparison of features (from Austin 1987).



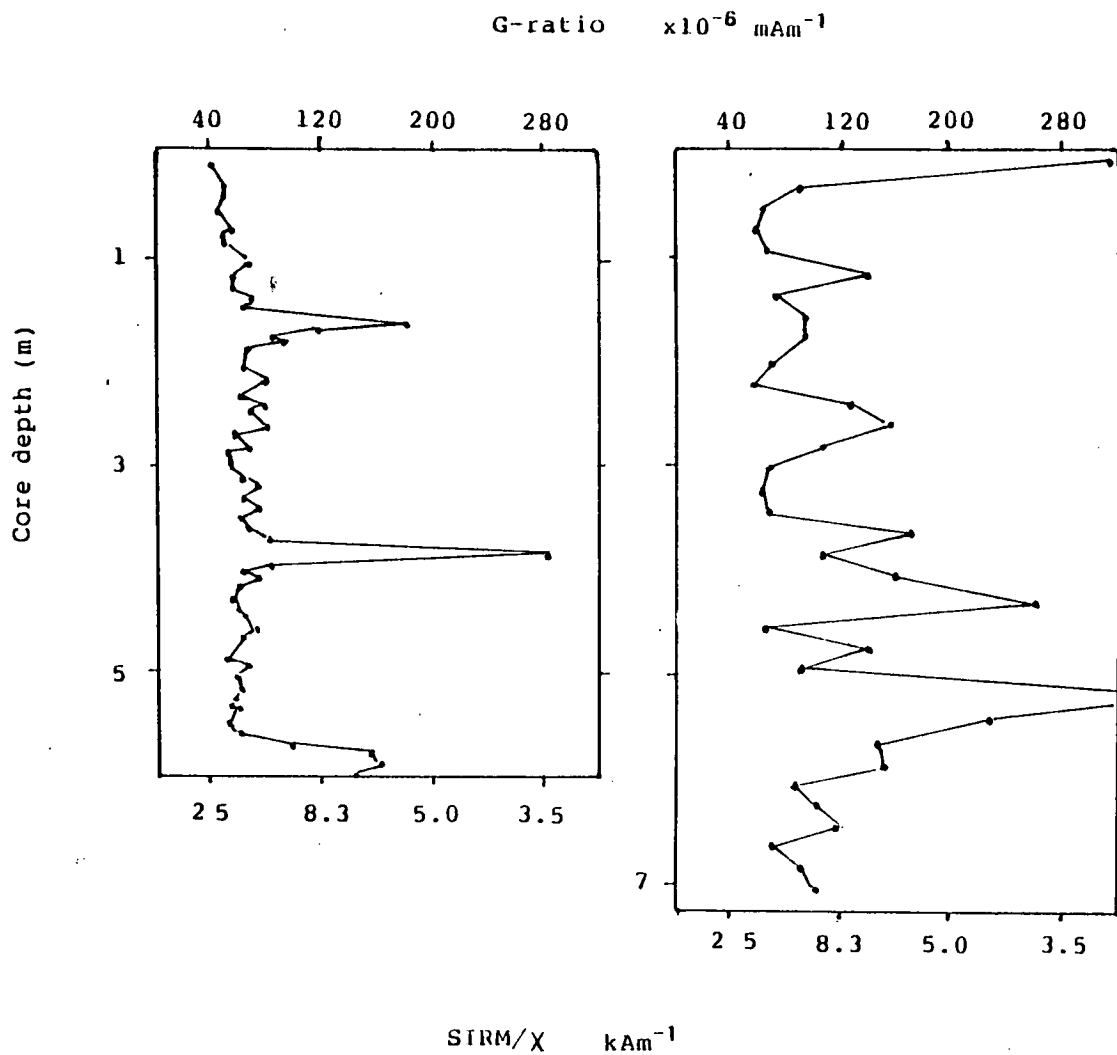
- Fig 8.5 Examples of long core inclination data from the Barents Shelf with visual correlation of features. (from Austin 1987).

NORWEGIAN SEA CORES.

BARENTS SHELF CORES.



- Fig 8.6 Correlation of palaeomagnetic records between cores from the Norwegian Sea and Barents Shelf. Correlation by visual comparison of features (Austin 1987)



- Fig 8.7 Examples of mineral magnetic analysis of Norwegian sea cores undertaken by Austin 1987. The G ratio is equivalent to χ/SIRM .

8.4 Results

Downcore ^{NRM} palaeomagnetic data for the sites is shown in figs 8.8–8.11. Data for the mineral magnetic parameters is shown in figs 8.12–8.15. These diagrams incorporate results for sample sets from both ship board work and laboratory subsampling.

1 Palaeomagnetic Results

Site 3 Fig 8.8.

The inclination data for site 3 starts at a low value of approximately 15° at the top of the core but rises rapidly to 80° at 50cm before decreasing to an average value of 40° in the remainder of the core.

Declination data for site 3 exhibits little variation downcore, except for a zone from 20cm to 60 cm where it swings quite rapidly from 100° to 150° .

Intensity data for site 3 has two distinct zones. Intensity values remain steady at 100 mAm^{-1} for the top 60cm where it jumps to 150 mAm^{-1} , a value which it retains in the remainder of the core.

Site 4 Fig. 8.9

The inclination data for site 4 starts with very low values for the top 70cm of core, varying between -10° and $+25^\circ$, before rising at 70cm to a steady 30° to 40° for the remainder of the core.

The declination record for site 4 is dominated by a large jump of 100° at 70 cm. The intensity record for site 4 also features a change at 70 cm with a rise from an average 50 to 80 mAm^{-1} at 70 cm.

Site 5 Fig. 8.10

Inclination starts low at 0° , rising to 50° by 15cm, dipping back to 0° at 20cm before rising to a high of 55° at 30cm. This high is followed by a gradual decline to 0° by the base of the core (80cm).

Declination remains very steady downcore, slowly fluctuating between by $+50^\circ$ and -50° .

Intensity is also steady for the majority of the core, with the exception of a sudden jump from 2 mAm^{-1} in the top 10cm before decreasing to a steady 25 mAm^{-1} for the remainder of the core.

Site 8 Fig 8.11

Inclination data for site 8 starts low at 0° , rising to 55° by 10 cm, followed by a steady decline to 25° by 40cm, where it remains steady for the rest of the core.

Declination data for site 8 is very constant downcore except for a 25° swing in the top 20cm.

Intensity data for site 8 exhibits a high of 200 mAm^{-1} in the top 50cm before decreasing to a value of 50 mAm^{-1} between 50cm and 60cm.

2 Mineral Magnetic Results

Site 3 Fig. 8.12

The mineral magnetic parameters for site 3 show only minor variations downcore.

χ is steady at approximately $0.125 \mu\text{m}^3\text{kg}^{-1}$

SIRM is steady at approximately $2.0 \text{ mAm}^2\text{kg}^{-1}$ downcore.

SIRM/ χ is steady at 18kAm^{-1} downcore.

S ratio is steady at 0.2 downcore.

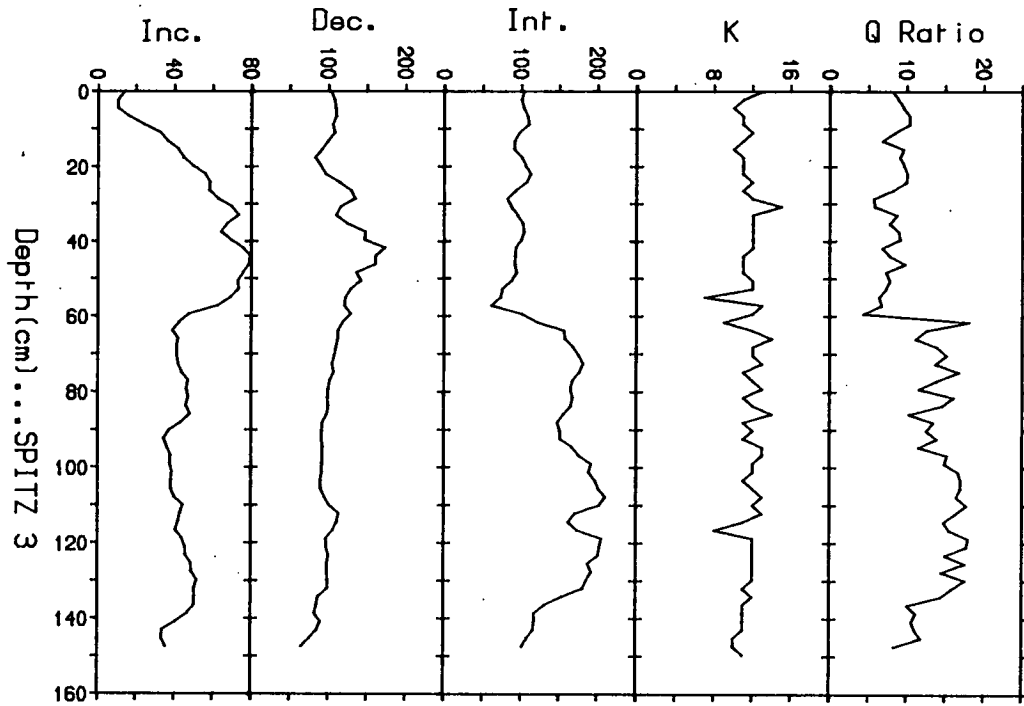
HIRM is steady at $0.8 \text{ mAm}^2\text{kg}^{-1}$ downcore.

Site 4 Fig. 8.13

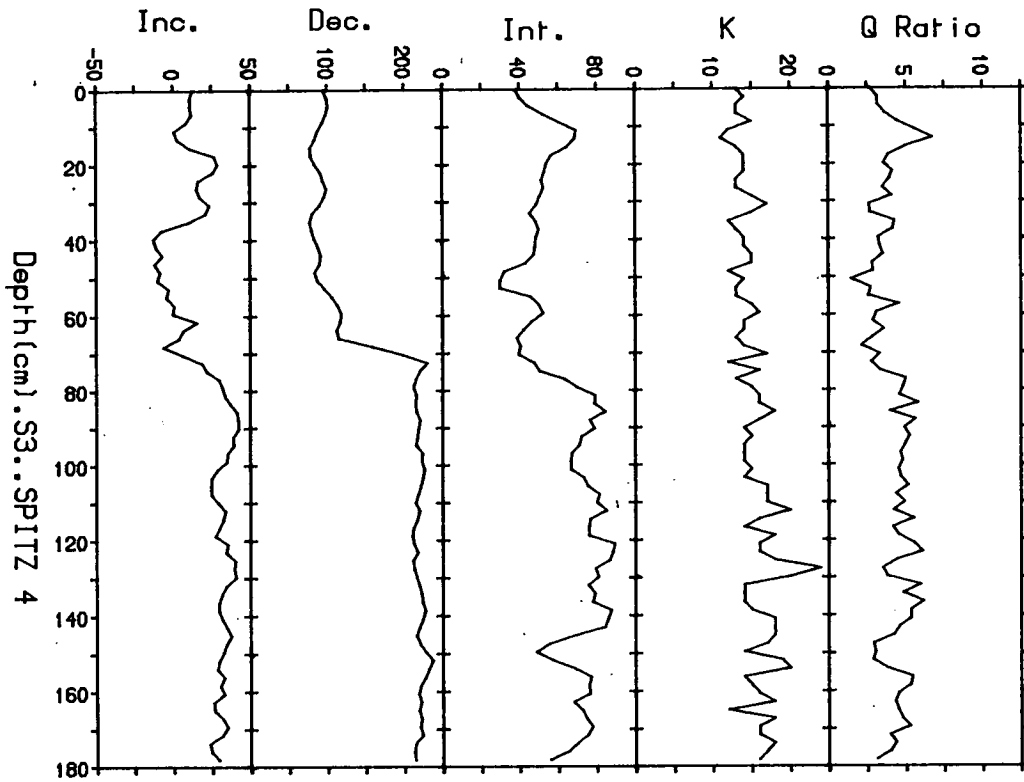
The mineral magnetic parameters for site 4 show contrasting stability characteristics downcore, with HIRM fluctuating whilst χ , SIRM, SIRM/ χ and S ratios remain steady.

χ is steady downcore at approximately $0.15 \mu\text{m}^3\text{kg}^{-1}$.

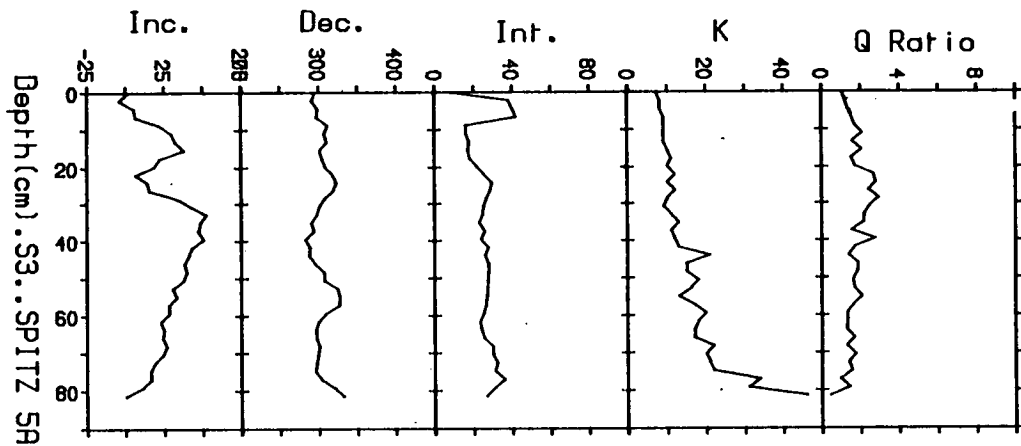
SIRM is steady downcore at approximately $2.5 \text{ mAm}^2\text{kg}^{-1}$.



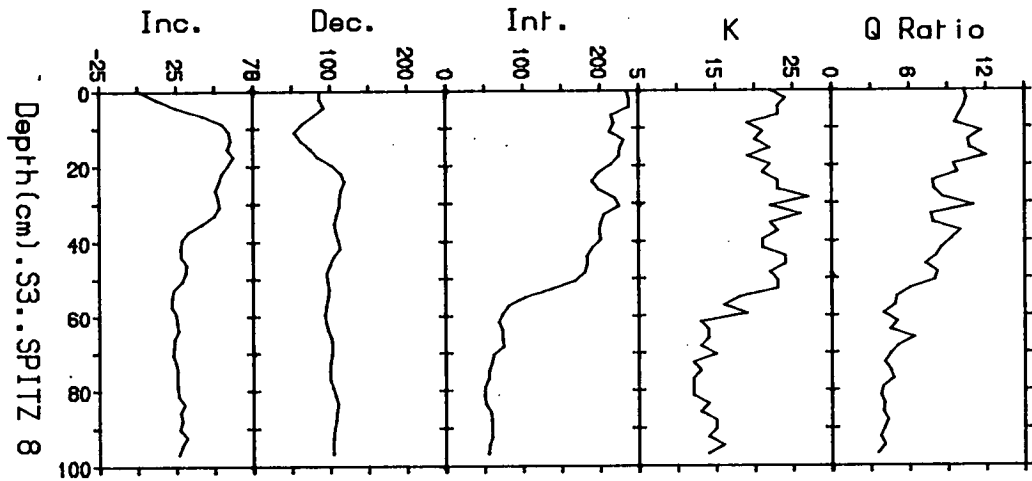
- Fig 8.8 Palaeomagnetic results for site 3 based on data from a contiguous subsample set. Units: Inclination and declination in degrees; intensity mAm^{-1} ; K and Q dimensionless.



- Fig 8.9 Palaeomagnetic results for site 4 based on data from a contiguous subsample set. Units: Inclination and declination in degrees; intensity mA m^{-1} ; K and Q dimensionless.



- Fig 8.10 Palaeomagnetic results for site 5 based on data from a contiguous subsample set. Units: Inclination and declination in degrees; intensity mAm^{-1} ; K and Q dimensionless.



- Fig 8.11 Palaeomagnetic results for site 8 based on data from a contiguous subsample set. Units: Inclination and declination in degrees; intensity mAm^{-1} ; K and Q dimensionless.

SIRM/ χ ratio is steady at approximately 18 kAm^{-1} downcore.

S ratio shows slight fluctuations between -0.2 and 0 downcore.

HIRM fluctuates considerably within the range 1.4 to $1.0 \text{ mAm}^2\text{kg}^{-1}$ downcore.

Site 5 Fig. 8.14

All mineral magnetic parameters for site 5 show considerable change downcore.

χ gradually increase from $1.0 \text{ }\mu\text{m}^3\text{kg}^{-1}$ to $2.3 \text{ }\mu\text{m}^3\text{kg}^{-1}$ from the top of the core to 75cm , followed by a rapid climb to $3.5 \text{ }\mu\text{m}^3\text{kg}^{-1}$ from 75cm to 80cm .

SIRM starts at $3.5\text{mAm}^2\text{kg}^{-1}$, dips to $3.0 \text{ mAm}^2\text{kg}^{-1}$ by 20cm where it remains steady until a sharp peak to $5.5 \text{ mAm}^2\text{kg}^{-1}$ at the base of the core.

SIRM/ χ shows a gradual downcore change from 32 kAm^{-1} at the top of the core to 12 kAm^{-1} at the bottom.

S ratio exhibits a gradual change downcore, from -0.6 at the top to $+0.7$ at the bottom.

HIRM shows a mirror image of S, starting at $2.5 \text{ mAm}^2\text{kg}^{-1}$ at the top and gradually decreasing to $7 \text{ mAm}^2\text{kg}^{-1}$ by the bottom of the core.

Site 8 Fig. 8.15

The mineral magnetic data for site 8 is characterized by a rapid change between 45cm and 60cm .

χ averages $3 \text{ }\mu\text{m}^3\text{kg}^{-1}$ for the top 50cm , but then dips rapidly to $1.5 \text{ }\mu\text{m}^3\text{kg}^{-1}$ by 60cm , a value that it retains for the remainder of the core.

SIRM averages $5 \text{ mAm}^2\text{kg}^{-1}$ for the top 45 cm , then drops rapidly over 50cm to 60cm to an average value of $1.1 \text{ mAm}^2\text{kg}^{-1}$ for the remainder of the core.

SIRM/ χ ratio decreases slightly from 18 kAm^{-1} to 12 kAm^{-1} over the top 50cm and then suddenly drops to 0.7 kAm^{-1} for the remainder of the core.

S ratio remains constant downcore at 0.69.

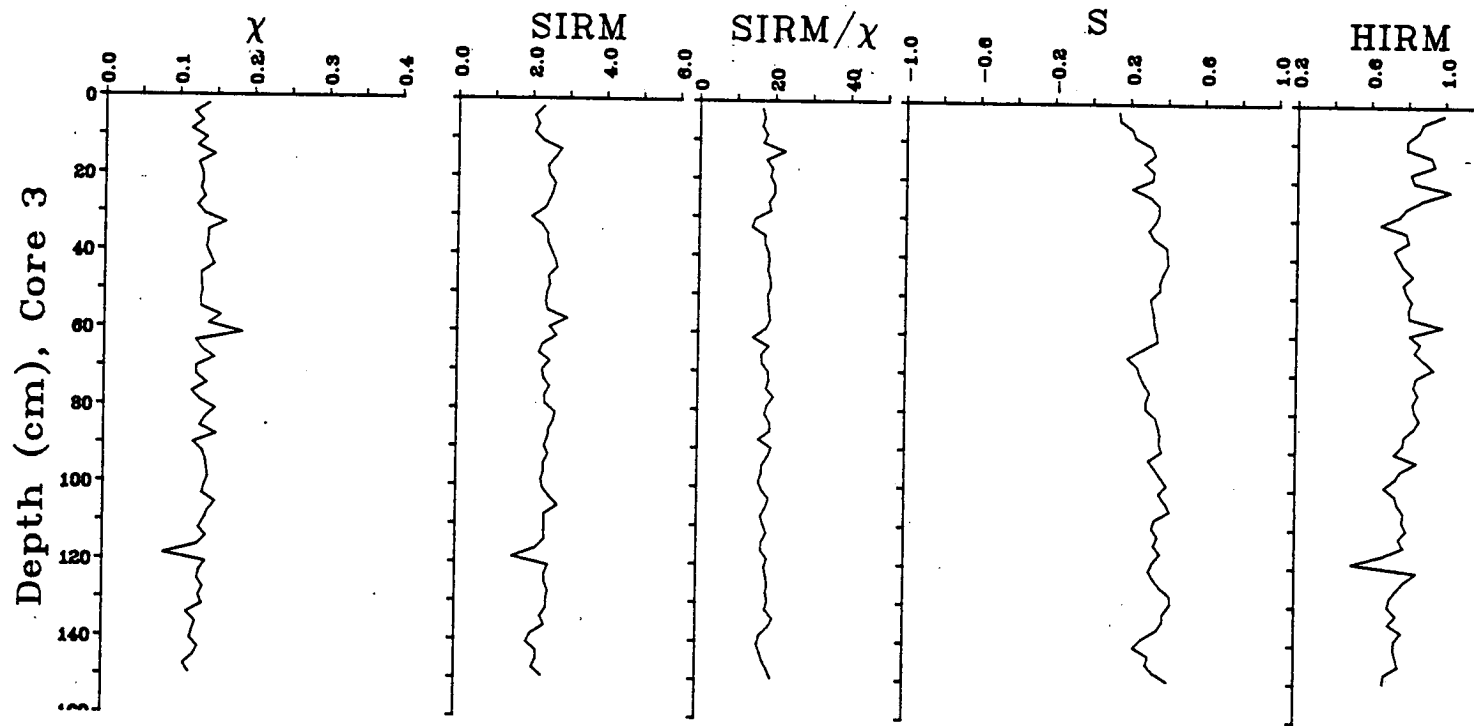
HIRM has an average value of $0.7 \text{ mAm}^2 \text{ kg}^{-1}$ in the top 50 cm and then drops rapidly at 55 cm to a value of $0.2 \text{ mAm}^2 \text{ kg}^{-1}$ for the remainder of the core.

After examination of the mineral magnetic data for sites 3 to 8, it was decided that the most distinguishing parameters both within and between cores were χ and HIRM. A biplot of these two parameters incorporating data from each core is shown in fig 8.16. In this figure, the data from sites 3 shows a very tight grouping of values, with χ ranging from 0.075 to $0.185 \text{ } \mu\text{m}^3 \text{ kg}^{-1}$ and HIRM ranging from 0.5 to $1.1 \text{ mAm}^2 \text{ kg}^{-1}$. Data from core 4 shows a limited spread of χ within the range 0.12 to $0.21 \text{ } \mu\text{m}^3 \text{ kg}^{-1}$ but a greater variation in HIRM, values falling within the range 0.8 to $1.8 \text{ mAm}^2 \text{ kg}^{-1}$. The wide spread of data in cores 5 and 8 contrasts with the tightly grouped data from cores 3 and 4. In the case of site 5, χ values lie within the range 0.10 to $0.38 \text{ } \mu\text{m}^3 \text{ kg}^{-1}$ with similarly widespread HIRM values (0.6 to $2.8 \text{ mAm}^2 \text{ kg}^{-1}$). The data from core 5 can be subdivided into two groups, one group having a narrow band of χ (0.8 to $1.5 \text{ } \mu\text{m}^3 \text{ kg}^{-1}$) and a wide range of HIRM (0.9 to $2.8 \text{ mAm}^2 \text{ kg}^{-1}$), the other group having a wide band of χ (1.25 to $3.75 \text{ } \mu\text{m}^3 \text{ kg}^{-1}$) and a narrow band of HIRM values (0.5 to $0.9 \text{ mAm}^2 \text{ kg}^{-1}$). Data from core 8 shows a linear spread with χ ranging from 0.15 to $0.36 \text{ } \mu\text{m}^3 \text{ kg}^{-1}$ and HIRM ranging from 0.1 to $1.1 \text{ mAm}^2 \text{ kg}^{-1}$.

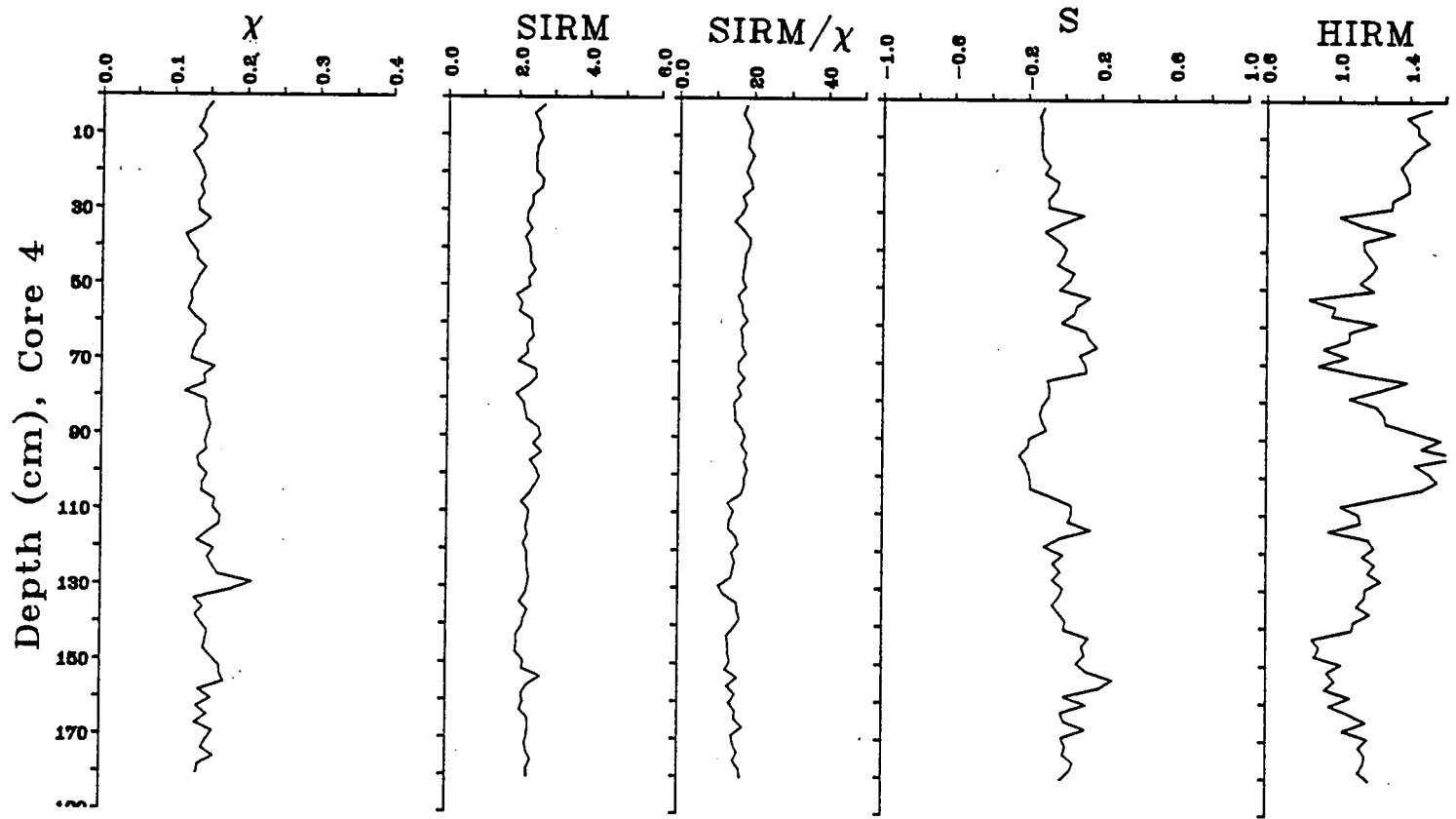
8.5 Discussion

1 Palaeomagnetic Results

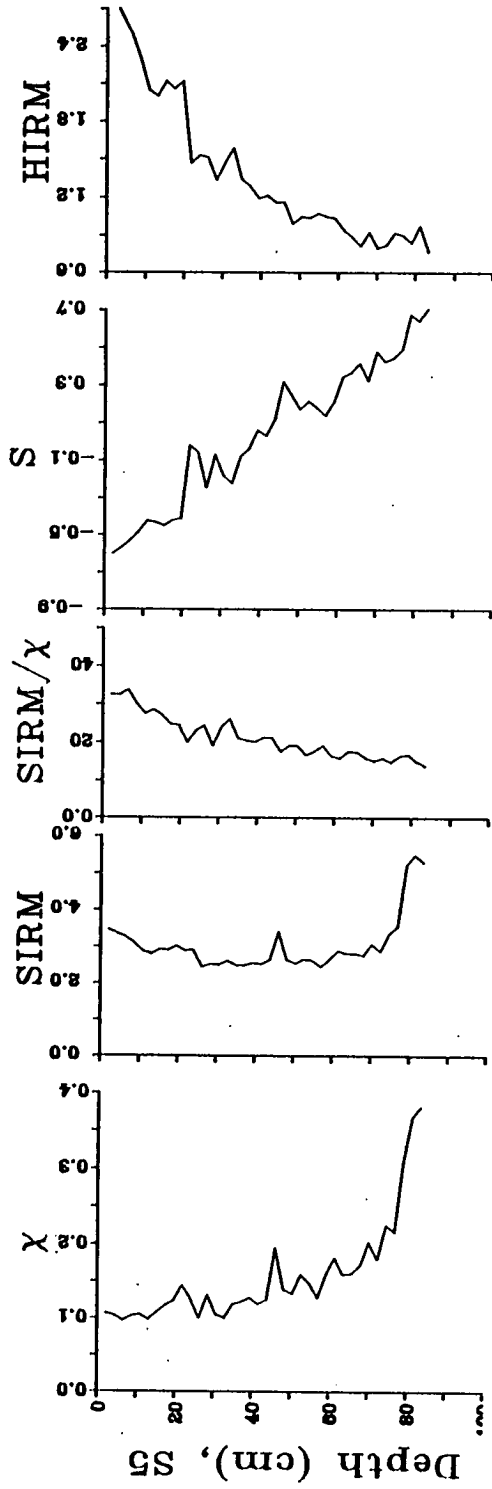
Examination of the palaeomagnetic data obtained in my study (figs 8.8–8.11) and by Austin (1987) (figs 8.4–8.6) show a range of variation in data patterns. In Austin's work, several palaeomagnetic features were identified as of geomagnetic origin and used as a basis for core correlation. Unfortunately, the cores provided by Prof. Boulton were too short to yield such a series of features. However, clearly identifiable in both data sets are inclinations shallower than would be expected from a geocentric axial dipole field model ($\tan I = 2 \tan \lambda$). At the latitude of Spitsbergen a palaeomagnetic inclination of approximately 80° is to be expected. The palaeomagnetic inclination data shown in figs 8.8–8.11 deviates greatly from the expected 80° . Such shallow



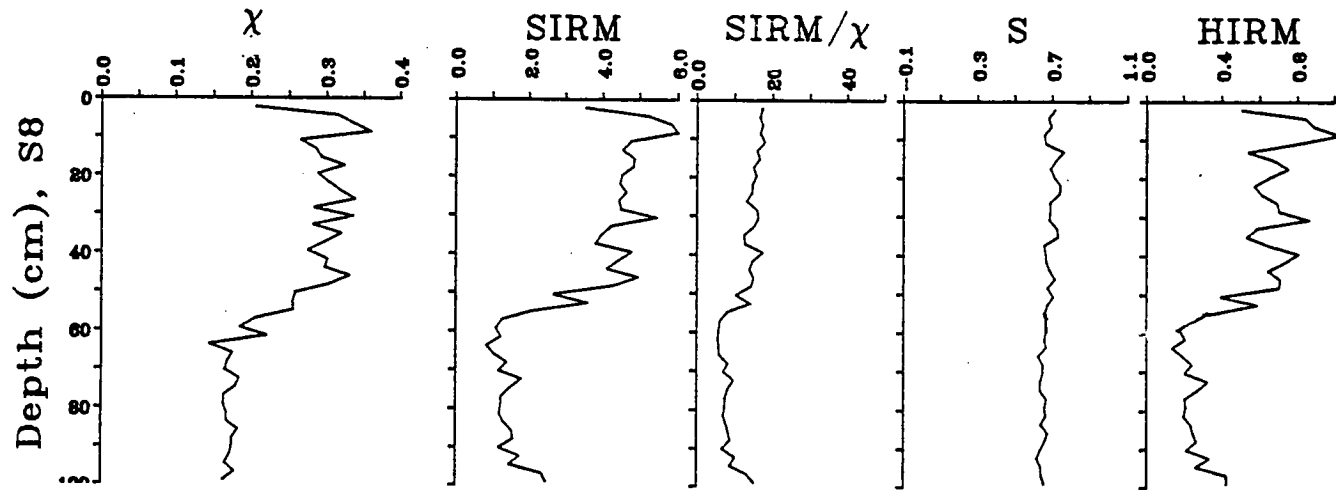
- Fig 8.12 Mineral magnetic data for site 3 based on a contiguous set of subsamples.
 Units; $\chi \mu\text{m}^3\text{kg}^{-1}$; SIRM $\text{mAm}^2\text{kg}^{-1}$; SIRM/ χ kAm^{-1} ; HIRM $\text{mAm}^2\text{kg}^{-1}$.



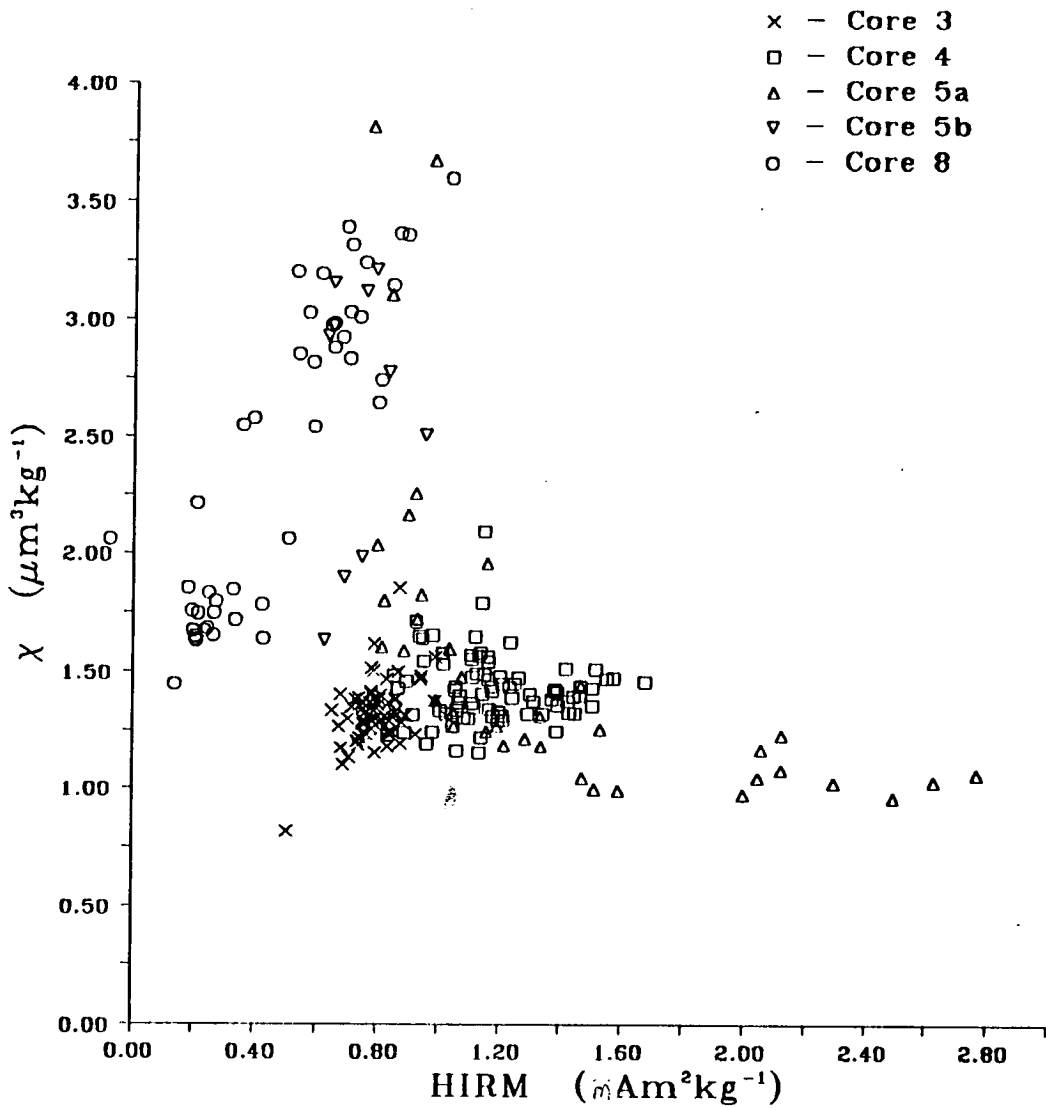
- Fig 8.13 Mineral magnetic data for site 4 based on a contiguous set of subsamples. Units; $\chi \mu\text{m}^3\text{kg}^{-1}$; SIRM $\text{mAm}^2\text{kg}^{-1}$; SIRM/ χ kAm^{-1} ; HIRM $\text{mAm}^2\text{kg}^{-1}$.



- Fig 8.14 Mineral magnetic data for site 5 based on a contiguous set of subsamples.
 Units: X $\mu\text{m}^3\text{kg}^{-1}$; SIRM $\text{mAm}^2\text{kg}^{-1}$; SIRM/X kAm^{-1} ; HIRM $\text{mAm}^2\text{kg}^{-1}$.



- Fig 8.15 Mineral magnetic data for site 8 based on a contiguous set of subsamples.
 Units; $\chi \mu\text{m}^3\text{kg}^{-1}$; SIRM $\text{mAm}^2\text{kg}^{-1}$; SIRM/ χ kAm^{-1} ; HIRM $\text{mAm}^2\text{kg}^{-1}$.



- Fig 8.16 Biplot of HIRM vs χ for samples from sites 3,4,5 and 8. Core 5a and core 5b represent the top section and base of the core from sample site 5.

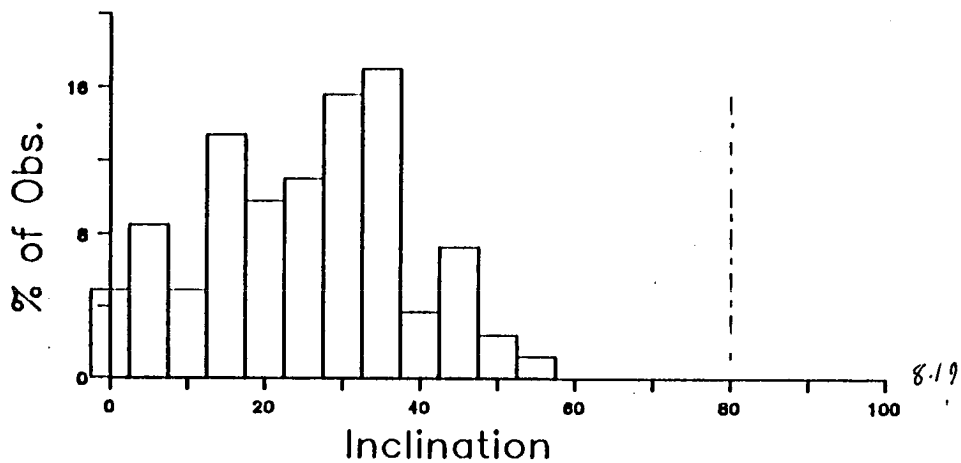
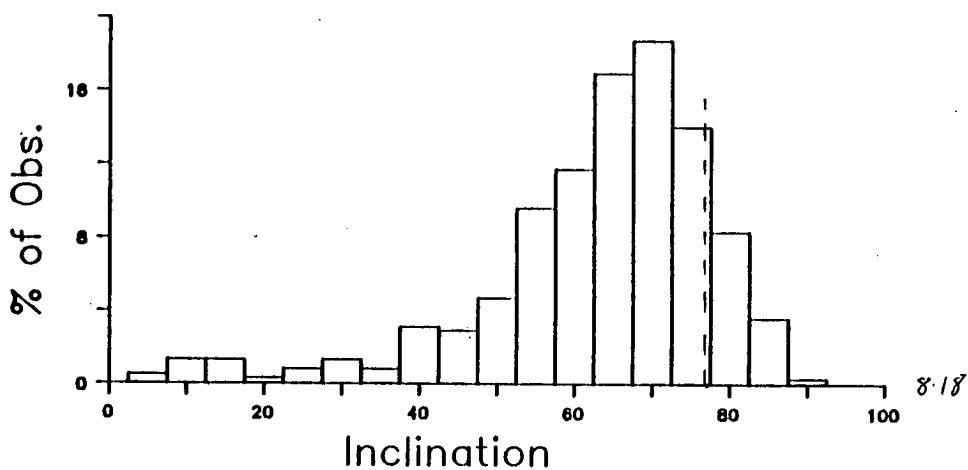
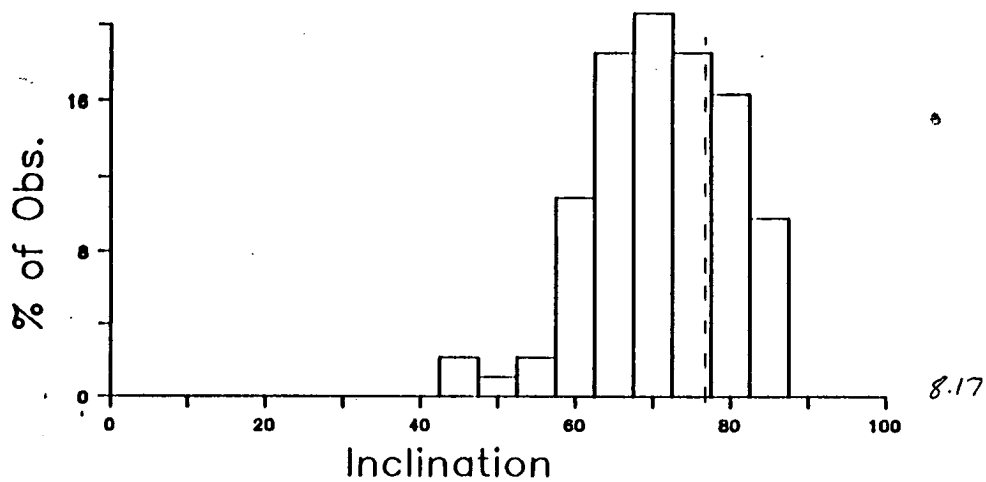
inclinations although of a less extreme nature were also observed in cores taken from the UK shelf (chapter 3-4). In the case of the UK sediments 'inclination errors' of the types described by Griffiths and King (1955) were offered as a possible explanation.

The low palaeomagnetic inclination data from the Spitsbergen sediments of Austin (1987) and this study could be explained either in terms of sedimentary 'inclination error' effects or in terms of prolonged low inclination excursions of the geomagnetic field. In any attempt to assess the separate effects of sedimentary derived inclination error and variations resulting from periods of low geomagnetic field inclination, additional independent information on the behaviour of the geomagnetic field at high latitudes is required. Palaeomagnetic data from Icelandic and Aleutian Island lava flows (Watkins et al, 1977 and McDougall et al, 1976) were analysed to see if they could yield additional information. They were examined for any consistent variation away from the expected dipole field inclination of 77° at Iceland and the Aleutians. The results shown in histogram form in figs. 8.17 and 8.18 are obviously free from any sedimentary derived inclination error, but nevertheless indicate a bias towards shallow values. Over 25% of the data lies 20° or more shallower than the dipole direction. When a direct comparison is made between typical data from the Spitsbergen sediments (drawn in histogram form in fig. 8.19) and the lava flow data it is apparent that there is a much greater deviation in palaeomagnetic inclinations in the sedimentary record than in the lavas. These greater deviations appear to support the concept of at least two sources of inclination error, one geomagnetic, the other sedimentary.

A further reduction in inclination could be attributed to the effect of an offset dipole field model (Wilson 1971). However, at the relatively high latitudes of Spitsbergen, Wilson's model could not be expected to contribute more than 5 degrees of shallowing. The shallow inclinations seen in cores described in this chapter far exceed the shallowing expected from both sedimentary inclination error and offset dipole effects, suggesting another as yet undetermined contributory factor to inclination error at high latitudes.

2 Mineral Magnetic Results

In the mineral magnetic data from the four Spitsbergen sites (figs 8.12-8.15), it is immediately apparent that there is considerable variation both between cores and within individual cores. Taking the sites individually, the following observations can be made



- Fig 8.17 Histogram of inclination data for Icelandic lava flows (Watkins et al 1977). The dotted line shows the inclination expected at the latitude of Iceland based on a dipole field model.

- Fig 8.18 Histogram of inclination data for Aleutian Island lava flows (Bingham and Stone 1972). The dotted line shows the inclination expected at the latitude of the Aleutians based on a dipole field model.

- Fig 8.19 Histogram of inclination data collected for site 8 of this study. The dotted line shows the inclination expected at the latitude of Spitzbergen.

At site 3 (fig 8.12) there is a constant magnetic mineralogy both in terms of total concentration and the proportion of magnetite to haematite. An S ratio of +0.2 suggests a significant amount of haematite is present. By comparing the value of HIRM ($0.8 \text{ mAm}^2\text{kg}^{-1}$) and SIRM ($2.0 \text{ mAm}^2\text{kg}^{-1}$) it can be seen that haematite accounts for some 40% of the saturation remanence. Because the IRM of magnetite is some twenty times stronger than haematite, these samples must have haematite to magnetite ratios of approximately 13:1.

At site 4 (fig 8.13) there is a slightly more complex mineralogical situation than at site 3. χ , SIRM and SIRM/ χ ratio at site 4 are nearly constant downcore pointing to little change in mineral concentration and composition. However, S and HIRM do vary downcore pointing to changing amounts of high coercivity haematite. A generally negative S value points to a considerable haematite presence. HIRM values approaching 50% of SIRM underline the importance of haematite in this core, with haematite/magnetite ratios of approximately 20:1.

At site 5 (fig. 8.14) considerable variations are seen in total magnetic mineral content and the relative proportions of high and low coercivity minerals. A trend of increasing concentration of magnetite downcore can be seen from the gradually increasing χ and SIRM values. As concentration increases, there is also a distinct shift between haematite and magnetite, seen in an S ratio changing from negative to positive and an increasing SIRM/ χ ratio with increasing depth. The increase in χ downcore may well be the result of haematite gradually being replaced by magnetite as the dominant magnetic mineral in newly arrived sediments. The gradual change in mineralogy downcore could be assigned to several causes. It may reflect a gradual shift in sediment source, a change in the redox conditions of deposition, or a post-depositional chemical change within the sediment body. Given the varied geology of Spitsbergen, and the proximity of site 5 to the shore, a change in sediment source is the most likely explanation. The proximity of a range of sandstone and igneous rock bodies to site 5 (see fig 8.3) which could provide a range of magnetic minerals from a relatively confined geographical area points to a shift in sediment source being very possible. The gradual nature of the magnetic mineral assemblage in core 5 suggests a long term and slow shift in sedimentation pattern. The gradual nature of the change points to a long term shift in sedimentation pattern.

At site 8 (fig 8.15), a more dramatic change in magnetic properties than at site 5 is seen. The dramatic drop in concentration dependent parameters (χ , SIRM and HIRM) at 60 cm is not echoed in S and is only just perceivable in SIRM/ χ ratio. The constant value of S suggests little change in the proportion of high and low coercivity magnetic minerals downcore. This in turn points to a constant sediment source, the change in overall concentration of magnetic minerals being attributable to depositional change. This depositional change could be a sudden change in sedimentation rate leading to varying degrees of dilution of magnetic minerals present. For example changes in χ downcore have been shown to inversely correlate with the amount of carbonate present (Robinson, 1986). The weakly magnetic carbonate effectively dilutes whatever magnetic minerals are present from other sources.

Comparison between sites can be best summarized by reference to a biplot of HIRM and χ (fig 8.16). Data patterns in this figure emphasize the varying mineralogical trends seen in core 3 to 8. The data from cores 3 and 4 is relatively tightly grouped reflecting a near constant magnetic mineralogy downcore whereas the spread of data from core 5 and 8 points to considerable changes, both in terms of concentration and coercivity, of magnetic minerals within core. The presence of haematite in the cores points to sandstone bodies being one of the principal sediment sources.

Comparisons are possible between Austin's G ratio (fig 8.7) and SIRM/ χ ratio used in this study (G ratio = χ /SIRM). Values for SIRM/ χ ratio have been superimposed on fig 8.7 which shows G ratio for Austin's cores. In this figure it is possible to see that both the SIRM/ χ ratio and the G ratio data groups fall within a similar range, but that Austin's data yield values slightly smaller (in SIRM/ χ ratio terms) than in this study. Austin uses the G ratio as an indicator of magnetite grain size. This approach is eminently satisfactory as long as magnetite is the dominant magnetic mineral. However, data from my study points to the existence of at least two principal magnetic mineralogies in the Spitsbergen area. The high HIRM values in cores from sites 5 and 8 point to the presence of haematite dominated magnetic mineralogies. Site 5 lies close to shore and its magnetic properties may reflect extremely local coastal sediments. However, site 8 lies a several kilometres offshore pointing to the presence of high coercivity magnetic minerals well out onto the Barents shelf. The presence of high coercivity mineralogies in the Barents sea casts some doubt on Austin's use of G ratio as a grain size indicator in these particular

sediments.

8.6 Significant Points

1) Palaeomagnetic data from sediment cores in my study differ from those expected for a dipole field model due to a combination of sedimentary derived inclination error (Griffiths and King 1955), and local effects in the prevailing geomagnetic field. Of these two error sources, sedimentary sources have a much greater significance.

2) Mineral magnetic data clearly shows the presence of significant amounts of magnetite and haematite.

3) Changes in the mineral magnetic properties of cores 5 and 8 point to significant changes in sediment sources and depositional conditions in the Spitsbergen area.

CHAPTER 9

CHEMICAL ANALYSIS

9.1 Introduction

Geochemical studies of sediments are widespread in the scientific literature. Many different analytical and interpretational approaches are employed. These approaches range from simple studies on the concentration of various elements in the environment and their relationship to specific problems, for example pollution studies or mineral exploration, to more complex assessments of chemical fluxes, environmental indicators and chemical budgets. The latter vary from ionic scale interactions to whole global chemical turnovers, for example in assessment of atmospheric levels of carbon dioxide.

In this study, attention was focused on the relationship of various elemental and oxide concentrations (see table 9.1) to the bulk magnetic susceptibility properties of sediments. This approach was similar to that employed by Currie and Bornhold, (1982); Puranen (1977) who studied the relationship of susceptibility and magnetite content in continental shelf sediments and glacial tills. Working on grab samples of surface sediments from the Canadian continental shelf, Currie and Bornhold (1982) demonstrated a strong positive relationship between iron content and magnetite content (see fig 1.6). Puranen (1977) had earlier demonstrated such a relationship in Finnish glacial tills.

The work of Currie and Bornhold, (1982) and Puranen (1977) was restricted to discrete sediment samples. Mineral magnetic work on marine sediment cores has tended to be centred on the examination of the chemical changes affecting the mineral carrier of the natural magnetic remanence. A range of chemical environments have been observed. Karlin and Levi (1985) demonstrated evidence of dissolution of fine grained magnetites in marine sediment cores whilst Henshaw and Merrill (1980) have found signs of diagenetic change downcore, including oxidation of NRM carrying titanomagnetites and the authigenic formation of some magnetic ferromanganese minerals leading to a strong CRM.

The main objective of this chemical study was to follow the line of investigation of Currie and Bornhold, (1982), and examine the relationship of

magnetite and susceptibility in marine sediments. However, instead of discrete surface sediment grab samples, samples from various depths in a range of UK continental shelf cores were used. Whole core susceptibility measurements were used as the principal magnetic parameter instead of mass specific susceptibility. This was primarily to test the effectiveness of whole core susceptibility as a mineral reconnaissance tool, without having to resort to time consuming subsampling.

9.2 Subsampling and Measurement Techniques

1 Sample selection

Sample positions were selected from whole core susceptibility profiles of Central North Sea and Flett area cores to give a representative range of susceptibility values. Care was taken to ensure that the samples were derived from an area in the core section where there was a constant value of susceptibility for at least 10cm on each side of the sampling point. 50 to 100g of material was used in order to provide adequate amounts for both XRF chemical analysis and carbonate content analysis.

Approximately 20g of sample was prepared for XRF analysis using the procedure outlined in chapter 2.

2 XRF measurement

X-Ray Fluorescence analysis was undertaken at Wolverhampton Polytechnic using a Philips PW140 X-Ray Spectrometer. Data interpretation was performed immediately using a software package written by Dr J.P. Smith which gave output in terms of 15 environmentally significant major and minor elements and oxides (table 9.1). This information was useful for comparing not only the relationship of iron to susceptibility, but for relating iron concentration to more economically important heavy minerals.

3 Carbonate Content Measurement

A carbonate bomb was used on part of each subsample to give a figure for percentage carbonate composition.

9.3 Results

Table 9.1 shows the percentage chemical composition of the 17 samples as produced directly from the J.P. Smith software package. In addition, the percentage of carbonate for each sample obtained from the carbonate bomb is also listed. Where SIRM/ χ data was available from previous work in chapters 4 and 5 for a particular sample position, it is listed as well.

A graph of percentage carbonate against volume susceptibility is shown in fig. 9.1a. This graph shows a tight band of data for 15 of the 17 samples, but with two samples showing relatively high carbonate concentrations.

Correlation coefficients between the various chemical constituents and volume susceptibility are shown in table 9.2. Correlation was between data not corrected for carbonate content as it was assumed that the dilution effect of the carbonate on the sediment would have an equal effect for all chemical constituents.

Graphs of significant relationships (ie those with a correlation coefficient of +/- 0.5 or greater) and fitted regression equations of susceptibility against chemical concentration are shown for Iron oxide (fig 9.1), manganese oxide (fig 9.2), aluminium oxide (fig 9.3), magnesium oxide (fig 9.4), zinc (fig 9.5), nickel (fig 9.6), phosphate (fig 9.7) and copper (fig 9.8). In all these cases, the correlations of chemical concentration to susceptibility are positive. Fig 9.9 shows the relationship of sulphate content and susceptibility, which are negatively correlated. Correlation coefficients (r) are shown on each graph. The correlation between volume susceptibility and elemental oxide shows a high of 0.82 for manganese. Much higher correlation coefficients, averaging 0.9 are seen for the relationship between iron and elemental oxides.

Iron/manganese ratios for various samples are shown in table 9.1. The majority of Fe/Mn ratios fall in the 60 to 80 range, but several samples from core 58-02 231VE have ratios in the 10 to 40 range.

Core no.	Depth in core	SiO ₂	Fe ₂ O ₃	K ₂ O	P ₂ O ₅	Sr	Pb	Cu	MgO	Al ₂ O ₃	CaO	SO ₃	Zr	MnO ₂	Zn	Ni
61-03 42CS	40-44	29.58181	4.92133	2.27646	0.05611	0.02351	0.00201	0.00568	2.28286	7.76061	7.51554	0.07416	0.01446	0.05807	0.01035	0.00608
60-05 28CS	36-40	27.47015	4.09641	1.80071	0.05157	0.03101	0.00205	0.00486	1.77522	6.04238	10.27080	0.09018	0.01392	0.06091	0.00855	0.00593
60-06 20CSi	80-84	29.75262	2.50344	2.00085	0.05148	0.03669	0.00193	0.00387	1.50213	5.48834	8.87311	0.13461	0.01538	0.04572	0.00107	0.00331
58-02 231VE	390-394	33.26689	0.35644	2.40715	0.04700	0.01137	0.00215	0.00284	1.14458	3.30924	2.43107	0.05450	0.02433	0.03034	0.00000	0.00055
58-02 231VE	26-30	20.26125	0.35493	1.03881	0.04966	0.12161	0.00210	0.00305	1.02063	0.00000	28.34794	0.22444	0.01998	0.02402	0.00000	0.00010
61-03 42CS	161-165	29.57583	4.97197	2.25729	0.05533	0.02317	0.00183	0.00638	2.15939	7.28985	7.69525	0.07963	0.01535	0.06367	0.00937	0.00513
61-03 42CS	186-190	28.92190	5.45964	2.81610	0.05451	0.02010	0.00171	0.00566	2.13553	8.31551	6.25429	0.08139	0.01286	0.06458	0.01178	0.00653
61-03 28CS	120-124	27.99994	3.15114	1.93347	0.05035	0.03882	0.00175	0.00453	1.81479	6.10096	10.07869	0.11168	0.01471	0.05576	0.00355	0.00419
61-03 42CS	25-29	30.94735	5.43285	1.66133	0.05545	0.01986	0.00219	0.00624	2.08201	7.19430	4.69868	0.07638	0.01685	0.07246	0.01010	0.00454
61-03 42CS	140-144	29.35265	4.77099	2.66125	0.05366	0.01926	0.00189	0.00541	2.11061	7.94009	7.11172	0.08356	0.01454	0.05866	0.00979	0.00505
58-02 231VE	222-226	29.61047	2.11959	2.13135	0.05597	0.02397	0.00188	0.00352	1.44622	5.23569	7.05542	0.15120	0.02836	0.04526	0.00100	0.00289
60-05 24CS	148-152	30.25503	3.89795	2.05156	0.05034	0.02525	0.00195	0.00483	1.76642	7.09334	7.87576	0.11037	0.01646	0.05038	0.00641	0.00419
60-05 24CS	40-44	28.02871	5.26518	2.33626	0.05500	0.02513	0.00175	0.00638	2.20219	8.01266	9.95892	0.09190	0.01423	0.06555	0.01084	0.00628
61-03 42CS	228-232	29.74175	5.28677	2.35371	0.05502	0.02169	0.00166	0.00608	2.06497	8.32912	5.72542	0.11232	0.01412	0.06444	0.00996	0.00620
61-03 42CS	58-62	27.96193	6.18443	2.13168	0.06165	0.02183	0.00184	0.00673	2.04654	7.54862	7.60490	0.06589	0.01315	0.06373	0.01222	0.00575
61-03 42CS	75-79	27.33729	4.98675	2.29850	0.05749	0.02218	0.00188	0.00614	1.99706	7.89277	8.36561	0.07940	0.01485	0.06094	0.01004	0.00608
58-02 231VE	154-158	21.98952	0.48309	1.10911	0.04825	0.14248	0.00214	0.00395	0.71463	0.07975	26.04295	0.19882	0.02707	0.02861	0.00000	0.00063

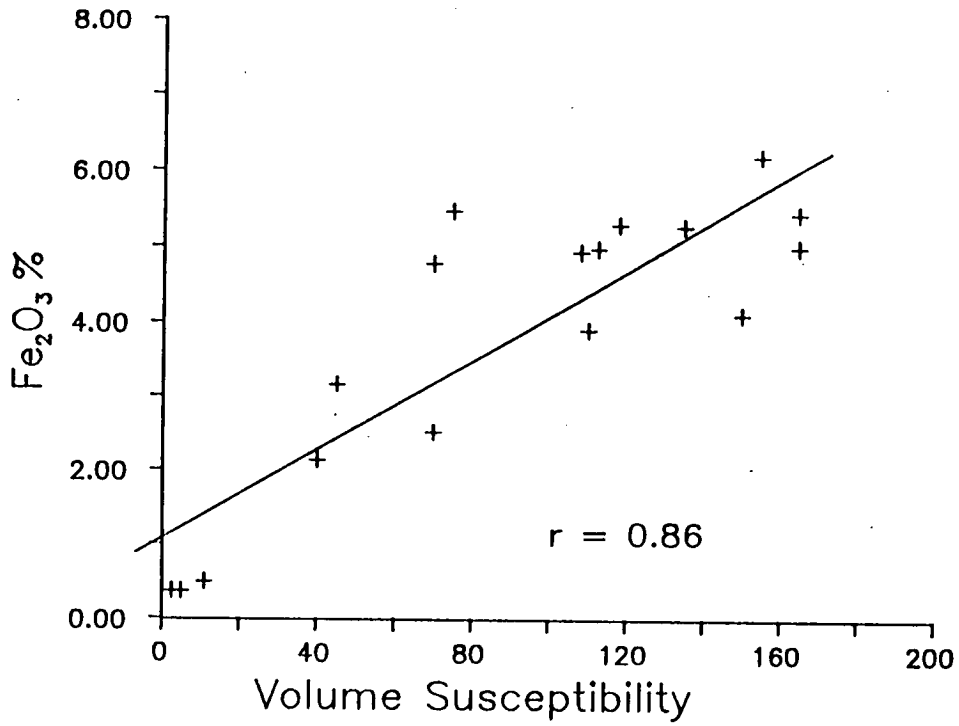
Core no.	Depth in core (cm)	Whole core susc.	SIRM/X kAm ⁻¹	Fe/Mn ratio
61-03 42CS	40-44	108	23	84.7
60-05 28CS	36-40	150	22	67.3
60-06 20CSi	80-84	70	18	54.8
58-02 231VE	390-394	3	37	11.7
58-02 231VE	26-30	5	13	14.8
61-03 42CS	161-165	113	24	78.1
61-03 42CS	186-190	75	24	84.5
61-03 28CS	120-124	45	16	56.5
61-03 42CS	25-29	165	24	75.0
61-03 42CS	140-144	70	24	81.3
58-02 231VE	222-226	40	18	46.8
60-05 24CS	148-152	110		77.3
60-05 24CS	40-44	135	21	80.3
61-03 42CS	228-232	118	20	82.0
61-03 42CS	58-62	155	22	97.0
61-03 42CS	75-79	165	20	81.8
58-02 231VE	154-158	11	77	16.9

- Tab 9.1a Chemical constituents (%) of some UK Continental Shelf core samples. Data derived by XRF analysis, with compositions calculated using software developed by Dr J.P. Smith.

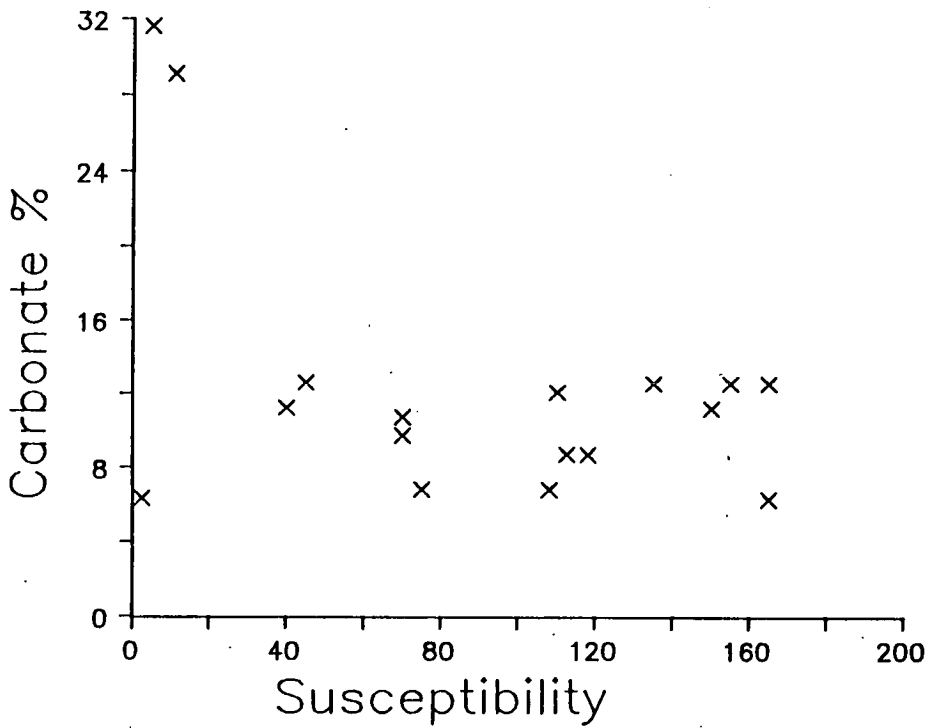
- Tab 9.1b Chemical ratio (derived from data in tab 9.1a) and mineral magnetic data

	Susc.	MgO	Al ₂ O ₃	CaO	SO ₃	Zr	MnO ₂	Zn	Ni	SiO ₂	Fe ₂ O ₃	K ₂ O	P ₂ O ₅	Sr	Pb
MgO	0.761														
Al ₂ O ₃	0.747	0.951													
CaO	-0.458	-0.654	-0.791												
SO ₃	-0.589	-0.729	-0.775	0.869											
Zr	-0.672	-0.801	-0.730	0.353	0.532										
MnO ₂	0.851	0.934	0.916	-0.635	-0.694	-0.741									
Zn	0.830	0.911	0.848	-0.486	-0.681	-0.778	0.902								
Ni	0.816	0.931	0.929	-0.572	-0.655	-0.803	0.931	0.917							
SiO ₂	0.294	0.495	0.642	-0.960	-0.789	-0.197	0.462	0.295	0.375						
Fe ₂ O ₃	0.862	0.948	0.919	-0.570	-0.675	-0.793	0.961	0.967	0.948	0.383					
K ₂ O	0.279	0.678	0.786	-0.812	-0.757	-0.434	0.549	0.558	0.635	0.723	0.574				
P ₂ O ₅	0.708	0.709	0.676	-0.399	-0.440	-0.446	0.713	0.740	0.707	0.192	0.793	0.403			
Sr	-0.539	-0.746	-0.852	0.971	0.873	0.471	-0.693	-0.570	-0.662	-0.896	-0.647	-0.833	-0.479		
Pb	-0.239	-0.569	-0.628	0.336	0.230	0.505	-0.519	-0.460	-0.634	-0.180	-0.547	-0.614	-0.452	0.410	
Cu	0.851	0.862	0.796	-0.406	-0.591	-0.715	0.897	0.942	0.862	0.228	0.948	0.428	0.777	-0.468	-0.479

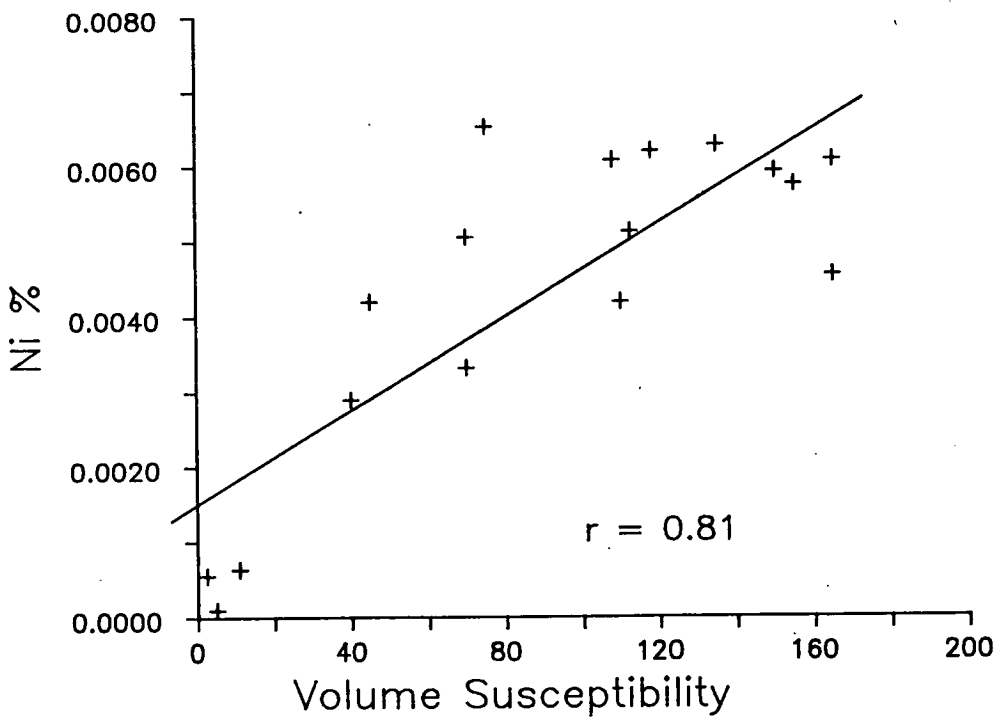
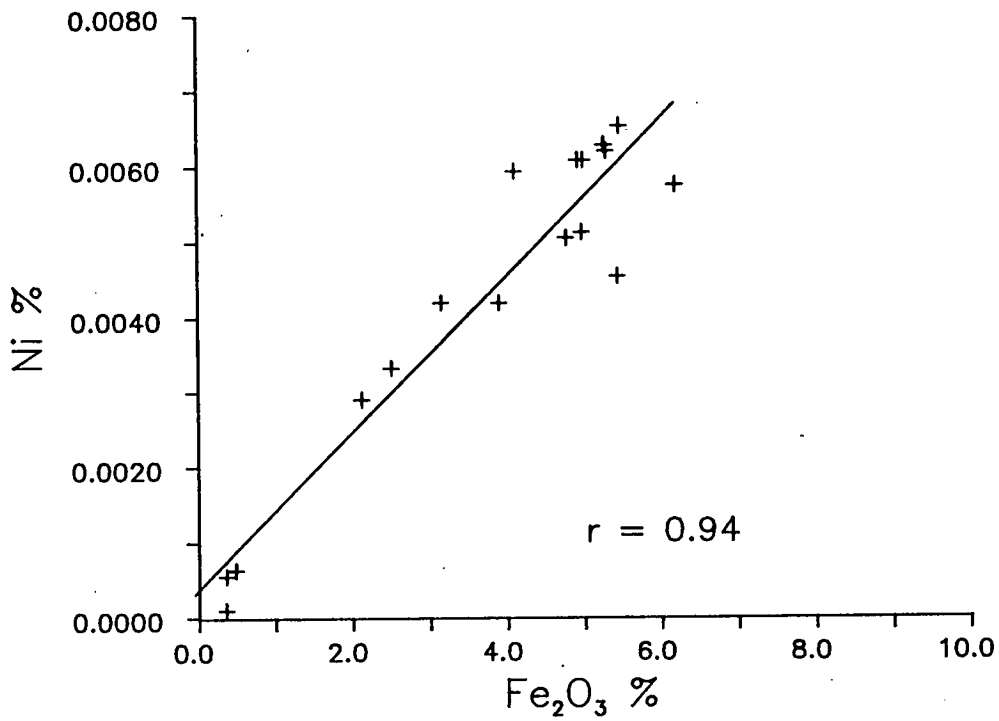
- Tab 9.2 Correlation coefficients between chemical constituents and volume susceptibility for some UK Continental Shelf sediments.



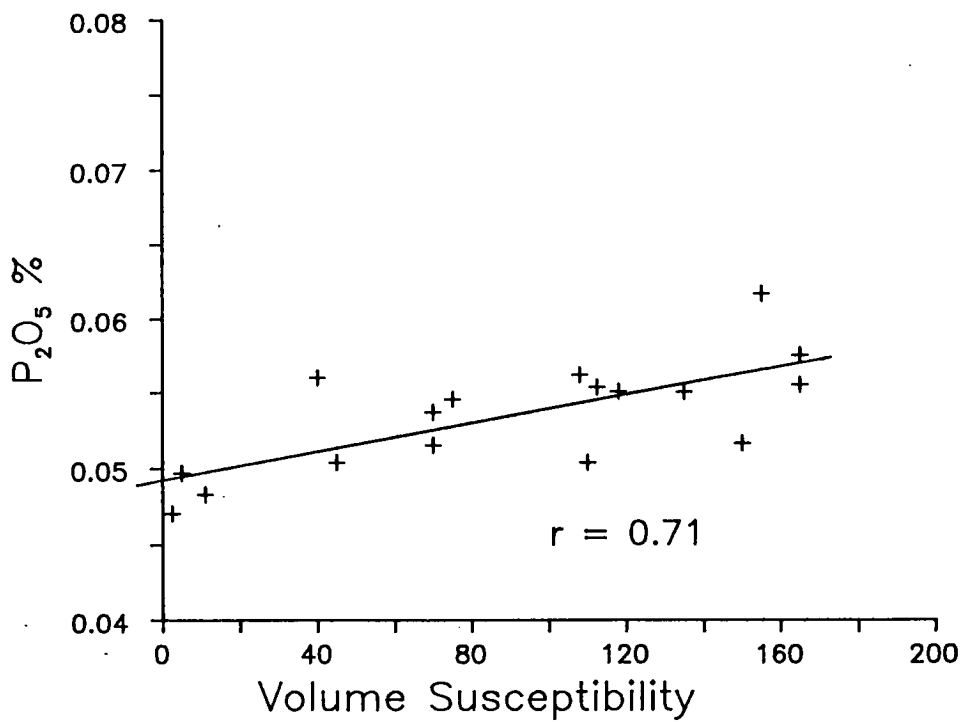
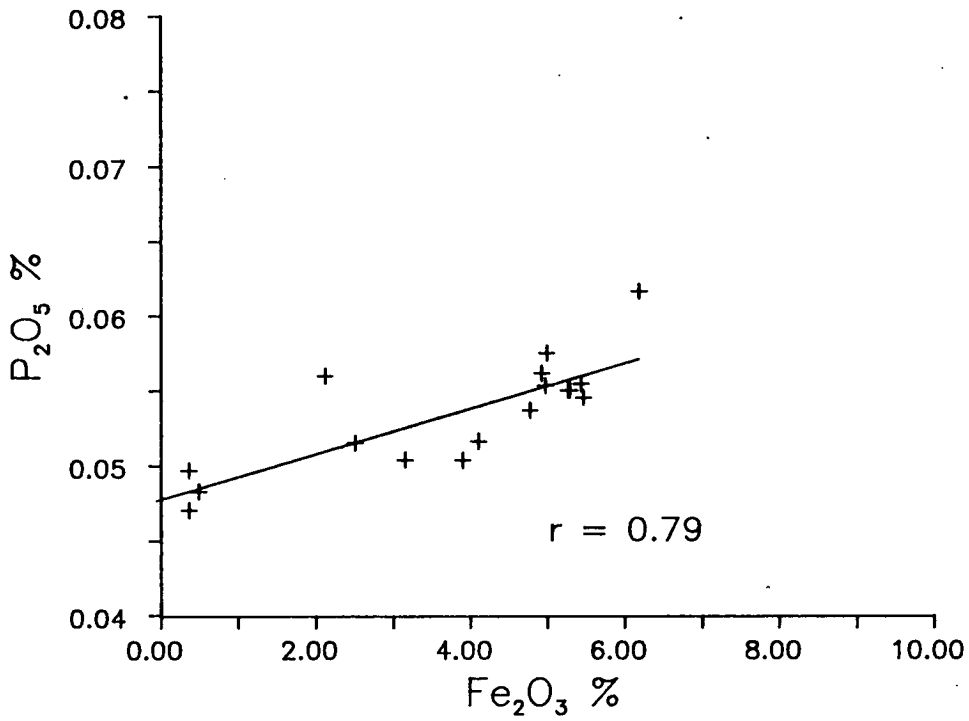
- Fig 9.1a The relationship of iron content and volume susceptibility for 17 continental shelf core samples.



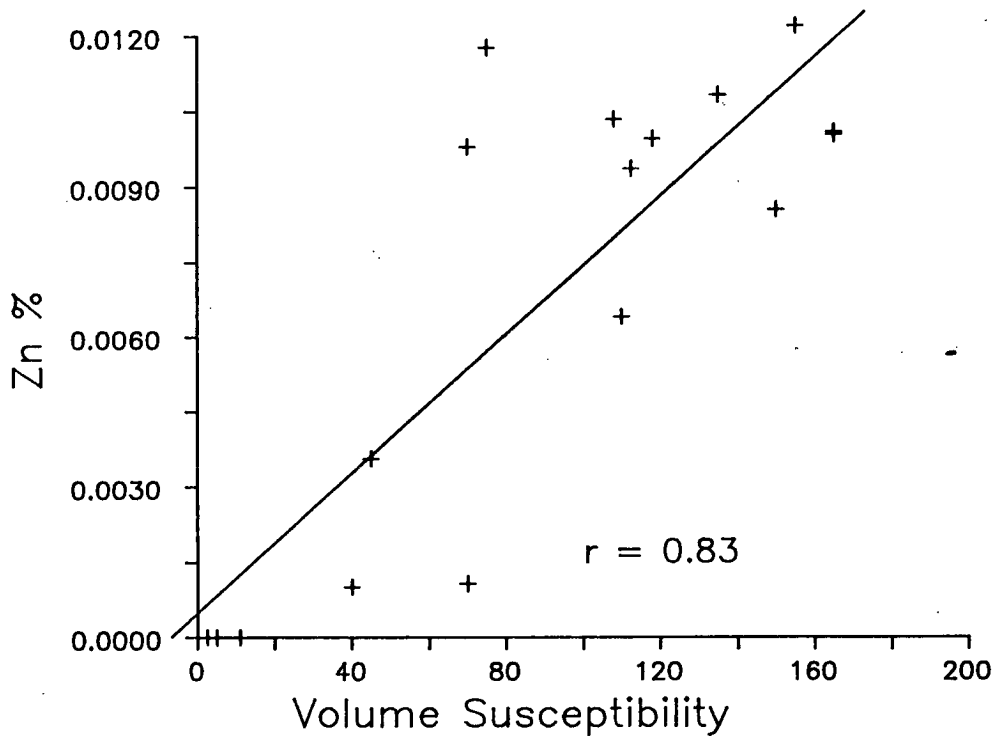
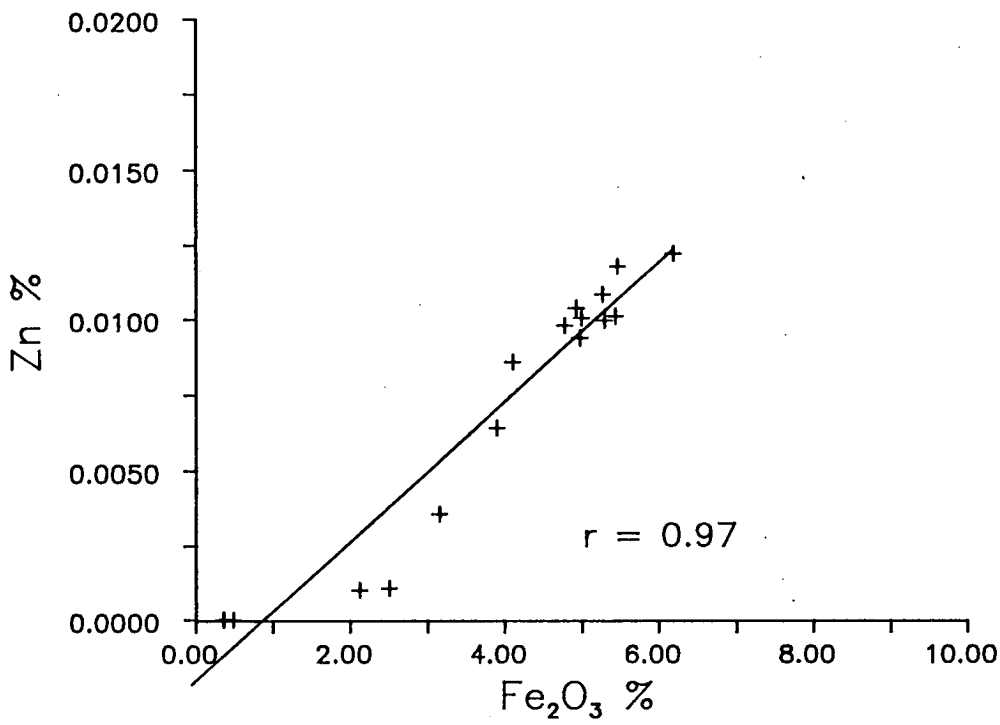
- Fig 9.1b The relationship of carbonate content and whole core susceptibility for 17 continental shelf samples.



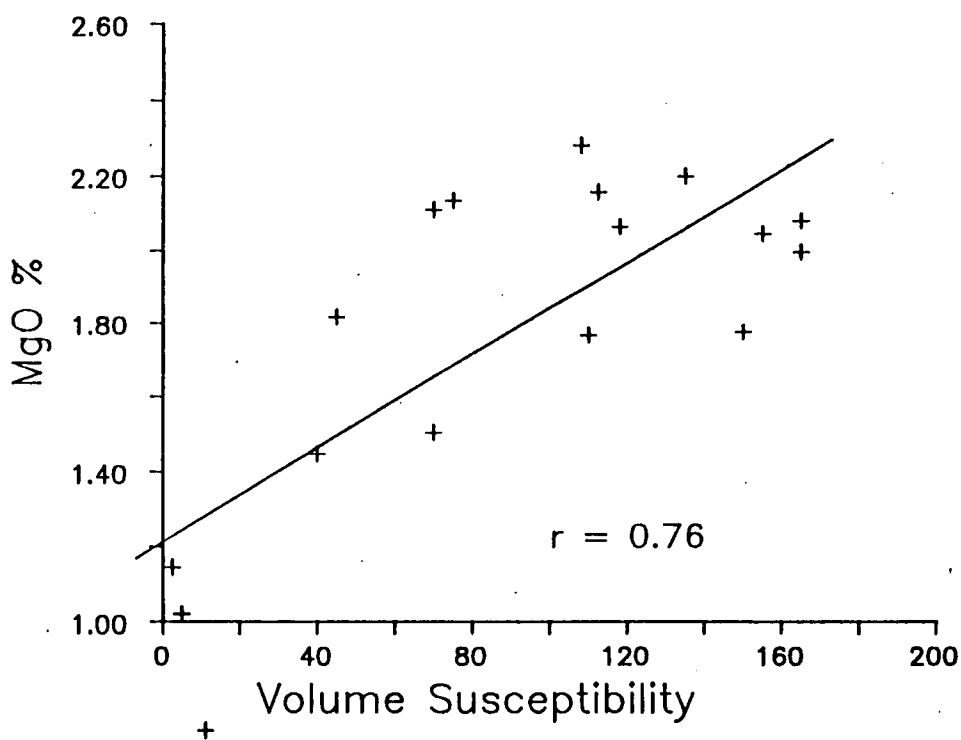
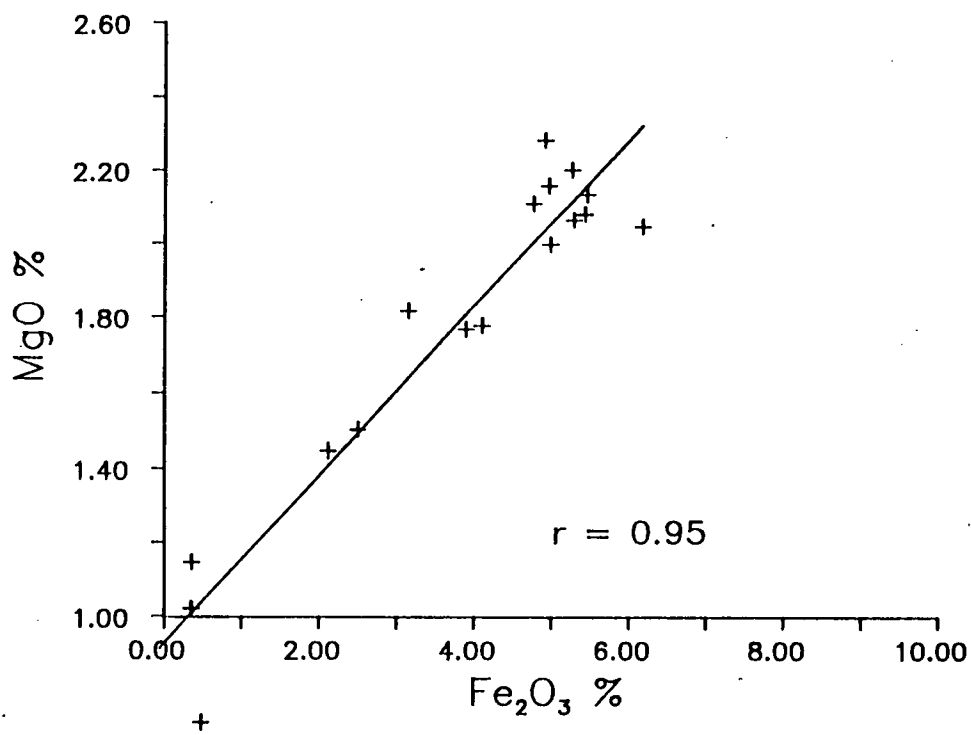
- Fig 9.2 The relationship between (a) nickel content and iron content, (b) nickel content and volume susceptibility for 17 continental shelf core samples.



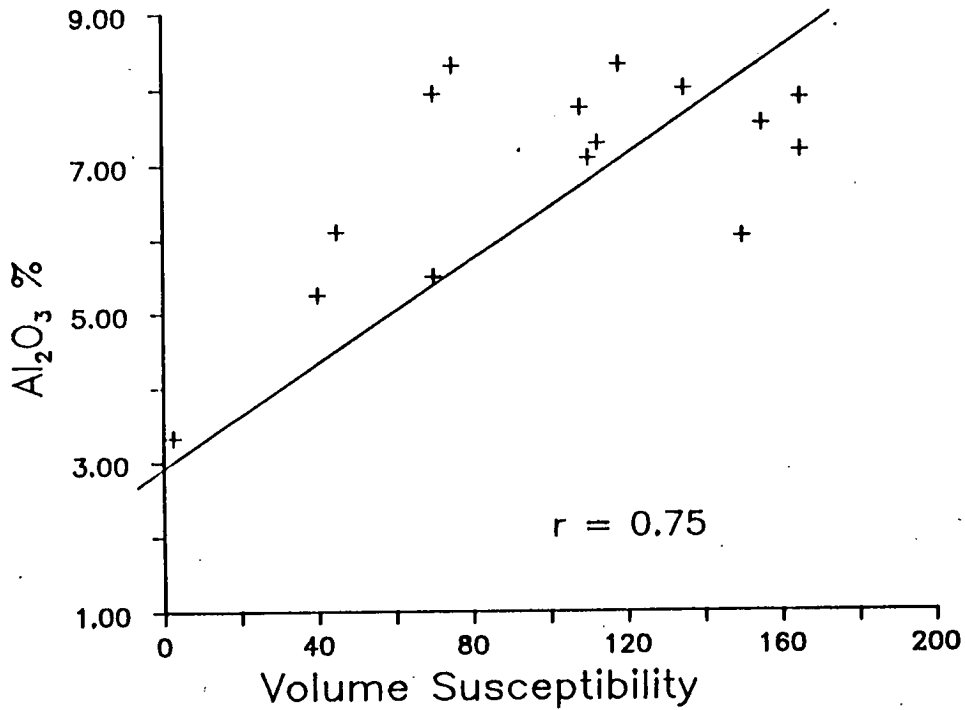
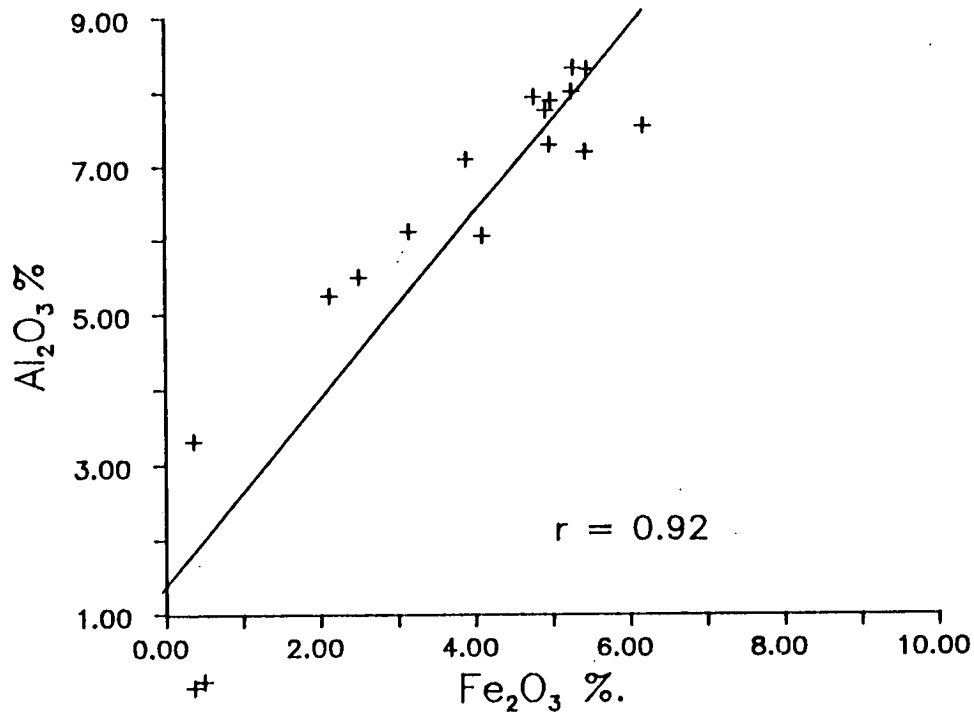
- Fig 9.3 The relationship between (a) phosphate content and iron content, (b) phosphate content and volume susceptibility for 17 continental shelf core samples.



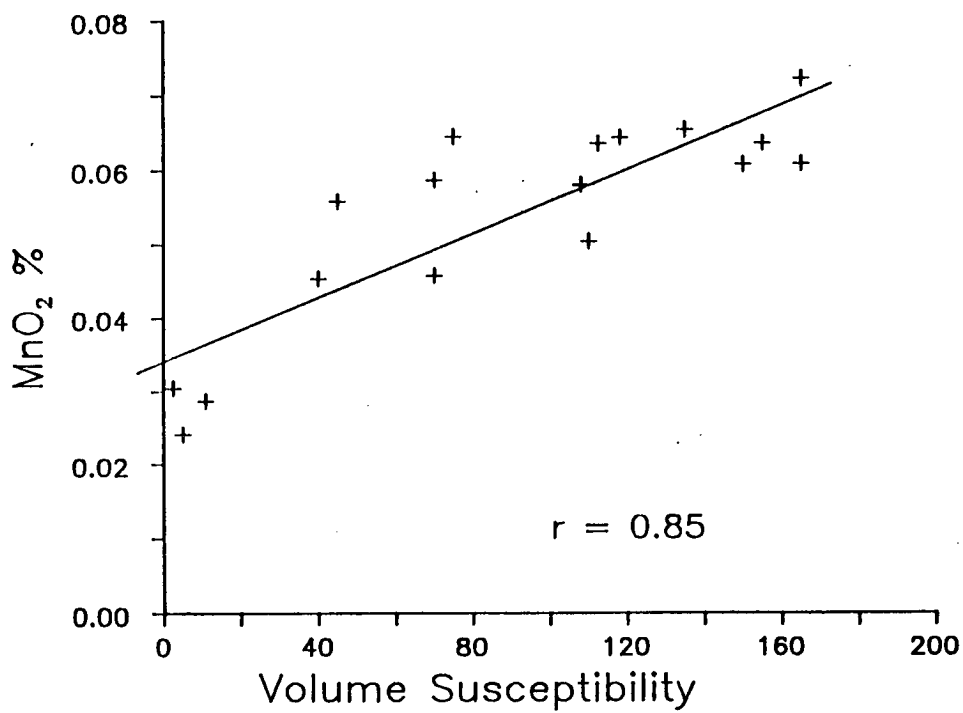
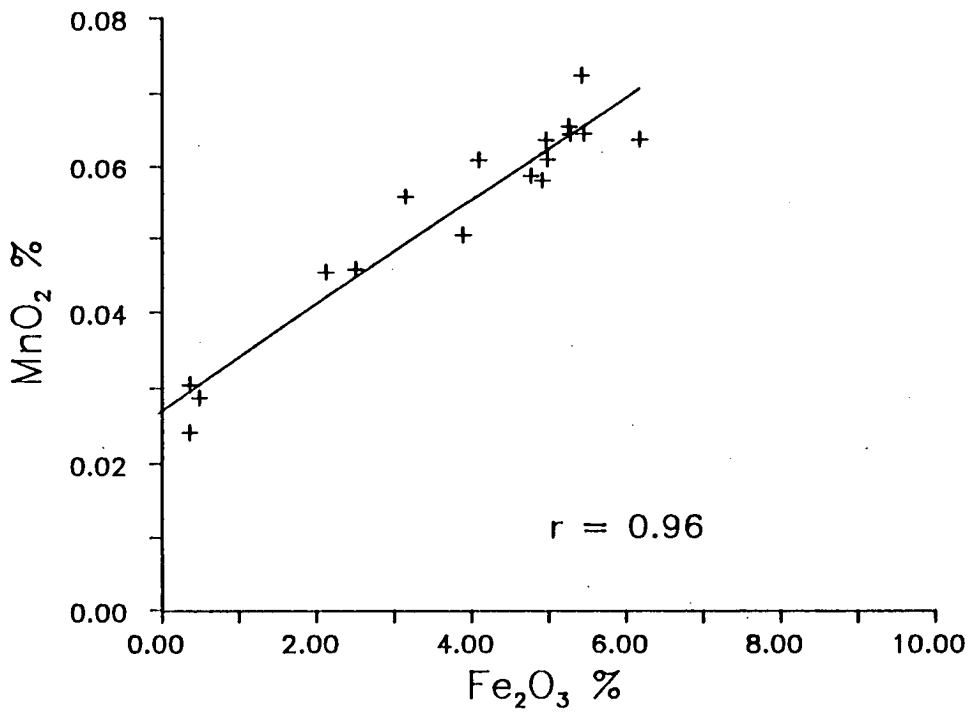
- Fig 9.4 The relationship between (a) zinc content and iron content, (b) zinc content and volume susceptibility for 17 continental shelf core samples.



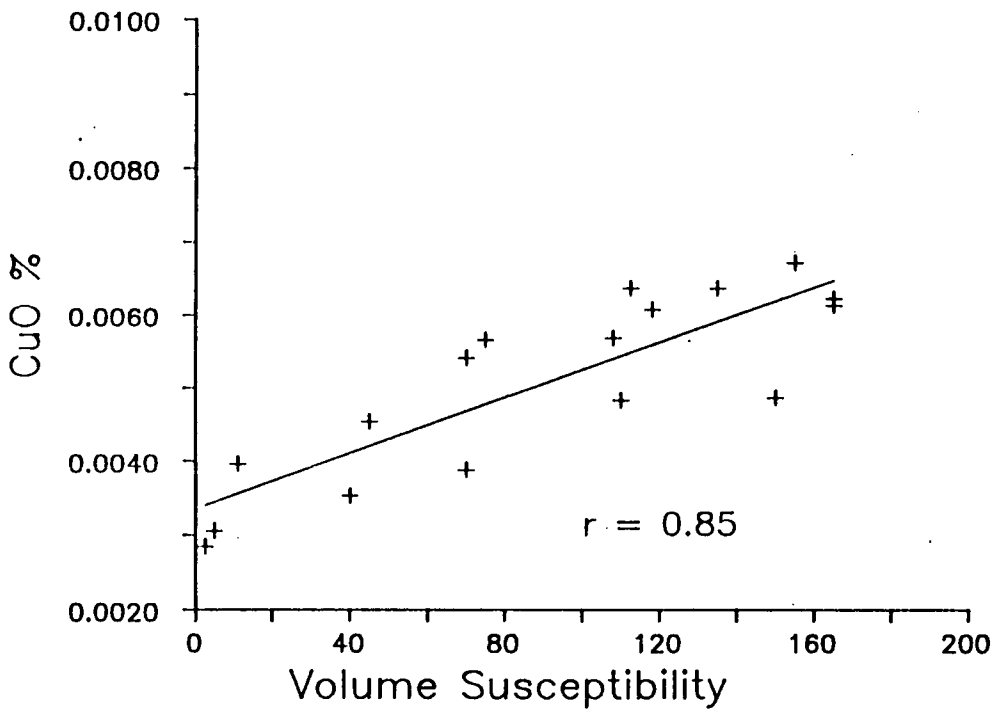
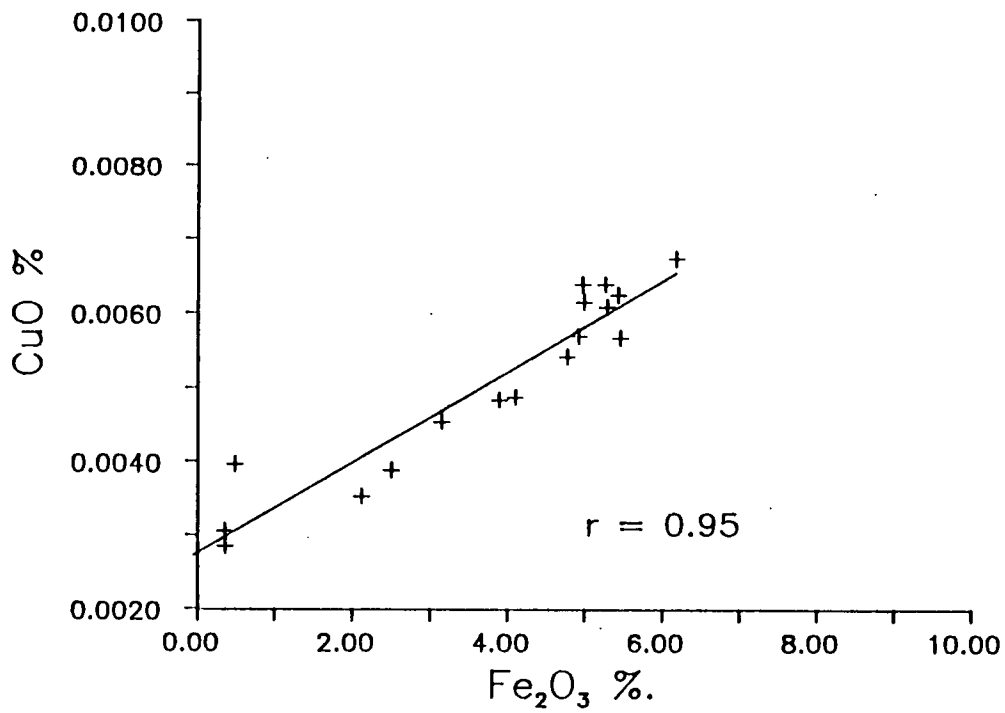
- Fig 9.5 The relationship between (a) magnesium oxide content and iron content, (b) magnesium oxide content and volume susceptibility for 17 continental shelf core samples.



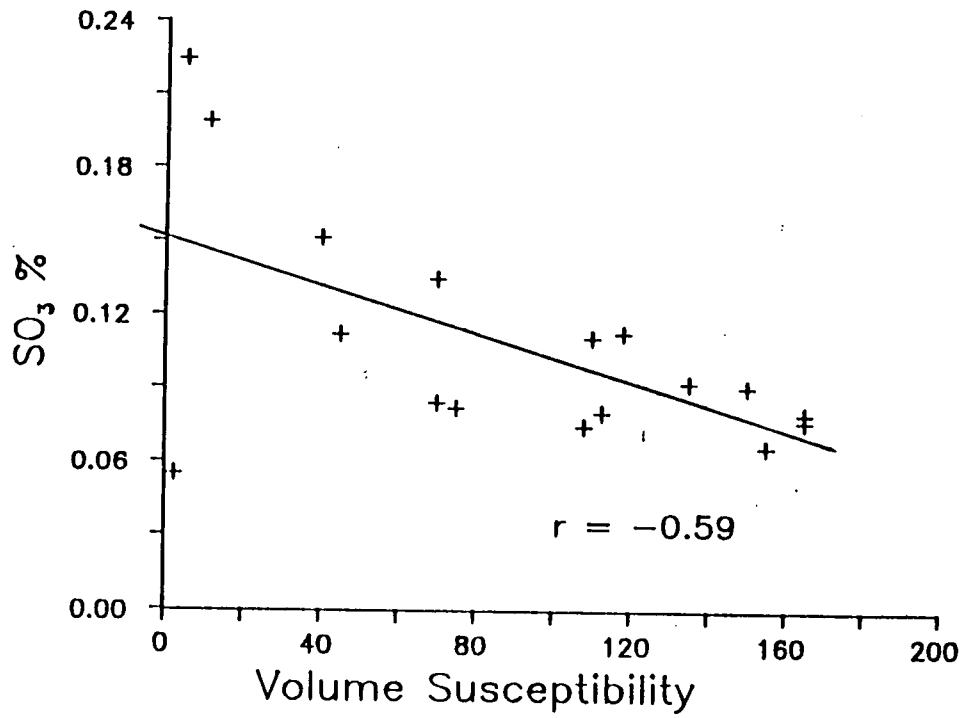
- Fig 9.6 The relationship between (a) aluminium oxide content and iron content, (b) aluminium oxide content and volume susceptibility for 17 continental shelf core samples.



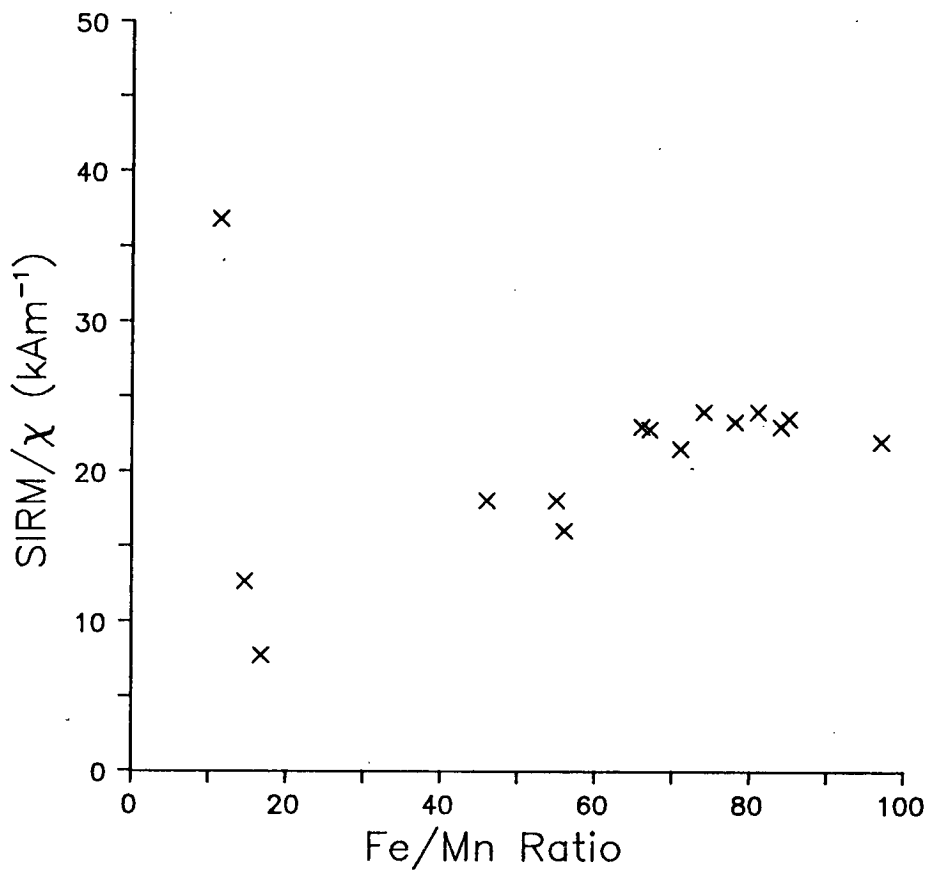
- Fig 9.7 The relationship between (a) manganese oxide content and iron content, (b) manganese oxide content and volume susceptibility for 17 continental shelf samples.



- Fig 9.8 The relationship between (a) copper content and iron content, (b) copper content and volume susceptibility for 17 continental shelf samples.



- Fig 9.9 The relationship of sulphate content and volume susceptibility for 17 continental shelf core samples.



- Fig 9.10 Plot of Fe/Mn ratio against SIRM/χ for samples from the UK continental shelf.

9.4 Discussion

Fig. 9.1_a shows the strong correlation ($r = 0.86$) between iron concentration and bulk susceptibility in continental shelf cores. This strong correlation echoes the results of Currie and Bornhold (1982) on grab sample from the Canadian continental shelf and the work of Puranen (1977) on Swedish glacial till deposits. It is interesting to note that the samples with the lowest susceptibility (from core 58-02 231VE) have abnormally high carbonate content for the data set, suggesting a possible dilution effect.

Besides demonstrating that susceptibility is an indicator of iron oxide concentration, chemical data provided by the XRF analysis show several other interesting relationships. The relationship between iron and other heavy minerals comes out strongly in several instances. It is known that iron concentrations tend to be associated with other heavy minerals (Basham, pers. comm 1987). The strong positive correlations between iron and nickel ($r = 0.94$), phosphate ($r = 0.79$), zinc ($r = 0.96$), magnesium ($r = 0.95$), aluminium ($r = 0.91$), manganese ($r = 0.96$) and copper ($r = 0.95$), (figs 9.2 to 9.8 respectively) are evidence of the close relationship between iron concentration and other elemental concentrations. In the case of zinc and nickel, there is still a strong positive relationship with iron concentration even when their concentrations are as low as 100 ppm. The close relationship between iron concentration and the presence of other elements as shown by the correlation coefficients listed above demonstrates the effectiveness of susceptibility as a prospecting tool in the regime of fine grained ($< 63\mu\text{m}$) sediments normally considered unsuitable for conventional (heavy liquid) mineral extraction.

In view of the recent work by Snowball and Thompson (1988) regarding the effect of iron sulphides on the magnetic properties of sediments in Loch Lomond, and the presence of pyrite and metastable monosulphides in marine sediments effected by dissolution (Karlin and Levi, 1983), it is significant to note that there is apparently no strong correlation ($r = -0.59$) between sulphate content, and susceptibility (fig 9.9). This lack of correlation suggests a stable chemical situation in respect of magnetic iron sulphides in the UK shelf cores.

In addition to the absolute concentrations of various chemical constituents, information can be derived from the ratios of chemicals found within individual samples. One of the most widely used chemical ratios is the iron/manganese

ratio which gives a good indication of the redox conditions during and after deposition of the sediment. Under oxidising conditions both elements exhibit low solubility, but in a reducing environment they become mobile, manganese more readily than iron due to its greater relative solubility (Engstrom and Wright 1984). Mackereth (1966) demonstrated how such a differential mobility could be utilised to assess depositional/sediment source environment in the form of the iron/manganese ratio. A low ratio represents a reduction stage during the depositional cycle with a higher ratio being representative of oxidising conditions. Typical iron/manganese ratios range from 10 to 190, the majority falling within the 30 to 100 range (Hirons 1986).

Data from this study (table 9.1) shows typical Fe/Mn ratios of 60–80, but with several extreme ratios in the region of 10 to 40. The samples with extreme Fe/Mn ratios were all taken from core 58–02 231VE originating in The Central North Sea. The Fe/Mn ratio data in table 9.1 suggests that core 58–02 231VE has been subjected to more severe reducing conditions during deposition than the other cores studied.

When SIRM/ χ ratios (where available) are plotted against Fe/Mn ratios for the cores, a distinct linear trend can be seen. This trend suggests that SIRM/ χ has some potential as an environmental indicator.

9.5 Significant Points

- 1) Iron content and susceptibility are positively related in UK continental shelf cores.
- 2) Iron deposits are associated with other metallic mineral concentrations.
- 3) It follows from (a) and (b) that susceptibility can be used as a reconnaissance tool for a range of metallic minerals.

CHAPTER 10 FINAL DISCUSSION

This thesis has explored various aspects of the application of palaeomagnetic and mineral magnetic techniques to continental shelf sediments. The results have given an insight into the limitations and strengths of such studies.

The sample material used was, in the case of BGS vibrocore, gravity core and shipex grab-samples, not originally intended for palaeomagnetic purposes. The emphasis in designing the BGS sampling systems had been to recover relatively large quantities of sediment for a variety of uses. The retention of a high quality sedimentary fabric was, of necessity, placed second to having systems robust enough to operate reliably in continental shelf conditions. The only core material examined in my study that was taken with a view employing detailed palaeomagnetic techniques was that from the Spitsbergen box cores. Nevertheless, the BGS core material proved technically suitable for palaeomagnetic studies as there was a clearly measurable NRM seen in cores from all UK areas studied. The only exceptions occurred when drying out through age or improper storage had taken place. For example, extensive damage through drying occurred in the case of cores from the Central North Sea area, (chapter 5). Originally, a reasonably clear NRM had been expected for the gravity cores but it was uncertain what quality of data would be obtained from vibrocores (see appendix A). In particular, it was not known if the vibration generated during the coring process would realign the magnetic grains within the sediment. However, as can be seen from, for example, the palaeomagnetic data for the Peach area, (chapter 3, figs 3.4, 3.5), vibrocores can carry a measurable NRM. The remanence has not been realigned to the earth's present field direction as would have been expected if the vibration during penetration was causing a realignment of magnetic grains. Indeed, there is very little sign of any secondary directional component under demagnetisation (fig 3.5). Gravity cores examined for the Flett area, (chapter 4, figs 4.5, 4.6), showed similar demagnetisation behaviour, suggesting, as expected for the gravity cores, negligible realignment of magnetic grains during coring.

One aspect of BGS core collection techniques which was found to hinder palaeomagnetic analysis was the lack of alignment between core sections

following division into one metre sections on deck, as shown in fig 3.4. The accuracy of alignment between core sections varied greatly with individual operators and is consequently difficult to quantify. Set against this alignment problem was the apparent lack of twisting of the core barrel whilst penetrating the sediment. Unlike the Mackereth coring technique commonly employed in lake sediments, the BGS coring equipment being of more sturdy design and steel construction (see appendix A), remained rigid throughout coring operations. There was also negligible flexing of the corer barrel during core recovery, a common and unquantifiable effect with Mackereth coring.

A problematical aspect of continental shelf coring was the depth of water. Depths of up to 1600 metres presented technical difficulties from a sampling equipment point of view and also had a knock-on effect in terms of sediment quality. The Peach area was the most extreme example, where cores were being recovered from below 1600 metres of water. Here the head of water produced considerable pressure on the unconsolidated sediments being sampled. As a result of the pressure release upon recovery to the surface, it was common to see cores expand out of their liners once the restraining gates on the barrel were removed. The effect of such expansion upon the sedimentary and magnetic fabrics of the core are difficult to quantify, but must be born in mind when looking at cores from deep water.

Moving on from the problems derived from the various coring techniques, the palaeomagnetic data itself was promising in that in most cases there was an NRM that proved stable under demagnetisation. Unfortunately, when the data downcore is viewed, the record of changes in NRM direction lack sufficient features for reliable comparison with secular variation master curves (eg Turner and Thompson, 1981) and were of insufficient length to record a reversal stratigraphy. During the course of my study, all cores examined palaeomagnetically had a strong, normal magnetic polarity. The only exceptions to normal polarity being a small number of samples at the base of cores from the Flett area that exhibited a negative polarity and proved unstable under demagnetisation (figs 4.5,4.6).

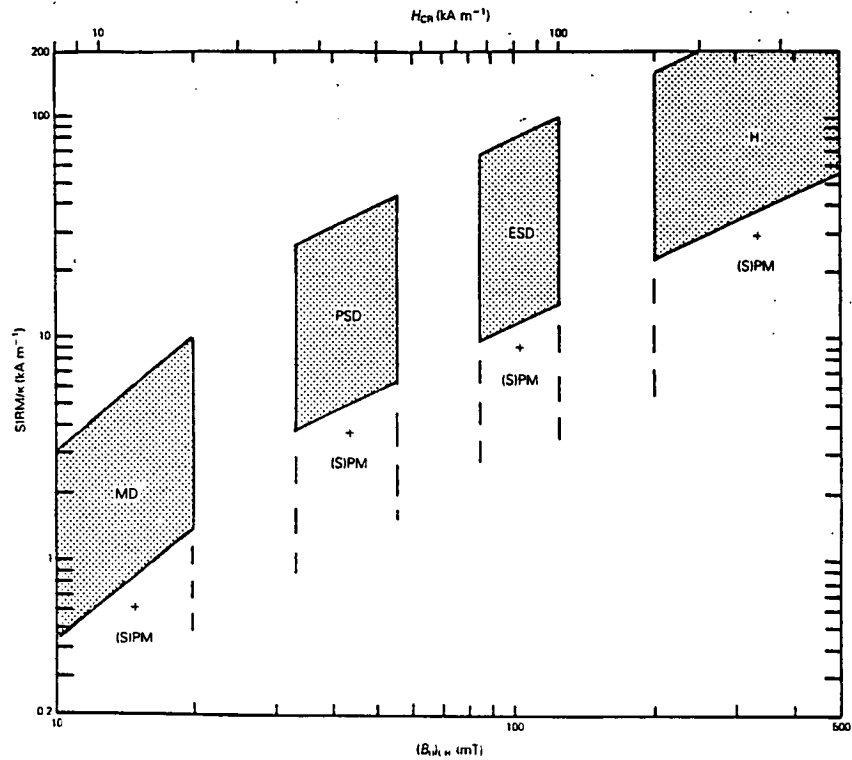
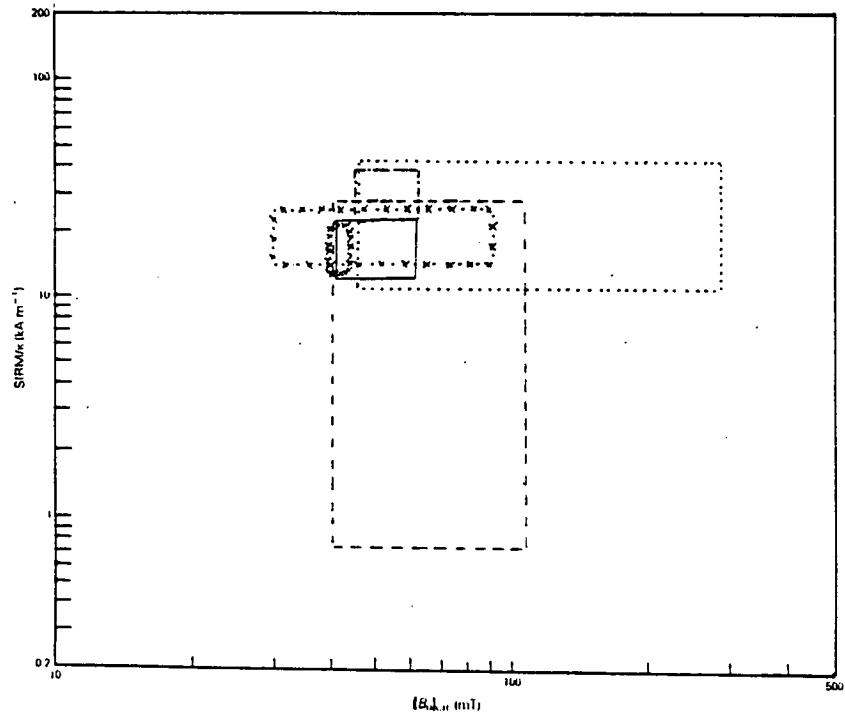
What could be seen in all core records, from the Peach area, northwards to Spitsbergen was an inclination shallower than would be expected at that latitude from a geomagnetic dipole field model. The common occurrence of shallow inclinations is discussed in chapter 8 in relation to Spitsbergen cores

which exhibited the greatest error. The shallow inclination problem was common to all types of core studied, that is vibrocore, gravity core and box-cores. The sediment type also varied between areas, as did the magnetic minerals that carried the remanence. These variations tend to reinforce the point made in chapter 8, that inclination error cannot be attributed solely to one particular piece of coring equipment, sediment type or magnetic remanence carrier. There is clearly some variation in geomagnetic field behaviour due to non-dipole elements of the earth's magnetic field at these latitudes.

The mineral magnetic data obtained in my study has a greater potential for constructive use than the palaeomagnetic approach. The technique of whole core susceptibility scanning has been established as viable in both laboratory and shipboard conditions (chapter 4). It fitted in well with routine deck procedures on the sampling vessel. Once interfaced to a computer, the Bartington whole core susceptibility equipment provided large quantities of easily interpretable data. This data could be used for several functions, from the detection of drop stones (chapter 3) to picking up changes in lithology changes downcore (chapters 4 and 5, fig 5.5). The chemical relationship between susceptibility and heavy minerals established in chapter 9 supports the possibility of using whole core susceptibility as a rapid mineral reconnaissance tool.

Other mineral magnetic parameters, χ , SIRM/ χ , HIRM and S, were shown to be useful in identifying lithologies (eg fig 5.6). The range of magnetic mineralogies was seen to vary greatly between cores and sometimes downcore. The variation in mineralogies ranged from the simple situation seen in Peach (chapter 3) with relatively constant concentration and coercivity downcore but varying concentrations between cores from adjacent areas to the complex situation found in the Central North Sea area (chapter 5). In the case of the Central North Sea, concentration and coercivity were seen to vary greatly both between cores and downcore, so reflecting the more complex and varied lithology of the area.

By using the biplot of SIRM/ χ and coercivity (fig 10.1) from Thompson and Oldfield (1986) and adding data from the various UK continental shelf sediments studied in this thesis, a distinct trend towards low coercivity magnetic minerals can be seen. The majority of UK continental shelf samples fall within the the



- | | | | |
|-------|---------|---------|--------------------|
| — | Peach | xxxx | Clyde (mud) |
| - - - | Flett | -y-y-y | Clyde (sand) |
| | Forties | - - - - | Moray Firth (sand) |

- Fig 10.1 Plot of $SIRM/\chi$ vs coercivity from Thompson and Oldfield (1986) with data for typical samples from the Peach, Flett, Forties sea areas included on identical axes. The grid on the Thompson and Oldfield (1986) figure is schematically divided into magnetic mineralogies and magnetisation states. Multidomain (MD), pseudo-single domain (PSD) and elongated single domain (ESD) magnetites fall in the upper left to centre of the diagram. Haematite (H) lies in the upper right corner, mixtures containing (super) paramagnetic grains lie further towards the lower right.

magnetite classification with varying magnetic grain sizes seen. Only a few samples from the Central North Sea fall within an exclusively haematite classification. The spread of data is least in the mud fraction of the Clyde grab sample sediments, and greatest in the North Sea cores. Haematite concentration is seen to increase with coarser grain sizes.

Within the Peach area, the variation in magnetite concentrations between cores was used as the basis for mapping sediment types as defined by whole core susceptibility and keyed to other geological data (fig 3.8). This mapping approach exploited the generally homogeneous lithology seen downcore in Peach, and is consequently not applicable to areas that show major lithological changes downcore.

In the case of varied coercivity and concentration of magnetic minerals, there is the potential for providing the basis for a system of sediment source identification. The most promising data for this sediment-source linkage program is from the Spitzbergen area as shown in biplot form in fig 8.16. The characteristics of sediments seen in fig 8.16 should be sufficient to allocate appropriate sources when compared to samples from potential sources.

Whole core susceptibility measurements were found to remain constant through time, as shown in chapter 4, fig 4.4a and 4.4b. This consistency through time supports the use of stored material in palaeomagnetic and mineral magnetic studies. Any change in susceptibility would have suggested a chemical change in magnetic mineralogy. Such a change may lead to the growth of CRMs which may alter the magnetic signature of the sediment.

The examination of grab samples provides a different approach to the magnetic studies of continental shelf sediments. The studies of the Clyde (chapter 6) and the Moray Firth (chapter 7) have shown the effectiveness of mass-specific susceptibility as a mapping tool (fig 6.5) and its potential for use as a sediment source identification tool through the use of a range of mineral magnetic parameters (fig 7.7). If the conclusions from chapter 9, that susceptibility is strongly related to heavy mineral concentration (figs 9.2-9.8), is added to the above result, it follows that susceptibility studies on grab samples provide the basis for a rapid mineral reconnaissance technique. Many thousands of grab samples from the UK continental shelf lie in store awaiting chemical analysis. Susceptibility would provide a rapid method of detecting

samples suitable for further investigation. The use of susceptibility as a reconnaissance tool has been successfully employed in heavy mineral studies currently being undertaken at the Applied Geology Dept., University of Strathclyde.

The results of this thesis provide a basis for a considerable amount of future work, particularly if the palaeomagnetic data is reinforced in several respects. A clearly measurable remanence is seen in most cores, but the lack of suitable dating control severely limits interpretation. At the time of writing (1989) carbon 14 accelerator dating is just becoming available and should be suitable for use on the very small amounts of organic carbon found in continental shelf cores. Thermoluminescence techniques are being developed for sediments, (Singhis and Mejdahl 1985) as well as more detailed tephra chronologies (Dugmore 1988, pers comm), both providing other means of gaining vital age control.

Longer cores are now also becoming available after a lull in BGS sampling activity during recent years. Recent (1989) BGS boreholes in the North Sea have recovered 270m of sediment with initial palaeomagnetic analysis showing a clear reversal stratigraphy.

One aspect of coring activity that still needs to be explored is the taking of duplicate vibrocores for palaeomagnetic analysis. The remanence records from sets of such cores could be stacked to provide a more reliable record of NRM variation in any one area.

Stacking techniques could also be applied to whole core susceptibility data from duplicate cores to give a clearer indication of any relationship to lithology and help eliminate variation attributable to localised impurities. Use of simple filtering techniques could help smooth out spikes in susceptibility due to drop stones or impurities from the time of recovery.

Simple actions, such as the use of non-magnetic cutting tools, the checking of magnetic field strengths within core barrels and rejecting or demagnetising highly magnetised barrels could lead to better quality palaeomagnetic data.

Specific suggestions for both mineral magnetic and palaeomagnetic work on BGS core material are summarised in 'A Guide to the Application of Palaeomagnetic and Mineral Magnetic Techniques in BGS sample material' (Watson 1990, in prep).

References

- Ager, D.V., 1980. *The Geology of Europe*. London: McGraw-Hill.
- Anderson, C.M., 1988. *Susceptibility studies in the Firth of Clyde*. Unpublished undergraduate project, University of Edinburgh, Dept. of Geophysics.
- As, J.A., 1967. The a.c. demagnetisation technique, in *Methods in palaeomagnetism*, D.W. Collinson, K.M. Creer and S.K. Runcorn (eds). Amsterdam: Elsevier.
- Austin, T.J.F., 1987. *Magnetostratigraphy and Late Quaternary History of the Barents Shelf*. Unpublished PhD. thesis, University of East Anglia.
- Barton, C.E., 1982. Spectral analysis of palaeomagnetic time series and the geomagnetic spectrum. *Phil. Trans. R. Soc. Lond. A* 306, 203-209.
- Barton, R.H., Tomlinson, W.D., and Bartington, G.W., 1988. Use of seabottom magnetic susceptibility measurements in hydrocarbon exploration. *Proc. of Remote Sensing for Exploration Geology*, Houston, 1988.
- Bent, A.J.A., 1986. *Aspects of pleistocene glaciomarine sequences in the North Sea*. Unpublished PhD thesis, University of Edinburgh.
- Bingham, D.K. and Stone, D.B., 1972. Palaeosecular variation of the geomagnetic field in the Aleutian Islands, Alaska. *Geophys. J. R. Astr. Soc.*, 28, 317-335.
- Bishop, P., 1975. The palaeomagnetism of muddy sediment cores from the Inner Sound, N.W. Scotland and the glacial and post-glacial history of sedimentation in the area. *Earth Planet. Sci. Lett.*, 27, 51-56.
- Bloemendal, J., 1983. Paleoenvironmental implications of the magnetic characteristics of sediments from deep sea drilling project site 514, southeast Argentine Basin. *Initial Reports of the D.S.D.P. Washington*, LXXI, 1097-1098.
- Bloemendal, J., Lamb, B., and King, J., 1988. Palaeoenvironmental implications of rock-magnetic properties of late quaternary sediment cores from the eastern equatorial Atlantic. *Paleoceanography*, 3, 61-87.
- Buchanan, J.Y., 1891. On the composition of oceanic and littoral manganese nodules. *Trans. R. Soc. Edinb.*, 36, 459-483.

Chesher, J.A. and Lawson, D., 1983. *The geology of the Moray Firth*. IGS report #83/5, H.M.S.O., London.

Collinson, D.W. and Wright, D., 1983. *Methods in rock magnetism and palaeomagnetism: techniques and instrumentation*. Chapman and Hall, London.

Cook, A.H., 1973. *Physics of the Earth and Planets*, Macmillan, London.

Creer, K.M., 1985. Review of lake sediment palaeomagnetic data. *Geophysical Surveys*, 7, 125-160.

Currie, R.G. and Bornhold, B.D., 1983. The magnetic susceptibility of continental-shelf sediments, West Coast Vancouver Island, Canada. *Marine Geology*, 51, 115-127.

Dankers, P.H., 1978. *Magnetic properties of dispersed natural iron oxides of known grain size*. PhD thesis, University of Utrecht.

Deegan, C.E., Kirby, R., Rae, I., and Floyd, R., 1973. *The superficial deposits of the Firth of Clyde and its sea lochs*. IGS report 73/9, H.M.S.O., London.

Dunlop, D.J., 1979. On the use of Zijderveld vector diagrams in multicomponent paleomagnetic studies. *Phys. Earth Planet Interiors*, 20, 12-24.

Elmore, R.D., Engel, M.H., Crawford, L., et al, 1987. Evidence for a relationship between hydrocarbons and authigenic magnetite *Nature*, 325, 428-430.

Evans, D. 1985. *1:250 000 Sheet 55N-06W 'Clyde', sea bed sediments and quaternary geology*. Ordnance Survey, Southampton.

Flood, R.D. et al, 1985. The magnetic fabric of surficial deep-sea sediments in the Hebble area (Nova Scotian continental rise). *Marine Geology*, 66, 149-167.

Griffiths, D.H., King, R.F., Rees, A.I. and Wright, A.E., 1960. The remanent magnetism of some recent varved sediments *Proc. R. Soc. Lond*, A256, 359-383.

Goree, W.S. and Fuller, M., 1976. Magnetometers using RF-driven squids and their applications in rock magnetism and palaeomagnetism *Rev. Geophys. and Space Phys.* 14, 591-608.

Harland, W.B., 1961. An outline structural history of Spitsbergen, in *Geology of the Arctic*, Raasch G.O. (ed) Univ. Toronto Press, Toronto.

Henshaw, P.C. and Merrill, R.T. 1980. Magnetic and Chemical Changes in Marine Sediments. *Rev. Geophysics and Space Physics*, 18, 483-504.

Hirons, K.R. and Thompson, R., 1986. Palaeoenvironmental application of magnetic measurements from inter-drumlin hollow lake sediments near Dungannon, Co. Tyrone, Northern Ireland. *Boreas*, 15, 117-135.

Housden, J., De Sa, A., and O'Reilly, W., 1988. The magnetic balance and its application to studying the magnetic mineralogy of igneous rocks. *J. Geomag. Geoelectr.*, 40, 63-75.

Howe, S.J., 1988. *A magnetic mineral study of surface sediments in the Moray Firth, Scotland*. Unpublished undergraduate project, University of Edinburgh, Dept. of Geophysics.

Hunt, A., 1986. The application of mineral magnetic methods to atmospheric aerosol discrimination. *Phys. Earth Planet Interiors*, 42 10-21.

Karlin, R. and Levi, S., 1983. Diagenesis of magnetic minerals in Recent haemipelagic sediments. *Nature*, 303, 327-330.

Karlin, R. and Levi, S., 1985. Geochemical and sedimentological control of the magnetic properties of hemipelagic sediments. *J. Geophys. Res.*, 90, 10373-10392.

Kent, D.V., 1982. Apparent correlation of palaeomagnetic intensity and climatic records in deep-sea sediments. *Nature*, 299, 538-539.

King, R.F., and Rees, A.I., Detrital magnetism in sediments: An examination of some theoretical models. *J. Geophys. Res.*, 71, 561-571.

Lancaster, D.E., 1966. Electronic metal detection. *Electronics Today*, (Dec), 39-62.

Long, D., 1979. Geotechnical subdivisions of the Witch Ground Beds in Northwest Forties. *IGS Engineering Geology Unit report No. 79/2*.

Lovlie, L., Markussen, B., Sejrup, H.P., Thiede, J., 1986. Magnetostratigraphy in three Arctic Ocean sediment cores; arguments for geomagnetic excursions within oxygen-isotope 2-3. *Phys. Earth Planet. Interiors*, 43, 173-184.

Mackereth, F.J.H., 1966. Some chemical observations on post-glacial lake sediments. *Phil. Trans. R. Soc.* 250B, 165-213.

Mackereth, F.J.H., 1971. On the variation in direction of the horizontal component of remanent magnetisation in lake sediments. *Earth Planet. Sci. Letters*, 12, 332-338.

McDougall, I., Watkins, N.D., and Kristjansson, L., 1976. Geochronology and palaeomagnetism of a Miocene-Pliocene lava sequence at Bessastadaa, Eastern Iceland. *American Journal of Science*, 276, 1078-1095.

Maher, B.A., 1986. Characterisation of soils by mineral magnetic measurements. *Phys. Earth Planet. Interiors*, 42, 76-92

Matthews, M.B., 1986. *Mineral magnetic contouring of Firth of Clyde surface sediments*. Unpublished undergraduate report, University of Edinburgh, Dept. of Geophysics.

Molyneux, L., and Thompson, R., 1973. Rapid measurement of the magnetic susceptibility of long cores of sediment. *Geophys. J. R. Astr. Soc.* 32, 479-481.

Parry, L.G., 1965. Magnetic properties of dispersed magnetite powders. *Phil. Mag.* 11, 303-312.

Petersen, N., von Dobeneck, T., Vali, H., 1986. Fossil bacterial magnetite in deep-sea sediments from the South Atlantic Ocean. *Nature*, 320, 611-615.

Puranen, R., 1977. Magnetic susceptibility and its anisotropy in the study of glacial transport in northern Finland. In: L.K. Lauranne (ed), *Prospecting in Areas of Glaciated Terrain*. Inst. of Mining and Metallurgy, London, pp 111-119.

Reid, G., and McManus, J., 1987. Sediment exchanges along the coastal margin of the Moray Firth, Eastern Scotland. *J. Geol. Soc. London*, 144, 179-185.

Richardson, N., 1986. The mineral magnetic record in recent ombrotrophic peat synchronised by fine resolution pollen analysis. *Phys. Earth Planet. Interiors*, 42, 48-56

Robinson, S.G., 1986. The late Pleistocene palaeoclimatic record of North Atlantic deep-sea sediments revealed by mineral-magnetic measurements. *Phys. Earth Planet. Interiors*, 42, 22-47.

Sachs, S.D., and Ellwood, B.B., 1987. Controls on magnetic grain-size variations

and concentration in the Argentine Basin, South Atlantic Ocean. *Deep-Sea Research*, 35, 929-942.

Shackleton, N.J. et al, 1984. Oxygen isotope calibration of the onset of ice-rafting and history of glaciation in the North Atlantic region. *Nature*, 307, 620-623.

Snape, C., 1971. An example of anhysteretic moments being induced by alternating field demagnetization apparatus. *Geophys. J.R. Astr. Soc.* 23, 361-364.

Snowball, I., and Thompson, R., 1988. The occurrence of Greigite in sediments from Loch Lomond. *Journal of Quaternary Science*, 3, 121-125.

Sommerville, D.Q.M., 1987. *Susceptibility studies of sediments in the waters surrounding Arran*. Unpublished undergraduate report, University of Edinburgh, Dept. of Geophysics.

Stober, J.C., 1978. *Palaeomagnetic secular variation studies on Holocene lake sediments*. PhD. thesis, University of Edinburgh.

Stober, J.C. and Thompson, R., 1979. An investigation into the source of magnetic minerals in some Finnish lake sediments. *Earth Planet. Sci. Letters*, 45, 464-474.

Stoker, M.S., Skinner, A.C., Fyfe, J.A., and Long, D., 1983. Palaeomagnetic evidence for early Pleistocene in the central and northern North Sea. *Nature*, 304, 332-334.

Strakhov, N.M., 1969. *Principles of Lithogenesis, volume 2*. Oliver and Boyd, Edinburgh.

Stumpp, C.C., Zudin, J.H., and Hailwood, E.A., 1986. Sample-deformation effects on magnetic fabric and remanence in soft sediments. *Abstract U.K.G.A. 10, Glasgow*.

Suttie, W., 1988. *A palaeomagnetic investigation of soft sediment core 58+00 122VE from the Witch Ground Basin area of the North Sea*. Unpublished undergraduate project, Dept. of Geophysics, University of Edinburgh.

Tarling, D.H., 1983. *Palaeomagnetism - Principles and Applications in Geology, Geophysics and Archaeology*. Chapman and Hall, London.

Thompson, R., 1975. Long period european geomagnetic secular variation confirmed. *Geophys. J. R. Astr. Soc.*, 43, 847-859.

Thompson, R., Barrerbee, R.W., O'Sullivan, P.E., Oldfield, F., 1975. Magnetic susceptibility of lake sediments. *Limnology and Oceanography*, 20, 687-698.

Thompson, R. et al 1980. Environmental applications of magnetic measurements. *Science*, 207, 481-486.

Thompson, R., 1986. Modelling magnetization data using SIMPLEX. *Phys. Earth Planet. Interiors*, 42, 113-127.

Thompson, R. and Oldfield, F., 1986. *Environmental Magnetism*. Allen and Unwin, London.

Turner, G.M., 1979. *Geomagnetic investigations of some recent British sediments*. Unpublished PhD thesis, University of Edinburgh.

Turner, G.M., and Thompson, R., 1981. Lake sediment record of the geomagnetic secular variation in Britain during Holocene times. *Geophys. J. R. Astr. Soc.*, 65, 703-725.

Veinberg, B.P. and Shibaev, V.P., 1969. *Catalogue. The results of magnetic determination at equidistant points and epochs, 1500-1940* (ed-in-chief A.N. Pushkov). Moscow: IZMIRAN. Translation no. 0031 by Canadian Dept. of the Secretary of State, Translation Bureau, 1970.

Walden, J., Smith, J.P., and Dackombe, R.V., 1987. The use of mineral magnetic analyses in the study of glacial diamicts: a pilot study. *Journal of Quaternary Science*, 2, 73-80.

Walling, D.E., Pearl, M.R., Oldfield, F., Thompson, R., 1979. Suspended sediment courses identified by magnetic measurements. *Nature*, 281, 110-113.

Watkins, N.D., McDougall, I., and Kristjansson, L., 1977. Upper miocene and pliocene geomagnetic secular variation in the Borgarfjordur area of Western Iceland. *Geophys. J. R. Astr. Soc.*, 49, 609-632.

Williams, T.M., 1988. *The geochemistry and magnetic mineralogy of Holocene strata in acid basins*. Unpublished PhD. thesis, University of Edinburgh.

Additional References

Papamarnopoulos, S., 1978. *Limnomagnetic studies on Greek Sediments*. Unpublished PhD. thesis, University of Edinburgh.

Singhis, A.K. and Mejdahl V., 1985. Thermoluminescence dating of sediments. *Nuclear Tracks*, 10, 137-161.

Tennent, R.M., 1971. *Science Data Book*, Oliver and Boyd, Edinburgh.

von Dobeneck, T., 1986. *Unpublished magnetic extraction equipment designs*, Inst. für Allg. und Angew. Geophysik, Ludwig-Maximilians-Universität München.

Wilson, R.L., 1971. Dipole-Offset - The time average palaeomagnetic field over the past 25 million years. *Geophys. J. R. astr. soc.*, 22, 481-504.

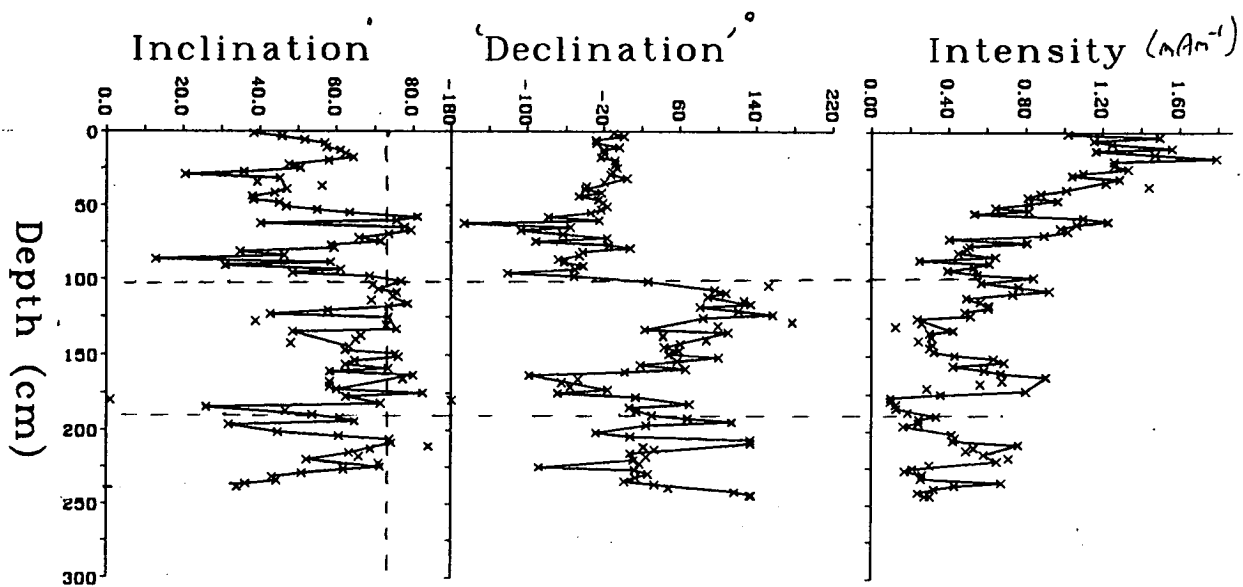
7 Palaeomagnetic results

All the subsamples recovered from Flett cores showed a strong normal magnetic polarity. As a continuous set of subsamples were available for core 61-03 42CS, it was decided to carry out more detailed palaeomagnetic analysis on the samples. Data for a contiguous set of subsamples from the core is shown in fig 4.8. In fig 4.8, data obtained for subsamples that came from disturbed horizons has been plotted in the figure as individual points. The inclination data for core 61-03 42CS varies between 10° and 80° . Variation between adjacent samples can be as much as 20° . The average inclination for the core is approximately 58° . A dotted line has been included on the figure to mark the inclination expected from an axial dipole field model. Relative declination data for core 61-03 42CS varies between -120 and $+140^{\circ}$. A particularly large swing is seen at 100cm, coincident with the division of the core into 1m sections. Intensity, unlike declination and inclination shows a distinct downcore trend, decreasing downcore from a peak value of 1.8 mAm^{-1} in the upper 25cm to a low of 0.1 mAm^{-1} by 150cm.

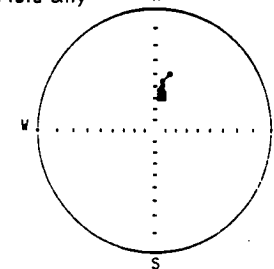
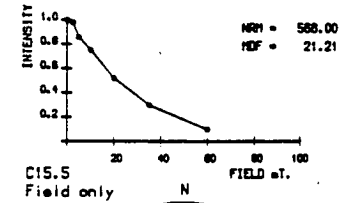
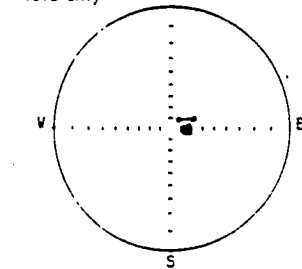
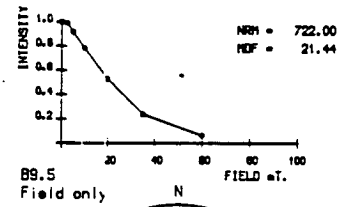
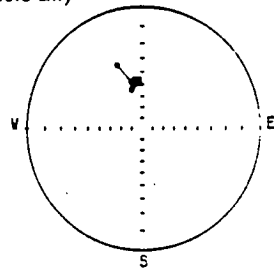
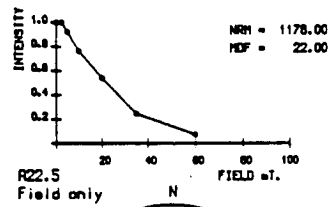
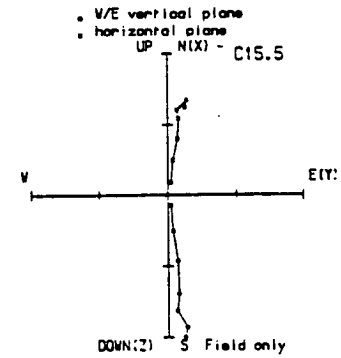
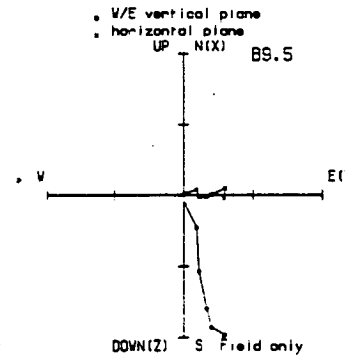
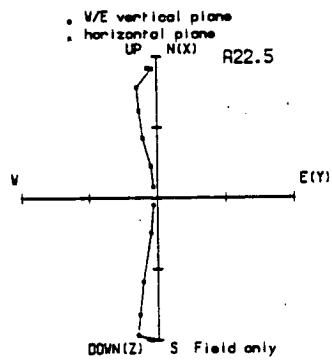
Demagnetisation data for 3 subsamples taken from core 61-03 42CS is shown in fig 4.9. The Zijderveld plots show a strong principal component of magnetisation for each sample. However, a smaller secondary component, removed by a 10mT demagnetisation is seen in each sample. The plots of intensity of remanence against demagnetising field show a steady decrease in intensity with increasing demagnetisation field. All samples had a median destructive field in the range 21-22mT. The stereographic projections for each sample show a tight grouping with any slight deviation attributable to the secondary component seen in the Zijderveld plots. The behaviour under demagnetisation of the three pilot samples in fig 4.9 typifies that of all subsamples from the Flett area.

8 Geological Data

The geological logs and geotechnical results shown in figs 4.10 and 4.11 are composed from data supplied by Dr A. Stevenson. The geological logs of cores 61-03 41CS and 61-03 43CS which typify the lithologies found in Flett cores are shown in fig 4.10a and 4.10b. Each core consists of varying bands of clay downcore, ranging in thickness between 2 and 100 cm. Superimposed on this clay background are small features, for example basalt fragments, dolerite pebbles, carbonaceous material and tuff layers. These small features are found



- Fig 4.8 Downcore palaeomagnetic data for core 61-03 42CS based on subsample results. Relative declination is shown. Position of core section boundaries are shown by horizontal dashed lines. The data points not joined to the main line are those identified as having come from disturbed horizons. The vertical dotted line shows the geocentric axial dipole field inclination at the coring site.



- Fig 4.9 Alternating field demagnetisation data for pilot samples from 61-03 42CS. Labels refer to section of core and depth of sample within that section. Units: NRM intensity - $\mu\text{Am}^2\text{kg}^{-1}$, MDF- mT.



Appendix B - BGS sample naming conventions

All BGS sample stations are assigned a standard coding to enable rapid identification of both origin of sample and the original method of recovery. The coding takes the form of

XX YY zzz mm
XX = latitude of grid square
YY = longitude of grid square (+ = East, - = West)
zzz = sequential number of sample station in grid square
mm = method of sample recovery,
VE = vibrocorer
CS = gravity corer
GS = shipex grab sample.

For example, sample 56-10 28VE is a vibrocore (VE), is positioned in grid square 56 North (56) 10 West (-10) and is the 28th sampling location in that square (28). The BGS labelling system is designed for UK waters, hence latitude is assumed to be North

Vibrocores are generally up to 6m in length, with approximately 5 m of material being the norm. Gravity cores are usually up to 3 m in length. Some gravity cores have been taken using a 6 m barrel, but none are examined in this thesis. Both vibrocores and gravity cores are approximately 100 mm in diameter.

Shipex grab samples vary in quantity from a few grams to several hundred grams.

Samples from vibrocore, gravity core and Shipex grab may exist for any one sample station. The following pages contain a list a sample locations for samples in the Peach, Miller, Flett, Judd and North Sea areas used in this study.

Peach Area

No.	Lat.	Long.	No.	Lat.	Long.
21	56.98617	-9.10917	157	56.18600	-8.57833
22	56.98850	-9.14833	159	56.18333	-8.91683
23	56.94867	-9.13467	164	56.50817	-8.40217
24	56.90883	-9.12717	165	56.88183	-8.04450
26	56.77183	-9.13183	166	56.87433	-8.03300
28	56.50667	-9.04663	167	56.75083	-8.03250
29	56.51450	-9.13750	168	56.44000	-8.03200
30	56.59200	-9.13583	169	56.42433	-8.03283
33	56.51983	-9.52967	171	56.22767	-8.15233
35	56.77917	-9.22150	172	56.18817	-8.02667
36	56.70950	-9.32750	173	56.28367	-8.39883
37	56.78767	-9.37333	174	56.47583	-8.40517
38	56.91433	-9.33783	175	56.50517	-8.57950
39	56.91583	-9.21167	177	56.50150	-8.82950
40	56.99017	-9.54433	178	56.58983	-8.74800
41	56.91000	-9.51833			
42	56.80067	-9.50283			
43	56.70467	-9.53417			
44	56.58667	-9.75900			
45	56.39017	-9.53900			
46	56.41900	-9.75467			
47	56.38700	-9.96633			
48	56.45083	-9.96650			
49	56.49933	-9.96483			
50	56.58217	-9.87733			
51	56.70183	-9.67417			
52	56.80083	-9.75433			
124	56.85667	-8.58250			
125	56.99100	-8.51733			
126	56.98283	-8.40483			
127	56.98483	-8.21283			
128	56.91033	-8.21267			
129	56.90150	-8.03200			
132	56.58383	-8.28933			
133	56.62383	-8.40133			
140	56.58783	-8.58367			
141	56.58083	-8.44200			
142	56.58683	-8.40700			
143	56.62400	-8.20867			
144	56.58167	-8.20750			
145	56.56067	-8.21433			
146	56.47783	-8.22400			
147	56.50083	-8.03433			
148	56.72117	-8.03400			
149	56.38733	-8.15150			
150	56.38633	-8.21533			
152	56.28500	-8.59083			
153	56.28500	-8.59083			
154	56.33467	-8.39933			
155	56.22517	-8.39833			
156	56.18683	-8.40083			

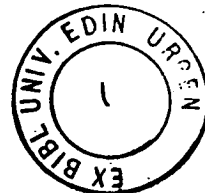
Central North Sea

Num.	Lat.	Long.
121	58.93796	-1.98136
122	58.94000	-1.75000
164	58.76334	-1.45837
231	58.67765	-1.74582
207	58.66891	-0.44955
208	58.86401	-0.46595
222	58.60792	-0.54950
224	58.56836	-0.83327
95	58.85898	0.16874
96	58.75914	0.40037
106	58.75681	0.60981
107	58.75818	0.83485
109	58.57591	0.83163
165	58.63089	0.40420
195	58.86412	0.87626
227	58.99440	0.01389
61	58.66770	1.46659
80	58.57880	1.16585
112	58.03571	1.62664
113	58.15085	1.60221
136	58.96718	1.47415

Miller, Flett and Judd

No.	Lat.	Long.
30	61.18250	-2.13267
31	61.18117	-2.33150
32	61.16600	-2.50150
34	61.22967	-2.67617
37	61.99617	-2.21567
38	61.99317	-2.52617
39	61.99367	-2.78233
40	61.93633	-2.98233
41	61.89067	-2.88167
42	61.91433	-2.62400
43	61.83333	-2.67150
14	60.06883	-5.06017
15	60.08267	-5.08967
16	60.10783	-5.13417
17	60.14133	-5.21050
18	60.18250	-5.29467
19	60.22383	-5.36950
24	60.78900	-4.14867
26	60.58467	-4.31350
27	60.50433	-4.39667
28	60.39150	-4.47567
29	60.30867	-4.57067

WATSON, David J.
Ph.D. 1990



Appendix A - Brief descriptions and photographs of British Geological Survey marine exploration equipment currently in use. Equipment of this kind was used to provide much of the background geological and geophysical data for the UK Continental Shelf sediments investigated in this thesis. (This material provided by the British Geological Survey marine exploration units).

The Marine Earth Sciences Directorate carries out geophysical and geological mapping of the UK Continental Shelf and Slope. The Marine Geophysics and Offshore Services Research Programme (MGOSRP) is responsible for the acquisition of geological and geophysical data, maintenance of the data base, interpretation and production of geophysical maps. The Marine Geology Research Programme (MGRP) is principally involved in the interpretation and production of geological maps and reports. The groups also carry out geological and geophysical surveys for industry and other groups world-wide, and provide a comprehensive consultancy and interpretation service, with further support available from a wide range of specialists within BGS.

Field operations

BGS use a variety of vessels under charter ranging from small inshore launches to large dynamically positioned vessels capable of working in over 2000 m water depth. The geological and geophysical surveys are undertaken from specially modified vessels and many of the BGS systems have been containerised or modularised to simplify mobilisation and demobilisation of equipment. Since 1966 over 200 000 km of geophysical traverse have been run, samples and cores collected from over 30 000 stations, and more than 500 shallow boreholes drilled.

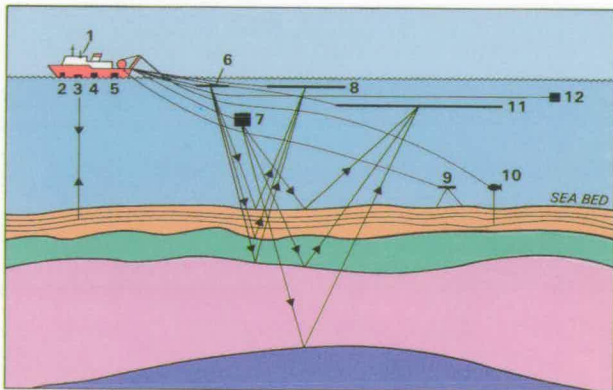


Figure 1 Towing configuration showing the deployment of the simultaneously operated geophysical equipment used in the BGS mapping programme.
 1 Satellite navigator; 2 Doppler sonar;
 3 Pinger; 4 Gravimeter;
 5 Echo sounder; 6 Sparker;
 7 Airgun; 8 Sparker hydrophone;
 9 Sidescan sonar; 10 Deep tow boomer;
 11 Airgun hydrophone;
 12 Magnetometer

In geophysical surveys the operation of the equipment has been integrated through the use of a special seismic control system developed by BGS to allow the operation of a variety of seismic sources (Figure 1). This enables the simultaneous collection along a single traverse of high quality records which provide high resolution information on the near surface sediments (pinger and deep tow boomer/sparker) or information from greater sub-seabed depth using sparker and small air/water guns. Additionally the ship will operate an echosounder, sidescan sonar, gravimeter and towed magnetometer.

For geological surveys the seabed is sampled using a variety of seabed grabs or dredges, and cores are collected using gravity corers designed to sample either hard rock or soft sediment. Stiff sediments and sands are sampled using a vibrocorer (Figure 2) and bedrock can be recovered using the BGS rockdrill. The latter is integrated with the 6-metre vibrocorer to provide a method of either 'jetting' or vibrating through sediment cover to core solid rock beneath. In shallow water, BGS geologist divers can also collect samples and make direct observations or measurements.



Figure 2 Deployment of the BGS 6-metre vibrocorer over the stern of the sampling vessel. The equipment weighs approximately four tons and can be operated in water depths down to 2000 m

Deeper penetration of the sea-bed is achieved using drilling ships designed for site investigation. BGS has developed its own suite of drilling equipment with bits especially designed to penetrate and core a variety of sediment and rock types. Over 500 boreholes have been drilled on the UK Shelf, in water depths of over 550 m and with a maximum penetration of 235 m below sea-bed. BGS has a special expertise in this type of drilling and has operated drilling vessels in many parts of the world.

Data archives

An aspect of the surveys carried out during the BGS offshore mapping programme is the accumulation of an extensive data set. Data collected by BGS are supplemented by information from a variety of commercial, academic and other sources and form an important national archive. Most of the data are publicly available, including the results of laboratory analysis and interpretation.

Gravity, magnetic, echosounding and navigational data are recorded at sea on digital tape and computer processed ashore to produce the ship's track charts and geophysical maps. Seismic records are collected in analogue form at sea, microfilmed ashore and paper copies made on a continuous copier. Digital seismic acquisition is being introduced. During seabed sampling and coring surveys, positional information and the results of onboard measurements and descriptions are fed into a computer and the results of further laboratory analyses are added.

These results, the seismic records, the preserved samples, cores and material from other sources all form part of the offshore archive. This resource, with the working map collection and the expertise of the BGS staff, are available for consultation to provide a comprehensive offshore service.

Deep crustal data acquired by the British Institutions' Reflection Profiling Syndicate (BIRPS) are also available for distribution, and small seismic processing studies can be carried out using the full-scale SKS processing package available on the BGS Vax computer.

Maps and report production

Solid Geology, Quaternary Geology, Sea Bed Sediment, Gravity Anomaly and Aeromagnetic Anomaly maps are published at 1:250 000 scale (Figure 3) as well as other maps at smaller scales. Computer techniques have been introduced into the map making, and it is now possible to select relevant field data from a digital data bank for presentation in graphical form using proprietary contouring and surface-trend analysis programs.

The Directorate has also embarked on the production of a series of Offshore Regional Reports which describe the geology around the UK in a form similar to the popular British Regional Guides onshore.

Special projects

Staff are involved in a wide variety of special investigation and research projects, often in collaboration with industrial or academic partners. These include a major appraisal of offshore sand and gravel resources, investigation of cable and pipeline routes, tunnel and barrage schemes, reclamation and major harbour developments and exploration for placer minerals. Studies of marine slope stability and problems associated with shallow gas or hazardous waste disposal have also been carried out. Academic studies have included the modelling of glacio-marine depositional environments, the development of new seismic processing techniques and the investigation of deep crustal structures around the UK. Consultancy services have been provided to overseas and national surveys and other government departments on the planning, management and interpretation of offshore surveys.

Further information should be obtained from:

Mr J H Hull (Assistant Director, Hydrocarbons and Marine Earth Sciences Directorate)

Mr D A Ardu (Manager, Marine Geology Research Programme)

Dr A Dobinson (Manager, Marine Geophysics and Offshore Services Research Programme)

British Geological Survey
Murchison House
West Mains Road
Edinburgh

Tel: 031-667 1000
Telex: 727343 SEISED G
Fax: 031 668 2683

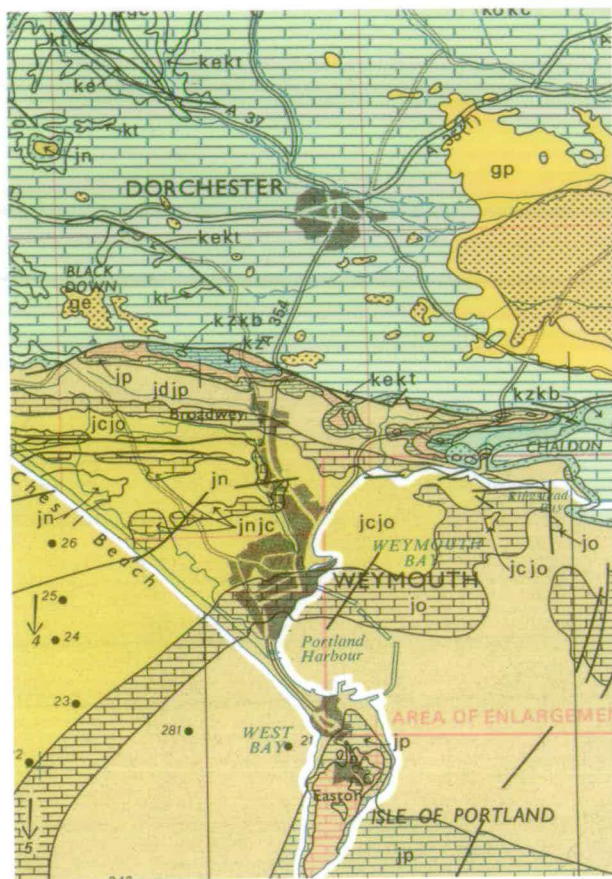


Figure 3 Portion of a 1:250 000 Solid Geology Map (Portland Sheet)

Mr D A C Mills
Marine Geology Research Programme
British Geological Survey
Keyworth
Nottingham NG12 5GG
Tel: 06077 6111
Telex: 378173 BGSKEY G
Fax: 06077 6602

MARINE EARTH SCIENCES DIRECTORATE

Offshore studies by BGS began in 1967 with extensive field programmes designed to regionally map the UK Designated Area. In the main chartered vessels were used and they were equipped, mobilised and operationally manned by BGS. To date, in excess of 200,000 km of seismic track have been run, and samples and cores collected from over 30,000 stations and over 500 boreholes to a maximum depth of 235m below seabed. In addition a large archive of data and core samples from commercial sources is held confidentially. Data from the mapping programmes are publically available and are presented in published maps, BGS publications, Scientific Journals and as part of the BGS Advisory and Enquiry Service.

The work has now extended to the provision of integrated geological and geophysical surveys to various Government departments, Public Bodies and Oil Companies, the provision of Offshore Consultancy for drilling programmes, geophysical and geological quality control, desk studies and Project Management and to utilising the equipment and personnel in sub-contract arrangements with the Offshore Industry.

Staff specialise in Geophysics, Geology and Hydrocarbon studies and further support is provided by Geochemists, Palaeontologists, Petrologists, Seismologists and Engineering geologists. Data from the Hydrocarbon assessment studies is confidential to the UK Department of Energy.

Geophysical studies include the use of shallow and deep tow Side Scan Sonars, Echo Sounders, Pingers, shallow and deep tow Boomers, Sparkers, small Air Guns and Gravity and Magnetic measurements. These instruments are normally operated simultaneously using a purpose built firing control system. A variety of positioning systems can be operated depending on individual survey requirements.

Geological studies utilise seabed Grabs and Dredges, sediment and rock Gravity Corers, Vibrocorers, seabed Rock Drills, Rotary Wireline rock and sediment coring from drilling vessels and Scuba Diving.

Core recovered is subjected to lithological, geotechnical, palaeontological, X-ray, palaeomagnetic, acoustic and various age dating studies. In addition studies of natural and induced radiation (down hole and underway on the seabed), seabed acoustic and resistivity properties and long term *in-situ* seismic observations have been made.

Special projects are also undertaken including studies of pockmarks, subglacial channelling, low angle slope stability, carbonate sediments, sediment fabric studies, sediment chemistry, (including large scale baseline programmes for mineral distribution and pollution studies) absolute dating techniques and seabed seismic monitoring.

Significant developments have been made in seismic control equipment, seabed sampling techniques, shallow soils drilling and geological coring in difficult offshore environments. These developments continue at present.

Staff have worked on projects in various parts of the world both on continental shelves and in deep water as well as in polar regions and have considerable experience in ship selection, contracting and mobilisation. Technical, operational and scientific consultancy is available and staff have experience of power cable and pipeline routing, tunnel and barrage schemes, geotechnical site investigation, mineral exploration and inshore surveys including aggregate investigation, dredging projects, beach reclamation and sewer outfall work.

Further information on the work, the expertise and the facilities available may be obtained from the Enquiries Officer, at the address below.

**British Geological Survey
Marine Earth Sciences Directorate
Murchison House
West Mains Road
Edinburgh EH9 3LA**

**Tel: 031-667 1000
Telex: 727343 SEISED G
Fax: 031-668 2683**

GRAVITY CORER

Use: To core unconsolidated sediments up to 6 metres below sea bed and rock at outcrop.



Description: The gravity corer consists of a 500 kg lead weighted chassis with an attached sediment or rock core barrel that is lowered to approximately 20 metres above the sea bed before being allowed to free-fall. The sediment barrels are 70 mm or 102 mm outside diameter, up to 6 metres in length and have an inner plastic liner to retain the sample. A stainless steel core catcher in the cutting head and a butterfly valve in the corer chassis ensure maximum core retention.

An electro hydraulic winch, complete with metering system, enables the gravity corer to be lowered at an approximate speed of 150 metres per minute.

A buoyant braidline rope or a steel wire can be used with the gravity corer.

A special recovery chute enables the gravity coring operation to be carried out in safety in adverse weather conditions.

Sample: The sediment samples are retained in a plastic liner tube of 57 mm and 83 mm internal diameter.

Operational depth: The present winch system limits operations to 3,000 metres.

Enquiries to:—

**British Geological Survey
Marine Geology Research Programme
Murchison House
West Mains Road
Edinburgh EH9 3LA**

**Telephone: 031-667 1000
Telex: 727343 SEISED G.**

VIBROCORER

Use: Sampling sediments, including stiff and stoney clays, and soft rock to a penetration depth of 6 metres.



Description: The vibrocorer consists of a twin vibrator motor housed in a pressure vessel driving a core barrel of 102 mm outside diameter with a vibration force of 6 tonnes at 50 Hz. The standard system weighing in the order of 3½ tonnes uses a 6 m barrel but smaller units with correspondingly lighter frames are available. A base mounted winch on the vibrocorer providing up to 12 tonnes withdrawal force enables full barrel retraction prior to recovery on the main lift wire. A penetrometer

with a chart recorder and analog display gives a precise measure of penetration rate and depth. The power requirements is 30 kva 415 v 3 ph 50 Hz.

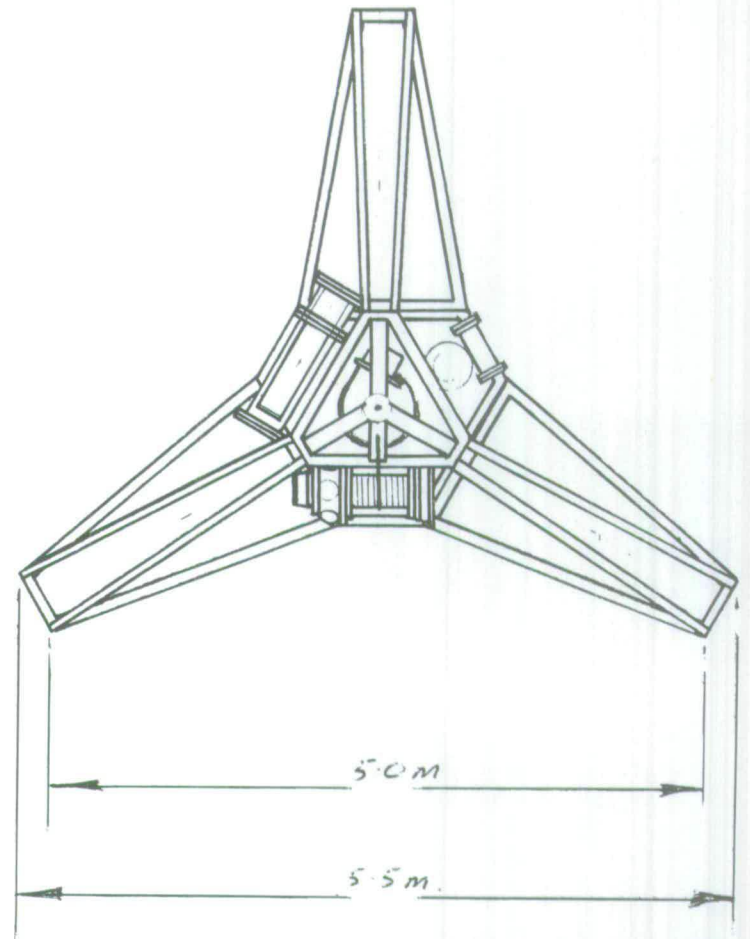
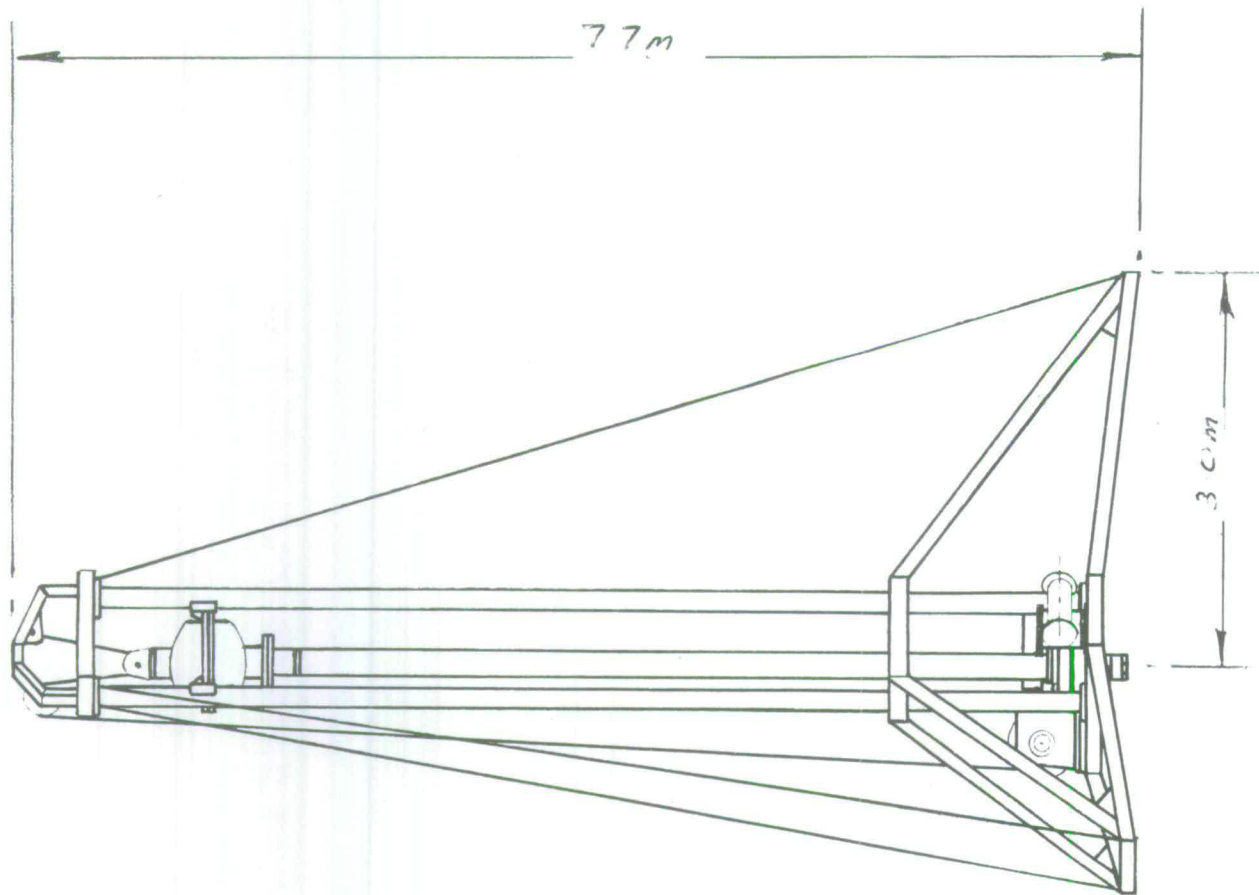
Sample: The samples are retrieved in a clear plastic liner tube of 83 mm internal diameter.

Operational depth: The system has been tested to depths in excess of 1,800 metres and is designed for use to 2,000 metres.

Enquiries to:—

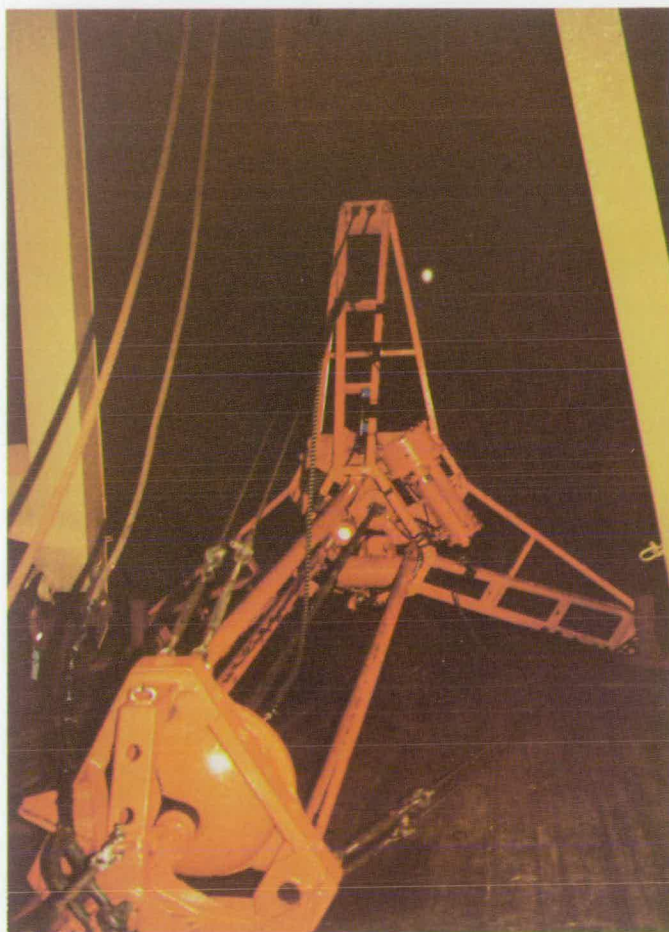
British Geological Survey
Marine Geophysics and Offshore Services
Murchison House
West Mains Road
Edinburgh EH9 3LA

Telephone: 031-667 1000
Telex: 727343 SEISED G
Fax: 031-668 2683



ROCKDRILL

Use: Coring in rock up to 5 metres below sea bed. Simply by fitting an alternative 6 m barrel assembly vibrocores may be taken in sediments or soft rocks.



Description: The rock drill is built within a modular steel structure identical to that of the vibrocorer. The sea bed system is electro hydraulic and fully self contained. The power swivel is base mounted and drives the hexagonal outer barrel at variable drilling speeds up to 600 rpm controlled water flushing is run while drilling. Insitu retraction is achieved by a base mounted hydraulic winch achieving a possible 12 tonnes withdrawal force. The drill uses microprocessor control. Penetration,

retraction and the status of all drilling functions are monitored and displayed.

Sample: The rock core (T.B.W. 44 mm diameter) is recovered in the steel inner barrel of the twinwall barrel system and archived in 1 metre long sections.

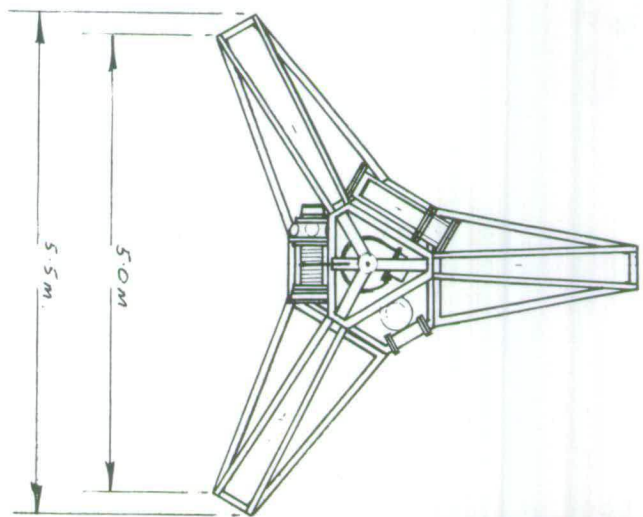
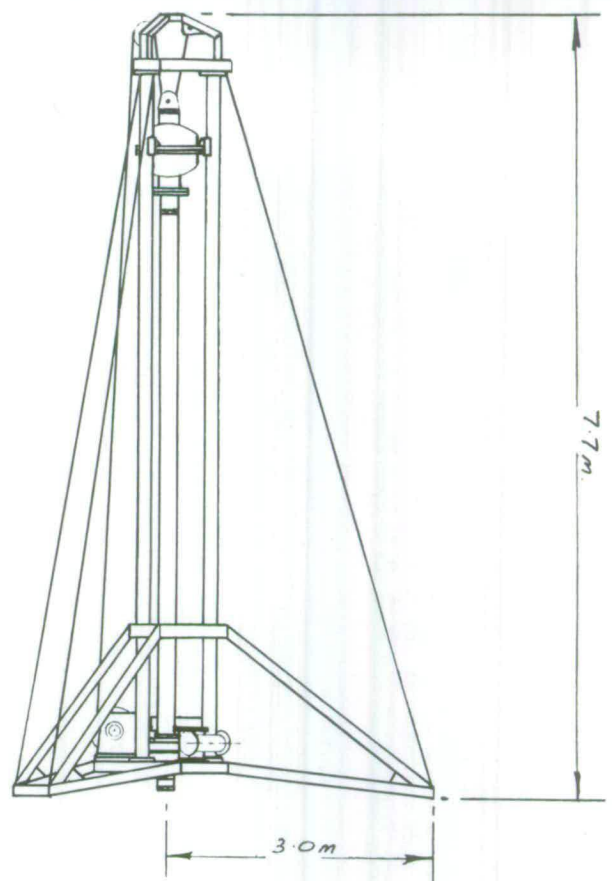
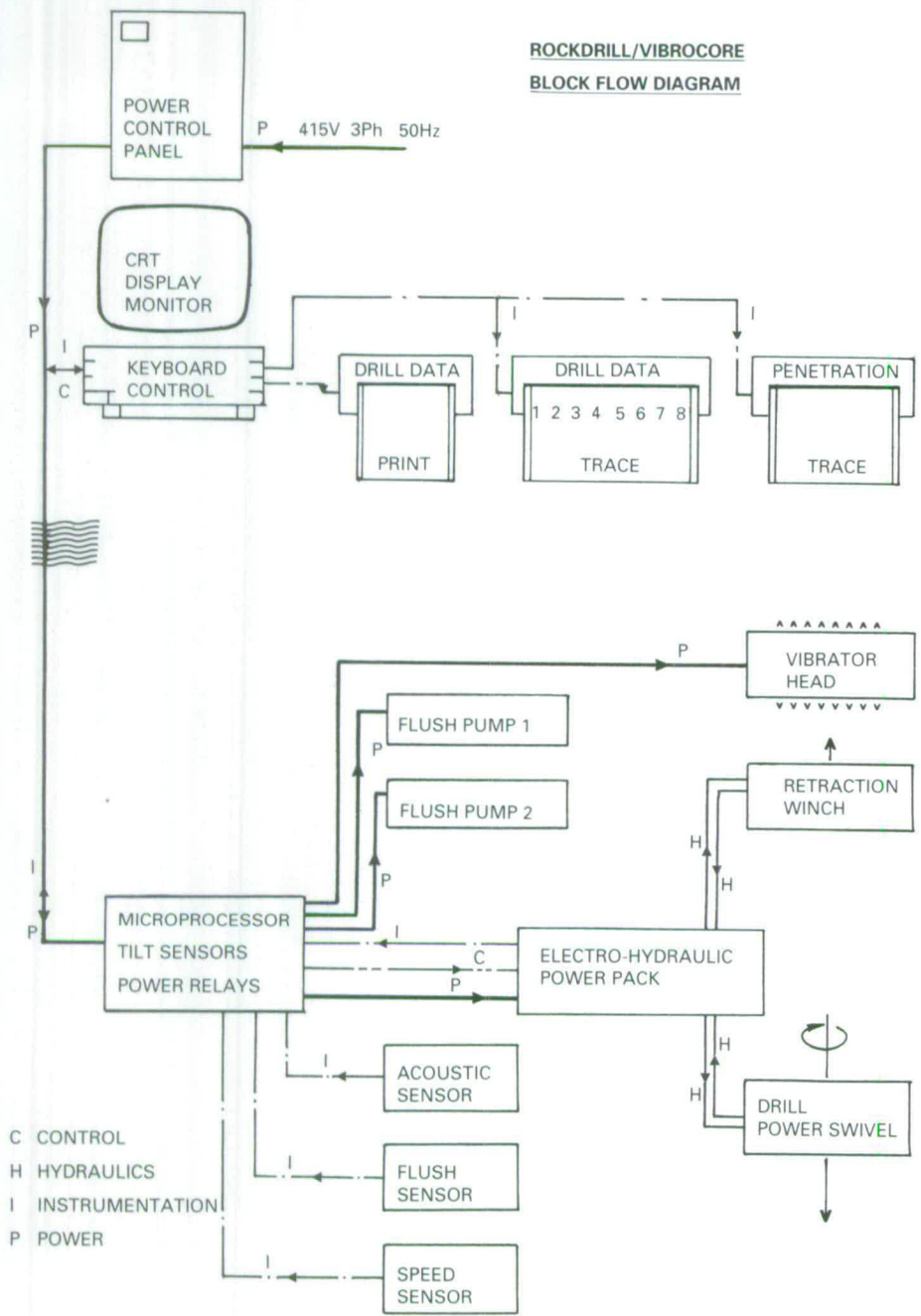
Operational Depth: The system is designed for use to 2000 metres water depth.

Enquiries to:—

British Geological Survey
Marine Geophysics and Offshore Services
Murchison House
West Mains Road
Edinburgh EH9 3LA

Telephone: 031-667 1000
Telex: 727343 SEISED G
Fax: 031-668 2683

**ROCKDRILL/VIBROCORE
BLOCK FLOW DIAGRAM**

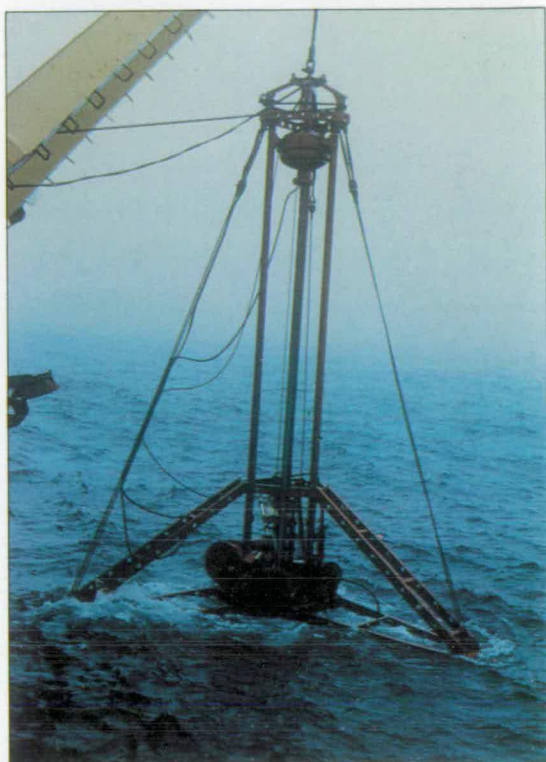


BRITISH GEOLOGICAL SURVEY

SAMPLING AND CORING OPERATIONS

VIBROCORER – ROCKDRILL

This seabed coring tool designed for use to 2000 metres water depth is a self-contained electro-hydraulic unit capable of coring in sedimentary and hard crystalline rock at or near seabed using diamond rotary coring and is also capable of coring seabed sediments using linear vibration forces. The systems are contained in an open geometry steel structure and require only a steel hoist cable and a simple electrical umbilical link to the surface vessel, alternatively a combined power hoist umbilical may be employed.

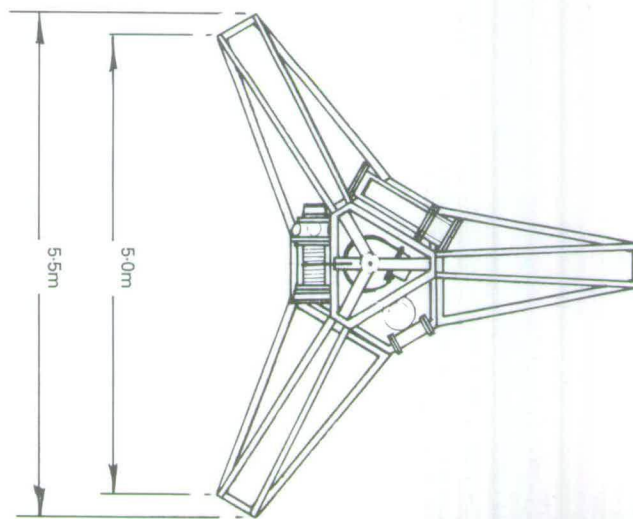
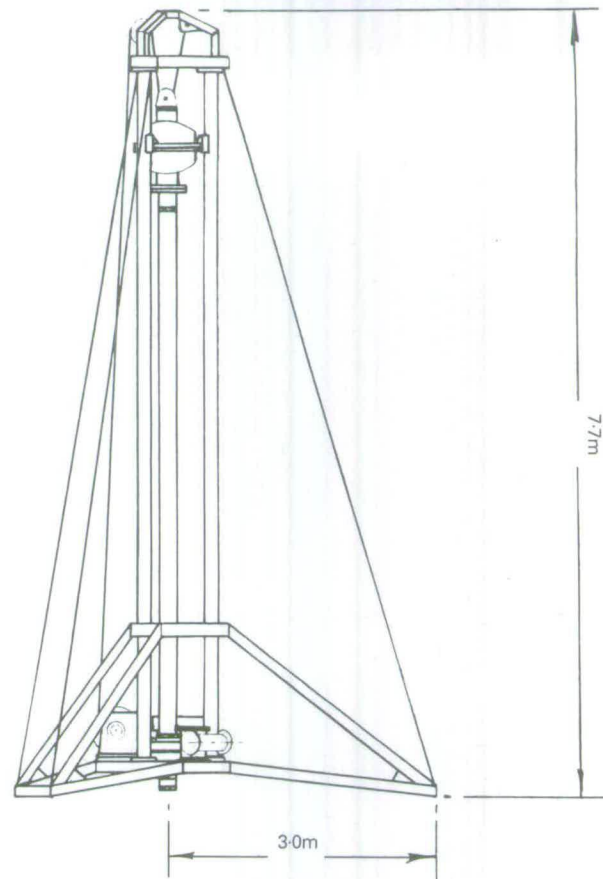
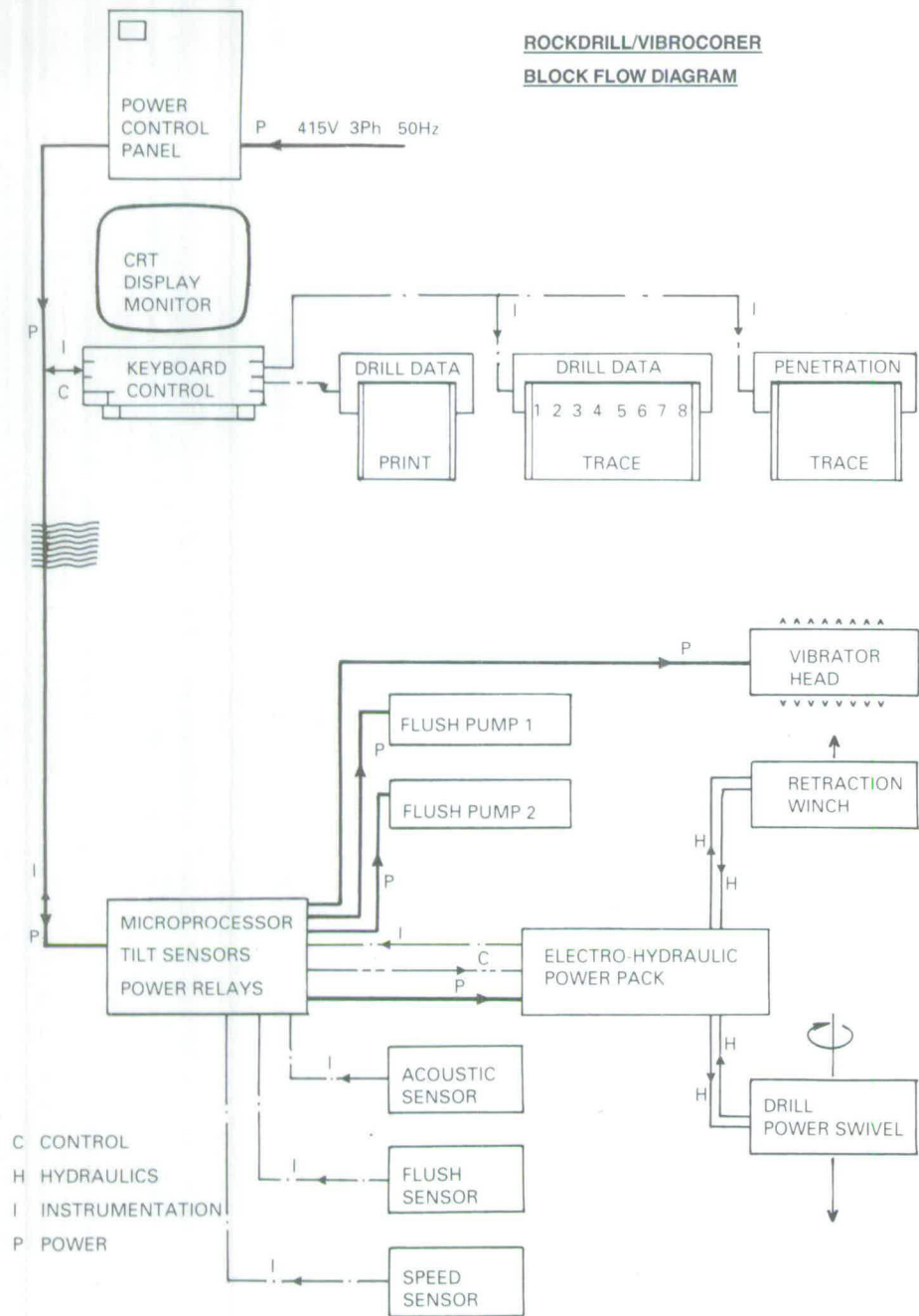


Rock Core – 44mm diameter (TBW) and up to 5 metres long is recovered in the steel non-rotating inner barrel of a twinwall barrel system and is typically archived in 1 metre long sections.

Sediment Core – 83mm diameter and up to 6 metres long is recovered in a clear butyrate or polycarbonate liner tube and is typically archived in 1 metre long sections.

Enquiries to:–
British Geological Survey
Marine Geophysics and Offshore Services
Murchison House
West Mains Road
Edinburgh EH9 3LA
Telephone: 031-667 1000
Telex: 727343 SEISD G
Fax: 031-668 2683

**ROCKDRILL/VIBROCORER
BLOCK FLOW DIAGRAM**



BRITISH GEOLOGICAL SURVEY

SAMPLING AND CORING OPERATIONS

WIRELINE DRILLING

Use: Drilling and continuous coring of sediments and rock formations.



Description: The equipment comprises a wireline core barrel with a selection of tungsten carbide, diamond and rock roller bits developed for BGS and able to core both unconsolidated sediments and rock formations. Various types of inner barrel assemblies can be interchanged during drilling; the non-rotating inner barrel is the most commonly used, but an extended coring assembly and push sampling assemblies are also available for soft and unconsolidated formations. 115 mm I.F. box thread on the core barrel head. 102 mm I.D. drill collars and drill pipe are required.

Handling equipment for running and preparing the core barrels, overshots, tools for make up and maintenance and spares are available.

A Mount Sopris model 2500 wireline logging equipment with combination stratigraphic probe is used to obtain gamma logs of boreholes. Neutron or gamma-gamma can be run with alternative probes.

With the exception of outer drill barrels all equipment is self-contained in a 20' x 8' x 8' container which is also fitted out for equipment assembly and logging.

Sample: 77 mm diameter core with non-rotating inner barrel, 64 mm core with extended coring system and 64 mm or 51 mm core with push sampling assembly.

Operational depth: The equipment is used to depths up to 300 metres below sea bed.

Enquiries to:—

**British Geological Survey
Marine Geology Research Programme
Murchison House
West Mains Road
Edinburgh EH9 3LA**

**Telephone: 031-667 1000
Telex: 727343 SEISED G.**



DEPARTMENT OF ENERGY
PETROLEUM ENGINEERING DIVISION

CORE STORE

For Hydrocarbons Commercial Well Samples

Storage space for 100,000 sample boxes.
Examination rooms and facilities available by
appointment.

Managed by the BRITISH GEOLOGICAL SURVEY
376 Gilmerton Road Edinburgh EH17 7QS
Telephone 031-664 7330



CORE STORE

As part of the obligations of a licence to drill for hydrocarbons on the UKCS and onshore the licensee is required to supply the Department of Energy with a portion of all core and cuttings samples taken. These are received, curated and administered on behalf of DE n by the BGS.

For many years these samples were stored at Kippax near Leeds and at several locations in and near Edinburgh. In 1982 the Department of Energy purchased the present site at 376 Gilmerton Road. The existing building, formerly used as a garage, was modified and equipped for storage and examination of samples. In the spring of 1984 all offshore commercial samples from the various stores were installed at Gilmerton Road. It was apparent that the existing building would require extension in order to allow for the continuing acquisition of cores and cuttings. By mid-summer 1984 the building was considerably extended and fitted out with racking.

Thus, currently the store houses approximately 50,000 trays and boxes of cuttings and cores with space to house a further 40,400 such boxes. Examination rooms equipped with running water, simple laboratory equipment, microscopes and photographic equipment are available for use by visiting geologists. A microfiche viewer is available for examination of released well data.



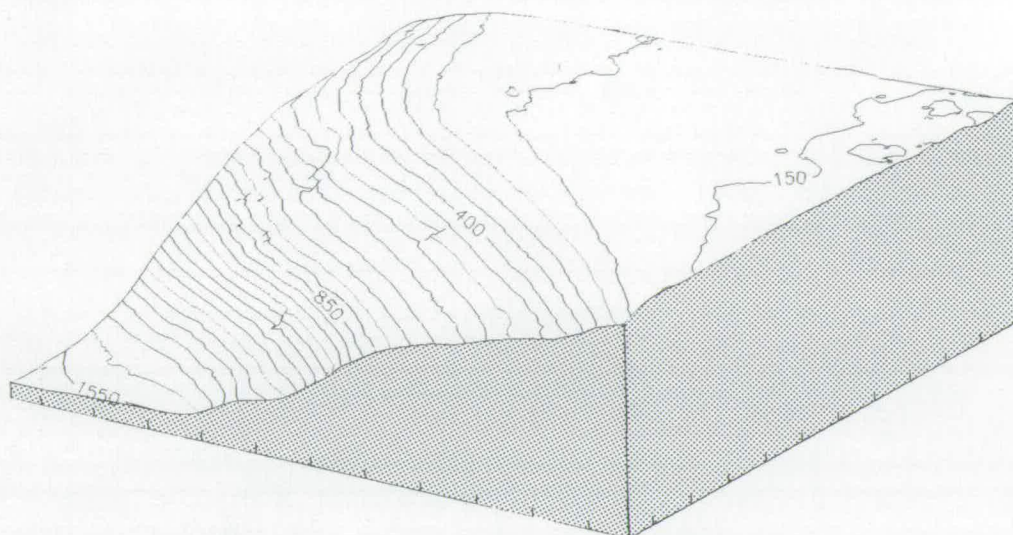
The store is visited regularly by oil company and academic geologists wishing to examine and sub-sample core and cuttings. The regulations governing the use of the store have been sent to all operating companies in the UK and to geology departments of British Universities.

The building also houses a large PRIME computer installation which carries the geological and geophysical databases for the Department of Energy funded BGS Hydrocarbons Research Programme.



Further information may be obtained from:
The Curator
DE n Core Store
376 Gilmerton Road
EDINBURGH EH17 7QS
Telephone 031-664 7330

OFFSHORE DATABASE



Perspective View — Northwest Scotland Continental Shelf

Since 1968, the Marine Directorate of the British Geological Survey has been responsible for surveying and mapping the greater part of the UK Continental Shelf. In that time, they have covered some 200,000 km of geophysical track and taken over 30,000 surface and core samples.

The geophysical data include gravity, magnetic and bathymetric measurements, which are held in digital form, as well as shallow analogue seismic records including airgun, sparker, boomer and sidescan.

The sample data include surface and core samples (of up to 6m penetration) and 500 boreholes to around 200m TD. Most of the surface samples have been subsequently analysed and data are available on particle size and carbonate content. Shipboard geotechnical strength measurements are available on a large number of core samples.

Data are held on a computer data base which can be accessed by BGS staff. Data can be presented in the form of listings and maps or extracted in digital form to tape or floppy disc. Seismic records can be copied as paper or microfilm or may be inspected at the Survey's Offices in Edinburgh.

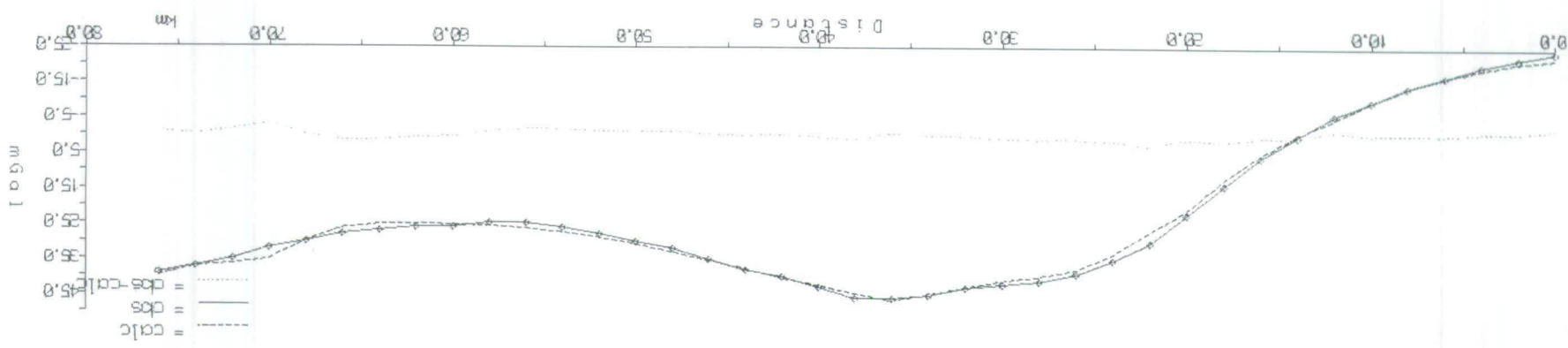
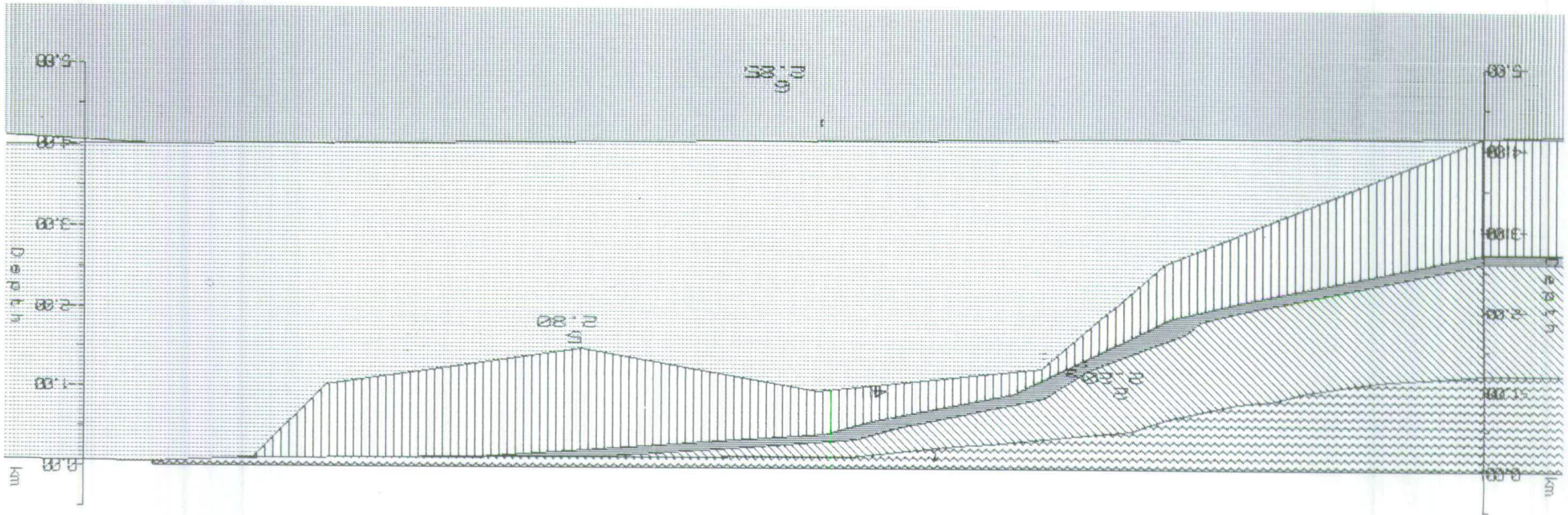
The British Geological Survey is also able to offer software developed for our own use but which may be of benefit to clients who buy our data. These include plotting and geophysical modelling programs, which may also be used by visitors to the Survey.

Enquiries to:

**British Geological Survey
Marine Geophysics and Offshore Services
Murchison House
West Mains Road
Edinburgh EH9 3LA**

**Tel: 031-667 1000
Telex: 727343 SEISED G
Fax: 031-668 2683**

Northwest Scotland Continental Shelf Gravity Model



= calc
 = obs
 = obs-calc

MARINE OPERATIONS

Through its extensive offshore survey programme over the past 20 years, the BGS has built up considerable experience in a very wide range of offshore geophysical and geological operations.

The following systems are operated:

GEOPHYSICAL

Gravity
Magnetics
Bathymetry
Positioning
Data logging
Shallow seismic profiling:
 Deep tow boomer/sparker
 Surface tow boomer
 Pinger
 Sparker
 Airguns
Side scan sonar

GEOLOGICAL

Sampling and coring:

Grabs
Gravity corers
Piston corers
Vibrocorers
Rockdrills
Diving (Scuba)
Photography and TV

Drilling:

Rotary wireline drilling
Electrical logging

Additional facilities include workshops and laboratories both shipboard and land based.

Individual information sheets are available for many of the above systems.

Enquiries to:

**British Geological Survey
Marine Geophysics and Offshore Services
Murchison House
West Mains Road
Edinburgh EH9 3LA**

**Tel: 031-667 1000
Telex: 727343 SEISED G
Fax: 031-668 2683**

GRAVITY



Since 1968 the Survey has built up a level of experience in marine gravity surveying that is unique in the United Kingdom. In our regional survey programme typically 15,000km of gravity data have been collected annually for input to our 1:250,000 map series covering the whole of the UK Continental Shelf.

The system currently employed is a La Coste and Romberg air-sea gravity meter with a Worden land meter providing harbour base ties. Digital data are logged on an integral Monitor Labs 9400 logger and on a Qubit TRAC IV logging system. The latter is the

primary logging device, also recording depth, magnetics and navigation parameters. Depth information is provided by an Atlas Deso 20 echo sounder and a variety of positioning systems can be operated depending on survey location.

All processing of gravity data is done in-house, including Eotvos, latitude and water depth corrections, smoothing and network analysis. All processed gravity data are incorporated in our Offshore Database and may be retrieved in a variety of graphical outputs or in digital form.

Enquiries to:—

**British Geological Survey
Marine Geophysics and Offshore Services
Murchison House
West Mains Road
Edinburgh EH9 3LA**

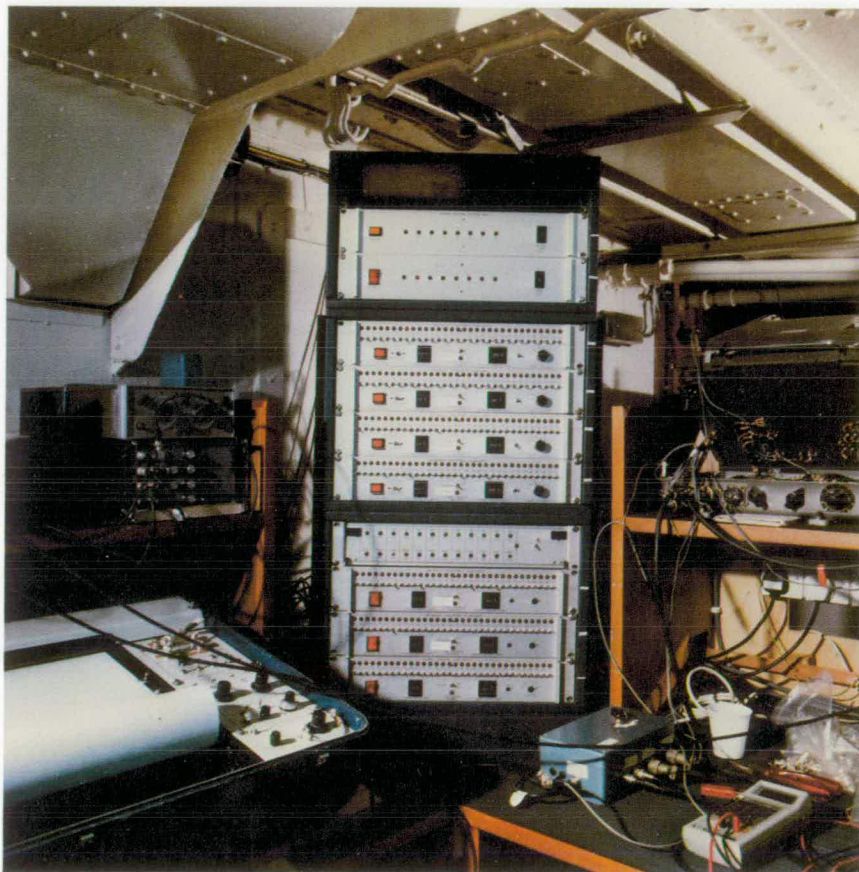
**Telephone: 031-667 1000
Telex: 727343 SEISED G
Fax: 031-668 2683**

BRITISH GEOLOGICAL SURVEY

MARINE GEOPHYSICAL OPERATIONS

SEISMIC CONTROL SYSTEM

Interference free multi-system seismic/sonar data acquisition.



The control system was designed and built in house and comprises a master unit and sub-units, one for each seismic/sonar system in operation.

Sub-units provide:—

1. Independent time control of firing and recording sequences, to 10msec, for each system within an overall timing cycle generated by the master unit. The latter time cycle is determined by the slowest rate of firing in operation.
2. Memories which permit reversible sweep display resulting in normalisation of seismic records.

3. Print delay—removal of water column.
4. Multiple print facility—stretches the horizontal scale reducing vertical distortion

The system has been in routine use over the last three years during which over 30,000km of multiple system data have been acquired in the BGS regional mapping programme. Typically, airgun, sparker, pinger and/or deep tow boomer, and sidescan sonar are operated simultaneously. An additional unit is used to control the magnetometer cycle to prevent sparker interference.

Enquiries to:—

**British Geological Survey
Marine Geophysics Research Programme
Murchison House
West Mains Road
Edinburgh EH9 3LA**

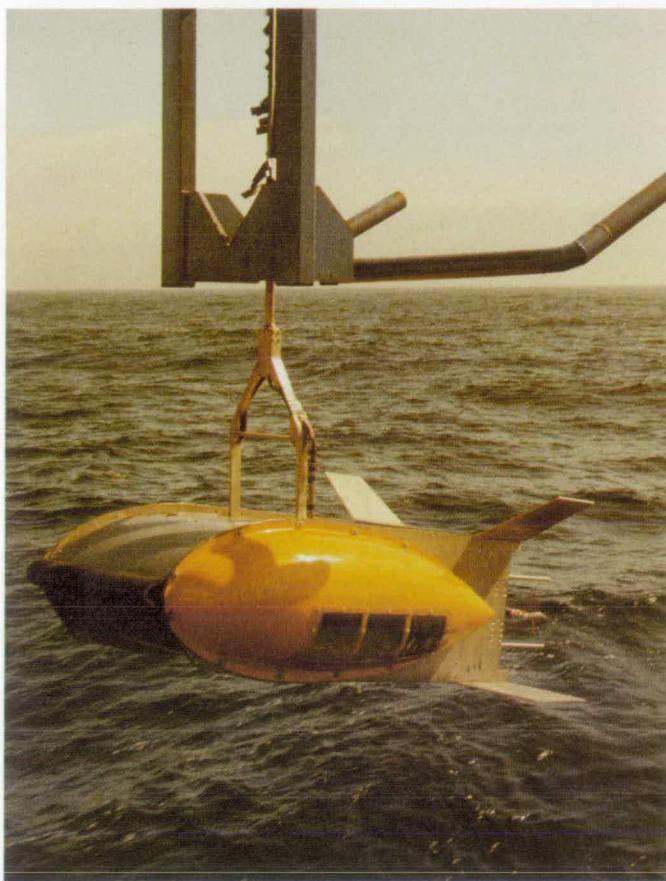
**Telephone: 031-667 1000
Telex: 727343 SEISED G.**

BRITISH GEOLOGICAL SURVEY

MARINE GEOPHYSICAL OPERATIONS

DEEP TOW BOOMER / SPARKER

High resolution sub-bottom profiling in water depths 100-2000m.



Developed by BGS from the Huntec deep tow boomer, the depth of operation of the tow fish has been extended to 1000m.

Boomer operation is successful throughout the full tow depth range and a penetration of 150msec has been achieved with a resolution of better than 1m. The alternative sparker source may be selected and produces a very comparable record but with depth of operation limited to approximately 300m.

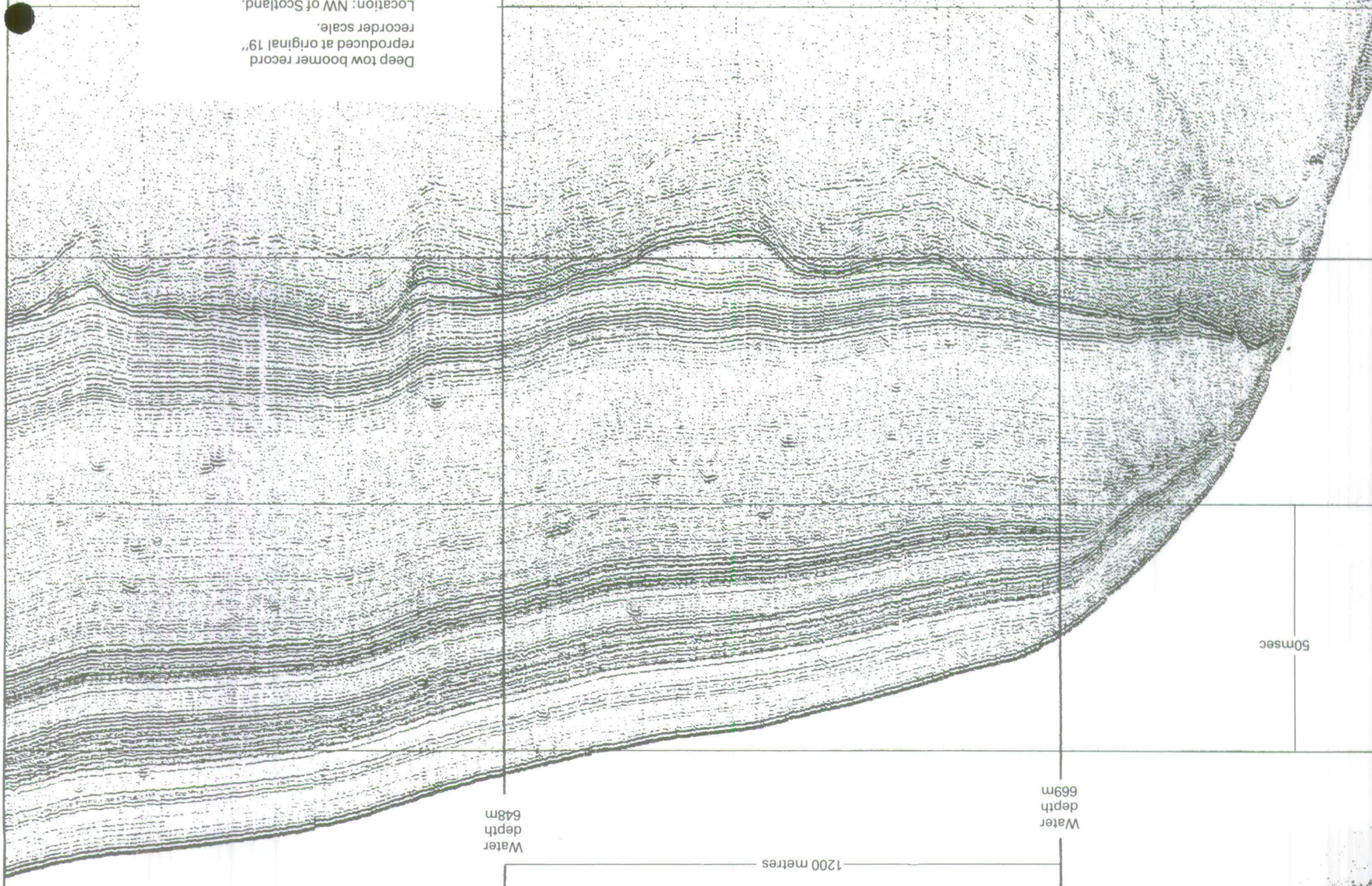
The system comprises tow fish (weight 800kg) with a

short trailing hydrophone array, A-frame with fish catcher assembly (weight 4.5 tons), remotely controlled electro-hydraulic winch with 2.5km tow cable and power pack (total weight 8 tons), HV power supply unit and a laboratory electronics package which includes depth compensation. Further signal processing is provided by a band pass filter, TSS 307 TVG amplifier, TSS 302 swell filter and display on an EPC 3200 graphic recorder. Firing control and additional features, such as print delay, are provided by the BGS Seismic Control System.

Enquiries to:—

**British Geological Survey
Marine Operations Research Programme
Murchison House
West Mains Road
Edinburgh EH9 3LA**

**Telephone: 031-667 1000
Telex: 727343 SEISED G.**



Deep tow boomer record
reproduced at original 19"
recorder scale.
Location: NW of Scotland.

50msec

Water
depth
669m

Water
depth
648m

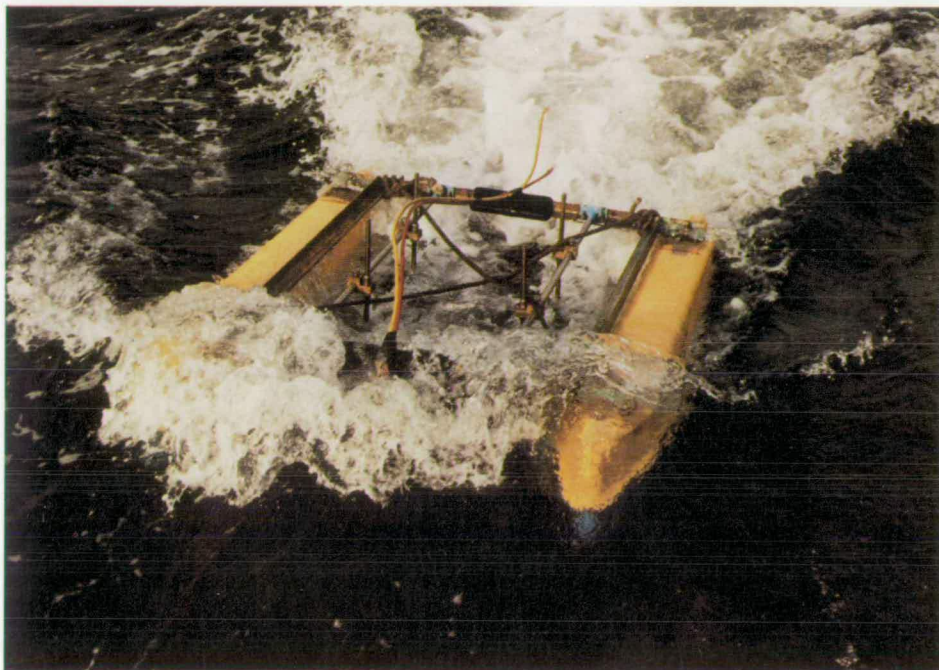
1200 metres

BRITISH GEOLOGICAL SURVEY

MARINE GEOPHYSICAL OPERATIONS

SURFACE TOW BOOMER

High resolution sub-bottom profiling for shallow water/inshore surveys.



Source: EG & G Model 230 boomer plate, catamaran mounted, 300J power capability. Typical penetration to 100m, resolution to 0.5m.

Hydrophone: Teledyne, 10m active section with 7 channels each of 4 elements. Number of channels selected dependent on resolution/penetration requirements.

Processing and Display: Seven channel in-house design seismic amplifiers and summing unit, Kemo or Kronhite bandpass filter, TSS Model 307 seabed tracking TVG amplifier, TSS Model 302 swell filter and display on an EPC 4600 or EPC 3200 graphic recorder. Reversible sweep, water column removal and multiple print facility provided by the Seismic Control System.

Enquiries to:—

British Geological Survey
Marine Geophysics Research Programme
Murchison House
West Mains Road
Edinburgh EH9 3LA

Telephone: 031-667 1000
Telex: 727343 SEISED G.

SPARKER

Medium resolution shallow seismic profiling over the Continental Shelf.



Source: EG & G System with up to 2kJ power capability. Nine candle array with multitip candles selectable from shipboard end in banks of three. Normally used at 500J per bank of three candles giving a discharge rate of 11J per tip. This discharge rate is maintained for powers of 1000 and 1500J permitting flexibility in power output whilst minimising changes in pulse characteristic. Pulse length is typically 5msec with penetration to 500m.

Hydrophone: Teledyne, 10m active section with 7 channels each of 4 elements.

Processing and Display: Seven channel in-house design seismic amplifiers and summing unit, Kemo or Kronhite bandpass filter, TSS Model 307 seabed tracking TVG amplifier, TSS Model 302 Swell Filter and display on an EPC 4600 or EPC 3200 graphic recorder. Reversible sweep, water column removal and multiple print facility provided by the Seismic Control System.

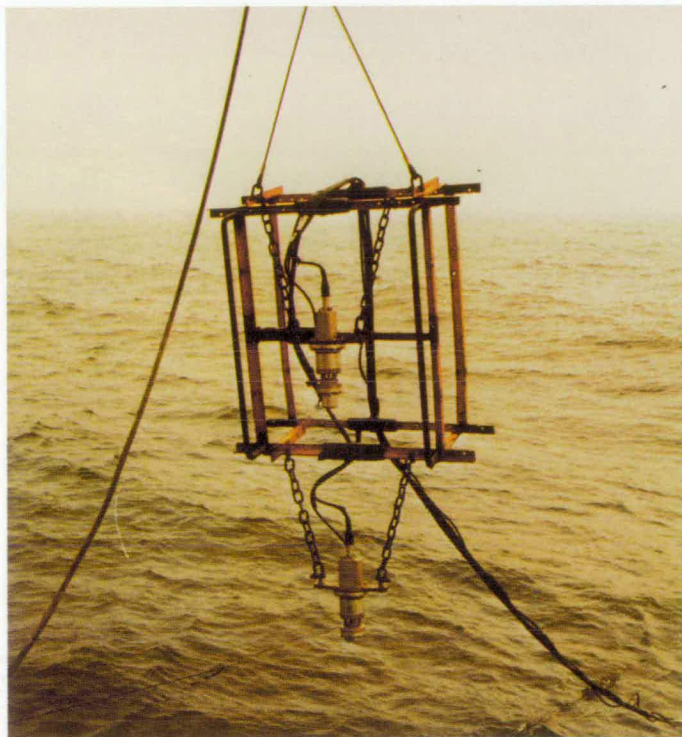
Enquiries to:—

**British Geological Survey
Marine Geophysics Research Programme
Murchison House
West Mains Road
Edinburgh EH9 3LA**

**Telephone: 031-667 1000
Telex: 727343 SEISED G.**

AIRGUN

Regional seismic profiling over the Continental Shelf and Slope.



Source: Combination of Bolt 600B airguns with a range of chamber sizes from 1 to 40 cu.in. Wave shape kits are used with the 40 cu.in chambers to eliminate the bubble pulse. Normally two guns are towed on the same frame and these can be used singly or in combination giving typical penetration to 1km. A tuned array of up to five guns is under development. A containerised Compair Reavell VHP 36 compressor system provides capability of firing 80 cu.in at an 8sec rate.

Hydrophone:

(a) 2 Channel, 30m, Geomecanique.

(b) In-house specification 80m hydrophone with two active 25m sections, isolating head and tail sections, depth sensor and depth controllers.

Processing and Display:

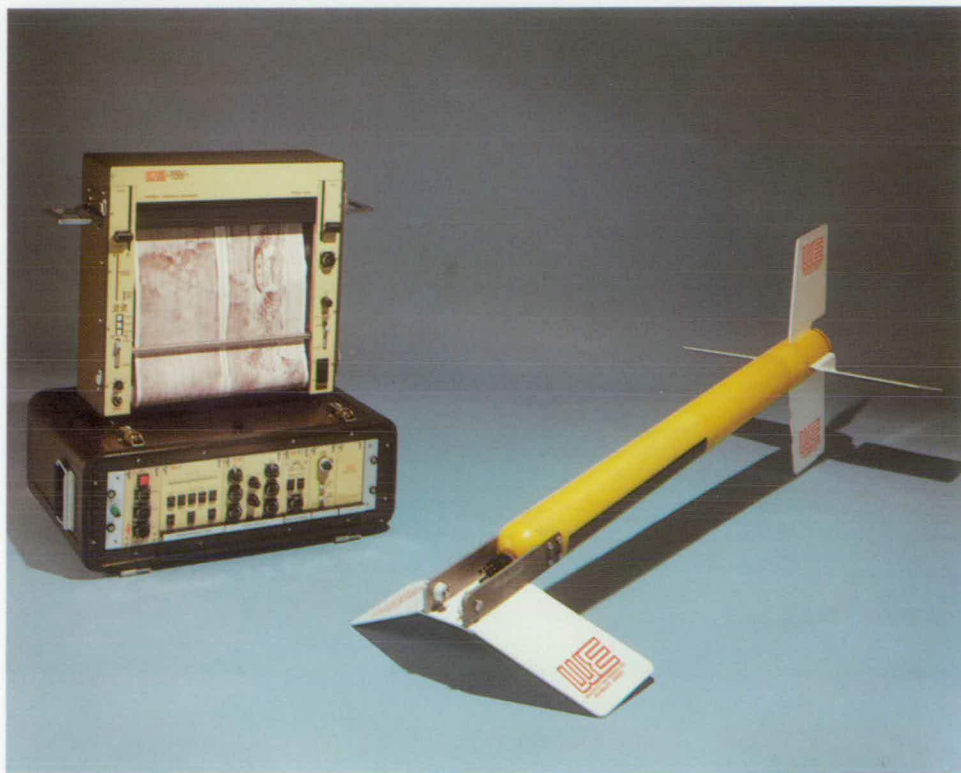
In-house design seismic amplifiers, Kemo or Kronhite bandpass filter, TSS Model 307 seabed tracking TVG amplifier and display on an EPC 4600 or EPC 3200 graphic recorder. Reversible sweep, water column removal and multiple print facility provided by Seismic Control System.

Enquiries to:—

**British Geological Survey
Marine Geophysics Research Programme
Murchison House
West Mains Road
Edinburgh EH9 3LA**

**Telephone: 031-667 1000
Telex: 727343 SEISED G.**

SIDE-SCAN SONAR



The Survey's primary sidescan sonar system is currently the Waverley Sonar 3000. This is a dual channel 100KHz system incorporating a signal processing unit with automatic adaptive gain control, a range expansion facility and display on a high definition thermal printer. The processing unit has been especially modified to permit a degree of external control which eliminates disruptive interface from other seismic sources without

significantly effecting sonar data quality. Other facilities include along course ship speed adjustment and a tape recording facility.

The system is available with either a 150m tow cable on a handwinch for shallow water operations or with a 600m tow cable on a powered winch giving full Continental Shelf capability.

Enquiries to:—

British Geological Survey
Marine Geophysics and Offshore Services
Murchison House
West Mains Road
Edinburgh EH9 3LA

Tel: 031-667 1000
Telex: 727343 SEISED G
Fax: 031-668 2683

BRITISH GEOLOGICAL SURVEY

SAMPLING AND CORING OPERATIONS

SHIPEK GRAB

Use: Sampling sea bed surface sediments.



Description: The grab is spring loaded and cocked by a lever before being lowered to the sea bed. On contact with the seabed a trigger weight on the grab strikes a release lever and the bucket snaps shut to take a sample of the sea bed sediment.

An electro-hydraulic winch, complete with metering system, is used to lower the grab to the sea bed on a 6mm wire at a speed of 60-70 metres/minute.

Sample: Up to 2kg.

Operational depth: The present winch system limits operations to 3,000 metres.

Enquiries to:—

British Geological Survey
Marine Geology Research Programme
Murchison House
West Mains Road
Edinburgh EH9 3LA

Telephone: 031-667 1000
Telex: 727343 SEISED G.